

**UNIVERSIDADE FEDERAL DE SÃO CARLOS
PROGRAMA DE PÓS-GRADUAÇÃO EM GENÉTICA EVOLUTIVA E
BIOLOGIA MOLECULAR**

Renata Luiza Rosa de Moraes

**Evolução cromossômica, diversidade genética e história
demográfica em espécies do gênero *Pyrrhulina*
(Characiformes, Lebiasinidae)**

SÃO CARLOS -SP
2024

Renata Luiza Rosa de Moraes

Evolução cromossômica, diversidade genética e história demográfica em espécies do gênero *Pyrrhulina* (Characiformes, Lebiasinidae)

Tese de doutorado apresentada ao Programa de Pós-Graduação em Genética Evolutiva e Biologia Molecular do Centro de Ciências Biológicas e da Saúde da Universidade Federal de São Carlos – UFSCar, como parte dos requisitos necessários para obtenção do título de Doutora em Ciências (Ciências Biológicas), área de concentração: Genética e Evolução.

Orientador: Prof. Dr. Marcelo de Bello Cioffi

São Carlos-SP
2024

Dedico esse trabalho a todas as pessoas que mudaram minha vida: minha família, amigos, e colegas de trabalho que participaram e me apoiaram intensamente nessa jornada.

A realização deste estudo foi possível devido:

À Universidade Federal de São Carlos e ao Programa de Pós-Graduação em Genética Evolutiva e Biologia Molecular (UFSCar).

Aos laboratórios de Citogenética Evolutiva (UFSCar), Laboratory of Molekulare Zytogenetik da Universitätsklinikum (Uni Jena).

À Fundação de Amparo à Pesquisa do Estado de São Paulo (FAPESP) pelo financiamento dos projetos: **“Evolução cromossômica, diversidade genética e história demográfica em espécies do gênero *Pyrrhulina* (Characiformes, Lebiasinidae)”** (Processo: FAPESP 2019/25045-3)

e
“Análise do Satelitoma em espécies do gênero *Pyrrhulina* (Characiformes, Lebiasinidae): Insights para evolução cariotípica e dos cromossomos sexuais” (BEPE – processo: FAPESP 2022/04964-3)

AGRADECIMENTO

Agradeço a todas as pessoas e instituições envolvidas que possibilitaram a realização deste projeto, em especial:

Ao meu orientador Dr. Marcelo de Bello Cioffi por todos os ensinamentos e oportunidades que compartilhou comigo ao longo de todos esses anos. Terei eterna gratidão pelo crescimento profissional que me ofereceu e pelas portas que me abriu. Muito obrigada!

Ao Dr. Orlando Moreira-Filho e Dr. Luiz Antônio Carlos Bertollo por toda sabedoria, respeito e admiração.

Aos funcionários do Departamento de Genética e Evolução, aos professores do Programa de Pós-Graduação em Genética Evolutiva e Biologia Molecular da UFSCar e a todos os colegas de pós-graduação.

A Manoela Maria Ferreira Marinho, por todo apoio prestado com relação a taxonomia dos indivíduos e pela identificação dos exemplares.

Aos técnicos de laboratório Luiz Henrique da Silva (Piau) e Antônio Aparecido Donizetti da Silva (Toninho) pelo suporte com as coletas.

Agradeço a todos os alunos e professores do Laboratory of Molekulare Zytogenetik da Universitätsklinikum na cidade de Jena (Alemanha), especialmente ao Dr. Thomas Liehr e Ahmed Al-Rikabi por toda a ajuda, paciência e ensinamentos oferecidos.

A todos que me auxiliaram e que estiveram comigo durante o período em que estive no exterior, especialmente à: Aida e Helena; Caio, Rodrigo, Francisco; Michelly, Luz e Fernando pela amizade, momentos de descontração e por toda parceria no laboratório.

Agradeço a cada um dos colegas que fiz ao longo de todos esses anos no Laboratório de

Citogenética Evolutiva: Ezequiel, Nathalia, Cássia, Geovana, Terumi, Manolo, Carla, Caio, Felipe, Pedro, Priscila, Gustavo, Mariannah, Guilherme, Alan, Nayori, Marina. E agradecimentos especiais aos alunos que admiro e que me apoiaram ao longo desse processo: Francisco, Fernando e Jhon agradeço pela parceria profissional e pela amizade cultivada e conquistada ao longo desses anos. E a Geize e Príncia, agradeço por todo carinho, amizade e paciência nesse longo processo, vocês são admiráveis. Foi um prazer trabalhar com vocês, cada um foi fundamental no meu crescimento profissional e pessoal.

Agradeço a todos os meus amigos, particularmente a Ana Carolina pelos nossos momentos de desabafos e torcida pelo meu sucesso. E em especial minha amiga Giovana, que me acompanhou e me incentivou todos os dias, tanto profissionalmente como pessoalmente, e hoje me protege e me guia do céu!

Agradeço incondicionalmente aos meus familiares que me apoiaram todos os dias. Em especial meus pais (Manoela e Sérgio) e minha irmã (Laura) que me auxiliaram, apoiaram, e me guiaram em cada minuto dessa minha jornada! Amo todos vocês!

Quero agradecer a toda a família do meu noivo pela torcida e carinho que foram essenciais. Em particular a minha cunhada Mayara que teve uma contribuição particularmente especial.

Um agradecimento especial ao meu noivo (futuro marido) meu parceiro de vida. Obrigada por todo apoio, incentivo, paciência e dedicação. Amo você!

“...Depois de muito esperar, num dia como outro qualquer,
decidi triunfar...

Decidi não esperar as oportunidades e sim, eu mesmo
buscá-las.

Decidi ver cada problema como uma oportunidade de
encontrar uma solução.”

(Walt Disney)

DADOS CURRICULARES DA AUTORA

Renata Luiza Rosa de Moraes iniciou sua graduação em Ciências Biológicas na Universidade Federal de São Carlos, *campus* São Carlos em 2015 e obteve seu título em 2019. Durante a graduação foi bolsista FAPESP de Iniciação Científica no Laboratório de Citogenética Evolutiva (LEC) com supervisão do Prof. Dr. Marcelo de Bello Cioffi durante quatro anos. Nesse período aprendeu e desenvolveu habilidades na área da Citogenética clássica e molecular de peixes com enfoque principal em pequenos peixes da família Lebiasinidae. Em 2017 realizou um estágio de dois meses no Laboratory of Molekulare Zytogenetik da Universitätsklinikum na cidade de Jena (Alemanha) liderado pelo Dr. Thomas Liehr onde efetuou experimentos de microdissecção e pintura cromossômica, além de aprimorar seus conhecimentos citogenéticos e culturais. Ingressou no mestrado pelo Programa de pós-graduação em Genética Evolutiva e Biologia molecular como bolsista CNPq e após dois meses iniciou doutorado direto pelo mesmo programa como bolsista FAPESP sob orientação do Prof. Dr. Marcelo de Bello Cioffi. Em 2023, retornou à cidade de Jena e realizou um estágio de seis meses no Laboratory of Molekulare Zytogenetik da Universitätsklinikum onde fez novos experimentos de microdissecção e pintura cromossômica, além de aprimorar seus conhecimentos com o estudo dos DNAs satélites. Durante o doutorado também participou de diversos projetos de pesquisa além de participar de eventos nacionais e internacionais da área com apresentação de trabalho. Até o momento publicou quinze artigos, sendo cinco deles de primeira autoria.

Lista de artigos com participação da aluna durante o doutorado

Moraes, RLR, Sassi, FMC, Bertollo, LAC, Marinho, MMF, Viana, PF, Feldberg, E, Oliveira, VCS, Deon, GA, Al-Rikabi, ABH, Liehr, T, Cioffi, MB. (2021). Tracking the Evolutionary Trends Among Small-Size Fishes of the Genus *Pyrrhulina* (Characiforme, Lebiasinidae): New Insights From a Molecular Cytogenetic Perspective. **Frontiers in Genetics**, 12, 769984.

Moraes RLR, Sassi FMC, Marinho MMF, Ráb P, Porto JIR, Feldberg E, Cioffi MB (2023). Small Body, Large Chromosomes: Centric Fusions Shaped the Karyotype of the Amazonian Miniature Fish *Nannostomus anduzei* (Characiformes, Lebiasinidae). **Genes**, 14(1), 192.

Moraes, RLR, Sassi, FMC, Vidal, JAD, Goes, CAG, dos Santos, RZ, Stornioli, JHF, Porto-Foresti, F, Liehr, T, Utsunomia, R, Cioffi, MB (2023). Chromosomal Rearrangements and Satellite DNAs: Extensive Chromosome Reshuffling and the Evolution of Neo-Sex Chromosomes in the Genus *Pyrrhulina* (Teleostei; Characiformes). **International Journal Molecular Science**, 24, 13654.

Moraes, RLR, Sassi, FMC, de Souza FMC, Deon GA, Marinho MMF, Cioffi MB. The evolution of Lebiasinidae (Teleostei: Characiformes): Insights from cytogenetics. **Genetic and Molecular Biology (Submetido)**

Sassi FMC, Hatanaka T, **Moraes RLR**, Toma GA, Oliveira EA, Liehr T, Rab P, Bertollo LAC, Viana PF, Feldberg E, Nirchio MT, Marinho MMF, Souza JFS, Cioffi MB. (2020). An insight into the chromosomal evolution of Lebiasinidae (Teleostei, Characiformes). **Genes**, 11(4), 365.

Leite PPM, Sassi FMC, Marinho MMF, Nirchio M, **Moraes RLR**, Toma GA, Bertollo LAC, Cioffi MB. (2022). Tracking the evolutionary pathways among Brazilian *Lebiasina* species (Teleostei: Lebiasinidae): a chromosomal and genomic comparative investigation. **Netropical Ichthyology**, 20 (1), e210153.

Ferreira PHN, de Souza FHS, **Moraes RLR**, Perez M, Sassi FMC, Viana PF, Feldberg E, Ezaz T, Liehr T, Bertollo LAC, Cioffi MB. (2022). The influence of chromosomal rearrangements and sex chromosomes in the genetic differentiation of *Pyrrhulina* (Teleostei, Characiformes). **Frontiers in Genetics**, 13, 869073.

Vidal JAD; Sassi FMC; **Moraes RLR**; Artoni RF; Liehr T; Cioffi MB; Almeida MC (2023). Giant Sex Chromosomes in *Omophoita* species (Coleoptera, Chrysomelidae): Structural and Evolutionary Relationships revealed by Zoo-FISH and Comparative Genomic Hybridization (CGH). **Insects**, v. 14, p. 440.

Tura V; Kretschmer R; Sassi FMC; **Moraes RLR**; Barcellos SA; Rosso VO; Souza MS; Cioffi MB; Gunski RJ; Garner AV (2023). Chromosomal evolution of Suboscines: Karyotype diversity and evolutionary trends in Ovenbirds (Passeriformes, Furnariidae). **Cytogenetic and Genome Research**, v. 1, p. 1.

Khensuwan S and Sassi FMC; **Moraes RLR**; Jantararat S; Seetapan K; Phintong K; Thongnet W; Kaewsri S; Jumruthanasan S; Supiwong W; Ráb P; Tanomtong A; Liehr T; Cioffi MB (2023). Chromosomes of Asian Cyprinid Fishes: Genomic Differences in Conserved Karyotypes of 'Poropuntiinae' (Teleostei, Cyprinidae). **Animals**, v. 13, p. 1415.

Khensuwan S and Sassi FMC; **Moraes RLR**; Ráb P; Liehr T; Supiwong W; Seetapan K; Tanomtong A; Tantisuwichwong N; Arunsang S; Buasriyot P; Tongnunui S; Cioffi MB (2024). Chromosomes of Asian cyprinid fishes: Novel insight into the chromosomal evolution of Labroninae (Teleostei, Cyprinidae). **PLoS One**, 19(2), e0292689

Molina, WF, Khensuwan, S, **Moraes, RLR**, Sassi, FMC, da Costa, GWWF, Miguel, DZ, Supiwong, W, Jantararat, S, Phintong, K, Seetapan, K, Ditcharoen, S, Tanomtong, A, Liehr, T, Cioffi, MB. (2024). Karyotypic stasis and its implications for extensive hybridization events in corallivores species of butterflyfishes (Chaetodontidae). **Heliyon**, 10(6).

RESUMO

A família Lebiasinidae (Teleostei, Characiformes) é composta por sete gêneros de pequenos peixes de água doce, que podem ser encontrados em riachos por toda América central e do Sul (exceto Chile). Os representantes desta família apresentam uma grande diversidade de formas e colorações, o que os torna muito atraentes no setor aquarista. Embora seja um grupo que se destaca dentro da ordem Characiformes por sua riqueza de espécies, tal família ainda é pouco explorada citogeneticamente principalmente por suas dificuldades de coleta, obtenção cromossômica e taxonomia confusa. Entretanto, diversos estudos citogenéticos e moleculares envolvendo o grupo vem sendo desenvolvidos ao longo dos anos, contribuindo significativamente no início do esclarecimento de diversas incertezas. Sendo assim, o presente estudo faz parte de grandes avanços citogenéticos e genômicos em andamento que buscam elucidar a história evolutiva dos peixes da família Lebiasinidae. Esta tese tem enfoque principal no gênero *Pyrrhulina*, onde foram combinadas análises citogenéticas, moleculares e de diversidade genética com o objetivo de i) analisar a evolução cariotípica do grupo, ii) compreender a influência do sistema sexual na diferenciação de espécies de *Pyrrhulina* e iii) organizar uma filogenia baseada em dados moleculares para a família Lebiasinidae. Foram analisadas cinco novas espécies de *Pyrrhulina* (*Pyrrhulina* aff. *marilynae*, *Pyrrhulina* cf. *laeta*, *Pyrrhulina marilynae*, *Pyrrhulina obermulleri* e *Pyrrhulina* sp.) por técnicas de citogenética clássica e molecular (Giemsa, bandamento C, mapeamento de DNA repetitivo, hibridização genômica comparativa (CGH) e pintura total cromossômica (WCP). Os resultados mostraram um $2n$ conservado para a maioria das espécies variando entre 40 e 42 cromossomos e um cariótipo majoritariamente acrocêntrico, sendo *P. marilynae* uma exceção, apresentando $2n=32$ e a notável presença de quatro pares de cromossomos metacêntricos, cujo status plesiomórfico é discutido. A distribuição de microssatélites não difere significativamente entre as espécies, entretanto o número e posição dos sítios de DNAr sofreram mudanças significativas em cada uma delas. Os experimentos de CGH interespecíficos apresentaram divergências moderadas no conteúdo de DNA repetitivo entre os genomas das espécies e notavelmente, os experimentos de WCP reforçaram a hipótese sobre a origem do sistema sexual múltiplo X_1X_2Y de *Pyrrhulina semifasciata*. A fim de compreender melhor a formação de tal sistema sexual e a redução cariotípica observada em *P. marilynae* também foram feitas análises com sequências de DNA satélites dessas espécies. Os resultados mostraram a possível influência dessas *sequências* na redução do cariótipo de *P. marilynae* e reforçou a hipótese sobre a formação do sistema sexual de *P. semifasciata*. Além disso, para concluir os estudos feitos aqui, o primeiro cariótipo de *Copella* foi descrito juntamente com uma filogenia baseada em dados moleculares dos representantes de cada um dos gêneros de Lebiasinidae contribuindo para as discussões feitas sobre as relações filogenéticas da família. Resumidamente podemos concluir que os dados sugerem que as diferenciações cariotípicas aqui estudadas foram impulsionadas por rearranjos estruturais acompanhados por uma alta dinâmica de DNAs repetitivos, principalmente quando diz respeito ao gênero *Pyrrhulina*.

Palavras-Chave: Peixes, DNAs repetitivos, Rearranjos Cromossômicos, Evolução

ABSTRACT

The Lebiasinidae family includes seven genera of tiny freshwater fishes that live in streams throughout Central and South America (except Chile). The family's representatives have a wide range of shapes and colors, making them highly desirable in the aquarium industry. Despite being a group that stands out within the Characiform order for its diversity of species, this family has received little attention, owing to collection challenges, chromosome obtaining, and complex taxonomy. Although they constitute a substantial challenge, multiple cytogenetic and molecular research involving the group have been developed throughout the years, contributing considerably to the beginning of the resolution of various uncertainties. Thus, our study is part of a larger cytogenetic and genomic effort to understand the evolutionary history of the Lebiasinidae family. Continuing the studies, with a primary focus on the genus *Pyrrhulina*, cytogenetic, molecular, and genetic analyses were combined with the goal of analyzing the group's karyotypic evolution, understanding the influence of the sex chromosome system in *Pyrrhulina* species differentiation, and organizing a phylogeny based on molecular data from the Lebiasinidae family. Five new *Pyrrhulina* species (*Pyrrhulina* aff. *marilynae*, *Pyrrhulina* cf. *laeta*, *Pyrrhulina marilynae*, *Pyrrhulina obermulleri* and *Pyrrhulina* sp.) were studied using conventional and molecular cytogenetic techniques, including Giemsa, C-banding, repetitive DNA mapping, comparative genomic hybridization (CGH), and whole chromosome painting (WCP). The results showed a conserved $2n$ for most species, ranging from 40 to 42 chromosomes and a predominantly acrocentric karyotype, with *P. marilynae* being an exception, with $2n=32$ and the unusual presence of four pairs of metacentric chromosomes, the plesiomorphic status of which is questioned. The distribution of microsatellites is similar among species, while the number and position of rDNA sites vary greatly. Interspecific CGH tests revealed moderate divergences in repetitive DNA content between the species' genomes. Surprisingly, the WCP studies supported the theory that *Pyrrhulina semifasciata*'s X_1X_2Y multiple sex chromosome system evolved. To better understand the formation of such a sex chromosome system and the karyotypic reduction observed in *P. marilynae*, analyses were also carried out using satellite DNA sequences from these species. The results showed the possible influence of these sequences on the karyotype reduction of *P. marilynae* and reinforced the hypothesis about the formation of the sex chromosome system of *P. semifasciata*. Furthermore, to conclude the studies conducted here, the first karyotype of *Copella* was described, along with a phylogeny based on molecular data of representatives from each of the genera of Lebiasinidae, which contributed to discussions about the family's internal phylogenetic relationships. In conclusion, the data point to the possibility that structural rearrangements combined with a high dynamic of repetitive DNAs drove the karyotypic differentiations under study, particularly in the case of the genus *Pyrrhulina*.

Key-Words: Fishes, Repetitive DNAs, Chromosomal rearrangements, Evolution

Lista de Ilustrações

INTRODUÇÃO

Figura 1: A) Mapa parcial da América do Sul, destacando em cores a distribuição de Lebiasinidae de acordo com GBIF (2024). B-G representantes dos gêneros *Copeina*, *Copella*, *Derhamia*, *Lebiasina*, *Nannostomus* e *Pyrrhulina*, respectivamente. *Copeina guttata* - <https://www.seriouslyfish.com/species/copeina-guttata>; *Copella arnoldi* - foto por Zikamoi - Inaturalist - <https://www.inaturalist.org/photos/76418963>; *Derhamia hoffmannorum* - <https://lifecatalog.ru/cont/1/le/Lebiasinidae.html>; *Lebiasina melanoguttata* - foto por Ezequiel A. de Oliveira; *Nannostomus beckfordi* - foto por Chen Hung-Jou - Inaturalist - <https://www.inaturalist.org/photos/923588> e *Pyrrhulina obermulleri* - foto por Francisco C.M. Sassi25

MATERIAL E MÉTODOS

Figura 2: Locais de coleta no Brasil das espécies de *Pyrrhulina* investigadas citogeneticamente em Moraes *et al.* (2021) (círculos vermelhos) e as anteriormente analisadas (círculos brancos: dados de (Moraes *et al.*, 2017; Moraes *et al.*, 2019)35

CAPÍTULO 1

Figure 1: Brazilian collection sites of the *Pyrrhulina* species cytogenetically investigated in the present study (red circles) and the ones previously cytogenetically analyzed (white circles: data from (Moraes *et al.*, 2017; Moraes *et al.*, 2019).49

Figure 2: Male and female karyotypes of *Pyrrhulina marilynae* (A, F, and K), *Pyrrhulina* aff. *marilynae* (B, G and L), *Pyrrhulina* sp. (C, H and M), *P. obermulleri* (D, I and N) and *Pyrrhulina* cf. *laeta* (E, J and O) arranged after Giemsa staining (A-E), C-banding (F-J), and dual-color *in situ* hybridization (FISH) with 18S (green) and 5S (red) ribosomal DNA probes (K-O). Chromosomes were counterstained with 4',6-diamidino-2-phenylindole (DAPI). Scale bar=5 μ m53

Figure 3: Male and female metaphase plates of *Pyrrhulina marilynae*; *Pyrrhulina* aff. *marilynae*; *Pyrrhulina* sp.; *P. obermulleri* and *Pyrrhulina* cf. *laeta* shows the general distribution of the microsatellites (GA)₁₅, (CA)₁₅ and (CGG)₁₀ on chromosomes. Bar=5 μ m54

Figure 4: Zoo-FISH with the PSEMI-Y probe on male metaphase plates of *P. marilynae* (A), *Pyrrhulina* aff. *marilynae* (B), *Pyrrhulina* cf. *laeta* (C), *Pyrrhulina* sp. (D), and *P. obermulleri* (F) shows the distribution of the telomeric (TTAGGG)_n repeats in *P. marilynae*. Bar = 5 μ m54

Figure 5: Comparative genomic hybridization (CGH) using male-derived genomic probes from *Pyrrhulina* species hybridized onto male chromosomes of *P. marilynae*. The common genomic regions are depicted in the 1st column in each line representing the experiments A-D.

Hybridization between the gDNA of *P. marilynae* (Pmar), *P. australis* (Paus) and *Pyrrhulina* aff. *australis* (Pafa) (A); *P. marilynae* (Pmar), *Pyrrhulina* aff. *marilynae* (Pafm) and *Pyrrhulina* sp. (Psp) (B); *P. marilynae* (Pmar), *P. brevis* (Pbre) and *P. semifasciata* (Psem) (C); *P. marilynae* (Pmar), *P. obermulleri* (Pobe) and *Pyrrhulina* cf. *laeta* (Pcfl) (D). Bar=5 μ m.....55

Figure 6: Representative idiograms of *Pyrrhulina* species showing the distribution of the 18S (green) and 5S rDNA (red) sites on chromosomes, based on the present study and some other previous data (Moraes *et al.*, 2017; Moraes *et al.*, 2019). Bar=5 μ m57

CAPÍTULO 2

Figure 1: Phylogenetic relationships of *Pyrrhulina* species analyzed and their distribution. (A)—Species tree recovered with SNAPP, with branch lengths measured in units of expected number of mutations per site, based on dataset I: *P. australis* (1), *P. brevis* (2), *P. obermulleri* (3); *P. marilynae* (4); and *P. semifasciata* (5). (B)—South America map indicating the origin of *Pyrrhulina* species analyzed. Colored areas indicate the distribution of the species: *P. australis*(blue), *P. brevis* (green), *P. obermulleri* (yellow); *P. marilynae* (purple); and *P. semifasciata* (pink). The numbered circles indicate the collection sites of each species. The red ellipse indicates syntopic species (sampled in the same area). (C)—Idiograms with partial karyotypes of each species and the sex chromosomes exclusively found in *P. semifasciata* are boxed.63

Figure 2: Pairwise Dxy per Species is represented in the upper diagonal, and Da in the lower diagonal. Higher values are shown in green, and as the values decrease the color changes to yellow, orange, and then red for lower values.....66

Figure 3: (A) Genetic diversity in *Pyrrhulina* species according to a PCoA. The PCoA recovered 37.7% of the total variation in the first principal coordinate (PC1), and 21.6% in the second principal coordinate (PC2). (B)—Results for fastStructure with K = 4 and K = 5. Each vertical bar represents an individual; the bar colors represent the group in which the fastStructure classified the individual; the legend below indicates their species.67

CAPÍTULO 3

Figure 1: Metaphase plates of PmaSatDNAs. The satDNA family names are indicated on the left top, in red (Atto550-labeled) or green (Atto488-labeled). Scale bar=10 μ m..79

Figure 2: Male metaphase chromosomes of *Pyrrhulina semifasciata* after FISH with 10 PseSatDNAs. The satDNA family names are indicated in the top left corner in red (Atto550-labeled) or green (Atto488-labeled). The sex chromosomes X₁, X₂, and Y are indicated. Scale bar = 10 μ m80

Figure 3: Male and female metaphase plates of *Pyrrhulina semifasciata* showing that the hybridization pattern of PseSat01 (first column) is coincident with the X₂ and Y sex chromosomes, as indicated by the whole-chromosome painting with the PSEMI-Y probe (second column), which is derived from the microdissection of the Y chromosome. Scale bar = 10 μm80

Figure 4: Metaphase plates of *Pyrrhulina obermulleri* (a–d), *P. brevis* (e–h), and *P. marilynae* (i–l) highlighting the chromosomal location of PseSatDNAs that were mapped in the sex chromosomes of *P. semifasciata*. The satDNA family names are indicated in the upper left in red (if labeled with Atto550-dUTP) or green (if labeled with Atto488-dUTP). The arrows indicate the proto-sex chromosomes. Scale bar = 10μm.....81

Figure 5: (A) *P. semifasciata* male (first column) and female (second column) sex chromosomes highlighting the hybridization pattern of the four PseSatDNAs that produced visible signals, with each line matching to a satellite sequence indicated on the left. The third, fourth, and fifth columns show the hybridization patterns of those satellites in the *P. obermulleri*, *P. brevis*, and *P. marilynae* chromosomes, respectively. Bar = 10 μm. (B) Phylogenetic relationships of *Pyrrhulina* species (green lines) based on Ferreira *et al.* (2022) plotted with main events of origin, loss, and T/R (transposition or recombination) of PseSatDNAs, and origin of the multiple sex of the chromosome system (MSC) (pink lines)82

Figure 6: Linear MSTs of PseSat55 obtained from reads of females (pink) and males (green). The diameter of the circle is proportional to the abundance of the haplotype. Black circles represent 01 base of divergence between haplotypes, and the black triangles represent 05 bases of divergence. The *in situ* mapping in male and female metaphase plates is highlighted in boxes. Bar = 5 μm.83

Figure S1: Females metaphase plates of *Pyrrhulina semifasciata* highlighting the chromosomal location of 10 satDNA. The satDNA family names are indicated on the left top, in red (ATTO550 labeled) or green (ATTO488 labeled). The sex chromosomes (X1X2Y) are shown. Scale bar = 10 μm89

CAPÍTULO 4

Figure 1: Map of South America with sampling sites indicated as dots. Each color represents a distinct species, with colors defined on the legend in the left corner. A *Copella callolepis* individual is presented above the legend, photo by José Luis Olivan Birindelli. The map was produced using the software QGis 3.4.4 (<https://qgis.org>), Inkscape 0.92 (<https://inkscape.org>), and Adobe Photoshop CC 2020 (San Jose, CA, USA).....100

Figure 2: Karyotypes of *Copella callolepis* arranged after different cytogenetic protocols. Giemsa staining (A), C-banding (B), and dual-color FISH with 18S (green) and 5S (red) rDNA probes (C). Chromosomes are counterstained with DAPI (blue). Scale bar= 10μm103

Figure 3: Schematic representation of chromosomes of Lebiasinidae and Ctenoluciidae species, highlighting the position of 18S rDNA (green) and 5S rDNA (red). The small box highlights a sex chromosome system in *Pyrrhulina semifasciata*, while the bigger box highlights the Ctenoluciidae members. FISH data were taken from Souza e Sousa *et al.* 2017; Sassi *et al.* 2019; Leite *et al.* 2022; Sember *et al.* 2020; Moraes *et al.* 2023a; Toma *et al.* 2019; Moraes *et al.*, 2017; 2019; 2021. Letters correspond to the genera: (A) *Boulengerella*, (B) *Lebiasina*, (C) *Nannostomus*, (D) *Copeina*, (E) *Copella*, and (F) *Pyrrhulina*.104

Figure 4: Principal component analysis results, each circle represents an individual, species are colored differently according to the names, percentage values indicate the explanatory capability of each axis, (A) displays the results for the PCA analysis with the full dataset; (B) displays the results for the dataset comprising only *Nannostomus* samples.....105

Figure 5: Maximum likelihood species tree (A), diamond symbols indicate nodes with bootstrap values of 100, gray boxes indicate relevant the main cytogenetic features of each clade. NeighborNet network circles are colored in the same scheme as the phylogenetic tree, each circle represents a sample that was collapsed into one in the phylogeny (B).....106

Figure S1: Maximum likelihood species tree with all sampled individuals in this study. Values close to each node indicate bootstrap values.....110

Lista de Tabelas

MATERIAL E MÉTODOS

Tabela 1: Coordenadas geográficas e número amostral das espécies de *Pyrrhulina* (Characiformes, Lebiasinidae) coletadas no Brasil36

Tabela 2: Dez satDNAs mais abundantes em *P. marilynae*. Destaques em azul são os PmaSatDNAs selecionados para FISH.....42

Tabela 3: 21 satDNAs selecionados para confecção de primer de *P. semifasciata*. Destaques em azul são os PseSatDNAs selecionados para FISH e os asteriscos (*) são todos aqueles que hibridizaram em algum dos cromossomos sexuais.....42

Tabela 4: Condições de PCR (primer, temperatura e concentração de DNA template) para a amplificação ideal de DNAs satélites de *P. marilynae* e *P. semifasciata*.....43

CAPÍTULO 1

Table 1: Geographical coordinates, sample size, and diploid number of *Pyrrhulina* (Characiformes, Lebiasinidae) species collected in Brazil.49

CAPÍTULO 2

Table 1: Species, diploid numbers (2n), sex chromosome systems, numbers of individuals cytogenetically analyzed, and the number of individuals sequenced.63

Table 2: Estimated genome-wide genetic diversity of genus *Pyrrhulina* by species.66

Table 3: AMOVA percentage of variation within and between each of the tested groups: 1) by species, 2) by the best K in the fast structure, 3) by the groups generated in PCoA, and 4) by the presence or absence of sex chromosomes.67

Table 4: Results of the ABBA-BABA test for admixture assessment.68

CAPÍTULO 3

Table 1: Species, locality, and number of individuals (N) used in the present study.....76

Table S1: Main characteristics of 71 satDNAs found in *Pyrrhulina marilynae*. The sequences highlighted in blue correspond to those selected for the FISH experiments.89

Table S2: Main characteristics of 70 satDNAs found in *Pyrrhulina semifasciata*, highlighting, in blue, those chosen for FISH mapping. The asterisk (*) indicates the satDNAs mapped in the sex chromosomes.90

Table S3: Shared SatDNA between *P. marilynae* and *P. semifasciata*. The sequences highlighted in blue correspond to those selected for the FISH experiments.92

Table S4: PCR conditions (primer, temperature, and concentration of template DNA) for the optimal amplification of satellite DNAs from *P. marilynae* and *P. semifasciata*.93

CAPÍTULO 4

Table 1: Samples used in this study.....101

LISTA DE ABREVIATURAS

2n	Número diploide
DNAr	DNA ribossômico
ITS	Sítio telomérico intersticial
mm	Milímetro
ml	Mililitro
mg/ml	Miligramma por mililitro
ng/ml	Nanograma por mililitro
µl	Microlitro
mM	Milimolar
µM	Micromolar
µm	Micrômetro
m	Cromossomo metacêntrico
sm	Cromossomo submetacêntrico
a	Cromossomo acrocêntrico
PCR	<i>Polymerase chain reaction</i>
dNTP	<i>Deoxynucleotide triphosphates</i>
dUTP	<i>Deoxyuridine Triphosphate</i>
DOP	<i>Degenerate oligonucleotide-primed</i>
FISH	<i>Fluorescence in situ hybridization</i>
WCP	<i>Whole chromosome painting</i>
CGH	<i>Comparative genomic hybridization</i>
DNAg	DNA genômico
DAPI	4',6-Diamidino-2-Phenylindole, Dihydrochloride
MgCl₂	Cloreto de Magnésio
rpm	Rotação por minuto
M	Molaridade
N	Normalidade
satDNA	DNA satélite

Sumário

1. INTRODUÇÃO	21
1.1. PEIXES: DIVERSIDADE E IMPORTÂNCIA NOS ESTUDOS EVOLUTIVOS E GENÉTICOS	21
1.1.1. <i>Família Lebiasinidae, com enfoque no gênero Pyrrhulina</i>	24
1.1.2. <i>Estudos citogenéticos em Pyrrhulina</i>	26
1.2. MARCADORES CITOGENÉTICOS	28
1.2.1 <i>Sequências de DNAs satélite e o estudo do Satelitoma</i>	30
1.3. CITOGENÉTICA EVOLUTIVA EM LEBIASINIDAE	31
2. OBJETIVOS	34
2.1. <i>OBJETIVO GERAL</i>	34
2.2. <i>OBJETIVOS ESPECÍFICOS</i>	34
3. MATERIAIS E MÉTODOS	35
3.1. <i>MATERIAL</i>	35
3.2. <i>MÉTODOS</i>	36
3.2.1. <i>Obtenção de cromossomos mitóticos</i>	36
3.2.1.1. <i>Preparação das lâminas</i>	37
3.2.2. <i>Deteção de heterocromatina constitutiva</i>	37
3.2.3. <i>Hibridização fluorescente in situ (FISH) - mapeamento de DNAs repetitivo</i>	37
3.2.5. <i>Pintura total cromossômica (WCP)</i>	40
3.2.6. <i>Análises de bioinformática</i>	40
3.2.6.1. <i>Procedimento de sequenciamento DArTseq e filtragem de dados</i>	40
3.2.6.2. <i>Avaliadores de marcação em seleção</i>	41
3.2.6.3. <i>Diversidade genética</i>	41
3.2.6.4. <i>Estrutura genética e análise de variância molecular (AMOVA)</i>	41
3.2.7. <i>Sequências DNA satélites</i>	42
3.2.7.1. <i>Sequenciamento</i>	42
3.2.7.2 <i>Análises Bioinformáticas e Biblioteca de satDNA</i>	42
3.2.7.3. <i>Design de Primer e Amplificação de DNA via Reação em Cadeia da Polimerase (PCR)</i>	43
3.2.8. <i>Análises</i>	46
4. RESULTADOS E DISCUSSÃO	47
CAPÍTULO 1	48
1. INTRODUCTION	49
2. MATERIALS AND METHODS	50
2.1. <i>ANIMALS</i>	50
2.2. <i>CHROMOSOMAL PREPARATIONS AND ANALYSIS OF THE CONSTITUTIVE HETEROCHROMATIN</i>	51
2.3. <i>REPETITIVE DNA MAPPING WITH FLUORESCENCE IN SITU HYBRIDIZATION (FISH)</i>	52
2.4. <i>FISH FOR WHOLE CHROMOSOME PAINTING</i>	52
2.5. <i>PROBES FOR COMPARATIVE GENOMIC HYBRIDIZATION</i>	53
2.6. <i>MICROSCOPY AND IMAGES PROCESSING</i>	54
3. RESULTS	54
3.1. <i>KARYOTYPES AND HETEROCHROMATIN DISTRIBUTION</i>	54
3.2. <i>CHROMOSOMAL MAPPING OF REPETITIVE DNA SEQUENCES</i>	55
3.3. <i>COMPARATIVE GENOMIC HYBRIDIZATION–CGH</i>	57
4. DISCUSSION	58
5. CONCLUSION	61

CAPÍTULO 2.....	62
1. INTRODUCTION	63
2. MATERIALS AND METHODS.....	64
2.1. SAMPLING	64
2.2. DARTSEQ SEQUENCING PROCEDURE AND DATA FILTERING.....	65
2.3. ASSESSMENT OF MARKERS UNDER SELECTION.....	66
2.4. GENETIC DIVERSITY.....	66
2.5. GENETIC STRUCTURE AND ANALYSIS OF MOLECULAR VARIANCE (AMOVA).....	66
2.6. SPECIES TREE	67
2.7. ANALYSIS OF INTROGRESSION.....	67
3. RESULTS	67
3.1. SEQUENCING, FILTERING, AND DETECTION OF MARKERS UNDER SELECTION	67
3.2. GENETIC DIVERSITY AND STRUCTURE.....	68
3.3. SPECIES TREE AND ANALYSIS OF INTROGRESSION.....	70
4. DISCUSSION.....	70
5. CONCLUSION.....	73
CAPÍTULO 3.....	75
1. INTRODUCTION	76
2. MATERIALS AND METHODS.....	77
2.1. MATERIAL, MITOTIC CHROMOSOMES AND DNA SEQUENCING	77
2.2. BIOINFORMATIC ANALYSES AND SATDNA LIBRARY.....	78
2.3. PRIMER DESIGN AND DNA AMPLIFICATION VIA POLYMERASE CHAIN REACTION (PCR).....	79
2.4. FLUORESCENCE IN SITU HYBRIDIZATION (FISH).....	79
2.5. IMAGES AND CONFIRMATION OF RESULTS	80
3. RESULTS	80
3.1. SATDNA CONTENT OF <i>P. MARILYNAE</i> AND <i>P. SEMIFASCIATA</i>	80
3.2. CHROMOSOMAL DISTRIBUTION OF PMA SATDNA IN <i>P. MARILYNAE</i>	81
3.3. CHROMOSOMAL DISTRIBUTION OF PSE SATDNA IN <i>P. SEMIFASCIATA</i>	81
3.4. CHROMOSOMAL DISTRIBUTION OF PSE SATDNA IN OTHER PYRRHULINA SPECIES.....	83
3.5. MINIMUM SPANNING TREES: MSTs	84
4. DISCUSSION.....	85
4.1. GENERAL FEATURES <i>P. MARILYNAE</i> AND <i>P. SEMIFASCIATA</i> SATELLITOMES.....	85
4.2. SATELLITE DNA CONTRIBUTION IN THE SIGNIFICANT 2N REDUCTION OBSERVED IN <i>P. MARILYNAE</i>	87
4.2. SATDNAs AND THE EVOLUTION OF MULTIPLE SEX CHROMOSOMES.....	88
CAPÍTULO 4.....	98
1. INTRODUCTION	99
2. MATERIAL AND METHODS	101
2.1. SAMPLING	101
2.2. CONVENTIONAL AND MOLECULAR CYTOGENETICS	102
2.3. SEQUENCING AND OBTENTION OF SNPs.....	103
2.4. PRINCIPAL COMPONENT ANALYSIS	104
2.5. SPECIES TREE.....	104

3. RESULTS	104
3.1. <i>CONVENTIONAL AND MOLECULAR CYTOGENETICS</i>	104
3.2. <i>PRINCIPAL COMPONENT ANALYSIS</i>	107
3.3. <i>SPECIES TREE AND NEIGHBOR-NET</i>	107
4. DISCUSSION.....	108
4.1. <i>CHROMOSOMAL FEATURES OF COPELLA CALLOLEPIS</i>	108
4.2. <i>TRENDS IN KARYOTYPE EVOLUTION OF LEBIASINIDAE IN LIGHT OF NEW GENOMIC DATA</i>	110
5. CONSIDERAÇÕES FINAIS	113
6. REFERÊNCIAS BIBLIOGRÁFICAS	115

1. Introdução

1.1. Peixes: diversidade e importância nos estudos evolutivos e genéticos

Os peixes são um grupo parafilético composto por uma riqueza taxonômica notável que explora uma diversidade de hábitos e habitats. Em geral, a maioria dos peixes se encontra nas regiões tropicais e subtropicais, se destacando principalmente na África tropical, no sudeste asiático e na Bacia do Rio Amazonas (Nelson *et al.*, 2016). Embora também seja caracterizada por um clima tropical, a América Central é relativamente pobre em diversidade de peixes, possivelmente em decorrência da sua história geológica (Nelson *et al.*, 2016; Tickner *et al.*, 2020; Albert *et al.*, 2021). Do total de espécies de peixes válidas, mais de 50% habitam ambientes de água doce, sendo assim, uma parcela significativa da diversidade ictiológica está desproporcionalmente distribuída em uma área relativamente pequena quando comparada com a superfície terrestre, já que apenas 1% da água do planeta é doce (Tagliacollo *et al.*, 2021).

Notavelmente, a região Neotropical apresenta o maior número de peixes de água doce, com uma alta proporção de espécies endêmicas (Albert *et al.*, 2020; Tonella *et al.*, 2022). Agrupados em cinco ordens predominantes: Siluriformes (peixes-gato), Characiformes (tetras, piranhas e aliados), Cyprinodontiformes (killifishes, rivulídeos e aliados), Cichliformes (ciclídeos) e Gymnotiformes (peixes elétricos neotropicais) (Van Der Sleen e Albert, 2017; Malabarba e Malabarba, 2020; Dagosta e de Pinna, 2019; Van Der Sleen e Albert, 2021), os peixes dessa região se caracterizam principalmente por sua diversidade e pela abundância de espécies de tamanho diminuto (Castro e Polaz, 2020).

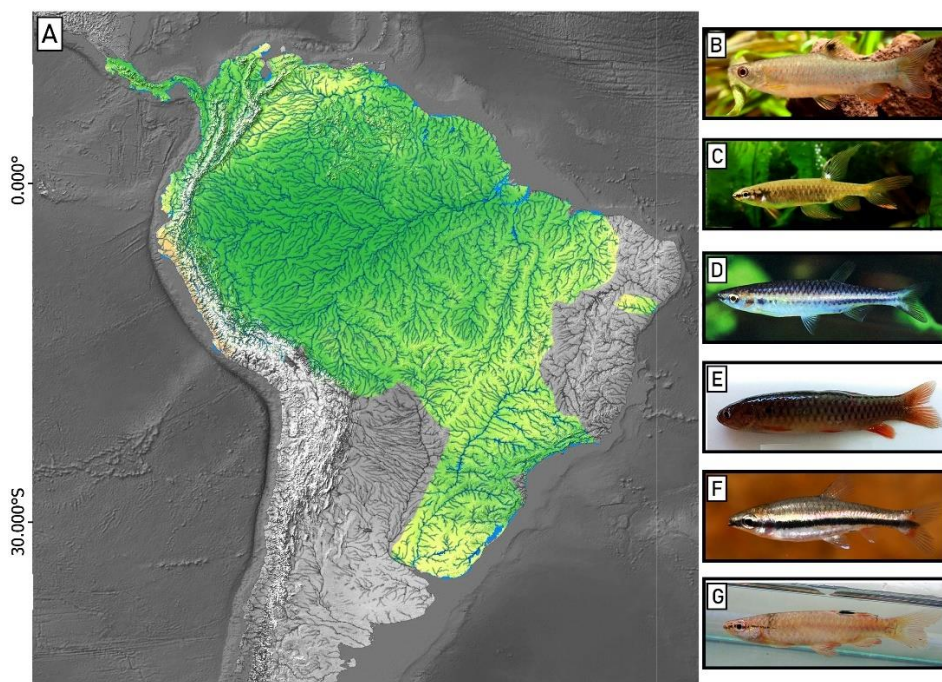
A ordem Characiformes mais especificamente, se destaca por apresentar peixes de baixa tolerância a água salgada e uma notável variação morfológica (Nelson *et al.*, 2016; Betancur-R *et al.*, 2019), o que os torna particularmente atrativos para estudos evolutivos. Por serem exclusivamente de água doce, os peixes dessa ordem podem apresentar relações evolutivas diretamente ligadas com a fragmentação dos continentes e o desenvolvimento de barreiras naturais durante a dispersão para habitats secundários (Betancur-R *et al.*, 2019; Melo *et al.*, 2022). Embora atualmente existam análises morfológicas e moleculares mais aprofundadas dentro da ordem Characiformes, ainda sim as relações filogenéticas são incertas em diversos grupos questionando sua monofilia (Arcila *et al.*, 2017; Dai *et al.*, 2018; Betancur-R *et al.*, 2019; Faircloth *et al.* 2020; Melo *et al.*, 2022).

Por apresentarem uma das primeiras linhagens a diversificar na filogenia dos vertebrados, os peixes são ótimos modelos para estudos genômicos e evolutivos (Shao *et al.*,

2019; Sember *et al.*, 2021), colaborando no esclarecimento da filogenia dos vertebrados como um todo, já que sua grande diversidade possivelmente ocorra por conta de mudanças genômicas rápidas, os diferenciando dos outros grupos (Ravi e Venkatesh, 2018). Uma vez que os peixes são um grupo muito abundante, essas grandes diversidades podem dificultar não só os arranjos taxonômicos desses animais, mas também uma compreensão mais aprofundada de suas relações evolutivas, fazendo com que sejam em boa parte inexplorados (Dornburg e Near, 2021; Parey *et al.*, 2023). Sendo assim, os estudos citogenéticos têm contribuído para o esclarecimento das relações filogenéticas dos peixes através de citogenética clássica e molecular, permitindo um avanço no aprofundamento dos estudos evolutivos nesse grupo tão diverso (Cioffi *et al.*, 2018).

1.1.1. *Família Lebiasinidae, com enfoque no gênero Pyrrhulina*

A família Lebiasinidae apresenta 7 gêneros (*Lebiasina*, *Piabusina*, *Derhamia*, *Nannostomus*, *Pyrrhulina*, *Copella*, *Copeina*) e aproximadamente 75 espécies válidas, endêmicas da região Neotropical, amplamente distribuídas nas Américas do Sul e Central (Costa Rica e Panamá), com exceção do Chile (Netto-Ferreira e Marinho, 2013; Fricke *et al.*, 2024; Froese e Pauly, 2024). Esse grupo é organizado em duas subfamílias: Lebiasininae e Pyrrhulininae (Netto-Ferreira e Marinho, 2013; Froese e Pauly, 2018; Fricke *et al.*, 2024), das quais a segunda representa o clado mais diversificado composto pelos gêneros *Nannostomus*, *Copeína*, *Copella* e *Pyrrhulina* (Netto-Ferreira e Marinho, 2013). De modo geral, a família é representada em maior quantidade por peixes de porte pequeno que variam de 1,5 a 7,0 cm de comprimento e apresentam grandes variações de formatos corporais e coloração, o que os tornam particularmente atrativos para a aquarofilia (Weitzman e Vari, 1988; Weitzman e Weitzman, 2003).



56

57 **Figura 1:** A) Mapa parcial da América do Sul, destacando em cores a distribuição de Lebiasinidae de
 58 acordo com GBIF (2024). B-G representantes dos gêneros *Copeina*, *Copella*, *Derhamia*, *Lebiasina*,
 59 *Nannostomus* e *Pyrrhulina*, respectivamente. *Copeina guttata* - <https://www.seriouslyfish.com/species/copeina-guttata>;
 60 *Copella arnoldi* - foto por Zikamoi - Inaturalist - <https://www.inaturalist.org/photos/76418963>;
 61 *Derhamia hoffmannorum* - <https://lifecatalog.ru/cont/1/le/Lebiasinidae.html>; *Lebiasina melanoguttata* - foto por Ezequiel A. de Oliveira;
 62 *Nannostomus beckfordi* - foto por Chen Hung-Jou - Inaturalist - <https://www.inaturalist.org/photos/923588> e
 63 *Pyrrhulina obermulleri* - foto por Francisco C.M. Sassi.
 64

65 Por muito tempo as relações filogenéticas da família Lebiasinidae eram incertas, sendo
 66 considerados grupo-irmão de diferentes grupos de peixes Neotropicais ao longo dos anos.
 67 Inicialmente, em decorrência de seus caracteres morfológicos a família Lebiasinidae era
 68 relacionada com Erythrinidae, Ctenoluciidae e Hepsetidae (Oyakawa, 1998; Buckup, 1998).
 69 Posteriormente, através de análises filogenéticas moleculares tal grupo foi considerado grupo
 70 irmão de Serrasalminidae, assim como Erythrinidae de Hepsetidae (Orti e Meyer, 1997). Anos
 71 mais tarde, diferentes estudos moleculares sugeriram uma relação entre Lebiasinidae e
 72 Ctenoluciidae (Calcagnotto *et al.*, 2005; Oliveira *et al.*, 2011), dados estes que foram
 73 corroborados por estudos moleculares posteriores (Arcila *et al.*, 2017; Betancur-R *et al.*, 2018;
 74 Melo *et al.*, 2022).

75 Em particular, o gênero *Pyrrhulina* é o mais especioso da subfamília Pyrrhulininae
 76 (junto com *Nannostomus*) sendo composto por 19 espécies válidas (Fricke *et al.*, 2024). Esse
 77 gênero está distribuído particularmente nas bacias Amazônica e Araguaia-Tocantins, bem
 78 como na rede hidrográfica Paraguai-Paraná-La Plata, e nos sistemas Laguna dos Patos e Rio
 79 Tramandaí no sul da América do Sul (Weitzman e Weitzman, 2003; Venere e Garutti, 2011;
 80 Bertaco *et al.*, 2016; Dagosta e de Pinna, 2019). Considerado o mais derivado da família,

81 *Pyrrhulina* abriga a maioria das incertezas taxonômicas atuais dentro dos Lebiasinidae (Netto-
82 Ferreira e Marinho, 2013), incluindo uma série de inconsistências nas descrições e diagnósticos
83 das espécies deste grupo (Gery, 1977), que são difíceis de distinguir com base em suas caracte-
84 rísticas morfológicas (Souza *et al.*, 2023). Por conta da variedade de espécies e suas caracte-
85 rísticas individuais, o gênero ainda apresenta sua taxonomia confusa, mesmo depois de análises
86 taxonômicas e moleculares recentes (Weitzman e Weitzman, 2003; Netto-Ferreira e Marinho,
87 2013; Souza *et al.*, 2023).

88 **1.1.2. Estudos citogenéticos em *Pyrrhulina***

89 Por conta do tamanho diminuto, a família Lebiasinidae por muito tempo foi pouco ex-
90 plorada citogeneticamente, possivelmente por conta das dificuldades de se obter boas prepara-
91 ções cromossômicas. Assim, os primeiros dados sobre a família se restringiam basicamente em
92 referências ao número cromossômico haploide e diploide em algumas poucas espécies (Scheel,
93 1973; Arai, 2011), ou a descrição do cariótipo de uma única espécie da família, *Pyrrhulina* cf.
94 *australis* (Oliveira *et al.*, 1991). Anos mais tarde, foram analisadas por técnicas de citogenética
95 mais avançadas duas espécies do gênero *Pyrrhulina* (*Pyrrhulina* aff. *australis* e *P. australis*)
96 que deram um salto aos estudos citogenéticos da família. Os resultados de tais análises eviden-
97 ciaram $2n=40$ (4st+36a) sem a presença de cromossomos sexuais morfológicamente diferen-
98 ciados em ambas as espécies (Moraes *et al.*, 2017). Um acúmulo de heterocromatina C-positiva
99 foi observado principalmente nas regiões centroméricas e teloméricas da maioria dos cromos-
100 somos de ambas as espécies, além disso foram evidenciadas bandas intersticiais presentes em
101 *Pyrrhulina* aff. *australis* e ausentes em *P. australis* (Moraes *et al.*, 2017). Os mapeamentos de
102 DNAs repetitivos, hibridização genômica comparativa (CGH) e pintura total cromossômica
103 (WCP) determinaram o número, a posição relativa dos DNAr 18S e 5S, e diversas particulari-
104 dades e divergências entre as espécies (Moraes *et al.*, 2017). Tais experimentos mostraram
105 ainda que embora essas espécies apresentem diferenças, ambas compartilham muitas caracte-
106 rísticas, corroborando sua proximidade taxonômica (Moraes *et al.*, 2017). Apesar das especifi-
107 cidades inerentes a cada grupo, algumas correlações quanto à estrutura cariotípica e distribui-
108 ção de classes de DNAs repetitivos foram evidenciadas entre *Pyrrhulina* e *Erythrinus erythri-*
109 *nus* (Erythrinidae) sugerindo na época uma proximidade entre os grupos (Moraes *et al.*, 2017).

110 Embora fosse um grupo desafiante em quesitos citogenéticos, os estudos dentro do
111 gênero continuaram e contribuíram significativamente para a compreensão da evolução
112 cariotípica do grupo. Mais duas espécies (*Pyrrhulina brevis* e *Pyrrhulina semifasciata*) foram

113 analisadas por diferentes técnicas citogenéticas e moleculares nos anos seguintes, trazendo
114 como principais resultados um cenário que condiz com o anteriormente observado. *P. brevis*
115 evidenciou um $2n=42$ para ambos os sexos sem diferenciação sexual. Assim como observado
116 em *Pyrrhulina* aff. *australis*, *P. brevis* apresentou acúmulo de heterocromatina C-positiva não
117 apenas nas regiões pericentroméricas como também nas regiões intersticiais o que a diferencia
118 das outras espécies até então estudadas (Moraes *et al.*, 2019). *P. semifasciata* por sua vez
119 apresentou um cariótipo com $2n=42$ para fêmeas e $2n=41$ para machos com a presença de três
120 cromossomos não pareados ($1m+2a$) sugerindo a formação de um sistema sexual múltiplo
121 X_1X_2Y , originado por fusão cêntrica, que se destaca por ser o único sistema sexual
122 heteromórfico evidente dentro da família (Moraes *et al.*, 2019).

123 Para compreender melhor as relações entre as espécies estudadas e a possível origem
124 do sistema sexual evidenciado em *P. semifasciata*, foram utilizadas ferramentas robustas como
125 hibridização genômica comparativa (CGH) e pintura total cromossômica (WCP). Assim, a
126 presença do sistema sexual múltiplo observado em *P. semifasciata* foi confirmada por
127 experimentos de WCP, os quais evidenciaram três cromossomos ($1m+2a$) não pareados e
128 totalmente marcado nos machos da espécie e dois pares de cromossomos totalmente marcados
129 tanto nas fêmeas da espécie como em outras espécies do gênero sugerindo que formação do
130 cromossomo neo-Y desse sistema fosse a fusão de dois cromossomos acrocêntricos não
131 homólogos (Moraes *et al.*, 2019). Além disso, com os experimentos intraespecíficos de CGH
132 foi possível observar sequências sexo específicas localizadas principalmente no cromossomo
133 metacêntrico de *P. semifasciata* macho (cromossomo neo-Y) dado esse que corrobora com a
134 presença de um sistema sexual múltiplo X_1X_2Y na espécie. Já os experimentos interespecíficos
135 feitos entre *P. brevis* e *P. semifasciata* produziram uma gama de sinais espécie específicos não
136 sobrepostos, sendo essa uma consequência de suas histórias evolutivas específicas (Moraes *et*
137 *al.*, 2019).

138 Portanto, em um contexto geral foi possível observar que embora as espécies de
139 *Pyrrhulina* compartilhem uma gama de características cariotípicas e genômicas como: i) um
140 $2n$ conservado variando entre 40-42 cromossomos; ii) acúmulo de heterocromatina C-positiva
141 principalmente nas regiões pericentroméricas/ centroméricas e teloméricas; iii) múltiplos sítios
142 de DNAr 18S e 5S; iiiii) cariótipos marcados majoritariamente por cromossomos acrocêntricos
143 (Moraes *et al.*, 2017; Moraes *et al.*, 2019), tais espécies também evidenciam características
144 particulares que as diferenciam entre si, identificando diferentes processos evolutivos entre elas
145 (Moraes *et al.*, 2017; Moraes *et al.*, 2019)

146 1.2. Marcadores citogenéticos

147 Os marcadores cromossômicos têm se mostrado como ferramentas cruciais na
148 caracterização da biodiversidade, principalmente de peixes (Moreira-Filho e Bertollo, 1991;
149 Bertollo *et al.*, 2000; Cioffi *et al.*, 2012). Os primeiros bandamentos cromossômicos
150 permitiram a comparação de bandas para o pareamento correto dos cromossomos homólogos
151 (Guerra, 1988), entretanto a citogenética molecular sofreu grandes aperfeiçoamentos ao longo
152 dos anos permitindo, em conjunto com a citogenética clássica, análises evolutivas mais robusta.
153 A seguir foram selecionadas algumas abordagens que vêm sendo utilizadas em análises
154 evolutivas de peixes.

155 Descrito pela primeira vez por Sumner (1972) o bandamento C se originou com o objetivo
156 de identificar regiões ricas em heterocromatina constitutiva. Tais regiões são comumente
157 encontradas nas regiões pericentroméricas e teloméricas dos cromossomos e se caracterizam
158 por serem compostas por diversas sequências de DNA repetitivo (Charlesworth, 1994; Plohl *et*
159 *al.*, 2008; López-Flores e Garrido-Ramos, 2012). Em espécies de peixes a distribuição de
160 heterocromatina constitutiva pode auxiliar na diferenciação de espécies, na identificação de
161 cromossomos acessórios ou até mesmo na evidência de sistemas cromossômicos sexuais
162 (Galetti Jr. *et al.*, 1991; Margarido e Galletti Jr., 1999; Margarido e Galetti Jr., 2000; Bertollo *et*
163 *al.*, 1997; Rocha-Reis *et al.*, 2018).

164 Proposta por Howell e Black (1980) a detecção das regiões organizadoras de nucléolos
165 (NORs) também é considerada uma ferramenta primordial. Tal técnica consiste na
166 impregnação de Nitrato de Prata nos cromossomos (Ag-86 NOR) com o objetivo de identificar
167 famílias de DNA ribossomal (DNAr), dado que as NORs são compostas por DNAr 45S e
168 proteínas acessórios. É digno de nota que os DNAr dão origem aos ribossomos e participam
169 ativamente na síntese proteica. De modo geral são divididos em duas famílias multigênicas:
170 DNAr 45S e DNAr 5S. No segmento DNAr 45S estão codificados os DNAs ribossomais 28S,
171 5,8S e 18S que se encontram separados por dois espaçadores internos transcritos (ITS1 e ITS2),
172 dois espaçadores externos transcritos (ETS1 e ETS2) e apenas um espaçador não transcrito
173 (NTS). Por sua vez, DNAr 5S é organizado por uma série de repetições, separadas por NTS ou
174 também podem ser encontrados na forma de pseudogenes dispersos nos cromossomos
175 (Lafontaine e Tollervey, 2001).

176 Entretanto, com o avanço da citogenética molecular foi possível investigar com mais pro-
177 priedade a real posição dos genes ribossomais, assim como o seu número de sítios. A partir do
178 surgimento das técnicas de hibridização fluorescente *in situ* (FISH) e do aperfeiçoamento das

179 sondas de DNAr, o mapeamento desses genes se revelou uma das principais opções na caracte-
180 rização de biodiversidade e estudos de sistemática (Sochorová *et al.*, 2018). É importante
181 ressaltar que apesar da sua alta conservação, as sequências ribossomais tendem a mudar em
182 número de sítios e sua posição nos cromossomos o que as torna *sequências* extremamente atra-
183 entes em estudos evolutivos (Roy *et al.*, 2005; McTaggart *et al.*, 2007; Wang e Lemos, 2017;
184 Sochorová *et al.*, 2018; Glugoski *et al.*, 2020; Sassi *et al.*, 2021).

185 Sequências como microssatélites também tem se demonstrado ótimas ferramentas em estu-
186 dos evolutivos. Tais *sequências* podem ser encontradas em todos os eucariotos (López- Flores
187 e Garrido Ramos, 2012; Cioffi e Bertollo, 2012) e se caracterizam por serem pequenas repeti-
188 ções em tandem que podem apresentar até seis nucleotídeos. Interessantemente, essas unidades
189 podem se agrupar formando longas sequências que podem se associar a diferentes regiões cro-
190 mossômicas incluindo regiões heterocromáticas (Martins, 2007; Cioffi *et al.*, 2011; Haerter *et*
191 *al.*, 2023). Especificamente em peixes, é muito comum observarmos essas *sequências* princi-
192 palmente em regiões centroméricas e teloméricas, e até mesmo em cromossomos sexuais (Ci-
193 offi e Bertollo, 2012; Schemberger *et al.*, 2019; Balini *et al.*, 2024).

194 Por fim, mas não menos importante temos as *sequências* teloméricas, que se destacam
195 principalmente por conter importantes informações sobre a evolução cromossômica (Merlo *et*
196 *al.*, 2007; Wang *et al.*, 2009). Ricas em guanina (TTAGGG)_n, as *sequências* teloméricas de-
197 sempenham papéis fundamentais na sobrevivência dos organismos estabilizando os cromosso-
198 mos e permitindo a replicação completa das suas regiões terminais (Blackburn, 1994). Embora
199 essas sequências se encontrem majoritariamente nas regiões terminais dos cromossomos, em
200 diferentes cenários elas podem ser detectadas em regiões intersticiais (sítios teloméricos inters-
201 ticiais (ITS) tendo como função principal identificar possíveis processos de fusão cromossô-
202 mica (Sola *et al.*, 2003; Cioffi *et al.*, 2010; Blanco *et al.*, 2012; Ocalewicz, 2013; Moraes *et al.*,
203 2022).

204 Dentre as ferramentas utilizadas na citogenética molecular temos a hibridização genômica
205 comparativa (CGH) e a Pintura total cromossômica (WCP). A técnica de CGH consiste na
206 utilização de sondas de genomas inteiros que possibilitam a comparação de regiões comparti-
207 lhadas entre sexos ou espécies, identificação de ganho ou perda de sequências de DNA entre
208 as espécies analisadas, bem como a variação do número de cópias de uma sequência genômica
209 específica. Entre os peixes tal procedimento vem se destacando cada vez mais, conforme ob-
210 servado na quantidade de trabalhos publicados nos últimos anos utilizando a abordagem (Oli-
211 veira e Sember *et al.*, 2017; Freitas *et al.*, 2017; Moraes *et al.*, 2019; Sassi *et al.*, 2020),

212 certamente CGH mostrando-se uma ferramenta valiosa na identificação de homologies entre
213 sistemas de cromossomos sexuais, bem como para estudos evolutivos como um todo.

214 Incrementando ainda mais os estudos citogenéticos os experimentos de pintura total cro-
215 mossômica (WCP) surgiram com um enfoque predominantemente clínico (Blough *et al.*,
216 1998), sendo posteriormente utilizados em estudos evolutivos envolvendo diferentes espécies
217 animais (Yang *et al.*, 2009). Aqui utilizamos sondas de cromossomos inteiros ou até mesmo de
218 segmentos cromossômicos, que são obtidos através de microdissecção ou citometria de fluxo,
219 seguido pela amplificação por primers degenerados (DOP-PCR) (Yang *et al.*, 2009). Os estu-
220 dos em peixes especificamente se iniciaram em 2010, permitindo estudos principalmente sobre
221 a origem e evolução de sistemas sexuais e autossomos em diferentes espécies (Oliveira e Sem-
222 ber *et al.*, 2017; Freitas *et al.*, 2017; Barby *et al.*, 2019; Sassi *et al.*, 2020; Yano *et al.*, 2021)

223

224 **1.2.1 Sequências de DNAs satélite e o estudo do Satelitoma**

225

226 DNAs satélites (satDNAs) são sequências repetidas em tandem não codificantes, com
227 comprimento de unidade, número de cópias e organização cromossômica variáveis (Tautz,
228 1993; Richard *et al.*, 2008; Garrido-Ramos, 2017). Os satDNAs são uma das *sequências* mais
229 abundantes da maioria dos genomas, constituindo longas matrizes localizadas principalmente
230 em regiões heterocromáticas centroméricas e teloméricas, além de já terem sido relatadas mais
231 de uma vez em regiões eucromáticas (Kuhn *et al.*, 2012; Plohl *et al.*, 2012; Brajković *et al.*,
232 2012; Pavlek *et al.*, 2015; Garrido-Ramos *et al.*, 2017; Šatović-Vukšić e Plohl, 2023).

233 Com a integração da citogenética e os sequenciamentos de próxima geração (NGS), as
234 coleções de diferentes famílias de satDNAs de diversas espécies foram caracterizadas,
235 fornecendo insights sobre diversas questões evolutivas, como evolução cariotípica, diversidade
236 do genoma e relações filogenéticas (Montiel *et al.*, 2021; Ruiz-Ruano *et al.*, 2016; Flynn *et al.*,
237 2023; Ferretti *et al.*, 2020; Bardella *et al.*, 2020; Vozdova *et al.*, 2021; Cabral-de-Mello *et al.*,
238 2021; Cabral-de-Mello *et al.*, 2023; Gržan *et al.*, 2023; Peona *et al.*, 2023). Em geral, grupos
239 de espécies relacionadas compartilham diversas famílias de satDNAs que geralmente evoluem
240 de forma independente dentro de cada linhagem, de acordo com a chamada hipótese de
241 biblioteca (Fry e Salser, 1977). Embora por muito tempo tenha sido caracterizado como DNA
242 “lixo”, estudos recentes evidenciaram que os satDNAs apresentam importantes papéis na
243 regulação de genes e genomas (revisado em Garrido-Ramos, 2017).

244 Acredita-se que sequências repetitivas são ótimas ferramentas para estudos da evolução
245 dos cromossomos sexuais, onde é comum observar um acúmulo diferencial significativo dessas
246 sequências entre machos e fêmeas, além de enfatizar a existência de vários satDNAs W/Y-

247 específicos (Flynn *et al.*, 2023; Ferretti *et al.*, 2020; Cabral-de-Mello *et al.*, 2023). Supõem-se
248 ainda que tais *sequências* desempenham papéis essenciais na evolução e organização de
249 cromossomos sexuais e na especiação cromossômica (Henikoff *et al.*, 2001; O'Neill *et al.*,
250 2004; Plohl *et al.*, 2012; Weissensteiner e Suh, 2019; Utsunomia *et al.*, 2019; Shatskikh *et al.*,
251 2020; Ferretti *et al.*, 2020; Flynn *et al.*, 2023), além de induzirem rearranjos cromossômicos,
252 impactando diretamente na evolução do cariótipo (Silva *et al.*, 2017; Utsunomia *et al.*, 2019;
253 Crepaldi *et al.*, 2021). Assim, a ocorrência de fusões e fissões cêntricas podem estar
254 frequentemente associadas a satDNAs que se encontram principalmente em regiões
255 centroméricas e pericentroméricas (Kopečna *et al.*, 2014; Vozdova *et al.*, 2019).

256 Embora os satDNAs tenham sido relacionados a diversas funções dentro do genoma,
257 ainda sim seu papel na evolução genômica e cariotípica é incipiente, necessitando de mais
258 investigações (Silva *et al.*, 2017; Utsunomia *et al.*, 2019; Crepaldi *et al.*, 2021).

259 **1.3. Citogenética Evolutiva em Lebiasinidae**

260 A família Lebiasinidae é um grupo desafiador. Por conter representantes de tamanhos
261 muito pequenos, o grupo apresenta grandes dificuldades de ser explorado tanto taxonomica-
262 mente como molecularmente. Entretanto, tal cenário vem sofrendo mudanças significativas
263 ao longo dos anos através de análises citogenéticas clássicas e moleculares em diferentes gê-
264 neros da família (Moraes *et al.*, 2017; Moraes *et al.*, 2019; Sassi *et al.*, 2019; Toma *et al.*,
265 2019; Sassi *et al.*, 2020; Sember *et al.*, 2020; Leite *et al.*, 2022; Moraes *et al.*, 2023a). Até
266 então, as análises mais específicas da família se resumiam com referências ao número cro-
267 mossômico haploide e diploide em algumas poucas espécies (Scheel, 1973; Arai, 2011), ou
268 com a descrição do cariótipo em uma única espécie da família, *Pyrrhulina* cf. *australis* (Oli-
269 veira *et al.*, 1991).

270 As primeiras análises citogenéticas mais aprofundadas em Lebiasinidae se deram durante
271 a Iniciação científica da presente aluna, na qual foram analisadas por citogenética clássica e
272 molecular quatro espécies do gênero *Pyrrhulina* (*Pyrrhulina* aff. *australis*, *Pyrrhulina* *aus-*
273 *tralis*, *Pyrrhulina* *brevis* e *Pyrrhulina* *semifasciata*) (Moraes *et al.*, 2017; Moraes *et al.*, 2019).
274 Posterior a esse cenário, outros trabalhos envolvendo os outros gêneros do grupo sofreram
275 destaque (Sassi *et al.*, 2019; Toma *et al.*, 2019; Sassi *et al.*, 2020; Sember *et al.*, 2020; Leite
276 *et al.*, 2022), contribuindo impreterivelmente para uma melhor compreensão da evolução ca-
277 riotípica e filogenética da família.

278 Mesmo antes com a escassez de dados, já era possível observar uma variação do número
279 diploide entre os Lebiasinideos, variando de $2n=22$ em *Nannostomus unifasciatus* a $2n=46$ em
280 *Nannostomus trifasciatus* (revisado em Oliveira *et al.*, 2007 e Arai, 2011). Com os avanços da
281 citogenética clássica juntamente com a molecular foi possível dar uma nova perspectiva aos
282 desafios enfrentados ao estudar o grupo, sendo possível contribuir com novos dados citogené-
283 ticos e moleculares. No total, 13 espécies de Lebiasinidae foram analisadas por estudos citoge-
284 néticos mais aprofundados, sendo três espécies de *Lebiasina* (*L. melanoguttata*, *L. bimaculata*
285 e *L. minuta*), uma de *Copeina* (*C. gutatta*), cinco de *Nannostomus* (*N. breckfordi*, *N. eques*, *N.*
286 *marginatus*, *N. unifasciatus* e *N. anduzei*) e quatro de *Pyrrhulina* (*Pyrrhulina* aff. *australis*, *P.*
287 *australis*, *P. brevis* e *P. semifasciata*). Tais estudos, além de corroborar com dados já existentes
288 contribuíram com dados inéditos sobre a família, possibilitando uma visão mais robusta sobre
289 as relações filogenéticas do grupo (Moraes *et al.*, 2017; Moraes *et al.*, 2019; Sassi *et al.*, 2019;
290 Toma *et al.*, 2019; Sember *et al.*, 2020; Leite *et al.*, 2022; Moraes *et al.*, 2023a).

291 Dentre os gêneros que compõem a família, *Lebiasina* é considerado o gênero basal, sendo
292 representado por um cariótipo conservado com $2n=36$ composto por cromossomos de dois bra-
293 ços (Sassi *et al.*, 2019; Leite *et al.*, 2022). Por sua vez os outros representantes da família apre-
294 sentam grandes variações na estrutura cariotípica e no $2n$, variando de 22 a 46 cromossomos.
295 *Copeina* por exemplo evidenciou um $2n=42$ ($2m + 4sm + 36\ st-a$) com um cariótipo majorita-
296 riamente acrocêntrico, reforçando a tendência evolutiva divergente entre as espécies de Lebia-
297 sinidae (Toma *et al.*, 2019). Já *Nannostomus* e *Pyrrhulina* são os dois grupos mais especiosos
298 da família, apresentando diferentes variações de $2n$ e estrutura cariotípica. Assim como as ou-
299 tras espécies do grupo, *Nannostomus* e *Pyrrhulina* apresentam em sua maioria cariótipos ma-
300 joritariamente acrocêntricos ou até mesmo exclusivamente acrocêntricos como é o caso de *N.*
301 *beckfordi* e *N. eques* (Moraes *et al.*, 2017; Moraes *et al.*, 2019; Sember *et al.*, 2020; Moraes *et*
302 *al.*, 2023a).

303 Embora de modo geral as espécies apresentem cariótipos relativamente conservados, al-
304 gumas espécies se destacam por se diferenciarem do grupo. *N. anduzei* e *N. unifasciatus*, por
305 exemplo, são as espécies que apresentam os menores números diploides já documentados para
306 peixes teleósteos ($2n=22$) (Arai, 2011), com cariótipo composto exclusivamente por grandes
307 cromossomos metacêntricos originados por possíveis fusões cêntricas (Sember *et al.*, 2020;
308 Moraes *et al.*, 2023a), cenário esse diferente ao observado para as outras espécies do gênero.
309 *P. semifasciata* por sua vez também se destaca entre as espécies do gênero apresentando o
310 único sistema sexual heteromórfico documentado na família até o presente momento (Moraes
311 *et al.*, 2019).

312 Embora os estudos em Lebiasinidae tenham apresentado grandes avanços, ainda sim as
313 relações filogenéticas dentro do grupo se apresentam incertas. Ao longo dos anos duas tendên-
314 cias evolutivas foram sugeridas, sendo i) um cariótipo conservado com $2n=36$ composto ex-
315 clusivamente por cromossomos meta/submetacêntricos representando a condição basal do
316 grupo, como visto em *Lebiasina*; e ii) um cariótipo com $2n$ mais elevado, rearranjos cromos-
317 sômicos estruturais e um cariótipo majoritariamente acrocêntrico (Sassi *et al.*, 2020). Sendo
318 assim, teríamos a subfamília Lebiasininae composta por *Lebiasina* e *Dehamia*, e Pyrrhulinae
319 composta por *Copeina*, *Copella*, *Nannostomus* e *Pyrrhulina*. Embora tais tendências tenham
320 sido reafirmadas mais de uma vez em diferentes estudos, e os dados citogenéticos e taxonômi-
321 cos até então relatados corroborem com essas tendências, estudos moleculares recentes propu-
322 seram algumas mudanças nesse cenário, tais como a inclusão de *Nannostomus* dentro de Lebi-
323 asininae (Casimiro *et al.*, 2023). Mesmo com o conjunto de todos esses dados ainda sim fica
324 evidente a necessidade de maiores estudos envolvendo principalmente as relações internas da
325 família, bem como a inclusão de estudo citogenéticos envolvendo *Dehamia* e *Copella* dados
326 esses ausentes até o presente momento.

327 Em suma, mesmo com todas as dificuldades e desafios encontrados ao trabalhar com a
328 família Lebiasinidae, recentes estudos vem conseguindo superar boa parte das dificuldades e
329 contribuir significativamente com dados citogenéticos e moleculares que auxiliaram no escla-
330 recimento de diversas dúvidas sobre as relações internas do grupo. Adicionalmente, é evidente
331 que a combinação de mais estudos moleculares, morfológicos e cromossômicos são muito bem-
332 vindos para superar as incertezas ainda existentes no grupo, bem como novas filogenias com
333 maiores números amostrais objetivando o esclarecimento das relações filogenéticas ainda in-
334 certas.

335

336 2. Objetivos

337 2.1. *Objetivo geral*

338 Avançar com os conhecimentos sobre a família Lebiasinidae, dando enfoque no gênero
339 *Pyrrhulina*, tendo em vista analisar as relações cromossômicas intragenérica e intrafamiliar,
340 possibilitando assim abordagens comparativas importantes do ponto de vista evolutivo.

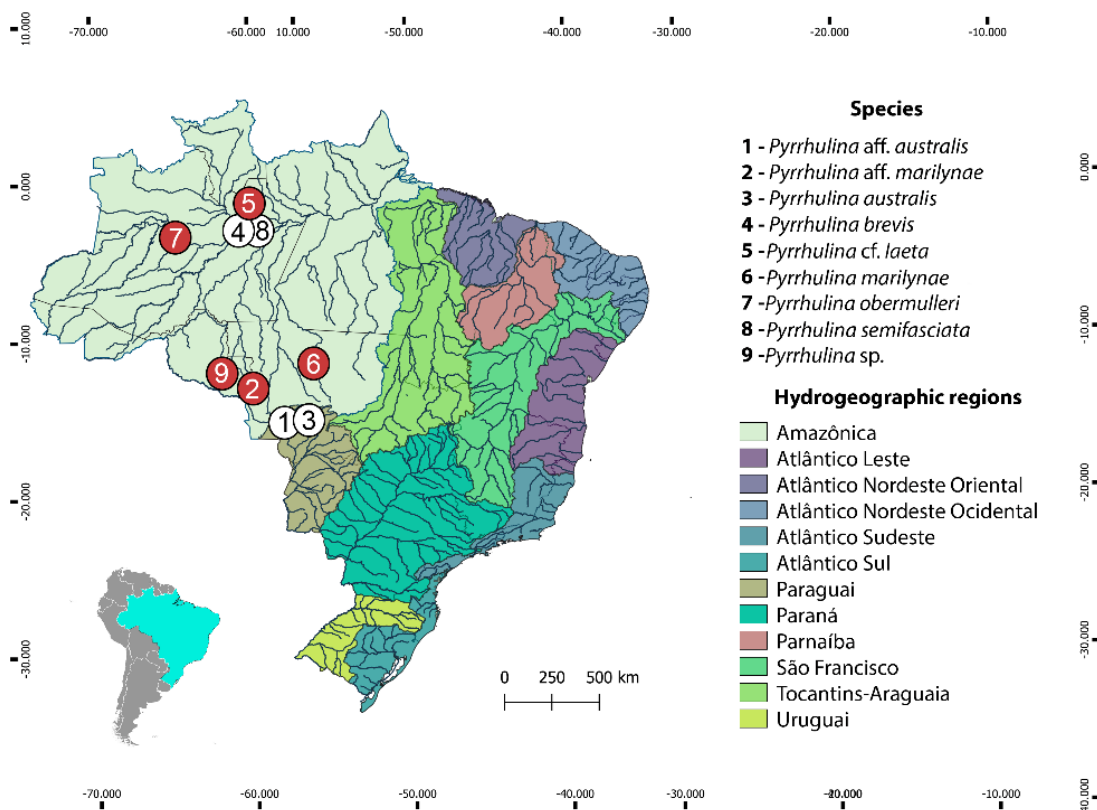
341 2.2. *Objetivos específicos*

- 342 1) Caracterizar o cariótipo de machos e fêmeas de cinco espécies de *Pyrrhulina* (*Pyrrhu-*
343 *lina* aff. *marilynae*, *Pyrrhulina* cf. *laeta*, *Pyrrhulina marilynae*, *Pyrrhulina obermul-*
344 *leri* e *Pyrrhulina* sp.) quanto ao número e morfologia cromossômica, assim como a
345 distribuição de heterocromatina C-positiva.
- 346 2) Investigar a distribuição e número de sítios de sequências de DNA repetitivo através
347 do mapeamento dos DNAs ribossomais 5S e 18S e sequências de microssatélites.
- 348 3) Avaliar o compartilhamento de frações do genoma entre todas as espécies de *Pyrrhu-*
349 *lina* analisadas citogeneticamente até o momento através da hibridização genômica
350 comparativa (CGH).
- 351 4) Identificar por experimentos de pintura total cromossômica (WCP) utilizando sondas
352 do cromossomo neo-Y (cromossomo Y de *Pyrrhulina semifasciata*) os possíveis cro-
353 mossomos sexuais putativos nas demais espécies de *Pyrrhulina* não portadoras de cro-
354 mossomos sexuais heteromórficos, visando auxiliar na compreensão da possível ori-
355 gem do sistema sexual múltiplo X_1X_2Y de *P. semifasciata*.
- 356 5) Analisar o papel dos rearranjos cromossômicos e a presença do sistema sexual na di-
357 ferenciação das espécies de *Pyrrhulina*.
- 358 6) Compreender a evolução e as tendências evolutivas em Lebiasinidae, através de aná-
359 lises filogenéticas da família baseada em dados moleculares.

360 3. Materiais e Métodos

361 3.1. Material

362 Para a realização desse trabalho foram amostradas nove espécies de peixes do gênero
363 *Pyrrhulina* localizadas principalmente na Bacia Amazônica. Os locais de coleta, número e sexo
364 dos espécimes investigados são apresentados na **Figura 1** e **Tabela 1**. Os animais foram
365 coletados com autorização do órgão ambiental brasileiro ICMBIO/SISBIO (licença n°48628-
366 14) e SISGEN (A96FF09). Todas as espécies foram devidamente identificadas por critérios
367 morfológicos pela Dra. Manoela Maria Ferreira Marinho e os exemplares depositados na
368 coleção de peixes do Museu de Zoologia da Universidade de São Paulo (MZUSP) sob os
369 números de comprovante (119077, 119079, 123073,123080) e da Universidade Federal da
370 Paraíba (UFPR) sob o número de voucher (12079, 12080, 12082, 12083). Todos os
371 experimentos seguiram condutas éticas e anestésicas, e foram aprovados pelo comitê de Ética
372 em Experimentação animal da Universidade Federal de São Carlos (processo número CEUA
373 1853260315)



374 **Figura 2:** Locais de coleta no Brasil das espécies de *Pyrrhulina* investigadas citogeneticamente em
375 Moraes *et al.* (2021) (círculos vermelhos) e as anteriormente analisadas citogeneticamente (círculos
376 brancos: dados de (Moraes *et al.*, 2017; Moraes *et al.*, 2019)

377 **Tabela 1** - Coordenadas geográficas e número amostral das espécies de *Pyrrhulina*
 378 (Characiformes, Lebiasinidae) coletadas no Brasil

Espécies	Localização	Número Amostrai
<i>Pyrrhulina</i> aff. <i>australis</i>	Rio Sepotuba, Lambari D'Oeste – MT (15°11'28.0"S 57°41'30.7"W)	16♂ 22♀
<i>Pyrrhulina</i> aff. <i>marilynae</i>	Igarapé 12 de Outubro, Comodoro – MT (12°58'41.0"S 60°00'34.0"W)	14♂ 10♀
<i>P. australis</i>	Barra do Bugres – MT (15°04'27.5"S 57°11'05.4"W)	18♂ 30♀
<i>P. brevis</i>	Reserva Florestal Adolpho Ducke, Manaus – AM (2°58'20.7"S 59°55'53.0"W)	17♂ 13♀
<i>Pyrrhulina</i> cf. <i>laeta</i>	Presidente Figueiredo – AM (1°59'10.8"S 60°03'40.8"W)	07♂ 05♀
<i>P. marilynae</i>	Ipiranga do Norte – MT (11°36'02.0"S 55°56'27.0"W)	14♂ 08♀
<i>P. obermulleri</i>	Tefé – AM (3°25'50.7"S 64°44'54.8"W)	21♂ 12♀
<i>P. semifasciata</i>	Careiro – AM (3°51'00.0"S 60°04'00.0"W)	12♂ 09♀
<i>Pyrrhulina</i> sp.	Represa, Alto Alegre dos Parecis – RO (12°11'58.0"S 61°46'47.7"W)	19♂ 29♀

379 **3.2. Métodos**

380 **3.2.1. Obtenção de cromossomos mitóticos**

381 Os cromossomos mitóticos foram obtidos de acordo com Bertollo *et al.* (2015). Todos
 382 os animais aqui coletados foram previamente submetidos a um tratamento com Colchicina (1
 383 ml de solução a 0,005%/100 gramas de peso), e mantidos em aquário aerado por um período
 384 de 45 minutos. Após procedimentos anestésicos, foram extraídos fragmentos do rim anterior,
 385 posterior e das guelras, que foram transferidos para uma cubeta contendo 10ml de solução
 386 hipotônica de cloreto de Potássio (KCl) 0,075M. Com o auxílio de uma seringa desprovida de
 387 agulha os tecidos foram dissociados com leves movimentos até se obter uma solução
 388 homogênea. Tal suspensão foi mantida em estufa a 37 °C durante 30min. Em seguida, toda a
 389 suspensão foi transferida para um tubo de centrifuga com auxílio de uma pipeta Pasteur de
 390 vidro, onde foi feito o processo de pré-fixação pingando dez gotas de fixador (proporção 3:1
 391 de álcool metílico e ácido acético) e deixando a temperatura ambiente por 15min.
 392 Posteriormente a solução foi colocada em uma centrifuga a 1000 rpm por 10min, foi feito o
 393 descarte do sobrenadante e o conteúdo celular foi ressuspendido em 10ml de fixador e
 394 centrifugado novamente nas mesmas condições por mais duas vezes. Na última centrifugação,
 395 o sobrenadante foi removido e descartado e cerca de 1,5 ml de fixador foi adicionado, na qual

396 a solução final foi transferida para um microtubo e armazenada a -20°C. Todos os
397 procedimentos seguiram as condutas éticas e de anestesia aprovadas pelo Comitê de Ética em
398 Experimentação e Uso Animal da Universidade Federal de São Carlos (Processo CEUA
399 7994170423)

400

401 **3.2.1.1. Preparação das lâminas**

402 Foram pingadas duas gotas de 10ul da suspensão celular sobre lâminas limpas e
403 aquecidas a 55°C. As lâminas foram secas ao ar e em seguida os cromossomos foram corados
404 com Giemsa 5% (pH 6.8) por 8 minutos. O excesso de corante foi removido e as lâminas
405 lavadas em água corrente. Após a análise em microscópio de campo claro e a marcação em
406 lâmina branca das melhores metáfases, o excesso de óleo de imersão foi retirado com álcool
407 100% e as lâminas descoradas em solução de fixador (proporção 3:1 de álcool metílico e ácido
408 acético) por 15 minutos em temperatura ambiente. Em seguida as lâminas foram lavadas em
409 água corrente e deixadas para secar em temperatura ambiente.

410 **3.2.2. Detecção de heterocromatina constitutiva**

411 Para a detecção de heterocromatina C-positiva foi utilizado o protocolo de Sammer *et*
412 *al.* (1972). Após os experimentos de FISH, as melhores metáfases foram selecionadas para os
413 experimentos sequência de Bandamento C. Sendo assim, as lâminas contendo preparações
414 cromossômicas foram tratadas em solução de ácido clorídrico (0,2N) a 45°C por 2 minutos e
415 lavadas em água destilada. Ainda úmidas as lâminas foram incubadas em solução recém
416 preparada e filtrada de Hidróxido de Bário Ba(OH)₂ a 45°C de 50 segundos a 1 minuto
417 dependendo da espécie, e em seguida foram lavadas em solução de HCl 0,2N e em água
418 corrente. Por fim, as lâminas foram incubadas em solução salina (2xSSC) durante 20 minutos
419 em estufa à 60°C. Passado esse período as lâminas foram lavadas com água destilada e deixadas
420 para secar ao ar. Os cromossomos foram corados com 20ul da solução antifading e iodeto de
421 Propídio (50 mg/ml) de acordo com Lui *et al.* (2012) e analisadas em microscópio de
422 fluorescência.

423 **3.2.3. Hibridização fluorescente in situ (FISH) - mapeamento de DNAs repetitivo**

424 Foram utilizadas sondas dos DNAs ribossomais 5S e 18S, isoladas do genoma de *Ho-*
425 *plias malabaricus* (Characiformes, Erythrinidae), clonadas em vetores plasmidiais e propaga-
426 das em células competentes de *Escherichia coli* DH5α (Invitrogen, San Diego, CA, USA). A
427 sonda de rDNA 5S incluiu 120 pares de bases (pb) da região codificadora do gene rDNA 5S e

428 200 pb de espaçador não transcrito (NTS) (Pendás *et al.*, 1994). A sonda de rDNA 18S foi
429 composta por um segmento de 1400 pb da região codificadora de rDNA 18S (Cioffi *et al.*,
430 2009). Ambas as sondas foram marcadas diretamente utilizando o *Nick-Translation Mix Kit*
431 (Jena Bioscience, Jena, Alemanha) – rDNA 18S com ATTO488-dUTP e rDNA 5S com
432 ATTO550-dUTP, de acordo com as instruções do fabricante. Além das famílias multigênicas
433 descritas, também foram utilizadas sondas de sequências repetitivas de pequeno tamanho, cor-
434 respondendo aos microssatélites (CA)₁₅, (GA)₁₅ e (CGG)₁₀. Tais microssatélites foram marca-
435 dos diretamente com Cy3 durante a síntese, segundo Kubat *et al.* (2008). Além disso, a sequên-
436 cia telomérica (TTAGGG)_n também foi utilizada. Tal sonda foi gerada por PCR na ausência
437 de molde de acordo com Ijdo *et al.* (1991) e posteriormente marcada por Nick-Translation Mix
438 Kit (Jena Bioscience, Jena, Alemanha) com ATTO550-dUTP.

439 Os experimentos de FISH seguiram a metodologia descrita em Yano *et al.* (2017) e
440 Sassi *et al.* (2022). Os cromossomos foram tratados com 100ul de solução de RNase (1ul de
441 RNase A + 100ul de 2xSSC) por 1,5 horas incubados em câmara úmida em estufa a 37°C.
442 Após esse tempo, as lâminas foram lavadas sob agitação em PBS 1x por 5 minutos, seguido
443 por um tratamento de solução de Pepsina (1ml de H₂O miliq autoclavada + 10µl HCl 1M + 3
444 µl Pepsina 2%) em câmara úmida por 10 minutos. Em seguida uma nova lavagem de PBS 1x
445 sob agitação por 5 minutos seguida por uma rápida lavagem em série alcóolica 70%, 85% e
446 100% por 2 minutos cada. Para a desnaturação dos cromossomos, as lâminas foram submetidas
447 ao tratamento de formamida 70% a 72°C por 3 minutos, sucedida de uma lavagem em série
448 alcóolica como no passo anterior com a alteração para álcool 70% gelado. Por fim o mix de
449 hibridização conteve 2ul de cada sonda desejada completando para 20ul com DS (sulfato de
450 dextrano – 2,5ng/ul, formamida 50% deionizada, 10% de sulfato de dextrano) sendo desnatu-
451 rado no termociclador a 86°C por 8 minutos + 4°C a 2 minutos. Após esse tempo, foi aplicado
452 20ul em cada lâmina e tudo foi incubado em câmara úmida a 37°C por no mínimo 16 horas.
453 Passado esse tempo, as lâminas foram lavadas sob agitação em SSC 1x a 65°C por 5 minutos,
454 seguido de uma lavagem de 4xSSC/Tween sob agitação por 5 minutos, uma rápida lavagem
455 sob agitação em PBS 1x, concluindo com uma lavagem em série alcóolica 70%, 85%, 100%
456 por 2 minutos cada. Após estarem completamente secas, os cromossomos foram corados com
457 20ul de DAPI + Antifading (Vectashield da Vector Laboratories, Burlingame, CA).

458 3.2.4. *Hibridização genômica comparativa (CGH)*

459 Os DNAs genômicos (gDNAs) de machos e fêmeas de *Pyrrhulina* aff. *australis*,
460 *Pyrrhulina* aff. *marilynae*, *Pyrrhulina australis*, *Pyrrhulina brevis*, *Pyrrhulina* cf. *laeta*,
461 *Pyrrhulina marilynae*, *Pyrrhulina obermulleri*, *Pyrrhulina semifasciata* e *Pyrrhulina* sp. foram
462 extraídos a partir do músculo e do fígado, seguindo o método de fenol-clorofórmio-álcool iso-
463 amílico (Sambrook e Russell, 2001). As comparações interespecíficas, os gDNAs derivados de
464 machos e fêmeas de *P. australis* (Paus), *Pyrrhulina* aff. *australis* (Pafa), *P. semifasciata*
465 (Psem), *P. brevis* (Pbre), *P. marilynae* (Pmar), *Pyrrhulina* aff. *marilynae* (Pafm), *Pyrrhulina*
466 sp (Psp), *P. obermulleri* (Pobe) e *Pyrrhulina* cf. *laeta* (Pcfl) foram hibridizados contra cromos-
467 somos metafásicos de *P. marilynae*. Tal espécie foi selecionada por apresentar o menor registro
468 de 2n (2n=32) até então identificado no gênero juntamente com uma notável diferenciação
469 cariotípica. Para esse propósito o gDNA derivado de machos de *P. marilynae* foi marcado para
470 todos os ensaios com ATTO550-dUTP, enquanto os gDNAs das outras espécies foram marca-
471 dos com ATTO488-dUTP (*P. australis*, *Pyrrhulina* aff. *marilynae*, *P. brevis* e *P. obermulleri*)
472 ou ATTO425-dUTP (*Pyrrhulina* aff. *australis*, *Pyrrhulina* sp., *P. semifasciata* e *Pyrrhulina* cf.
473 *laeta*) todos marcados por Nick-Translation (Jena Bioscience, Jena, Alemanha).

474 As comparações foram divididas em um conjunto de quatro lâminas: 1) Na primeira, a
475 mistura final de sondas foi composta por 500ng de gDNA + 10ug de Cot-1 DNA de macho das
476 seguintes espécies: *P. marilynae*, *P. australis* e *Pyrrhulina* aff. *australis*. 2) Na segunda a mis-
477 tura final de sondas foi composta por 500ng de gDNA + 10ug de Cot-1 DNA derivado de
478 macho das seguintes espécies: *P. marilynae*, *Pyrrhulina* aff. *marilynae* e *Pyrrhulina* sp. 3) Na
479 terceira a mistura final de sondas foi composta por 500ng de gDNA + 10ug de Cot-1 DNA
480 derivado de macho das seguintes espécies: *P. marilynae*, *P. brevis* e *P. semifasciata*. 4) Final-
481 mente, na quarta lâmina, a mistura final de sondas foi composta por 500ng de gDNA + 10ug
482 de Cot-1 DNA derivado de macho das seguintes espécies: *P. marilynae*, *P. obermulleri* e
483 *Pyrrhulina* cf. *laeta*. Para todos os ensaios a proporção de sonda versus a quantidade de Cot-1
484 DNA foi baseada em experimentos anteriormente realizados em nossos estudos com peixes
485 (Moraes *et al.*, 2019; Toma *et al.*, 2019 e Sassi *et al.*, 2020) e os experimentos de CGH segui-
486 ram a metodologia descrita por Sember *et al.* (2018).

487 **3.2.5. Pintura total cromossômica (WCP)**

488 Como *Pyrrhulina semifasciata* representa a única espécie de *Pyrrhulina* com a presença
489 de um sistema sexual múltiplo X₁X₂Y, uma sonda do cromossomo Y (PSEMI-Y) foi
490 previamente preparada por microdissecção como descrito em Moraes *et al.* (2019).
491 Aproximadamente 20 cópias do cromossomo Y de *P. semifasciata* foram microdissectadas
492 manualmente usando agulhas de vidro, sob um microscópio invertido (Zeiss Axiovert 135). Os
493 cromossomos foram amplificados por PCR, seguindo o protocolo descrito em Yang *et al.*
494 (2009). Em seguida, 1ul do produto de amplificação primária foi usado como DNA modelo
495 para uma marcação secundária de DOP-PCR com Spectrum Orange-dUTP (Vysis, Downers
496 Grove, EUA) em 30 ciclos, seguindo Yang e Graphodatsky (2009).

497 Metáfases de macho e fêmea de *Pyrrhulina* aff. *marilynae*, *Pyrrhulina* cf. *laeta*, *P.*
498 *marilynae*, *Pyrrhulina* sp., *P. obermulleri* foram utilizadas para experimentos Zoo-FISH com
499 a sonda PSEMI-Y, de acordo com os procedimentos descritos em Yano *et al.* (2017) e Sassi *et*
500 *al.* (2022). A mistura final de sonda foi composta por 500ng da sonda PSEMI-Y e 25ug de Cot-
501 1 DNA isolado do genoma de machos de *P. semifasciata*. As hibridizações foram realizadas
502 em câmara úmida a 37°C por um período de 72h, seguido por duas lavagens sob agitação de
503 1xSSC por 5 minutos a 65°C, mais duas lavagens sob agitação de 4xSSC/Tween por 5 minutos,
504 uma lavagem rápida em 1xPBS, finalizando com a serie alcóolica 70%, 85% e 100% por dois
505 minutos cada. Os cromossomos foram corados com 20ul de DAPI + Antifading (Vectashield
506 da Vector Laboratories, Burlingame, CA).

507

508 **3.2.6. Análises de bioinformática**

509 **3.2.6.1. Procedimento de sequenciamento DArTseq e filtragem de dados**

510 O tecido hepático de todos os indivíduos foi usado para realizar procedimentos de
511 sequenciamento DArTseq na Diversity Arrays Technology Pty Ltd. Esse método de
512 sequenciamento usa uma combinação de enzimas de restrição (SbfI e PstI) que enriquecem
513 regiões hipometiladas (Kilian *et al.*, 2012). O sequenciamento das bibliotecas obtidas foi
514 realizado na plataforma Illumina HiSeq2500.

515 Os dados brutos foram processados de duas maneiras gerando os seguintes conjuntos
516 (I) uma matriz de SNPs usando Ipyrad v. 0.9.84 (Eaton e Overcast, 2020) e (II) um arquivo de
517 sequência em fases obtido com pyRAD v3.0.66 (Eaton, 2014). Em ambos, os adaptadores de
518 sequenciamento foram aparados, e todas as sequências menores que 35pb ou aparentando mais
519 de cinco bases de baixa qualidade (Q<20) não foram consideradas. No conjunto de dados I, um
520 único SNP por locus foi selecionado, para reduzir a inclusão de SNPs vinculados, e os SNPs

521 foram codificados como 0 para homozigotos de estado de referência, 1 para heterozigotos e 2
522 para homozigotos de estado alternativo.

523 Os dados brutos estão disponíveis no banco de dados do National Center for
524 Biotechnology Information, com o código de acesso PRJNA804560 (link de acesso:
525 https://www.ncbi.nlm.nih.gov/Traces/study/?acc=PRJNA804560&o=acc_s%3Aa).

526

527 **3.2.6.2. Avaliadores de marcação em seleção**

528 Uma análise BayeScan foi realizada para procurar marcadores potenciais sob seleção
529 em ambos os conjuntos de dados (Foll e Gaggiotti, 2008). Realizamos um total de 5.000
530 execuções MCMC (Markov Chain Monte Carlo) e desbaste de 10, com um valor de
531 probabilidades anterior de 100. Valores de False Discovery Rate (FDR) foram usados para
532 classificar outliers, e apenas loci com valores menores que 0,01 foram considerados outliers e
533 removidos da análise subsequente.

534

535 **3.2.6.3. Diversidade genética**

536 Utilizando o conjunto de dados II, foi realizada uma análise no software DnaSP v.
537 6.12.03 (Rozas et al., 2019), para obter a diversidade de haplótipos (Hd), D de Tajima (D) e
538 duas medidas de diversidade de nucleotídeos por sítio, π e teta de Watterson (θ_w). A
539 diferenciação também foi estimada a partir da divergência de nucleotídeos entre amostras
540 usando o número médio de substituições de nucleotídeos por sítio entre pares de amostras de
541 espécies diferentes (D_{xy}) e a divergência líquida, corrigida para variação dentro das amostras
542 analisadas (D_a).

543

544 **3.2.6.4. Estrutura genética e análise de variância molecular (AMOVA)**

545 Uma análise de coordenadas principais (PCoA) no pacote R dartR (Gruber et al., 2018)
546 foi usada para investigar a estrutura genética entre as espécies. A estrutura genética também
547 foi investigada com fastSTRUCTURE (Raj et al., 2014), usando o pipeline “Lizards-are-
548 awesome” (Melville et al., 2017). Usamos o comando chooseK.py para selecionar o número
549 de clusters que maximiza a probabilidade e é mais informativo para a estrutura do nosso
550 conjunto de dados. Os resultados do fastStructure foram visualizados com Clumpak (Kopelman
551 et al., 2015). Além disso, uma análise de variância molecular (AMOVA) também foi realizada
552 usando o conjunto de dados I, com amostras agrupadas da seguinte forma: 1) por espécie, 2)
553 pelos clusters do melhor valor K no fastStructure, 3) pelo padrão de agrupamento gerado no
554 PCoA e 4) pela presença ou ausência do sistema de cromossomos sexuais múltiplos.

555

556 **3.2.6.5. *Árvore de espécies***

557 Usamos o pacote SNAPP no BEAST 2.6.4 (Bouckaert et al., 2014) para inferir a
558 topologia da árvore de espécies. Incluímos apenas locais polimórficos, usamos o pior padrão
559 para taxa de coalescência e calculamos taxas de substituição para trás e para frente
560 (parâmetros u e v) com base nos dados empíricos. Aplicamos um comprimento de cadeia de
561 dois milhões de gerações, amostramos a cada 5000 interações. A convergência foi avaliada
562 no Tracer 1.7.1 (Rambaut et al., 2018). Obtivemos a árvore MCC com base em alturas
563 ancestrais comuns no TreeAnnotator, com as primeiras 25% das árvores geradas descartadas
564 com burn-in. Exportamos a árvore de consenso no FigTree 1.4.4.

565

566 **3.2.6.6. *Análise de introgressão***

567

568 Avaliamos a mistura entre linhagens calculando as estatísticas D de Patterson (teste
569 ABBA-BABA) no Ipyrad v. 0.9.84 (Eaton e Overcast, 2020) usando frequências de SNP
570 agrupadas de indivíduos de cada espécie (Durand et al., 2011). Realizamos testes de 4 táxons
571 de acordo com a topologia SNAPP recuperada, usando *P. marilynae* ou *P. australis* como
572 grupo externo, *P. brevis* como P_3 e *P. semifasciata* e *P. obermulleri* como P_1 ou P_2 . A
573 significância foi medida com 1.000 réplicas bootstrap por reamostragem de loci com
574 substituição (seguindo Eaton e Ree, 2013). Os resultados foram considerados significativos de
575 acordo com seus escores Z (valores significativos > 3), que quantificam o número de desvios-
576 padrão do bootstrap nos quais os valores da estatística D se desviam de seu valor esperado de
577 zero.

578

579 **3.2.7. *Sequências DNA satélites***

580 **3.2.7.1. *Sequenciamento***

581 Para o sequenciamento de DNA, selecionamos um macho *P. marilynae* e um macho e
582 uma fêmea de *P. semifasciata*. O DNA total de tais espécies foi extraído dos tecidos musculares
583 utilizando um protocolo baseado em spin-column (Cellco Biotech, São Carlos – SP, Brasil).
584 Os DNAs purificados foram *sequenciados* pela plataforma BGISEQ-500 (2 x 150 pb; BGI
585 Shenzhen Corporation, Shenzhen, China). O sequenciamento de Short-read rendeu entre 2,14
586 GB (*P. semifasciata*) e 2,44 GB (*P. marilynae*). Todos os dados brutos foram depositados em
587 um arquivo de leitura de sequências (SRA-NVBI) e estão disponíveis sob os números de acesso
588 (SRR25467276, SRR25476502 e SRR25476501).

589

590 **3.2.7.2 *Análises Bioinformáticas e Biblioteca de satDNA***

591 Inicialmente, foram cortadas as leituras brutas com Trimmomatic (Bolger et al., 2014)
592 para selecionar as leituras finais do par com $Q > 20$ para todos os nucleotídeos. Em seguida, os

593 catálogos de satDNA de *P. semifasciata* e *P. marilynae* foram caracterizados
594 independentemente no TAREAN (Novák *et al.*, 2020) com o pipeline satMiner (Ruiz-Ruano
595 *et al.*, 2016). As *sequências* de consenso de satDNA produzidas no TAREAN foram filtradas
596 das bibliotecas genômicas com DeconSeq (Schmieder e Eswards, 2011) e interações
597 subsequentes foram realizadas no TAREAN até que nenhum satDNA fosse encontrado. Em
598 seguida, foi realizada uma busca de homologia com RepeatMasker (Smith *et al.*, 2020) para
599 agrupar as *sequências* em: Variantes, famílias e superfamílias conforme sugeridas por Ruiz-
600 Ruano (2016). Também foram calculados os valores de abundância e divergência das famílias
601 de satDNA selecionando 10.000.000 leituras (2 x 5.000.000) de cada biblioteca genômica e
602 mascarando seu próprio catálogo de satDNAs com RepeatMasker (Smith *et al.*, 2020). Depois
603 disso, foram nomeadas as famílias de satDNA de acordo com sua abundância em cada espécie.

604 Como *P. semifasciata* apresenta um sistema de cromossomos sexuais múltiplos, foi
605 calculada a razão de abundância machos/fêmeas (M/F) de cada família de satDNA, em seguida
606 foram selecionados aqueles que apresentavam uma relação $M/F > 1,2$ como satDNAs sexo
607 específicos, acumulados supostamente em machos. Finalmente todos os satélites foram
608 pesquisados pelo BLAST (Altschul *et al.*, 1990) contra a coleção de nucleotídeos do NCBI
609 para verificar a presença de satDNAs conservados. Além disso, foi construída uma árvore
610 geradora mínima (MST) para PseSat55 usando PHYLOIZ (Nascimento *et al.*, 2017) para
611 descrever as proporções dos haplótipos de machos e fêmeas.

612 3.2.7.3. Design de Primer e Amplificação de DNA via Reação em Cadeia da Polimerase 613 (PCR)

614 Para a confecção dos primers, foram projetados primers para 21 dos 70 PseSatDNAs e
615 para 10 dos 71 PmaSatDNAs que foram caracterizados. Como critério de seleção para
616 produção dos primers, foram selecionados os dez mais abundantes para *P. marilynae* (**Tabela**
617 **2**), os cinco mais abundantes e aqueles com alguma diferença de abundância entre os sexos
618 para *P. semifasciata* (**Tabela 3**). Para os procedimentos de PCR foram usadas temperaturas e
619 concentrações de DNA ideais para cada DNA satélite, de acordo com Ruiz-Ruano (2016).

620

621

622 **Tabela 2** – Dez satDNAs mais abundantes em *P. marilynae*. Destaques em azul são os
623 PmaSatDNAs selecionados para FISH.

624

Família satDNA	RUL	Abundância	Divergência	A+T (%)
PmaSat01-1627	1627	0.0395879278883	1.33	58.6
PmaSat02-68	68	0.0126290012853	2.63	66.2
PmaSat03-45	45	0.0083896090511	2.92	44.4
PmaSat04-50	50	0.00772308401902	3.93	60
PmaSat05-226	226	0.00728803566553	9.69	64.2
PmaSat06-198	198	0.00647761332963	9.25	67.2
PmaSat07-45	45	0.00639111613516	5.97	62.2
PmaSat08-33	33	0.00268802096213	2.10	57.6
PmaSat09-335	335	0.00220671410467	9.24	70.1
PmaSat10-4663	4663	0.00209498220866	5.93	43.6

625 **Tabela 3** – 21 satDNAs selecionados para confecção de primer de *P.semifasciata*. Destaques
626 em azul são os PseSatDNAs selecionados para FISH e os asteriscos (*) são todos aqueles que
627 hibridizaram em algum dos cromossomos sexuais.
628

Família SatDNA	RUL	Abundância (M)	Abundância (F)	Abundância (M/F)	Divergência (M)	Divergência (F)	A+T (%)
PseSat01- 304*	304	0,005606905	0,006386826	0,877885927	9,78	9,65	68
PseSat02- 45	45	0,005289071	0,00496321	1,065655359	4,97	4,98	62,2
PseSat03- 68	68	0,005288433	0,005331731	0,991879186	2,52	2,54	66,1
PseSat04-226*	226	0,004975278	0,005546355	0,897035567	9,76	9,62	64,6
PseSat05 - 45	45	0,004215905	0,004087883	1,03131743	4,4	4,43	44,4
PseSat06- 198	198	0,002799141	0,003195114	0,876069106	8,88	8,81	66,6
PseSat27- 422	422	0,000581057	0,000722512	0,804218246	6,35	6,6	0,575829
PseSat32- 186	186	0,000390964	0,000658971	0,593294997	8,44	8,02	0,709677
PseSat34-165	165	0,000282004	0,000328703	0,857928629	6,61	6,58	0,642424
PseSat38- 300*	300	0,000230661	0,000059944	3,847935851	4,96	6,47	0,576667
PseSat39- 80	80	0,000225943	0,000317697	0,711188427	15,55	15,44	0,6625
PseSat40- 39	39	0,000215363	0,000275735	0,781050911	10,74	9,56	0,641026
PseSat50- 1125	1125	0,000160486	0,000123408	1,300450538	9,97	12,7	0,656
PseSat54- 159	159	0,00013754	0,000194867	0,705815943	5,1	4,7	0,672956
PseSat55- 43*	43	0,000133589	0,000159353	0,838325057	8,62	7,99	0,488372
PseSat56- 87	87	0,000126526	0,000159655	0,792494666	6,25	5,81	0,678161
PseSat57- 162	162	0,000124983	8,86007E-05	1,410636489	4,99	5,06	0,67284
PseSat61- 213	213	0,000109063	0,000137659	0,792264963	5,14	5,29	0,615023
PseSat63- 463	463	0,000100169	0,000113188	0,884981918	3,94	3,69	0,591793
PseSat64- 182	182	0,000098656	5,97373E-05	1,651496552	10,95	13,61	0,681319
PseSat67- 198	198	8,07013E-05	0,000103397	0,780502273	4,81	4,26	0,60101

629 Para cada uma das *sequências* foi usado o seguinte ciclo: desnaturação inicial a 95°C
630 por 5 min; 29-35 ciclos com desnaturação a 95°C por 15s; anelamento de 50°C a 62°C (**Tabela**
631 **4**); extensão a 72°C por 10s e extensão final a 72°C por 10 min. Para validar a amplificação e
632 garantir a integridade dos satDNAs, os produtos de PCR foram analisados por eletroforese em
633 géis de agarose a 1% e 2%. Por fim todos os produtos foram quantificados no

634 espectrofotômetro NanoDrop (ThermoFisher Scientific, Branchburg, NJ, EUA).

635

636 **Tabela 4** - Condições de PCR (primer, temperatura e concentração de DNA template) para a
637 amplificação ideal de DNAs satélites de *P. marilynae* e *P. semifasciata*

638

Satélite	Primer F	Primer R	Faixa de temperatura de anelamento	[DNA] ng/μl
PmaSat01-1627	5'CACACCTTTGGCATTCTAGC	5'TCTGTTAAGCATGGTGGAGG	56°C – 57,4°C	100
PmaSat04-50	5'GGGTGTGGTTATCTCTGTAC	5'CCCCTCTAAACAGAGTATAAAC	50°C – 51,7°C	100; 10; 1; 0,1
PmaSat05-226	5'GCAAGCTGAATACATTCTATG	5'GACTGTCTGAGAGCACAAAC	53°C - 54,5°C	100; 10; 1; 0,1
PmaSat06-198	5'AAGACAGCTTCTGCATCCATG	5'TTGCAGATTTGCCCCAAAAAC	55°C - 55,6°C	100; 10; 1; 0,1
PmaSat07-45	5'CCTCTGTAACACATTA AACTGT	5'TAGGAGAGTGTAGTGTTAGTCT	51,7°C – 58°C	100; 10
PmaSat09-335	5'CTGCAACCACTTCCAGTGAT	5'ACACTTAGTTGTGTCTGAAA	53°C - 53,5°C	100; 10; 1; 0,1
PmaSat10-4663	5'AGAACGGAGGTCTCTT GCGT	5'TCCATTTCATTTCCATCACGC	56°C – 62,5°C	100
PseSat01-304	5'CTGCAACCACTTCCAGTGAT	5'ACACTTAGTTGTGTCTGAAA	53°C - 53,5°C	100; 10; 1; 0,1
PseSat04-226	5'GCAAGCTGAATACATTCATG	5'GACTGTCTGAGAGCACAAAC	53°C - 54,5°C	100; 10; 1; 0,1
PseSat06-198	5'AAGACAGCTTCTGATCCATG	5'TTGCAGATTTGCCCCAAAAAC	55°C - 55,6°C	100; 10; 1; 0,1
PseSat32-186	5'TGAGAGAAGAC TTTACAAGC	5'TGACACATTTAAGGCATTC	50°C - 54,9°C	100
PseSat34-165	5'CATGGCTGATAGGGTAAAAG	5'ATGTGACCACACTGTATCCC	56,5°C - 63°C	1; 0,1
PseSat38-300	5'ATAGACGGATGGATTAACGG	5'AAAGACTGACAGACCATTAT	53°C - 61°C	100; 10; 1; 0,1
PseSat39-80	5'CTTACTGTCTCATATCTGTG	5'AGTTAAGACCAGTATCTCTA	50,5°C - 57,4°C	100
PseSat50-1125	5'CTGTACAGTGGA TTATGGAG	5'TTCGTGTTACTCAGAATGTC	53 - 53,5	100; 10
PseSat54-159	5'AATCTCTGCATATAAAATGGC	5'AGATGGACCAAAAGGTGTAT	50°C - 58°C	100; 10; 1; 0,1
PseSat55-43	5'CTGTGGTGCCTAACCAGA	5'CCCTATCATTTCAGTACA	50°C - 58°C	100; 10; 1; 0,1
PseSat56-87	5'CACCCAGCCACTTTTAA	5'TGGAGGTAGTTAGTTAGATG	50°C - 51,5°C	100
PseSat57-162	5'AGGGTCAGTACTCTCACT	5'CACTTCATAACAGTCATTTTAA	52°C - 60°C	100; 10; 1; 0,1
PseSat61-213	5'ATTCCAGGCAATAATCTGCC	5'CAGGCGAGAATCTACCACT	53°C - 57,9°C	100; 10; 0,1
PseSat63-463	5'ATTGGTCAGATATTGTGAAG	5'ATTGCGCCGTTTATATTCAC	52°C - 60°C	100; 10
PseSat64-182	5'TTTACTGCTGTTAAGATTTTC	5'CCTTTGGTAGGCATGTAGC	50°C - 50,7°C	100; 10; 1; 0,1
PseSat67-198	5'CTAACTTCATTCGGCGTTCT	5'CCACCATGGCACACCTGATA	55°C - 55,6°C	10; 1; 0,1

639 **3.2.8. Análises**

640 Aproximadamente 20 metáfases por indivíduo foram analisadas para confirmar o nú-
641 mero diploide, as estruturas cariotípicas de cada espécie e os resultados de FISH. As imagens
642 foram capturadas usando microscópio de epifluorescência Olympus BX50 (Olympus Corpora-
643 tion, Ishikawa, Japão) e Axioplan II (Carl Zeiss Jena GmbH, Jena, Alemanha) acoplado a uma
644 câmera CoolSNAP e as imagens processadas no ISIS (MetaSystems Hard e Software GmbH,
645 Altussheim, Alemanha). Os cromossomos foram classificados em metacêntricos (m), subme-
646 tacêntricos (sm), subtelocêntricos (st) ou acrocêntricos (a), de acordo com suas proporções de
647 braços (Levan *et al.*, 1964). Além disso, a elaboração dos mapas foi realizada no QGIS Desktop
648 3.6.3, Inkscape 0.92 e Adobe Photoshop CC 2020, sendo esse último também utilizado para as
649 montagens de cariótipos, pranchas, ideogramas e tratamentos de imagem.

650 **4. Resultados e Discussão**

651 Os resultados obtidos no presente estudo e suas respectivas discussões foram compilados
652 e organizados na forma de capítulos, os quais correspondem aos artigos científicos listados
653 abaixo que se encontram publicados ou submetidos para publicação:

CAPÍTULO 1:

Tracking the Evolutionary Trends Among Small-Size Fishes of the Genus *Pyrrhulina* (Characiforme, Lebiasinidae): New Insights From a Molecular Cytogenetic Perspective

CAPÍTULO 2:

The Genetic Differentiation of *Pyrrhulina* (Teleostei, Characiformes) Species is Likely Influenced by Both Geographical Distribution and Chromosomal Rearrangements

CAPÍTULO 3:

Chromosomal Rearrangements and Satellite DNAs: Extensive Chromosome Reshuffling and the Evolution of Neo-Sex Chromosomes in the Genus *Pyrrhulina* (Teleostei; Characiformes)

CAPÍTULO 4:

The evolution of Lebiasinidae (Teleostei: Characiformes): Insights from cytogenetics

Tracking the Evolutionary Trends Among Small-Size Fishes of the Genus *Pyrrhulina* (Characiforme, Lebiasinidae): New Insights From a Molecular Cytogenetic Perspective

Renata Luiza Rosa de Moraes, Francisco de Menezes Cavalcante Sassi, Luiz Antônio Carlos Bertollo, Manoela Maria Ferreira Marinho, Patrik Ferreira Viana, Eliana Feldberg⁴, Vanessa Cristina Sales Oliveira, Geize Aparecida Deon, Ahmed B. H. Al-Rikabi, Thomas Liehr and Marcelo de Bello Cioffi

Frontiers in Genetics (2021) – DOI: 10.3389/fgene.2021.769984

655

Abstract

656

657

658

659

660

661

662

663

664

665

666

667

668

669

670

671

672

673

674

675

676

Miniature fishes have always been a challenge for cytogenetic studies due to the difficulty in obtaining chromosomal preparations, making them virtually unexplored. An example of this scenario relies on members of the family Lebiasinidae which include miniature to medium-sized, poorly known species, until very recently. The present study is part of undergoing major cytogenetic advances seeking to elucidate the evolutionary history of lebiasinids. Aiming to examine the karyotype diversification more deeply in *Pyrrhulina*, here we combined classical and molecular cytogenetic analyses, including Giemsa staining, C-banding, repetitive DNA mapping, comparative genomic hybridization (CGH), and whole chromosome painting (WCP) to perform the first analyses in five *Pyrrhulina* species (*Pyrrhulina* aff. *marilynae*, *Pyrrhulina* sp., *P. obermulleri*, *P. marilynae* and *Pyrrhulina* cf. *laeta*). The diploid number (2n) ranged from 40 to 42 chromosomes among all analyzed species, but *P. marilynae* is strikingly differentiated by having 2n = 32 chromosomes and a karyotype composed of large meta/submetacentric chromosomes, whose plesiomorphic status is discussed. The distribution of microsatellites does not markedly differ among species, but the number and position of the rDNA sites underwent significant changes among them. Interspecific comparative genome hybridization (CGH) found a moderate divergence in the repetitive DNA content among the species' genomes. Noteworthy, the WCP reinforced our previous hypothesis on the origin of the X1X2Y multiple sex chromosome system in *P. semifasciata*. In summary, our data suggest that the karyotype differentiation in *Pyrrhulina* has been driven by major structural rearrangements, accompanied by high dynamics of repetitive DNAs.

6771. Introduction

678

679 Characiformes comprise a very diverse and abundant freshwater order (Nelson *et al.*, 2016),
680 in which the family Lebiasinidae is represented by 75 valid species (Fricke *et al.*, 2021) widely
681 distributed across South and Central America (Weitzman and Weitzman, 2003). The
682 phylogenetic relationships of the Lebiasinidae remained in doubt for a long time, but more
683 recent phylogenetic analysis indicate their proximity to the Ctenoluciidae (Calcagnotto *et al.*,
684 2005; Oliveira *et al.*, 2011), which was also reinforced by the different studies (Arcila *et al.*,
685 2017; Betancur-R *et al.*, 2019; Melo *et al.*, 2021). Most Lebiasinidae species reach about 60
686 mm of Standard Length (SL), but miniature species, not surpassing a maximum of 26 mm SL,
687 is found within the Pyrrhulinae, whereas medium-sized species up to 150 mm SL can be
688 found within Lebiasininae (Weitzman and Weitzman, 2003).

689 Because of their small sizes and difficulties in obtaining good chromosomal preparations,
690 species of Lebiasinidae were, for a long time, little analyzed in terms of cytogenetics, with
691 scarce references mainly on the chromosomal number of few species (Scheel, 1973; Oliveira
692 *et al.*, 1991; Arai, 2011). However, this scenario has recently undergone significant changes
693 with the methodological advance of cytogenetics and its applicability among small to miniature
694 fishes of *Pyrrhulina*, *Lebiasina*, *Copeina*, and *Nannostomus* genus (Moraes *et al.*, 2017,
695 Moraes *et al.*, 2019; Sassi *et al.*, 2019; Toma *et al.*, 2019; Sassi *et al.*, 2020; Sember *et al.*,
696 2020).

697 *Pyrrhulina* is one of the most speciose genera of the subfamily Pyrrhulinae, with 19 valid
698 small species (Fricke *et al.*, 2021), ranging from 30.4 to 85 mm SL (Weitzman and Weitzman,
699 2003; Netto-Ferreira and Marinho, 2013). The genus is among the most problematic, with
700 many poorly known species, species complexes, and old taxonomic problems (Netto-Ferreira
701 and Marinho, 2013). The first *Pyrrhulina* species to have some chromosomal data evidenced
702 was *Pyrrhulina* cf. *australis*, with $2n = 40$ chromosomes, mainly acrocentric ones (Oliveira *et*
703 *al.*, 1991). Taxonomic boundaries of *P. australis* are still poorly defined, demonstrated in
704 subsequent studies (Moraes *et al.*, 2017; Moraes *et al.*, 2019) of two morphotypes. Both *P.*
705 *australis* and *Pyrrhulina* aff. *australis* showed similar data $2n = 40$ (4st + 36a), distinct from
706 *P. brevis*, $2n = 42$ (2sm + 4st + 36a), with no evidence of heteromorphic sex chromosomes in
707 the three species (Moraes *et al.*, 2017; Moraes *et al.*, 2019). Another species, *P. semifasciata*,
708 was analyzed, presenting $2n = 42$ (4st + 38a) in females, and $2n = 41$ (1m + 4st + 36a) in males,
709 the latter with three unpaired chromosomes because of a multiple X1X1X2X2/X1X2Y sex

710 chromosome system (Moraes *et al.*, 2019). This occurrence was also confirmed by comparative
711 genomic hybridizations (CGH) and whole-chromosome painting (WCP), with some
712 indications that the Y chromosome originated by centric fusions of non-homologous
713 acrocentric chromosomes (Moraes *et al.*, 2019).

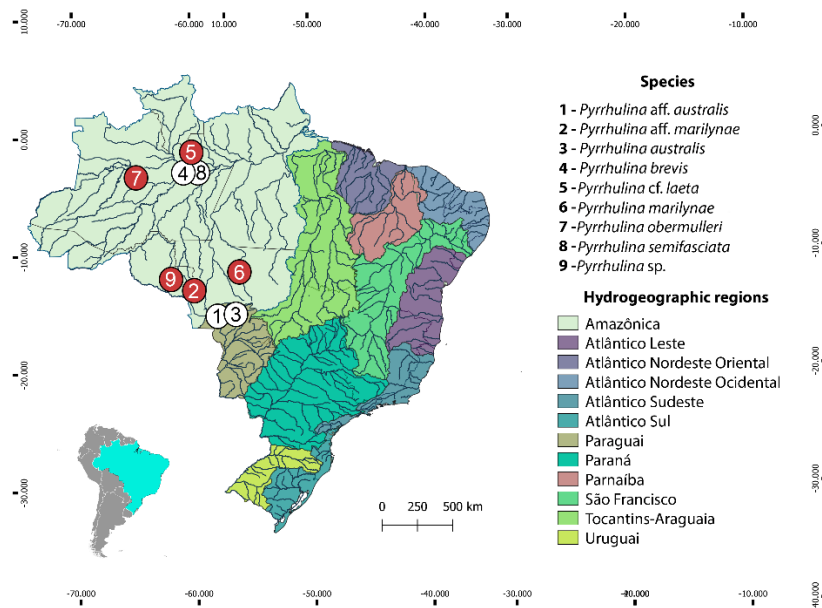
714 To improve the knowledge of the evolutionary processes within the genus *Pyrrhulina*, we
715 combined classical and molecular cytogenetic analyses, including Giemsa staining, C-banding,
716 repetitive DNA mapping, comparative genomic hybridization (CGH), and whole chromosome
717 painting (WCP to perform the first analyses in five *Pyrrhulina* species (*Pyrrhulina* aff.
718 *marilynae*, *Pyrrhulina* sp., *P. obermulleri*, *P. marilynae* and *Pyrrhulina* cf. *laeta*). The results
719 highlighted relationships and particular evolutionary paths at the chromosomal and genomic
720 levels among the species. In addition, the hypothesis on the origin of the multiple sex
721 chromosome system in *P. semifasciata* is validated.

722. Materials and Methods

723 2.1. Animals

724 The collection sites, number, and sex of the specimens investigated are presented in **Figure**
725 **1, Table 1**. Part of the sampling (**Figure 1**, white circles) resembles the one previously analyzed
726 by Moraes *et al.* (2017), Moraes *et al.* (2019) with different cytogenetic and molecular meth-
727 ods. Animals were collected with the authorization of the Brazilian environmental agency IC-
728 MBIO/SISBIO (license no. 48628-14) and SISGEN (A96FF09). All species were properly
729 identified by morphological criteria, and the specimens were deposited in the fish collection of
730 the Museu de Zoologia da Universidade de São Paulo (MZUSP) under the voucher numbers
731 (119077, 119079, 123073, 123080) and the Universidade Federal da Paraíba (UFPB) museum
732 under the voucher number (12079, 12080, 12082 and 12083). Experiments followed ethical
733 and anesthesia conducts and were approved by the Ethics Committee on Animal Experimenta-
734 tion of the Universidade Federal de São Carlos (process number CEUA 1853260315).

735



736

737 **Figure 1:** Brazilian collection sites of the *Pyrrhulina* species cytogenetically investigated in the present
 738 study (red circles) and the ones previously cytogenetically analyzed (white circles: data from (Moraes
 739 *et al.*, 2017; Moraes *et al.*, 2019).

740

741 **Table 1.** Geographical coordinates and sample size of *Pyrrhulina* (Characiformes, Lebiasinidae)
 742 species collected in Brazil.

Species	Locality	Sample Size
<i>Pyrrhulina</i> aff. <i>australis</i>	Rio Sepotuba, Lambari D'Oeste – MT (15°11'28.0"S 57°41'30.7"W)	16♂ 22♀
<i>Pyrrhulina</i> aff. <i>marilynae</i>	Igarapé 12 de Outubro, Comodoro – MT (12°58'41.0"S 60°00'34.0"W)	14♂ 10♀
<i>P. australis</i>	Barra do Bugres – MT (15°04'27.5"S 57°11'05.4"W)	18♂ 30♀
<i>P. brevis</i>	Reserva Florestal Adolpho Ducke, Manaus – AM (2°58'20.7"S 59°55'53.0"W)	17♂ 13♀
<i>Pyrrhulina</i> cf. <i>laeta</i>	Presidente Figueiredo – AM (1°59'10.8"S 60°03'40.8"W)	07♂ 05♀
<i>P. marilynae</i>	Ipiranga do Norte – MT (11°36'02.0"S 55°56'27.0"W)	14♂ 08♀
<i>P. obermulleri</i>	Tefé – AM (3°25'50.7"S 64°44'54.8"W)	21♂ 12♀
<i>P. semifasciata</i>	Careiro – AM (3°51'00.0"S 60°04'00.0"W)	12♂ 09♀
<i>Pyrrhulina</i> sp.	Represa, Alto Alegre dos Parecis – RO (12°11'58.0"S 61°46'47.7"W)	19♂ 29♀

743 2.2. *Chromosomal Preparations and Analysis of the Constitutive Heterochromatin*
 744 Mitotic chromosomes were obtained from kidney cells by the protocol described in
 745 Bertollo *et al.* (2015). The distribution of constitutive heterochromatin was observed by the C-
 746 banding method according to (Sumner, 1972).

747 2.3. *Repetitive DNA Mapping with Fluorescence in situ Hybridization (FISH)*

748 The 5S rDNA probe included 120 base pairs (bp) of the 5S rDNA gene coding region
749 and 200 bp of non-transcribed spacer (NTS) (Pendás *et al.*, 1994). The 18S rDNA probe was
750 composed of a 1,400-bp-long segment of the 18S rDNA coding region (Cioffi *et al.*, 2009).
751 Both probes were directly labeled with the Nick-Translation Mix Kit (Jena Bioscience, Jena,
752 Germany)—18S rDNA with ATTO488-dUTP and 5S rDNA with ATTO550-dUTP, according
753 to the manufacturer's instructions. The (CA)₁₅, (GA)₁₅, (CGG)₁₀ microsatellite probes were
754 directly labeled with Cy3 during the synthesis, according to Kubat *et al.* (2008). In addition,
755 since it contains the lowest 2n, telomeric (TTAGGG)_n sequence was also used as probe in *P.*
756 *marylinae*. This probe was generated by PCR in the absence of a template according to Ijdo *et al.*
757 *et al.* (1991) and later labeled with ATTO550-dUTP with the Nick-Translation Mix Kit (Jena
758 Bioscience, Jena, Germany). FISH experiments followed the methodology described in Yano
759 *et al.* (2017). Metaphase chromosomes were treated with RNase A (40 µg/ml) for 1.5 h at 37°C
760 and the DNA denatured in 70% formamide/2× SSC at 72°C for 3.15 min. A hybridization
761 mixture (2.5 ng/µL probes, 50% deionized formamide, 10% dextran sulfate) was then dropped
762 on the slides, and the hybridization process was performed overnight at 37°C in a moist
763 chamber. The first post-hybridization wash was performed with 1× SSC for 5 min at 65°C,
764 followed by the second one performed with 4xSSC/Tween for 5 min, at room temperature.
765 Chromosomes were then counterstained with DAPI, and the slides were mounted with an
766 antifade solution (Vectashield from Vector Laboratories, Burlingame, CA).

767

768 2.4. *FISH for Whole Chromosome Painting*

769 As *P. semifasciata* represents the only *Pyrrhulina* species that harbors an X1X2Y
770 multiple sex system, a Y-chromosome probe, named PSEMI-Y, was previously prepared by
771 microdissection, as described in (Moraes *et al.*, 2019) Male and female metaphases of *P.*
772 *marylinae*, *Pyrrhulina aff. marylinae*, *Pyrrhulina sp.*, *P. obermulleri*, *Pyrrhulina cf. laeta* were
773 used for Zoo-FISH experiments with the PSEMI-Y probe, according to procedures described
774 in Yano *et al.* (2017). The hybridization was performed for 72 h at 37°C in a moist chamber,
775 with post-hybridization washes with 1xSSC for 5 min at 65°C, and in 4xSSC/Tween (RT). 10
776 µg of male-derived C0t-1 DNA from *P. semifasciata* was used as suppressor in each
777 experiment. Chromosomes were stained with DAPI (1.2 µg/ml) and the slides were mounted
778 with an antifade solution, as described above.

779

780 2.5. *Probes for Comparative Genomic Hybridization*

781 The genomic DNAs (gDNAs) from male and female specimens of *P. marilynae*,
782 *Pyrrhulina* aff. *marilynae*, *Pyrrhulina* sp., *P. obermulleri*, *Pyrrhulina* cf. *laeta*, *P. australis*,
783 *Pyrrhulina* aff. *australis*, *P. brevis*, and *P. semifasciata* were extracted from liver tissue by the
784 standard phenol-chloroform-isoamyl alcohol method (Sambrook and Russell, 2001). For
785 intraspecific comparisons, the male-derived gDNAs of all species were labeled with ATTO550-
786 dUTP and the female gDNAs with ATTO 488-dUTP, by nick translation (Jena Bioscience, Jena,
787 Germany). The repetitive sequences were blocked using unlabeled C0t-1 DNA in all
788 experiments, according to (Zwick *et al.*, 1997). The final hybridization mixture for each slide
789 (20 µL) was composed of male- and female-derived gDNAs (500 ng each), plus 25 µg of female-
790 derived C0t-1 DNA from the respective species. The probe was ethanol-precipitated, and the dry
791 pellets were mixed in a hybridization mixture containing 50% formamide, 2× SSC, 10% SDS,
792 10% dextran sulfate, and Denhardt's buffer, pH 7.0.

793 For interspecific comparisons, the gDNA of male specimens of *P. australis* (Paus),
794 *Pyrrhulina* aff. *australis* (Pafa), *P. semifasciata* (Psem), *P. brevis* (Pbre), *P. marilynae* (Pmar),
795 *Pyrrhulina* aff. *marilynae* (Pafm), *Pyrrhulina* sp. (Psp), *P. obermulleri* (Pobe) and *Pyrrhulina* cf.
796 *laeta* (Pcfl) were hybridized against metaphase chromosomes of *P. marilynae*. This species was
797 selected since it harbors the lowest 2n = 32 until now register for the genus, coupled with a
798 remarkable karyotype differentiation. For this purpose, male-derived gDNA of *P. marilynae* was
799 labeled with ATTO 550-dUTP, while the gDNAs of the other species were labeled with ATTO
800 488-dUTP (*P. australis*, *Pyrrhulina* aff. *marilynae*, *P. brevis* and *P. obermulleri*) or ATTO 425-
801 dUTP (*Pyrrhulina* aff. *australis*, *Pyrrhulina* sp., *P. semifasciata* and *Pyrrhulina* cf. *laeta*), both
802 through nick translation (Jena Bioscience, Jena, Germany).

803 The interspecific comparisons were divided into a set of four slides. In the first slide, the
804 final probe mixture was composed of 500 ng of male-derived gDNA plus 10 µg of male-derived
805 C0t-1 DNA of each of the following species: *P. marilynae*, *P. australis*, and *Pyrrhulina* aff.
806 *australis*. In the second slide, the final probe mixture was composed of 500 ng of male-derived
807 gDNA plus 10 µg of male-derived C0t-1 DNA of each one of the following species: *P.*
808 *marilynae*, *Pyrrhulina* aff. *marilynae* and *Pyrrhulina* sp. In the third slide, the final probe
809 mixture was composed of 500 ng of male-derived gDNA plus 10 µg of male-derived C0t-1 DNA
810 of each one of the following species: *P. marilynae*, *P. brevis*, and *P. semifasciata*. Finally, in the
811 fourth slide, the final probe mixture was composed of 500 ng of male-derived gDNA plus and
812 10 µg of male-derived C0t-1 DNA of each one of the following species: *P. marilynae*, *P.*
813 *obermulleri*, and *Pyrrhulina* cf. *laeta*. The chosen ratio of probe vs. C0t-1 DNA amount was

814 based on previous experiments performed in our fish studies (Moraes *et al.*, 2019; Toma *et al.*,
815 2019; Sassi *et al.*, 2020). The CGH experiments followed the methodology described in Sember
816 *et al.* (2018).

817

818 2.6. *Microscopy and Images Processing*

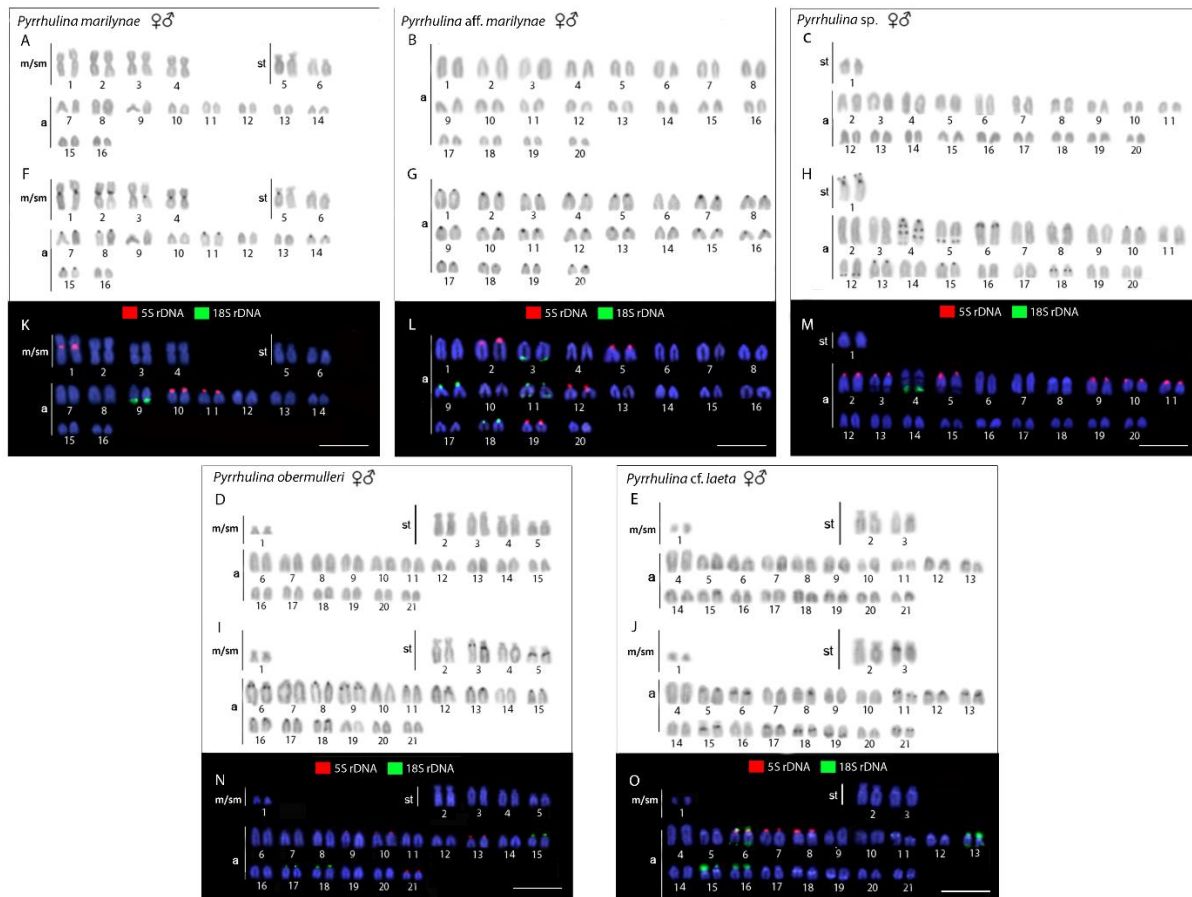
819 To confirm the diploid number, karyotype structure and FISH results in at least 30
820 metaphase spreads were analyzed per individual. The microscopy images were captured using
821 an Olympus BX50 epifluorescence microscope (Olympus Corporation, Ishikawa, Japan)
822 coupled with a CoolSNAP camera, and the images were processed using Image-Pro Plus 4.1
823 Software (Media Cybernetics, Silver Spring, MD, United States). Final images were optimized
824 and arranged using Adobe Photoshop, version CC 2020. Chromosomes were classified as
825 metacentric (m), submetacentric (sm), subtelocentric (st), or acrocentric (a), according to their
826 arm ratios (Levan, 1964). As the males and females results showed no differences, only male
827 metaphases were represented in the figures.

828

829 3. Results

830 3.1. *Karyotypes and Heterochromatin Distribution*

831 The diploid number ranged from $2n = 40$ to 42 among the following four species:
832 *Pyrrhulina* sp. ($2n = 40$; $2st+38a$), *Pyrrhulina* aff. *marilynae* ($2n = 40$; $40a$), *P. obermulleri* ($2n =$
833 42 ; $2m/sm+8st+32a$) and *Pyrrhulina* cf. *laeta* ($2n = 42$; $2m/sm+4st+36a$), the two latter also
834 sharing a characteristic small metacentric/submetacentric pair. On the other hand, *P. marilynae*
835 differed by presenting a very distinct karyotype composition ($2n = 32$; $8m/sm+4st+20a$). These
836 results represent the first cytogenetic data for the abovementioned species. The constitutive
837 heterochromatin was distributed at the pericentromeric region of several chromosome pairs in
838 *P. marilynae* and *Pyrrhulina* aff. *marilynae*. In its turn, *Pyrrhulina* sp., *P. obermulleri*, and
839 *Pyrrhulina* cf. *laeta* presented a remarkable series of interstitial and pericentromeric C-bands, in
840 addition to telomeric ones (**Figure 2**). In our sampling, we did not observe any karyotype
841 differences between males and females.



842

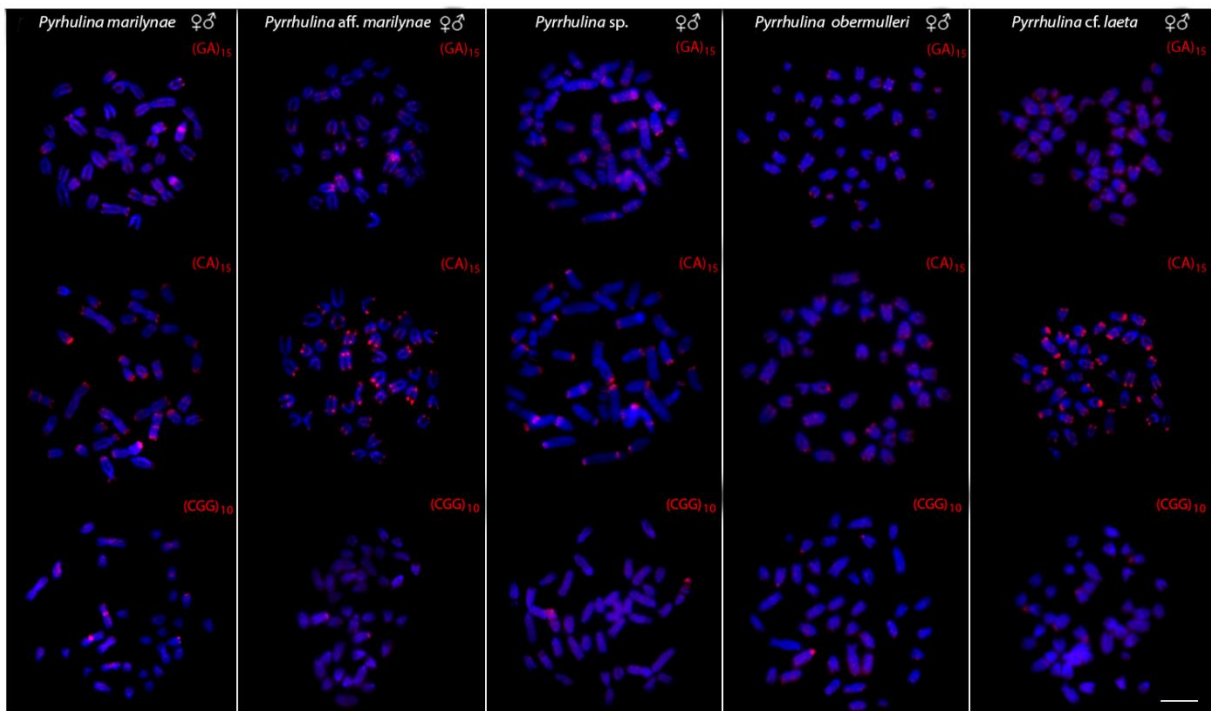
843 **Figure 2.** Male and female karyotypes of *Pyrrhulina marilynae* (A, F, and
 844 **K**), *Pyrrhulina aff. marilynae* (B, G and L), *Pyrrhulina* sp. (C, H and M), *P. obermulleri* (D, I and
 845 **N**) and *Pyrrhulina cf. laeta* (E, J and O) arranged after Giemsa staining (A-E), C-banding (F-J), and
 846 dual-color *in situ* hybridization (FISH) with 18S (green) and 5S (red) ribosomal DNA probes (K-O).
 847 Chromosomes were counterstained with 4',6-diamidino-2-phenylindole (DAPI). Scale bar = 5 μm.

848

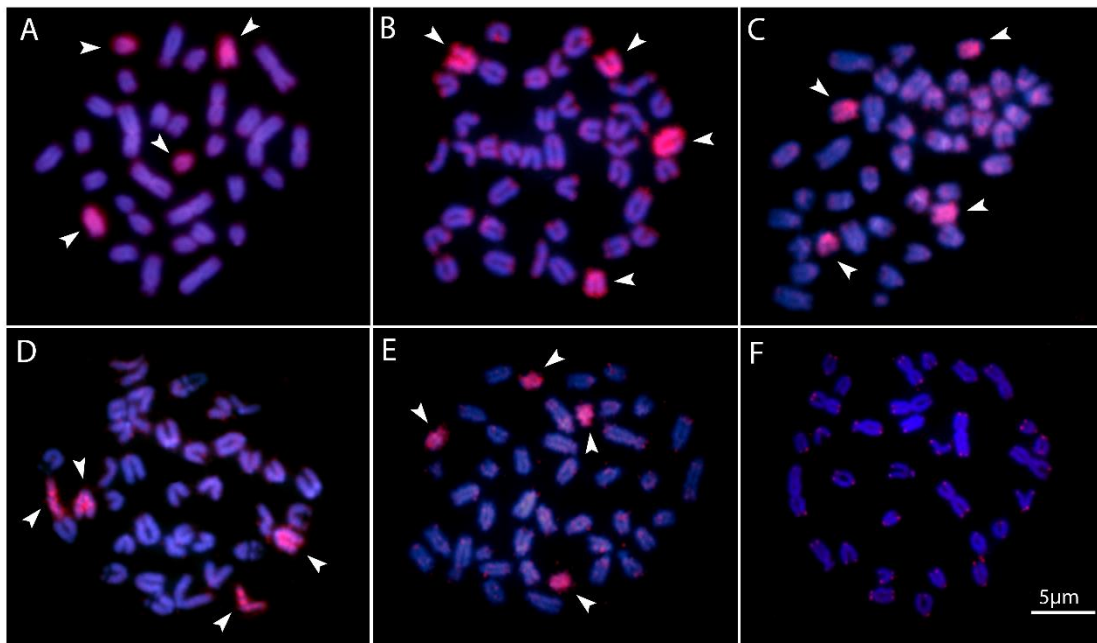
849 3.2. Chromosomal Mapping of Repetitive DNA Sequences

850 All the five species differ by the distribution of the multigene rDNA families. *Pyrrhulina*
 851 sp. and *P. marilynae* were the only species with only one chromosome pair bearing 18S rDNA
 852 sites, found at the telomeric region of acrocentric pairs 4 and 9, respectively. Six to twelve
 853 centromeric or telomeric sites occur in the other three species, including bitelomeric sites in
 854 *Pyrrhulina aff. marilynae* (pair 11) and *Pyrrhulina cf. laeta* (pairs 6 and 13). As for the 5S rDNA,
 855 from six to twelve centromeric sites occurred among species, including a syntenic condition for
 856 the 5S and 18S rDNA repeats in the chromosome pair 6 of *Pyrrhulina cf. laeta*, the same pair
 857 that displays bitelomeric 18S rDNA signals in this species (**Figure 2**). The distribution of the
 858 microsatellites (CA)₁₅, (GA)₁₅, and (CGG)₁₀ does not differ significantly among species,
 859 having a preferential location in the centromeric and telomeric regions of the chromosomes, in
 860 addition to some interstitial sites. However, (CA)₁₅ differs quantitatively, with a greater number
 861 of conspicuous sites compared to the other microsatellites, especially in *Pyrrhulina* aff.

862 *marilynae* and *Pyrrhulina* cf. *laeta*. In the same way, (CGG)10 occurs in smaller amounts in the
 863 five species (**Figure 3**). The (TTAGGG)*n* repeats showed the expected hybridization signals on
 864 telomeres of *P. marylinae* (**Figure 4F**). Whole chromosome painting–WCP.



865
 866 **Figure 3.** Male and female metaphase plates of *Pyrrhulina*
 867 *marilynae*; *Pyrrhulina* aff. *marilynae*; *Pyrrhulina* sp.; *P. obermulleri* and *Pyrrhulina* cf. *laeta* shows
 868 the general distribution of the microsatellites (GA)₁₅, (CA)₁₅ and (CGG)₁₀ on chromosomes. Bar =
 869 5 μm.



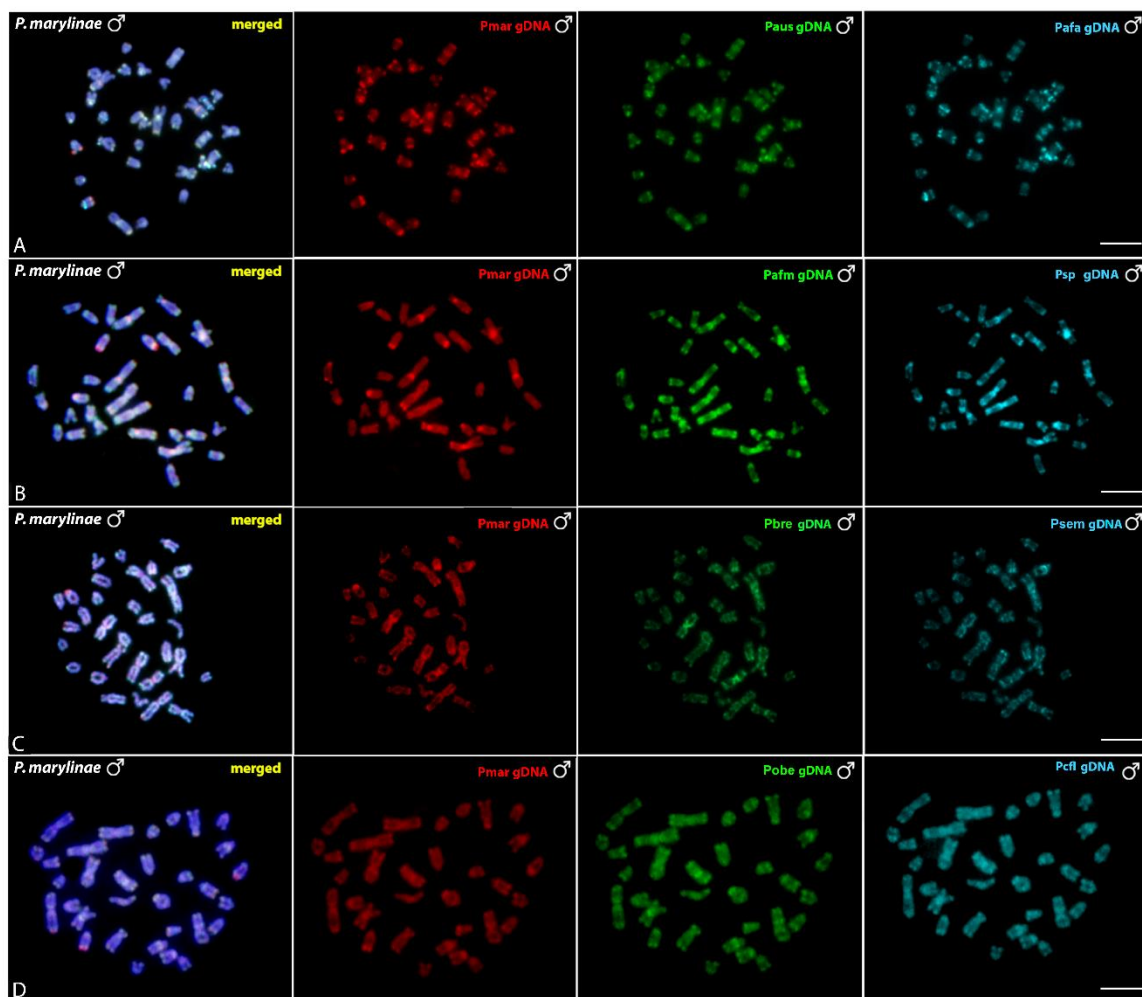
870
 871 **Figure 4.** Zoo-FISH with the PSEMI-Y probe on male metaphase plates of *P.*
 872 *marilynae*(A), *Pyrrhulina* aff. *marilynae* (B), *Pyrrhulina* cf. *laeta* (C), *Pyrrhulina* sp. (D), and *P.*
 873 *obermulleri* (E) shows the distribution of the telomeric (TTAGGG)*n* repeats in *P. marilynae*.
 874 Bar=5 μm.

875 Two acrocentric chromosome pairs were entirely painted with the PSEMI-Y probe in
876 *Pyrrhulina marilynae*, *P. obermulleri*, *Pyrrhulina* sp., *Pyrrhulina* aff. *marilynae* and *Pyrrhulina*
877 cf. *laeta* (Figures 4A–E).

878

879 3.3. Comparative Genomic Hybridization–CGH

880 The interespecific genomic comparison among *Pyrrhulina marilynae* and other
881 *Pyrrhulina* species (*P. semifasciata*, *P. australis*, *P. brevis*, *P. obermulleri*, *Pyrrhulina* aff.
882 *australis*, *Pyrrhulina* sp., *Pyrrhulina* aff. *marilynae*, *Pyrrhulina* cf. *laeta*) revealed a high level
883 of DNA compartmentalization, within all species presenting a distinct composition of repetitive
884 DNA sequences and specific signals. However, *P. marilynae* shows more evident species-
885 specific arrangements when compared to the other species. (Figure 5). Intraspecific genomic
886 hybridization between males and females did not show any clustering for sex-specific sequences
887 in all species (data not shown).



888

889 **Figure 5.** Comparative genomic hybridization (CGH) using male-derived genomic probes

890 from *Pyrrhulina* species hybridized onto male chromosomes of *P. marilynae*. The common genomic
891 regions are depicted in the 1st column in each line representing the experiments A-D. Hybridization
892 between the gDNA of *P. marilynae* (Pmar), *P. australis* (Paus)
893 and *Pyrrhulina* aff. *australis* (Pafa) (A); *P. marilynae* (Pmar), *Pyrrhulina* aff. *marilynae* (Pafm)
894 and *Pyrrhulina* sp. (Psp) (B); *P. marilynae* (Pmar), *P. brevis* (Pbre) and *P. semifasciata* (Psem) (C); *P.*
895 *marilynae* (Pmar), *P. obermulleri* (Pobe) and *Pyrrhulina* cf. *laeta* (Pcfl) (D). Bar = 5 μ m.
896

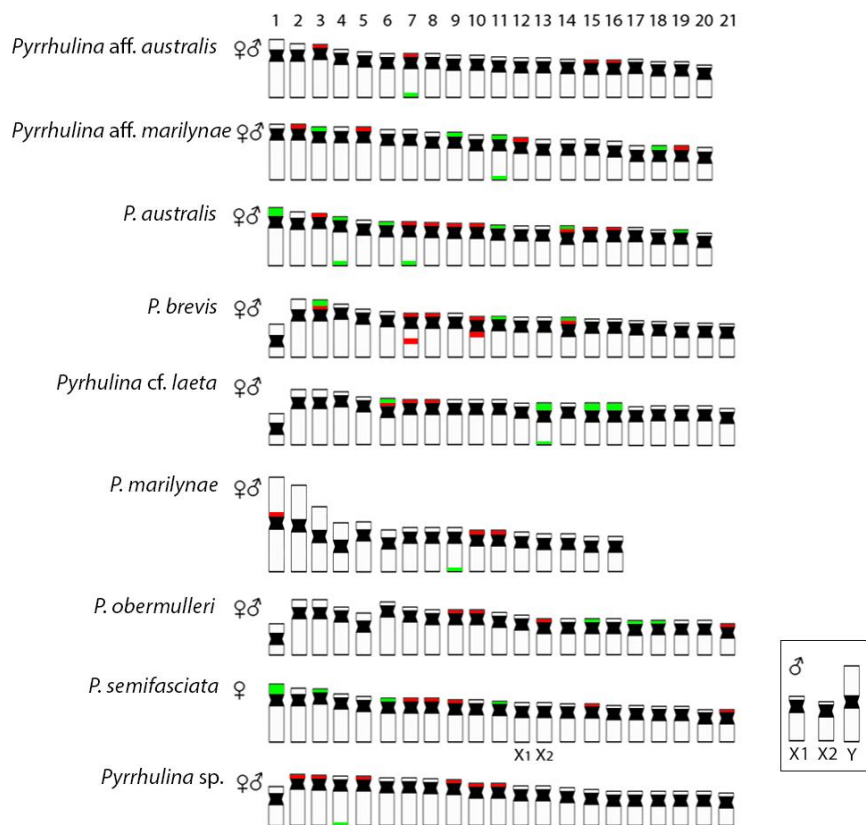
897 4. Discussion

898 Overall, two main evolutionary trends are proposed for the karyotypic evolution of the
899 Lebiasinidae: 1) the conservation of a plesiomorphic karyotype in the subfamily Lebiasininae,
900 with $2n = 36$ bi-armed chromosomes and, 2) high variations in diploid numbers and karyotypic
901 structures in the subfamily Pyrrhulininae, with the predominance of acrocentric chromosomes
902 (Sassi *et al.*, 2020). It is noteworthy that the karyotypic structure of Lebiasininae, $2n = 36$
903 biarmed chromosomes, is similar to that found in the sister family Ctenoluciidae (de Souza e
904 Sousa *et al.*, 2017; Sassi *et al.*, 2019; de Souza e Sousa *et al.*, 2021). Therefore, in this scenario,
905 the majority of the acrocentric chromosomes found in the species of the Pyrrhulininae are
906 probably derived from rearrangements such as centric fissions (Sassi *et al.*, 2020). However,
907 unlike other *Pyrrhulina* species, *P. marilynae* has the smallest $2n$ identified in the genus so far,
908 $2n = 32$, including four typical meta/submetacentric pairs. Some exceptions within the subfamily
909 showed secondary fusion events of acrocentric chromosomes giving rise to metacentric
910 chromosomes, reducing the diploid number as observed in *Nannostomus unifasciatus* (Sember
911 *et al.*, 2020). Biarmed chromosomes could also represent remnants of the ancestral karyotype
912 condition that were maintained during the evolutionary processes. However, no ITS was found
913 in any chromosome of *P. marilynae*, but such a scenario does not exclude the hypothesis of
914 fusion, given that telomeric regions can be lost after the rearrangement occurs (Bolzán, 2017).
915 Thus, to corroborate such hypotheses and to determine whether the evolutionary trajectory of
916 karyotype change in *Pyrrhulina* is directed mainly towards centric fusions or fissions,
917 cytogenetic data should be discussed in a larger phylogenetic framework of interspecific and
918 intergeneric relationships of Lebiasinidae.

919 CGH procedures have greatly assisted cytogenetic studies (Symonová *et al.*, 2013; Cioffi
920 *et al.*, 2017; Cioffi *et al.*, 2019), as among all *Pyrrhulina* studied so far. In fact, despite showing
921 close genomic similarities, the species also show considerable divergences, in addition to
922 species-specific repetitive DNA and C-band patterns, thus helping to understand their
923 differential evolutionary paths, considering the taxonomic problems still pending in this fish
924 group. In addition, multiple and syntenic ribosomal sites are not frequently observed among

925 fishes, but these chromosomal features are very informative cytotaxonomic markers regarding
 926 Pyrrhulinae species. Comparatively, they occur more frequently among *Pyrrhulina* than in
 927 other species of this subfamily (Moraes *et al.*, 2017; Moraes *et al.*, 2019; Sassi *et al.*, 2019; Sassi
 928 *et al.*, 2020; Toma *et al.*, 2019; Sember *et al.*, 2020). Like *Pyrrhulina* aff. *australis* (Moraes *et*
 929 *al.*, 2017), *Pyrrhulina* sp., and *P. marilynae* present multiple 5S rDNA sites and only one 18S
 930 rDNA site, thus differentiating them from *Pyrrhulina* aff. *marilynae*, *P. obermulleri*, and
 931 *Pyrrhulina* cf. *laeta*, as well as from some other *Pyrrhulina* species (Moraes *et al.*, 2017; Moraes
 932 *et al.*, 2019), which have multiple 5S and 18S rDNA sites. Furthermore, the syntenic condition
 933 for the 18S/5S rDNAs in *Pyrrhulina* cf. *laeta* is shared with *P. brevis* and *P. australis*, indicating
 934 a high rDNA diversity. (**Figure 6**). In its turn, the 18S rDNA clusters are distributed on distal
 935 chromosome positions for all investigated *Pyrrhulina* species (Moraes *et al.*, 2017; Moraes *et*
 936 *al.*, 2019; this study), as also occur among *Copeina* (Toma *et al.*, 2019), *Lebiasina* (Sassi *et al.*,
 937 2019), and *Nannostomus* (Sember *et al.*, 2020), so as in the species of the sister family,
 938 Ctenoluciidae (de Souza e Sousa *et al.*, 2017; de Souza e Sousa *et al.*, 2021).

939



940

941 **Figure 6.** Representative idiograms of *Pyrrhulina* species showing the distribution of the 18S
 942 (green) and 5S rDNA (red) sites on chromosomes, based on the present study and some other previous
 943 data (Moraes *et al.*, 2017; Moraes *et al.*, 2019). Bar = 5 μm.

944

945 Microsatellite distribution patterns have significantly contributed to evolutionary studies
946 in fish species, especially regarding sex chromosome differentiation (Kubat *et al.*, 2008; Cioffi
947 *et al.*, 2012; Terencio *et al.*, 2012; Kejnovský *et al.*, 2013; Poltronieri *et al.*, 2014; Yano *et al.*,
948 2014; de Freitas *et al.*, 2018). Among the five *Pyrrhulina* species now investigated, as well as in
949 other previous analyzed ones (Moraes *et al.*, 2017; Moraes *et al.*, 2019), the distribution of the
950 microsatellites did not significantly differ among them, although the (CA)₁₅ repeats present a
951 greater number of more conspicuous sites than the other microsatellites, especially in *Pyrrhulina*
952 *aff. marilynae* and *Pyrrhulina cf. laeta*. It is noteworthy that microsatellites have a preferential
953 location in the telomeric and centromeric regions of fish chromosomes (Cioffi and Bertollo,
954 2012), as occur with the (CA)₁₅ and (GA)₁₅ motifs in *Pyrrhulina*, despite some interstitial and
955 pericentromeric signs in *Pyrrhulina cf. laeta*, *P. marilynae*, *Pyrrhulina aff. marilynae* and
956 *Pyrrhulina sp.*, thus differentiating these species from others previously studied (Moraes *et al.*,
957 2017; Moraes *et al.*, 2019). Furthermore, it is also frequent that microsatellites and other
958 repetitive sequences occur in the association among fish (Cioffi and Bertollo, 2012), such as in
959 *Hepsetus odoe* (Carvalho *et al.*, 2017), *Lebiasina bimaculata* (Sassi *et al.*, 2019), and *Silurichthys*
960 *phaiosoma* (Ditcharoen *et al.*, 2020), for example. This is the scenario that also occurs in
961 *Pyrrhulina sp.*, in which the (CGG)₁₀ microsatellite located in the telomeric region of pair 4
962 shares the same chromosomal region with 18S rDNA repeats.

963 Fish, besides presenting high diversity in morphological and genetic characteristics, also
964 have a variety of sex chromosome systems (Sember *et al.*, 2021). About nine differentiated
965 systems, involving the XX/XY and ZZ/ZW sex chromosomes and their variations, have been
966 identified among species, including several Neotropical ones (Sember *et al.*, 2021). It is
967 noteworthy that among the multiple systems, the ♀X₁X₁X₂X₂/♂X₁X₂Y is the most prevalent
968 one, and commonly originated by centric or tandem fusions of the ancestral Y with an autosomal
969 member of the karyotype, giving rise to neo-Y chromosomes, as identified in a variety of fish
970 species (Sember *et al.*, 2021). That includes *P. semifasciata*, the only Lebiasinidae representative
971 highlighting heteromorphic sex chromosomes so far (Moraes *et al.*, 2019), in addition to a
972 putative ZZ/ZW sex system present in *Lebiasina bimaculata* (Sassi *et al.*, 2019). Although our
973 intraspecific CGH results in the current analyzed species did not reveal any sex-specific
974 differentiated region, our WCP experiment with the Y-derived probe of *P. semifasciata* entirely
975 painted two acrocentric pairs, suggesting that putative proto-XY chromosomes may occur in
976 these species. Thus, it supports our previous hypothesis on the origin of the *P. semifasciata* sex
977 chromosome system through centric fusion between the non-homologous acrocentric, giving rise

978 to the large metacentric Y chromosome. That can be considered as an apomorphy of this species
979 when compared to others of the genus. Furthermore, the experiments also showed that although
980 the karyotype of *P. marilynae* has large metacentric chromosomes, these do not correspond to
981 the heteromorphic sex chromosome of *P. semifasciata* (**Figure 4**).

982 5. Conclusion

983 Our data advances the understanding of evolutionary trends of the Lebiasinidae,
984 particularly concerning *Pyrrhulina*. Karyotypes with $2n = 40-42$, with the predominance of
985 mono-armed chromosomes, are more frequent among its species, except for *P. marilynae*, which
986 has a smaller diploid number ($2n = 32$), and several atypical biarmed chromosomes, a
987 characteristic that differentiates this species from the others analyzed in the genus. However, we
988 cannot rule out the hypothesis that this karyotypic reduction ($2n = 32$) may have been generated
989 by secondary fusions that allowed the formation of the four meta/submetacentric pairs identified
990 in *P. marilynae*. The present data also highlighted the putative proto-XY chromosomes that may
991 occur in these species and support the occurrence, through centric fusion, of the multiple sex
992 chromosome system of *P. semifasciata* as an independent evolutionary event of this Lebiasinidae
993 species. Our results highlight the importance of chromosomal data as valuable markers for
994 understanding the evolutionary relationships among Lebiasinidae species.

995

996 References

997 All references are compiled in the end of this thesis.

998 .

999

1000

1001

1002

1003

1004

1005

1006

1007

1008

1009

1010

1011

1012

1013

The Genetic Differentiation of *Pyrrhulina* (Teleostei, Characiformes) Species is Likely Influenced by Both Geographical Distribution and Chromosomal Rearrangements

Pedro Henrique Narciso Ferreira, Fernando Henrique Santos de Souza, Renata Luiza Rosa de Moraes, Manolo Fernandez Perez, Francisco de Menezes Cavalcante Sassi, Patrik Ferreira Viana, Eliana Feldberg, Tariq Ezaz, Thomas Liehr, Luiz Antônio Carlos Bertollo and Marcelo de Bello Cioffi

Frontiers in Genetic (2022) – DOI: 10.3389/fgene.2022.869073

1015

1016

1017

Abstract

1018

1019 Allopatry is generally considered to be one of the main contributors to the remarkable

1020 Neotropical biodiversity. However, the role of chromosomal rearrangements including neo-sex

1021 chromosomes for genetic diversity is still poorly investigated and understood. Here, we assess

1022 the genetic divergence in five *Pyrrhulina* species using population genomics and combined the

1023 results with previously obtained cytogenetic data, highlighting that molecular genetic diversity

1024 is consistent with their chromosomal features. The results of a principal coordinate analysis

1025 (PCoA) indicated a clear difference among all species while showing a closer relationship of

1026 the ones located in the same geographical region. This was also observed in genetic structure

1027 analyses that only grouped *P. australis* and *P. marilynae*, which were also recovered as sister

1028 species in a species tree analysis. We observed a contradictory result for the relationships

1029 among the three species from the Amazon basin, as the phylogenetic tree suggested *P.*1030 *obermulleri* and *P. semifasciata* as sister species, while the PCoA showed a high genetic1031 difference between *P. semifasciata* and all other species. These results suggest a potential role

1032 of sex-related chromosomal rearrangements as reproductive barriers between these species.

1033

1034

1035

1036

1037

1038

1039

1040

1041 1. Introduction

1042

1043 The Neotropical region harbors most of the known fish diversity, with more than 5,200
1044 valid species, however, there is additional evidence that many of them are yet to be described
1045 (Fricke *et al.*, 2021). Several reasons are suggested to be related to this huge diversity, and
1046 among them, the evolution of reproductive barriers reducing gene flow plays a key role in
1047 creating reproductive incompatibilities between species (Mayr, 1963). The evolution of strong
1048 reproductive barriers is essential for coexistence of species, especially for sympatric ones
1049 (those whose geographical distribution overlaps), even if the isolation in sympatry has preceded
1050 the overlap of species that currently coexist in the same region, in a secondary contact (Mayr,
1051 1999; Coyne and Orr, 2004).

1052 Among animals, most cases of post-zygotic isolation are caused by genetic
1053 incompatibilities, among which chromosomal rearrangements including specific sex
1054 chromosome-systems are of fundamental importance (Bateson, 1909; Dobzhansky, 1933;
1055 Muller, 1942; Coyne and Orr, 2004). Such chromosomal rearrangements can prevent
1056 introgression and reduce gene flow by suppressing recombination (Machado *et al.*, 2007;
1057 Yannic *et al.*, 2009; McGaugh and Noor, 2012; Ostberg, *et al.*, 2013; Presgraves, 2018; Potter,
1058 *et al.*, 2021). However, the contribution of these processes for biodiversity in Neotropical fish
1059 species is still poorly understood.

1060 The Lebiasinidae family is distributed throughout Central and South America, with 75
1061 species divided into two subfamilies: Lebiasininae and Pyrrhulininae (Weitzman and
1062 Weitzman, 2003; Froese and Pauly, 2014; Fricke *et al.*, 2021). The subfamily Pyrrhulininae is
1063 the most diverse, including the genera *Derhamia*, *Nannostomus*, *Copella*, *Copeina*, and
1064 *Pyrrhulina* (Fricke *et al.*, 2021). Recent cytogenetic and molecular data have added significant
1065 contributions to understanding evolutionary relationships of these genera (Moraes *et al.*, 2017,
1066 Moraes *et al.*, 2019, Sassi *et al.*, 2019; Toma *et al.*, 2019; Sember *et al.*, 2020; Moraes *et al.*,
1067 2021). Particularly, concerning *Pyrrhulina*, its diploid number (2n) ranges from 32 to 42
1068 chromosomes, with *Pyrrhulina* aff. *australis*, *P. australis* (Eigenmann and Kennedy, 1903),
1069 *Pyrrhulina* aff. *marilynae* and *Pyrrhulina* sp. present 2n = 40 chromosomes, whereas *P. brevis*
1070 (Steindachner, 1876), *P. obermulleri* (Allen *et al.*, 1926), and *Pyrrhulina* cf. *laeta* have 2n =
1071 42 chromosomes, both in males and females. Differently from the others, *P. semifasciata*
1072 (Steindachner, 1876) has divergent 2n among sexes (2n = ♀42 and ♂41) due to its exclusive
1073 multiple ♀X1X1X2X2/♂X1X2Y sex chromosome system (Moraes *et al.*, 2017; Moraes *et al.*,
1074 2019). In addition, *P. marilynae* (Netto-Ferreira and Marinho, 2013) also differs from its

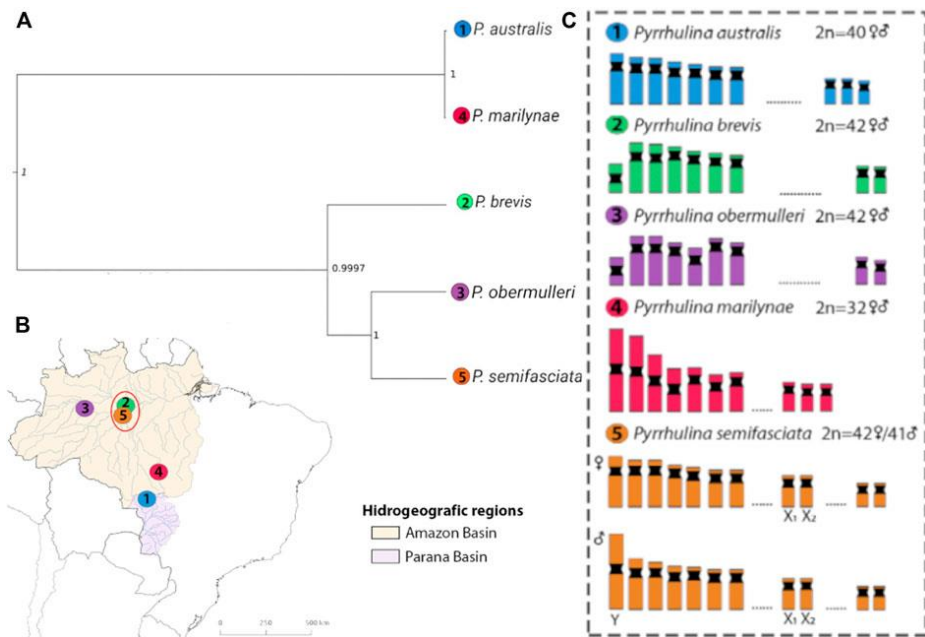
1075 congeneric species having $2n = 32$ chromosomes, due to a series of chromosomal fusions
1076 (Moraes *et al.*, 2021).

1077 The development and improvement of large-scale genotyping-by-sequencing (GBS)
1078 procedures allowed high-resolution analysis using Single Nucleotide Polymorphisms (SNPs)
1079 for genetic diversity studies in non-model organisms (Steane *et al.*, 2011; Yang *et al.*, 2013;
1080 Sánchez-Sevilla *et al.*, 2015; Alkimin *et al.*, 2018; Souza *et al.*, 2019; Oliveira *et al.*, 2020;
1081 Sassi *et al.*, 2021). Combining such genomic and cytogenetic data for pairs of
1082 species/populations in which there are variations related to geographic distribution, analysis of
1083 chromosomal rearrangements, and sex chromosome systems provide a critical tool to
1084 understanding the role of these events to generate biodiversity. The present study applies
1085 cytogenetic and genomic approaches in five *Pyrrhulina* species with distinct geographic
1086 distributions. Here, we aimed to assess the genetic diversity in five *Pyrrhulina* species by
1087 combining population genomic with previously obtained cytogenetic data. Our results
1088 highlighted that genomic diversity is consistent with the chromosomal features and provided
1089 hypothesis on the potential role of chromosomal rearrangements, especially those involving
1090 the sex chromosomes, in fostering genetic differentiation.

1091 2. Materials and Methods

1092 2.1. *Sampling*

1093 Collection sites, number, and sex of the specimens are given in **Figure 1; Table 1.**
1094 Sampling authorizations were obtained from the Brazilian Environmental Agency, Instituto
1095 Chico Mendes de Conservação da Biodiversidade/Sistema de Autorização e Informação em
1096 Biodiversidade (ICMBio/SISBIO - license no. 48628-14) and Sistema Nacional de Gestão do
1097 Patrimônio Genético e do Conhecimento Tradicional Associado (SISGEN - A96FF09). The
1098 distribution data was obtained from the analysis of scientific collection materials and previous
1099 literature (Bertaco *et al.*, 2016; Dagosta and Depinna, 2021).



1100

1101 **Figure 1:** Phylogenetic relationships of *Pyrrhulina* species analyzed and their distribution. (A)—
 1102 Species tree recovered with SNAPP, with branch lengths measured in units of expected number of
 1103 mutations per site, based on dataset I: *P. australis* (1), *P. brevis* (2), *P. obermulleri* (3); *P. marilynae*
 1104 (4); and *P. semifasciata* (5). (B)—South America map indicating the origin of *Pyrrhulina* species
 1105 analyzed. Colored areas indicate the distribution of the species: *P. australis* (blue), *P. brevis* (green), *P.*
 1106 *obermulleri* (yellow); *P. marilynae* (purple); and *P. semifasciata* (pink). The numbered circles indicate
 1107 the collection sites of each species. The red ellipse indicates syntopic species (sampled in the same
 1108 area). (C)—Idiograms with partial karyotypes of each species and the sex chromosomes exclusively
 1109 found in *P. semifasciata* are boxed.

1110

1111

1112 **Table 1.** Species, diploid numbers (2n), sex chromosome systems, numbers of individuals
 1113 cytogenetically analyzed, and the number of individuals sequenced

1114

Species	2n	Sex chromosomes	Sampling location	Latitude/Longitude	Cytological analysis	Sequence analysis	References
<i>P. australis</i>	♀♂40	Homomorphic	Barra do Bugres—MT	-15.04275,-57.11054	18♂ 30♀	6	Moraes et al. (2017)
<i>P. brevis</i>	♀♂42	Homomorphic	Adolpho Ducke Reserve—AM	-2.58207,-59.55530	17♂ 13♀	6	Moraes et al. (2019)
<i>P. semifasciata</i>	♀♂42 ♂41	X ₁ X ₁ X ₂ X ₂ /X ₁ X ₂ Y	Careiro—AM	-3.51000,-60.04000	12♂ 07♀	6	Moraes et al. (2019)
<i>P. obermulleri</i>	♀♂42	Homomorphic	Tefé—AM	-3.25507,-64.44548	21♂ 12♀	6	Moraes et al. (2021)
<i>P. marilynae</i>	♀♂32	Homomorphic	Ipiranga do Norte—MT	-11.36020,-55.56270	14♂ 08♀	6	Moraes et al. (2021)

Abbreviations: AM, Amazonas; MT, Mato Grosso Brazilian states. Chromosomal data refer to previous studies, according to references.

1115

1116

1117

1118 2.2. DArTseq Sequencing Procedure and Data Filtering

1119 Liver tissue from all individuals was used to perform DArTseq sequencing procedures at
 1120 Diversity Arrays Technology Pty Ltd. This sequencing method uses a combination of restriction

1121 enzymes (SbfI and PstI) that enrich hypomethylated regions (Kilian *et al.*, 2012). Sequencing of
1122 the obtained libraries was carried out on the Illumina HiSeq 2500 platform.

1123 The raw data were processed in two different ways to generate the following datasets (I)
1124 a matrix of SNPs using Ipyrad v. 0.9.84 (Eaton and Overcast, 2020) and (II) a phased sequence
1125 file obtained with pyRAD v3.0.66 (Eaton, 2014). In both, the sequencing adapters were trimmed,
1126 and all sequences shorter than 35 base pairs or presenting more than five low-quality bases ($Q <$
1127 20) were not considered. In dataset I, a single SNP per locus was selected, to reduce the inclusion
1128 of linked SNPs, and the SNPs were coded as 0 for reference state homozygotes, 1 for
1129 heterozygotes, and 2 for alternative state homozygotes.

1130 The raw data is available in the database of the National Center for Biotechnology
1131 Information, whose project access code is PRJNA804560 (access link:
1132 https://www.ncbi.nlm.nih.gov/Traces/study/?acc=PRJNA804560&eo=acc_s%3Aa).
1133 Additionally, datasets one and two are available at [https://github.com/PHnarciso/Dataset-1-and-](https://github.com/PHnarciso/Dataset-1-and-2)
1134 [2---Manuscript-Pyrrhulina](https://github.com/PHnarciso/Dataset-1-and-2).

1135

1136 2.3. *Assessment of Markers Under Selection*

1137 A BayeScan analysis was carried to search for potential markers under selection in both
1138 datasets (Foll and Gaggiotti, 2008). We performed a total of 5,000 MCMC (Markov Chain
1139 Monte Carlo) runs and thinning of 10, with a prior odds value of 100. Values of False Discovery
1140 Rate (FDR) were used to classify outliers, and only loci with values lower than 0.01 were
1141 considered outliers and removed from subsequent analysis.

1142

1143 2.4. *Genetic Diversity*

1144 Using dataset II, an analysis was performed in the DnaSP software v. 6.12.03 (Rozas *et*
1145 *al.*, 2019), to obtain the haplotype diversity (H_d), Tajima's D (D), and two measures of
1146 nucleotide diversity per site, π and Watterson's θ_w . Differentiation was also estimated
1147 from the nucleotide divergence between samples using the average number of nucleotide
1148 substitutions per site between pairs of samples from different species (D_{xy}) and the net
1149 divergence, corrected for variation within the samples analyzed (D_a).

1150

1151 2.5. *Genetic Structure and Analysis of Molecular Variance (AMOVA)*

1152 A principal coordinate analysis (PCoA) in the R package dartR (Gruber *et al.*, 2018) was
1153 used to investigate the genetic structure among species. The genetic structure was also
1154 investigated with fastSTRUCTURE (Raj *et al.*, 2014), using the "Lizards-are-awesome" pipeline

1155 (Melville *et al.*, 2017). We used the chooseK.py command to select the number of clusters that
1156 maximizes likelihood and is more informative for the structure from our dataset. The results
1157 from fastStructure were visualized with Clumpak (Kopelman *et al.*, 2015). Additionally, an
1158 analysis of molecular variance (AMOVA) was also performed using dataset I, with samples
1159 grouped as follows: 1) by species, 2) by the clusters from the best K value on fastStructure, 3)
1160 by the clustering pattern generated on the PCoA, and 4) by the presence or absence of the
1161 multiple sex chromosome system.

1162

1163 2.6. *Species Tree*

1164 We used the package SNAPP in BEAST 2.6.4 (Bouckaert *et al.*, 2014) to infer the species
1165 tree topology. We included only polymorphic sites, used the default prior for coalescence rate,
1166 and calculated backwards and forward substitution rates (parameters u and v) based on the
1167 empirical data. We applied a chain length of two million generations, sampling every 5000
1168 iterations. Convergence was evaluated in Tracer 1.7.1 (Rambaut *et al.*, 2018). We obtained the
1169 MCC tree based with common ancestor heights in TreeAnnotator, with the first 25% generated
1170 trees discarded as burn-in. We exported the consensus tree in FigTree 1.4.4.

1171

1172 2.7. *Analysis of Introgression*

1173 We assessed admixture between lineages by calculating Patterson's D-statistics (ABBA-
1174 BABA test) in Ipyrad v. 0.9.84 (Eaton and Overcast, 2020) using pooled SNP frequencies of
1175 individuals from each species (Durand *et al.*, 2011). We performed 4-taxon tests according to
1176 the recovered SNAPP topology (**Figure 1**), using either *P. marilynae* or *P. australis* as the
1177 outgroup, *P. brevis* as P3 and *P. semifasciata* and *P. obermulleri* as either P1 or P2. Significance
1178 was measured with 1,000 bootstrap replicates by resampling loci with replacement (following
1179 Eaton and Ree, 2013). Results were considered significant according to their Z-scores
1180 (significant values >3), which quantifies the number of bootstrap standard deviations in which
1181 the D-statistic values deviates from its expected value of zero.

1182

1183 3. Results

1184 3.1. *Sequencing, Filtering, and Detection of Markers Under Selection*

1185 Sequencing of DArTSeq resulted in two million reads per sample, on average, a total of
1186 5,149 SNP-markers were obtained after performing all filtering steps in dataset I, and a total of
1187 5,604 loci were obtained in dataset II. According to the BayeScan result, none of the loci were

1188 potentially under selection, as all FDR values were higher than 0.65 and 0.97 for dataset I and
 1189 dataset II respectively. Thus, all markers were maintained in subsequent analyses.

1190

1191 3.2. Genetic Diversity and Structure

1192 In general, all species showed low diversity values. Values of π and θ_w were closely
 1193 related across all sampled groups, with slightly higher estimates in *P. obermulleri* and *P.*
 1194 *semifasciata*, while *P. marilynae* showed the lowest values. (**Table 2**).

1195 **Table 2.** Estimated genome-wide genetic diversity of genus *Pyrrhulina* by species.

Species	Sample size	Hd	π	θ_w	D
<i>P. australis</i>	6	0.1230	0.0024	0.0026	-0.2004
<i>P. brevis</i>	6	0.1048	0.0020	0.0024	-0.3512
<i>P. obermulleri</i>	6	0.2033	0.0042	0.0044	-0.1656
<i>P. marilynae</i>	6	0.0338	0.0007	0.0006	0.1380
<i>P. semifasciata</i>	6	0.1712	0.0033	0.0039	-0.4412

Abbreviations: Hd - haplotype diversity; π - nucleotide diversity; θ_w - Watterson theta per site and D - Tajima's D.

1196

1197

1198 The nucleotide divergence (Dxy values) and net divergence (Da values) estimates
 1199 between individuals sampled of different species ranged from 0.01770 to 0.00660 as shown in
 1200 **Figure 2**. The lowest divergence values estimates were presented for *P. australis* and *P.*
 1201 *marilynae*, and the highest values were observed for comparisons of *P. semifasciata* with these
 1202 species.

1203

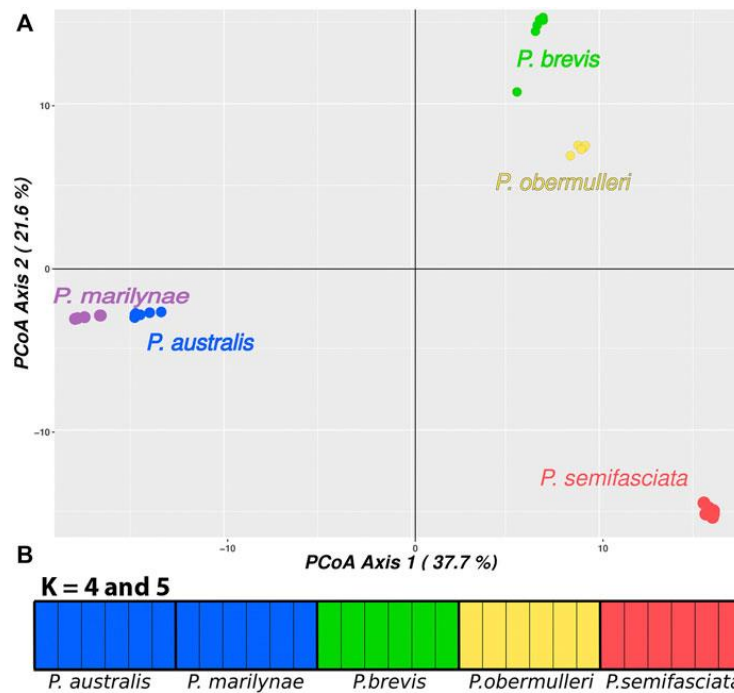
	<i>P. australis</i>	<i>P. brevis</i>	<i>P. obermulleri</i>	<i>P. marilynae</i>	<i>P. semifasciata</i>
<i>P. australis</i>		0.01320	0.01550	0.00800	0.01710
<i>P. brevis</i>	0.01110		0.01210	0.01380	0.01380
<i>P. obermulleri</i>	0.01230	0.00900		0.01600	0.01460
<i>P. marilynae</i>	0.00660	0.01250	0.01360		0.01770
<i>P. semifasciata</i>	0.01440	0.01120	0.01090	0.01580	

1204

1205 **Figure 2.** Pairwise Dxy per Species is represented in the upper diagonal, and Da in the lower diagonal.
 1206 Higher values are shown in green, and as the values decrease the color changes to yellow, orange, and
 1207 then red for lower values.

1208

1209 The PCoA results separate all species and indicate a higher similarity for species in the
 1210 same regions, as *P. brevis* and *P. obermulleri* are more similar to each other, as are *P. australis*
 1211 and *P. marilynae*. In turn, *P. semifasciata* appeared as the most different species of the group
 1212 (**Figure 3**).



1213

1214 **Figure 3.** (A) Genetic diversity in *Pyrrhulina* species according to a PCoA. The PCoA recovered 37.7%
 1215 of the total variation in the first principal coordinate (PC1), and 21.6% in the second principal coordinate
 1216 (PC2). (B)—Results for fastStructure with K = 4 and K = 5. Each vertical bar represents an individual;
 1217 the bar colors represent the group in which the fastStructure classified the individual; the legend below
 1218 indicates their species.

1219

1220 Results from fastStructure suggested K = 4 as the number of clusters that maximizes both
 1221 likelihood and is more informative for genetic structure, being the one that best explains the
 1222 complexity of the data. It is worth mentioning that the clusterization presented in K = 5 is
 1223 identical to that presented by K = 4, with both results combining *P. australis* and *P. marilynae*.
 1224 AMOVA results suggested that the clustering strategy presenting the highest variation between
 1225 groups and the lowest variation within groups was achieved when each separate species was
 1226 considered (83.66% variation between groups), followed by the fastStructure K = 4 result and
 1227 by the PCoA (**Table 3**).

1228

1229 **Table 3.** AMOVA percentage of variation within and between each of the tested groups:
 1230 1) by species, 2) by the best K in the fast structure, 3) by the groups generated in PCoA, and 4)
 1231 by the presence or absence of sex chromosomes.

Clustering	Species	FastStructure K = 4	PCoA	Presence/absence of sex chromosomes
Variation between groups	83.664	73.916	61.593	46.534
Variation within group	2.016	12.465	25.087	41.805

1232

1233 3.3. *Species Tree and Analysis of Introgression*

1234 The species tree recovered in SNAPP showed a relationship between species similar to
 1235 the structure shown in PCoA (**Figure 3**), showing *P. australis* and *P. marilynae* as sister species.
 1236 A sister species relationship was also recovered for *P. semifasciata* and *P. obermulleri*, with *P.*
 1237 *brevis* closer to this last two (**Figure 1**). Results of the admixture tests using D-statistics were
 1238 not able to detect significant introgression in *P. semifasciata* or *P. obermulleri*, regardless of
 1239 whether *P. marilynae* or *P. australis* were considered as the outgroup (Table 4). This result
 1240 agrees with the lack of admixture suggested by fastSTRUCTURE (**Figure 3**).

1241

1242 **Table 4.** Results of the ABBA-BABA test for admixture assessment.

Outgroup	P ₃	P ₂	P ₁	D	Z	ABBA	BABA
<i>P. marilynae</i>	<i>P. brevis</i>	<i>P. obermulleri</i>	<i>P. semifasciata</i>	-0.0214164	0.44500958	180.753565	188.665185
<i>P. australis</i>	<i>P. brevis</i>	<i>P. obermulleri</i>	<i>P. semifasciata</i>	0.00523111	0.1052923	182.665167	180.764028
<i>P. marilynae</i>	<i>P. brevis</i>	<i>P. semifasciata</i>	<i>P. obermulleri</i>	-0.0052311	0.1035013	180.764028	182.665167
<i>P. australis</i>	<i>P. brevis</i>	<i>P. semifasciata</i>	<i>P. obermulleri</i>	-0.0052311	0.10302304	180.764028	182.665167

Abbreviations: D, overrepresentation of ABBA against BABA patterns as measured by the D-statistics; Z, Z-score test to assess whether the D-statistics is significantly ($Z > 3$) different from zero; ABBA, frequency of ABBA patterns; BABA, Frequency of BABA patterns.

1243

1244

1245 4. Discussion

1246 Here the first genomic evaluation of five *Pyrrhulina* species was performed. Our results
 1247 highlight that genetic diversity among the analyzed *Pyrrhulina* species is consistent with their
 1248 chromosomal features. In addition, evidence was found that the occurrence of chromosomal
 1249 rearrangements including variation in sex chromosome systems might have contributed to
 1250 increase differentiation.

1251 Overall, the genetic diversity indexes (π ; θ_W) (**Table 2**) were low, being the highest ones
 1252 observed in *P. obermulleri* and *P. semifasciata* and the lowest in *P. marilynae* followed by *P.*
 1253 *brevis*. Low diversity values are somewhat expected due to the nature of our sequencing
 1254 technique (see methods) and similar results were found in populations from *Hoplias malabaricus*
 1255 under the same sequencing technique (Souza *et al.* submitted). According to Dxy and Da values
 1256 (**Figure 2**), *P. semifasciata* and *P. marilynae* are very distinct from each other, presenting the
 1257 highest observed values (0.01770 and 0.0158). They are also distinct morphologically (Netto-
 1258 Ferreira and Marinho, 2013) and present non-overlapping distributions in the Amazon basin.
 1259 *Pyrrhulina semifasciata* occur in the Purus, Juruá, Negro, Branco rivers, Amazonas main
 1260 channel (Dagosta and De Pinna, 2021), and Madeira River while *P. marilynae* is restricted to the
 1261 upper portions of Tapajós and Xingu (Netto-Ferreira e Marinho, 2013) (**Figure 1**). Similarly,
 1262 values of Dxy and Da between *P. semifasciata* and *P. australis* are also very high (0.0171 and

1263 0.0144), indicating their genetic distinctiveness. Furthermore, their distribution does not overlap
1264 (**Figure 1**) and they are also quite distinct morphologically and probably distantly related
1265 species, according to a morphology-based phylogenetic analysis (Marinho, 2014). This results
1266 are also in agreement with the species tree, as *P. marilynae* and *P. australis* were recovered as
1267 sister species in a distinct clade (**Figure 1**). However, it is important to emphasize that a more
1268 comprehensive species-level sampling is still necessary before claiming sister species
1269 relationships, especially in taxa that are apparently divergent such as *P. brevis* and *P.*
1270 *obermulleri*.

1271 *Pyrrhulina semifasciata*, the only species in the family up to now analyzed with
1272 heteromorphic sex chromosomes, presents high genetic differentiation values when compared
1273 to all other species. This could suggest that the presence of such multiple sex system promoted
1274 genetic differentiation in the species. The association of sex chromosomes and a high genetic
1275 differentiation was also evidenced in previous studies for some populations of other species such
1276 as the wolf fishes *Hoplias malabaricus* (Souza *et al.*, submitted) and *Erythrinus erythrinus*
1277 (Souza *et al.*, 2022). In addition, other studies suggest that an event of sex chromosome turnover
1278 in plants could have promoted the reduction of gene flow between groups of *Rumex hastatulus*,
1279 which could have contributed to further accumulation of genetic differences (Beaudry *et al.*,
1280 2019). Furthermore, the emergence of a neo-sex chromosome system is suggested as a factor
1281 that may have driven the speciation process in sticklebacks (Kitano *et al.*, 2009). Therefore, the
1282 emergence of sex neo-chromosomes could result in a rapid evolutionary mechanism fixing
1283 genetic variation in different species (Beaudry *et al.*, 2019). Indeed, our results suggest that *P.*
1284 *semifasciata*, which was collected in syntopy with *P. brevis* and presents a different
1285 chromosomal structure with a multiple sex chromosome system, is also genetically highly
1286 divergent from that latter species.

1287 Therefore, we present three main hypotheses for the observed scenario (I) *P. brevis* and
1288 *P. semifasciata* evolved in allopatry. Later, their distribution overlapped and the current genetic
1289 differences are the result of this previous allopatric period and not related to the sex
1290 chromosomes emergence (II) these species evolved in allopatry and the sex chromosomes
1291 present in *P. semifasciata* may have acted as an additional barrier to introgression, fostering their
1292 genetic differentiation after they became sympatric, and (III) the emergence of a multiple sex
1293 chromosome system of the X₁X₂Y-type in *P. semifasciata* have acted as key factor to reduction
1294 of the gene flow and contributed to the speciation process and the significant genetic
1295 differentiation observed for this species.

1296 The PCoA result also suggested that *P. semifasciata* stayed isolated from all other
1297 species, while *P. brevis* clustered with *P. obermulleri* (**Figure 3**). Many works highlight the
1298 important role of neo-sex chromosomes in preventing introgression, which is agreement with
1299 the lack of introgression between sympatric species detected here (**Table 4**), due to pairing
1300 problems associated with meiotic segregation of heterozygous rearrangements (e.g., McKee *et*
1301 *al.*, 1998; Kitano and Peichel, 2012; Beaudry *et al.*, 2019). Similarly, sex chromosomes might
1302 promote speciation, as some genes that play a role in reproductive isolation between populations
1303 can be accumulated in neo-sex chromosomes (Reinhold, 1998; Lindholm and Breden, 2002;
1304 Kitano and Peichel, 2012). Haldane's rule postulates that hybrids of the heterogametic sex from
1305 closely related species are often sterile, thus hybrid incompatibility also may act as a
1306 reproductive isolating barrier and contribute to prevent introgression (Haldane, 1922; Coyne and
1307 Orr, 2004). In both scenarios, the neo-sex chromosomes system could have contributed to
1308 genetic differentiation or speciation. Hence, it may be possible that the chromosomal
1309 rearrangements present in *P. semifasciata* may have had an impact on the diversity of *Pyrrhulina*
1310 species.

1311 In contrast, some species showed low differentiation, indicating that they are more
1312 similar genetically. The Dxy and Da values between *P. marilynae* and *P. australis* were the
1313 lowest ones (0.008 and 0.0066 respectively) and these two species were recovered as sister
1314 species in our phylogenetic analysis (**Figure 1**). Also, both species share with *P. vittata* a series
1315 of unique morphological characters which indicate that they form a monophyletic clade (Netto-
1316 Ferreira and Marinho, 2013). *Pyrrhulina brevis* and *P. obermulleri* presented low Dxy and Da
1317 values as well (0.0121 and 0.0090) in addition to be close to each other in the PCoA analysis
1318 (**Figure 3**) and be recovered in the same clade in the species tree, although not as sister species
1319 (**Figure 1**). All Tajima's D values were negative except for *P. marilynae*. Negative results may
1320 suggest a recent event of population expansion, or that purifying selection is acting mainly in *P.*
1321 *semifasciata* and *P. brevis*. The small positive value presented by *P. marilynae* could indicate a
1322 bottleneck event, but this seems unlikely due to the low value.

1323 The results of PCoA indicated a clear clustering of species sampled in the same
1324 geographical region, except for *P. semifasciata*, which was collected in sympatry with *P. brevis*
1325 and did not cluster with any other species (**Figure 3**). In fastStructure K = 4 result, only *P.*
1326 *australis* and *P. marilynae* were grouped. In both fastStructure and PCoA results, *P. australis*
1327 and *P. marilynae* were closely related, and such a connection is also presented in the speciestree
1328 (**Figure 1**) and supported by the species tree presented by Marinho (2014).

1329 In addition, AMOVA results suggest that grouping individuals by species maximize the
1330 variation between groups, although the groups generated by fastStructure and PCoA have also
1331 shown informative values (**Table 3**). Therefore, AMOVA results show that the clustering of
1332 individuals by species best explains the complexity of the data and therefore suggests that the
1333 species are well separated. The relationships between river reorganizations and biodiversity are
1334 a complex issue, as previously isolated habitats and populations can be merged, increasing
1335 dispersal and local diversity, and reducing speciation and extinction rates. They can also separate
1336 previously connected environments, leading to increased genetic isolation and speciation, and
1337 extinction rates (Tagliacollo *et al.*, 2015; Albert *et al.*, 2018). Therefore, the complex
1338 biogeographic history of the region complicates the understanding of *Pyrrhulina* genetic
1339 diversity considering that the current geographic distribution of species may not be the same as
1340 in the past and a comprehensive species-level phylogeny is still necessary to infer past
1341 geographic distributions.

1342 It is widely known that chromosomal rearrangements might have a role in speciation
1343 (Rieseberg, 2001; Navarro and Barton, 2003; Basset *et al.*, 2008). Chromosomal rearrangements
1344 have the potential to limit introgression, thus facilitating the origin and maintenance of
1345 reproductive isolation through recombination suppression (Faria and Navarro, 2010; Sichová *et*
1346 *al.*, 2015). Here, *P. australis* and *P. marilynae* were recovered as sister species in our
1347 phylogenetic analysis. This suggests a low genetic difference despite their different
1348 chromosomal formulae. Conversely, the species *P. semifasciata*, the only with a multiple sex
1349 chromosome system, showed high differentiation to all other species. This furnishes additional
1350 evidence for the role of chromosomal rearrangements, especially those associated with sex
1351 chromosomes, as potential important reproductive barriers between these species.

1352

1353 5. Conclusion

1354 Our results highlighted the distribution of the genetic diversity among the analyzed
1355 *Pyrrhulina* species and contributed to our understanding of their evolutionary history. However,
1356 the scarcity of phylogenetic data involving all *Pyrrhulina* species does not permit us to do a
1357 cause-and-effect correlation. Besides, the occurrence of chromosomal rearrangements leading to
1358 the presence of the X1X2Y sex chromosome system in *P. semifasciata* could have led to an
1359 intensification of the genetic differentiation of this species by preventing introgression with the
1360 other species. Future work with a better population and species-level sampling is still needed to
1361 bring new insights to 1) species delimitation, 2) infer demographic trends, 2) infer past

1362 distributional ranges, and 4) study the tempo and mode of speciation, including chromosomal
1363 rearrangements as a mechanism for isolation.

1364

1365 **References**

1366 All references are compiled in the end of this thesis.

1367

1368

Chromosomal Rearrangements and Satellite DNAs: Extensive Chromosome Reshuffling and the Evolution of Neo-Sex Chromosomes in the Genus *Pyrrhulina* (Teleostei; Characiformes)

Renata Luiza Rosa de Moraes, Francisco de Menezes Cavalcante Sassi, Jhon Alex Dziechciarz Vidal, Caio Augusto Gomes Goes, Rodrigo Zeni dos Santos, José Henrique Forte Stornioli, Fábio Porto-Foresti, Thomas Liehr, Ricardo Utsunomia and Marcelo de Bello Cioffi

International Journal of Molecular Sciences (2023) – DOI: 10.3390/ijms241713654

1370

1371

1372

1373

Abstract

1374 Chromosomal rearrangements play a significant role in the evolution of fish genomes, being
1375 important forces in the rise of multiple sex chromosomes and in speciation events. Repetitive
1376 DNAs constitute a major component of the genome and are frequently found in
1377 heterochromatic regions, where satellite DNA sequences (satDNAs) usually represent their
1378 main components. In this work, we investigated the association of satDNAs with chromosome-
1379 shuffling events, as well as their potential relevance in both sex and karyotype evolution, using
1380 the well-known *Pyrrhulina* fish model. *Pyrrhulina* species have a conserved karyotype
1381 dominated by acrocentric chromosomes present in all examined species up to date. However,
1382 two species, namely *P. marilynae* and *P. semifasciata*, stand out for exhibiting unique traits
1383 that distinguish them from others in this group. The first shows a reduced diploid number (with
1384 $2n = 32$), while the latter has a well-differentiated multiple X_1X_2Y sex chromosome system. In
1385 addition to isolating and characterizing the full collection of satDNAs (satellitomes) of both
1386 species, we also in situ mapped these sequences in the chromosomes of both species. Moreover,
1387 the satDNAs that displayed signals on the sex chromosomes of *P. semifasciata* were also
1388 mapped in some phylogenetically related species to estimate their potential accumulation on
1389 proto-sex chromosomes. Thus, a large collection of satDNAs for both species, with several
1390 classes being shared between them, was characterized for the first time. In addition, the possible
1391 involvement of these satellites in the karyotype evolution of *P. marilynae* and *P. semifasciata*,
1392 especially sex-chromosome formation and karyotype reduction in *P. marilynae*, could be
1393 shown.

1394 1. Introduction

1395 Fishes are an incredibly diverse group with many chromosomal variations, including
1396 polyploidy, supernumerary chromosomes, distinct sex chromosome systems, and
1397 polymorphisms (Oliveira *et al.*, 2009). In fact, most cases of postzygotic isolation are caused by
1398 genetic incompatibilities, among which chromosomal rearrangements play a fundamental role
1399 (Bateson, 1909; Dobzhansky, 1933; Muller, 1942). Chromosomal changes have the potential to
1400 limit introgression, thus facilitating the origin and maintenance of reproductive isolation through
1401 recombination suppression (Faria and Navarro, 2010; Šíchová *et al.*, 2015). However, one of the
1402 most interesting evolutionary events refers to the emergence of neo-sex systems, when multiple
1403 sex chromosomes arise because of rearrangements between an autosome and a sex chromosome.
1404 This evolutionary step, also known as sex chromosome turnover, has the potential to suppress
1405 recombination next to breakpoints, creating new linkage groups between genes from distinct
1406 chromosomes, increasing the number of sex-linked genes, and accelerating the accumulation of
1407 genetic incompatibilities between populations (Vieira *et al.*, 2003).

1408 The impact of chromosomal rearrangements in fish karyotype evolution has been
1409 studied primarily from a cytogenetic point of view, with a particular emphasis on the
1410 chromosomal mapping of repetitive DNA sequences. The latter has proven to be a valuable
1411 source of information on the role of such sequences in genome organization and evolution
1412 (Biémont and Vieira, 2006; Khosraviani *et al.*, 2019). Satellite DNAs (satDNAs) are one of the
1413 most common repeated sequences, forming extensive arrays of largely similar repeating units
1414 (monomers) that make up a significant percentage of genomes (reviewed in Šatović-Vukšić and
1415 Plohl, 2023). Recently, given the integration of cytogenetics with high-throughput sequencing
1416 data from next-generation sequencing methods (NGS), the whole collection of different satDNA
1417 families (satellitome) of several species has been characterized, providing insights into several
1418 evolutionary issues, such as karyotype evolution, genome diversity, and phylogenetic
1419 relationships (Ruiz-Ruano *et al.*, 2016; Ferretti *et al.*, 2020; Bardella *et al.*, 2020; Cabral-de-
1420 Mello *et al.*, 2021; Montiel *et al.*, 2021; Vozdova *et al.*, 2021; Cabral-de-Mello *et al.*, 2023;
1421 Flynn *et al.*, 2023; Gržan *et al.*, 2023; Peona *et al.*, 2023). These satellites (satDNAs) are also
1422 thought to play a role in the evolution and structure of sex chromosomes, as well as chromosome-
1423 based speciation (Henikoff *et al.*, 2001; O'Neill *et al.*, 2004; Plohl *et al.*, 2012; Weissensteiner
1424 and Suh, 2019; Ferretti *et al.*, 2020; Shatskikh *et al.*, 2020; Flynn *et al.*, 2023).

1425 *Pyrrhulina* Valenciennes 1846 (Characiformes, Lebiasinidae) is the most diverse genus
1426 of the fish subfamily Pyrrhulininae, with 19 valid species (Frecke *et al.*, 2023). Many species
1427 remain unexplored due to their small sizes and, thus, difficult sampling; consequently, the genus

1428 presents unsolved taxonomic issues (Netto-Ferreira and Marinho, 2013). Recent research,
1429 however, has led to a better understanding of the evolution of Lebiasinidae species, including
1430 several *Pyrrhulina* ones, particularly from a cytogenetic and molecular genetics standpoint
1431 (Benzaquem *et al.*, 2015; Moraes *et al.*, 2017; Moraes *et al.*, 2019; Sassi *et al.*, 2019; Toma *et*
1432 *al.*, 2019; Sember *et al.*, 2020; Liu *et al.*, 2020; Moraes *et al.*, 2021; dos Santos *et al.*, 2022). In
1433 general, about half (i.e., nine out of the 19) *Pyrrhulina* species have been cytogenetically
1434 documented, demonstrating a quite conserved diploid chromosome number, ranging from 40 to
1435 42 chromosomes with karyotypes predominantly formed by acrocentric chromosomes (Moraes
1436 *et al.*, 2017; Moraes *et al.*, 2019; Moraes *et al.*, 2021; Froese and Pauly, 2023). Aside from
1437 distinctive karyotypes and diploid numbers, genomic content comparisons among all analyzed
1438 species reveal a significant degree of similarity between their genomes, with most of the
1439 variations related to their repetitive content (Moraes *et al.*, 2021). Most species have multiple 5S
1440 rDNA and 18S rDNA sites, with some species having a syntenic arrangement of these rDNAs
1441 (Moraes *et al.*, 2017; Moraes *et al.*, 2019; Moraes *et al.*, 2021). Among all *Pyrrhulina* species,
1442 *P. marilynae* and *P. semifasciata* stand out for exhibiting characteristics that distinguish them
1443 from other species in the genus. In the first case, *P. marilynae* shows a significant karyotypic
1444 reduction, presenting $2n = 32$ chromosomes with four metacentric pairs not observed in other
1445 species, presumably due to secondary fusions (Moraes *et al.*, 2021). *P. semifasciata*, on the other
1446 hand, contains the sole morphologically differentiated sex chromosome system found in the
1447 genus, i.e., the multiple $X_1X_1X_2X_2/X_1X_2Y$ system (Moraes *et al.*, 2019).

1448 In this study, we selected those two *Pyrrhulina* species that underwent substantial,
1449 cytogenetically visible chromosomal rearrangements to examine the involvement of satDNAs in
1450 these chromosome-shuffling events and their putative role in both sex and karyotype evolution.
1451 Apart from performing a comprehensive analysis of their satellitomes, the satDNAs located on
1452 *P. semifasciata*'s sex chromosomes were also mapped in two phylogenetically related species
1453 (*P. brevis* e *P. obermulleri*) to check their possible accumulation on proto-sex chromosomes.

1454

1455 2. Materials and Methods

1456 2.1. Material, Mitotic Chromosomes and DNA Sequencing

1457 Samples of four *Pyrrhulina* species were collected in Brazilian rivers, according to **Table**

1458 **1**. To obtain mitotic metaphase chromosomes, the animals were euthanized with eugenol, as
1459 approved by the Ethics Committee on Animal Experimentation of the Universidade Federal de
1460 São Carlos, Brazil (Process number CEUA 7994170423), and cell suspensions were obtained

1461 from kidney cells (Bertollo, 1978). For DNA sequencing, we selected *P. marilynae* (one male)
 1462 and *P. semifasciata* (one male and one female) individuals. Then, total DNA was extracted from
 1463 muscle tissues using a spin-column-based protocol (Cellco Biotech, São Carlos–SP, Brazil). The
 1464 purified DNAs were then sequenced in the BGISEQ-500 platform (2 × 150 bp; BGI Shenzhen
 1465 Corporation, Shenzhen, China). Short-read sequencing yielded between 2.14 Gb (in *P.*
 1466 *semifasciata* female) and 2.44 Gb (in *P. marilynae*). Raw reads were deposited in the sequence
 1467 read archive (SRA-NVBI) and are available under the accession numbers (SRR25467276,
 1468 SRR25476502, and SRR25476501).

1469

1470 **Table 1.** Species, locality, and number of individuals (N) used in the present study.

Species	Locality	N	Voucher
<i>P. brevis</i>	Adolfo Ducke Reserve- Igarapé Barro Branco, Manaus - AM (2°56'04.6"S 59°58'10.6"W)	04♂; 07♀	MZUSP 123077
<i>P. marilynae</i>	Ipiranga do Norte - MT (11°36'02"S 55°56'27"W)	13♂; 04♀	UFPB 12080
<i>P. obermulleri</i>	Tefé- AM (3°25'50.7"S 64°44'54.8"W)	06♂; 04♀	UFPB 12079
<i>P. semifasciata</i>	Adolfo Ducke Reserve- Igarapé Barro Branco, Manaus - AM (2°56'04.6"S 59°58'10.6"W)	07 ♀; 12 ♂	MZUSP 123080

1471

1472 2.2. Bioinformatic Analyses and satDNA Library

1473 Firstly, we trimmed the raw reads with Trimmomatic (Bolger *et al.*, 2014) to select the
 1474 pair-end reads with Q > 20 for all nucleotides. Then, the satDNA catalogs from *P. semifasciata*
 1475 and *P. marilynae* were independently characterized on TAREAN (Novák *et al.*, 2020) with the
 1476 satMiner pipeline (Ruiz-Ruano, 2016). Specifically, the consensus satDNA sequences outputted
 1477 in TAREAN were filtered from the genomic libraries with DeconSeq (Schmieder and Eswards,
 1478 2011), and subsequent iterations were performed on TAREAN until no satDNA was found.
 1479 Then, a homology search with RepeatMasker (Smith *et al.*, 2020) was performed to group the
 1480 sequences into variants, families, and superfamilies, as suggested by (Ruiz-Ruano, 2016). We
 1481 also calculated the abundance and divergence values of the satDNA families by selecting
 1482 10,000,000 reads (2 × 5,000,000) from each genomic library and masking against their own
 1483 catalog of satDNAs with RepeatMasker (Smith *et al.*, 2020). After that, we named the satDNA
 1484 families according to their abundance in each species.

1485 Since *P. semifasciata* exhibits a multiple-sex chromosome system, we calculated the male:
 1486 female (M/F) abundance ratio of each satDNA family in this species (quotient between the

1487 abundance of the same satellite DNA in male and female). Then, we selected those with an M/F
1488 ratio greater than 1.2 as putatively sex-specific accumulating satDNAs. Finally, both satellitomes
1489 were BLAST-searched (Altschul *et al.*, 1990) against the NCBI nucleotide collection to check
1490 for the presence of conserved satDNAs. We constructed a minimum spanning tree (MST) for
1491 PseSat55 using PHYLOVIZ (Nascimento *et al.*, 2017) to describe the proportions of the male
1492 and female haplotypes.

1493

1494 2.3. *Primer Design and DNA Amplification via Polymerase Chain Reaction (PCR)*

1495 We designed primers for 21 out of the 70 PseSatDNAs and for 10 of the 71 PmaSatDNAs
1496 that were characterized. As a criterion for primer selection, we selected the ten most abundant
1497 ones (in *P. marylinae*, **Table S1**), the five most abundant, and those with some difference in
1498 abundance between sexes (in *P. semifasciata*, **Table S2**). PCR procedures used the optimal
1499 amplification temperatures and DNA template concentrations for each satDNA, according to
1500 (Ruiz-Ruano, 2016). For each sequence, the following cycles were used: initial denaturation at
1501 95 °C for 5 min; 29–35 cycles with denaturation at 95 °C for 15 s; annealing at 50 °C to 62 °C
1502 for 30 s (**Table S3**); extension at 72 °C for 10 s, and final extension at 72 °C for 10 min. To
1503 validate the amplification and ensure the integrity of the satDNAs, the PCR products were
1504 checked by electrophoresis on 2% and 1% agarose gels. Finally, they were quantified using the
1505 NanoDrop spectrophotometer (ThermoFisher Scientific, Branchburg, NJ, USA).

1506

1507 2.4. *Fluorescence In Situ Hybridization (FISH)*

1508 The probes derived from the satDNA's PCRs were labeled with Atto550-dUTP or
1509 Atto488-dUTP by Nick-Translation (Jena Biosciences, Jena, Germany) and used for FISH
1510 experiments. The hybridization mixes were composed of 100 ng of each labeled satellite DNA
1511 plus 50% formamide, 2 × SSC, 10% SDS, 10% dextran sulfate, and Denhardt's buffer at pH 7.0
1512 in a total volume of 20 µL, following high-stringency conditions for FISH (Pinkel *et al.*, 1986).
1513 We hybridized the above-mentioned selected sequences in both species (i.e., *P. marylinae* and
1514 *P. semifasciata*), then selected those satDNAs that displayed positive signals on the sex
1515 chromosomes of *P. semifasciata* to hybridize in *P. brevis* and *P. obermulleri* chromosomes. For
1516 the satDNA FISH experiments, glass slides containing metaphase chromosomes were aged for
1517 1 h at 60 °C, following a treatment at 37 °C for 5 min with 0.005% pepsin solution (99 µL H₂O,
1518 10 µL HCl, and 2.5 µL pepsin (20 mg/mL). Chromosomes were denatured in 70% formamide/2
1519 × SSC at 72 °C for 3 min, while probes were at 85 °C for 10 min, then cooled at 4 °C for 2 min
1520 before application. Hybridization occurred overnight in a moist chamber at 37 °C. Next, the

1521 slides were washed for 5 min in $1 \times$ SSC at 65°C and $4 \times$ SSC/Tween at room temperature,
1522 following a quick wash in $1 \times$ PBS for 1 min. The slides were dehydrated in an ethanol row
1523 (70%, 85%, and 100%) before the counterstaining of the chromosomes with DAPI mounted in
1524 Vectashield (Vector Laboratories, Burlingame, USA). We also used whole-chromosome
1525 painting (WCP) using a Y-specific probe (Psemi-Y) previously obtained (Moraes *et al.*, 2019)
1526 to detect the sex chromosomes of *P. semifasciata* and the proto-sex pairs in *P. brevis* and *P.*
1527 *obermulleri*. For this, sequential FISH/WCP was performed following (Sassi *et al.*, 2022). In
1528 total, 10 PseSatDNAs showed visible FISH signals in *P. semifasciata*, and 07 PmaSatDNA
1529 showed a visible FISH signal in *P. marilynae*.

1530

1531 2.5. Images and Confirmation of Results

1532 To confirm the FISH results, we analyzed a minimum of 30 metaphase spreads per
1533 individual. Images were captured with CoolSNAP on an Axioplan II microscope (Carl Zeiss
1534 Jena GmbH, Jena, Germany) and processed with ISIS (MetaSystems Hard e Software GmbH,
1535 Altlussheim, Germany).

1536

1537 3. Results

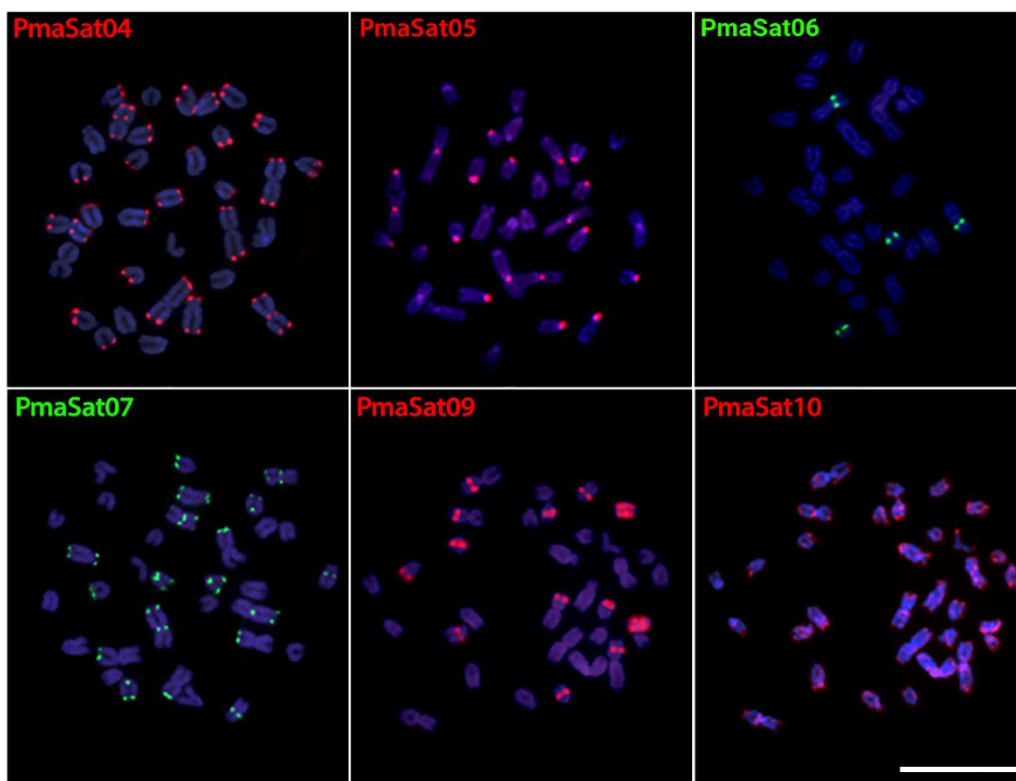
1538 3.1. SatDNA Content of *P. marilynae* and *P. semifasciata*

1539 We applied the satMiner pipeline using short-read libraries of *P. semifasciata* (female)
1540 and *P. marilynae* (for more detailed information, see the material and methods section). After
1541 three iterations of each of the satMiner protocols, we found 70 and 71 satDNA families for *P.*
1542 *marilynae* (Pma) and *P. semifasciata* (Pse), respectively. The repeat unit lengths ranged from 23
1543 to 4663 bp, with a median of 443.5 bp for *P. marilynae*, and from 6 to 2510 bp, with a median
1544 of 39 bp in *P. semifasciata*. In *P. marilynae*, the A + T content of satDNAs ranged from 39.2 to
1545 71.8% with a mean of 60%, whereas in *P. semifasciata*, it ranged from 39.2 to 78.5% with a
1546 mean of 60%. In total, 64 and 77 satDNAs in *P. marilynae* and *P. semifasciata*, respectively,
1547 had an A + T content of more than 50%. Long satDNAs (>100 bp sensu (Ruiz-Ruano *et al.*,
1548 2012) were predominant in both satellitomes, with 39 and 44 satDNA families in *P. marilynae*
1549 and *P. semifasciata*, respectively. The complete results for each satellitome are described in
1550 Tables S1 and S2. Sequences are available on the NCBI-Genbank, under the accession numbers
1551 OR094701-OR094771 (*P. semifasciata*) and OR094772-OR094841 (*P. marilynae*).

1552

1553 3.2. *Chromosomal Distribution of PmaSatDNA in P. marilynae*

1554 To examine the chromosomal location and distribution of the PmaSatDNAs, we used
1555 both female and male mitotic metaphase plates of *P. marylinae* in our two-color fluorescence in
1556 situ hybridization (FISH) experiments. Within 10 successfully amplified satDNAs families, six
1557 of them produced visible FISH signals, yielding the same result in both sexes (**Figure 1**).
1558 PmaSat04, PmaSat07, and PmaSat10 were mostly found in the telomeric and centromeric
1559 regions of most chromosomes, with the presence of bitelomeric signals for PmaSat04 and
1560 PmaSat10 (**Figure 1**). In addition, PmaSat06, PmaSat07, PmaSat09, and PmaSat10 were
1561 observed in the pericentromeric regions of some chromosomes (**Figure 1**). The satDNAs
1562 PmaSat02, PmaSat03, and PmaSat08 did not produce any FISH signal.



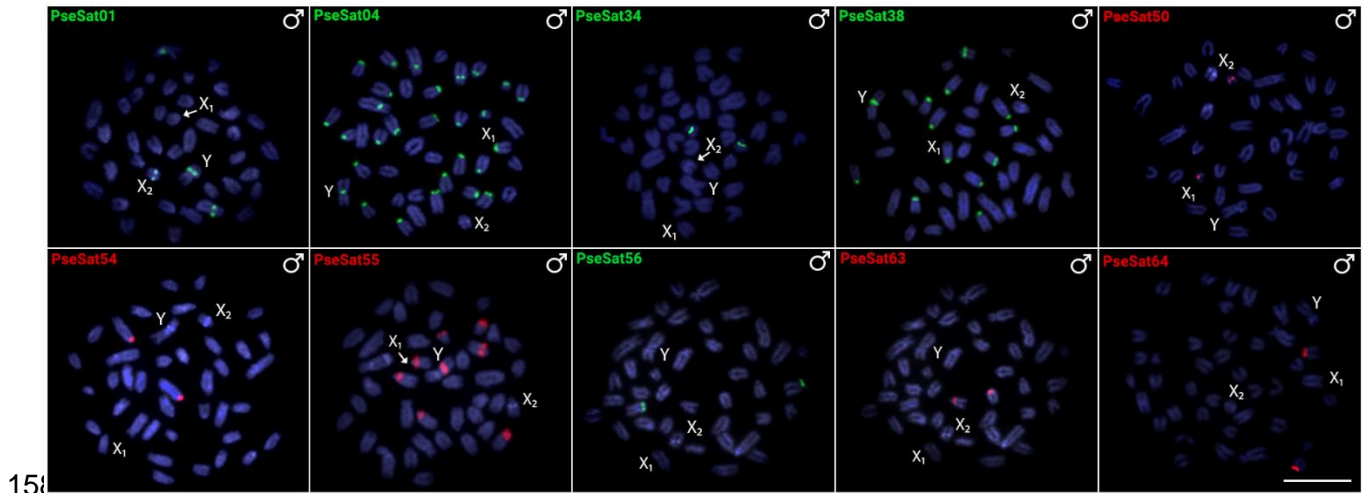
1563
1564 **Figure 1.** Metaphase plates of *Pyrrhulina marilynae* highlighting the chromosomal location
1565 PmaSatDNAs. The satDNA family names are indicated on the left top, in red (Atto550-labeled) or green
1566 (Atto488-labeled). Scale bar = 10 μ m.

1567
1568

1569 3.3. *Chromosomal Distribution of PseSatDNA in P. semifasciata*

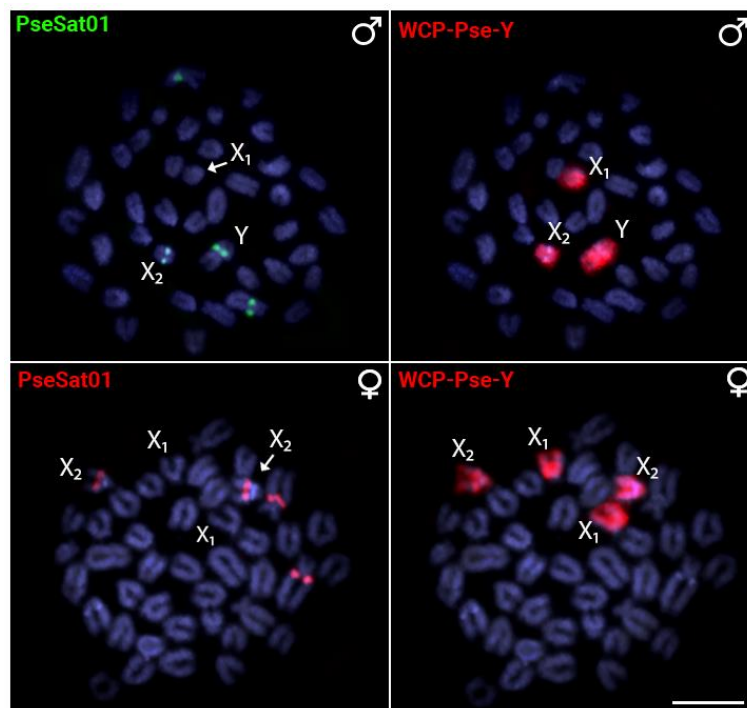
1570 To examine the chromosomal location and distribution of PseSatDNAs, we used both
1571 female and male mitotic metaphase plates of *P. semifasciata* in the same two-color FISH sets as
1572 before for *P. marilynae*. Within the 16 successfully amplified satDNA families, ten produced
1573 visible FISH signals, yielding the same result in both sexes, except the ones located on the sex
1574 chromosomes. Most of the analyzed PseSatDNAs were found in the centromeric and

1575 pericentromeric regions of the autosomal chromosomes (**Figure 2**). PseSat01, PseSat04,
 1576 PseSat38, and PseSat55 hybridized in the autosomes and sex chromosomes of *P. semifasciata*
 1577 (**Figure 2**). PseSat01, the most abundant satellite DNA, was located on two autosomes, the X2
 1578 and the Y chromosome (**Figure 2** and **Figure S1**). The sequences PseSat06, PseSat32, PseSat39,
 1579 PseSat57, PseSat61, and PseSat67 did not produce any visible FISH signals.



1581 **Figure 2.** Male metaphase chromosomes of *Pyrrhulina semifasciata* after FISH with 10 PseSatDNAs.
 1582 The satDNA family names are indicated in the top left corner in red (Atto550-labeled) or green
 1583 (Atto488-labeled). The sex chromosomes X1, X2, and Y are indicated. Scale bar = 10 μ m.
 1584

1585 In all experiments, a second FISH experiment using PseSat01 and/or the Y-specific
 1586 PSEMI-Y probe was carried out to accurately identify the X1, X2, and Y sex chromosomes
 1587 (**Figure 3**).

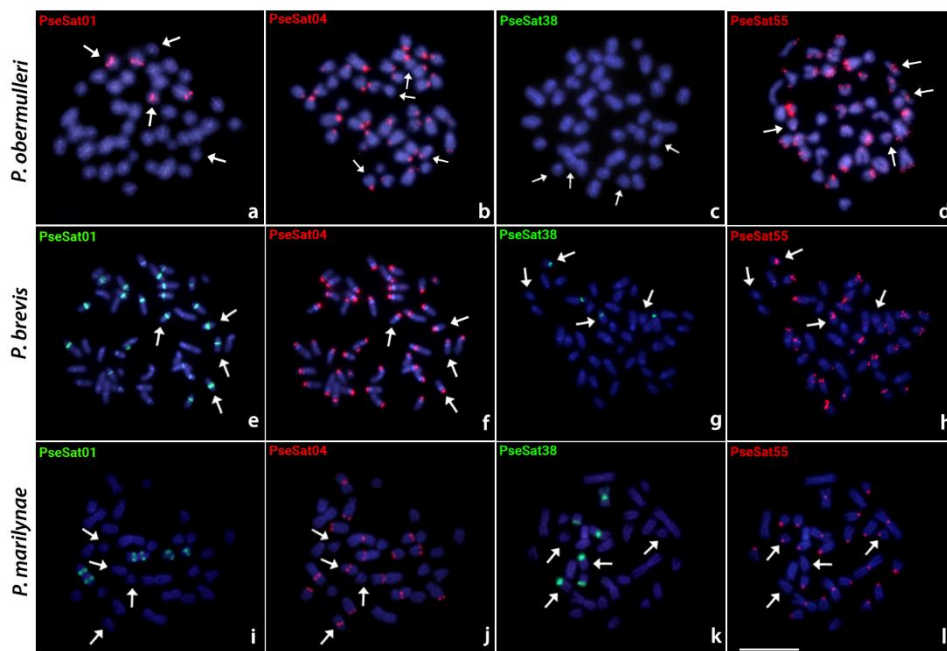


1588 **Figure 3.** Male and female metaphase plates of *Pyrrhulina semifasciata* showing that the hybridization
 1589

1590 pattern of PseSat01 (first column) is coincident with the X2 and Y sex chromosomes, as indicated by
 1591 the whole-chromosome painting with the PSEMI-Y probe (second column), which is derived from the
 1592 microdissection of the Y chromosome. Scale bar = 10 μ m.
 1593

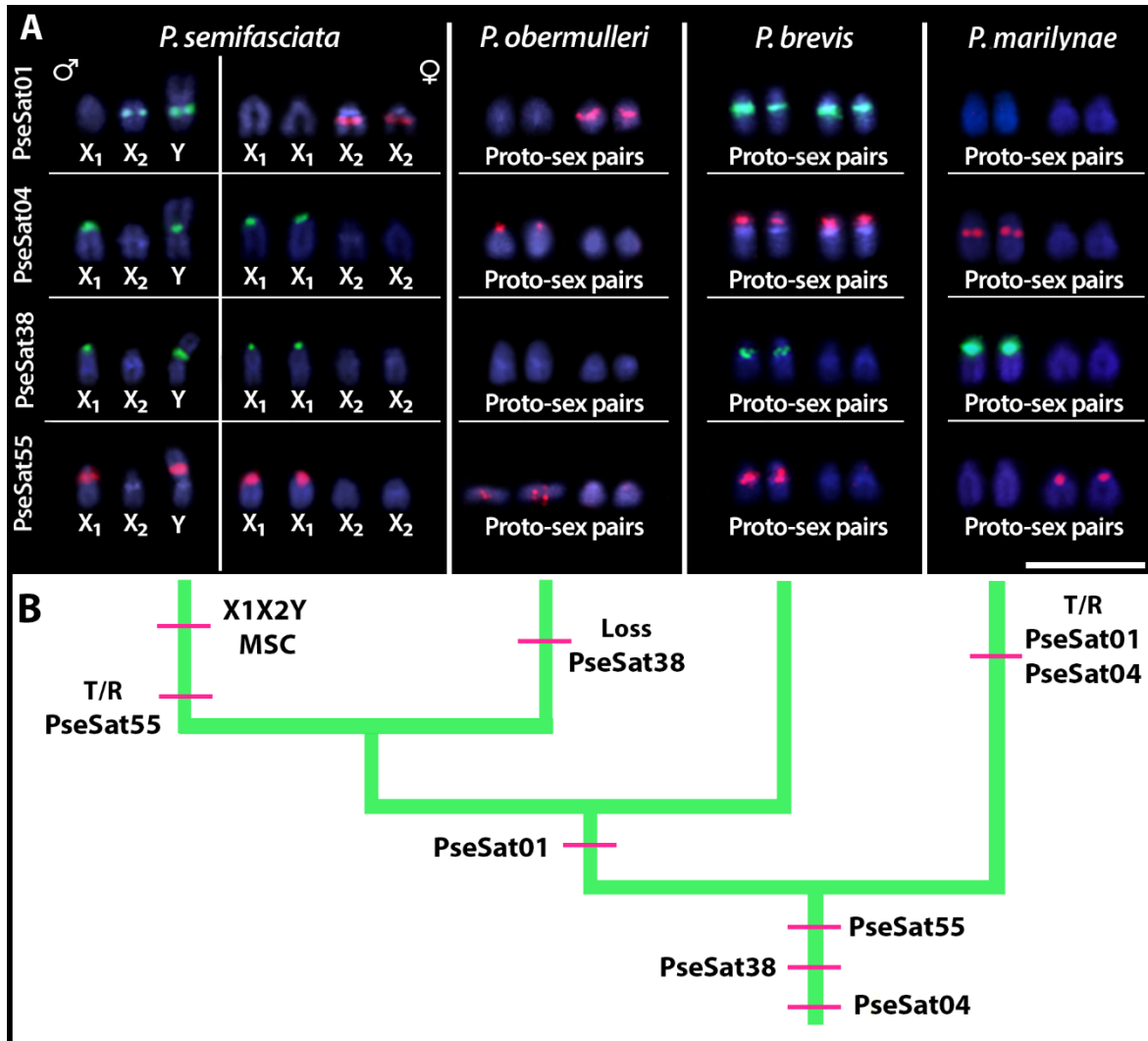
1594 **3.4. Chromosomal Distribution of PseSatDNA in Other *Pyrrhulina* Species**

1595 All PseSatDNAs located on the sex chromosomes of *P. semifasciata* (i.e., PseSat01,
 1596 PseSat04, PseSat38, and PseSat55) were also hybridized against *P. obermulleri*, *P. brevis*, and
 1597 *P. marilynae* metaphase chromosomes. All these satDNAs delivered evaluable results in all
 1598 species (**Figure 4**), except for PseSat38, which was not visible in the chromosomes of *P.*
 1599 *obermulleri* (**Figure 4c**). PseSat04 hybridized in the centromeric region of almost all
 1600 chromosomes in *P. obermulleri* and *P. brevis* (**Figure 4b,f**), whereas in *P. marilynae*, visible
 1601 signals were seen in the centromeric, pericentromeric, or telomeric regions on most
 1602 chromosomes (**Figure 4j**). PseSat01, on the other hand, was present in only two chromosome
 1603 pairs in *P. obermulleri* and *P. marilynae* (**Figure 4a,i**) and in nearly all chromosomes in *P. brevis*
 1604 (**Figure 4e**). PseSat55 was found in the centromeric and telocentromeric regions of most *P.*
 1605 *obermulleri* and *P. brevis* chromosomes (**Figure 4d,h**). In *P. marilynae*, on the other hand, it
 1606 was mapped exclusively in the centromeric region of most chromosomes (**Figure 4l**). Except for
 1607 PseSat38, which was not present in *P. obermulleri*, and PseSat01, which did not exhibit visible
 1608 signals in *P. marilynae* proto-sex pairs, all three species had at least one pair of putative proto-
 1609 sex pairs that exhibited positive signals for each of the selected PseSatDNAs (**Figure 5**). Again,
 1610 in all slides, a second FISH experiment with the Y-specific PSEMI-Y probe was carried out to
 1611 accurately identify the proto-sex chromosomes.



1612
 1613 **Figure 4.** Metaphase plates of *Pyrrhulina obermulleri* (a–d), *P. brevis* (e–h), and *P. marilynae* (i–l)

1614 highlighting the chromosomal location of PseSatDNAs that were mapped in the sex chromosomes of
 1615 *P. semifasciata*. The satDNA family names are indicated in the upper left in red (if labeled with
 1616 Atto550-dUTP) or green (if labeled with Atto488-dUTP). The arrows indicate the proto-sex
 1617 chromosomes. Scale bar = 10 μ m.
 1618

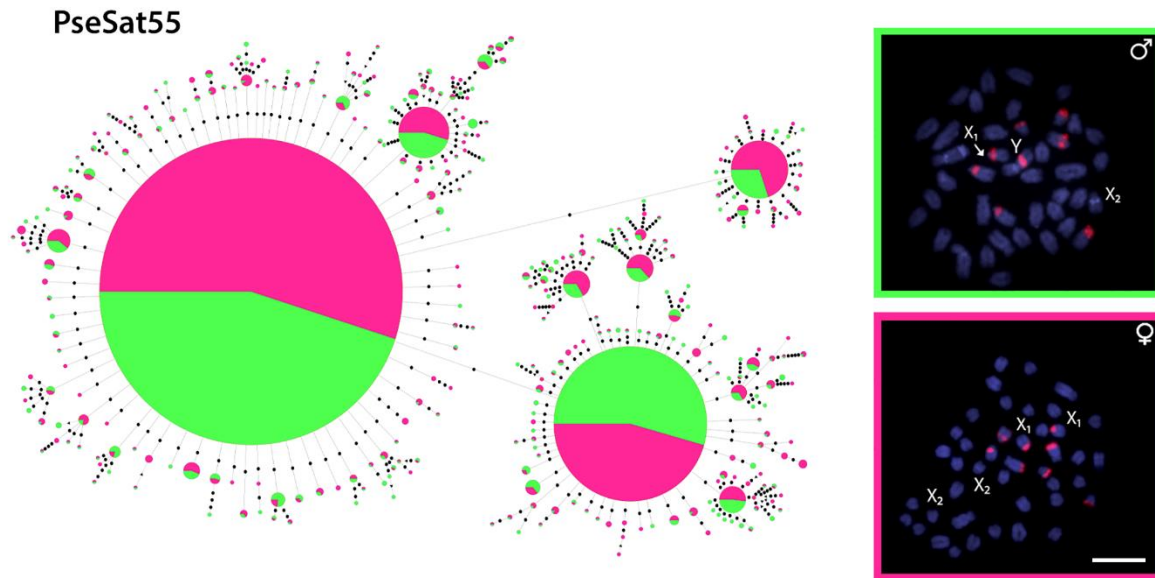


1619
 1620
 1621 **Figure 5.** (A) *Pyrrhulina semifasciata* male (first column) and female (second column) sex
 1622 chromosomes highlighting the hybridization pattern of the four PseSatDNAs that produced visible
 1623 signals, with each line matching to a satellite sequence indicated on the left. The third, fourth, and fifth
 1624 columns show the hybridization patterns of those satellites in the *P. obermulleri*, *P. brevis*, and *P.*
 1625 *marilynae* chromosomes, respectively. Scale bar = 10 μ m. (B) Phylogenetic relationships of *Pyrrhulina*
 1626 species (green lines) based on Ferreira *et al.* (2022) plotted with main events of origin, loss, and T/R
 1627 (transposition or recombination) of PseSatDNAs, and origin of the multiple sex chromosome system
 1628 (MSC) (pink lines).
 1629

1630 3.5. Minimum Spanning Trees: MSTs

1631 We have chosen PseSat55 to generate minimum spanning trees (MST). The other satDNAs
 1632 clustered in *P. semifasciata*'s sex chromosomes contain more than 150 bp, making it impossible
 1633 to create an MST. In addition to the identical locations of the X1 and Y chromosomes, PseSat55
 1634 is found in the pericentromeric regions of six autosomes in both males and females (**Figure 6**).

1635 Even among the less common haplotypes, this sharing is observed, with only a few sequences
 1636 being exclusive, mostly in females. The MST results show that PseSat55 is homogeneous in both
 1637 sexes, with just a few unique haplotypes, suggesting a certain degree of recombination between
 1638 the X and Y chromosomes.



1639 **Figure 6.** Linear MSTs of PseSat55 obtained from reads of females (pink) and males (green). The
 1640 diameter of the circle is proportional to the abundance of the haplotype. Black circles represent 01 base
 1641 of divergence between haplotypes, and the black triangles represent 05 bases of divergence. The in situ
 1642 mapping in male and female metaphase plates is highlighted in boxes. Bar = 5 μ m.
 1643
 1644

1645 4. Discussion

1646 4.1. General Features *P. marylinae* and *P. semifasciata* Satellitomes

1647 Here, we show that a significant proportion of satDNA families (38 satDNAs) are shared
 1648 between the satellitomes of *P. marylinae* (70 satDNAs) and *P. semifasciata* (71 satDNAs)
 1649 (**Table S4**). Such a scenario (i.e., the conservation and sharing of satDNA families) is not an
 1650 exclusive feature of *Pyrrhulina* but is also observed in other fish species (Silva *et al.*, 2017; dos
 1651 Santos *et al.*, 2021; Goes *et al.*, 2023), as well as several vertebrates such as snakes (Lisachov *et*
 1652 *al.*, 2023), primates (Ahmad *et al.*, 2020), and true toads (Guzmán-Markevich *et al.*, 2022).
 1653 According to the library hypothesis (Fry and Salser, 1977), satellite sequences are preserved over
 1654 long evolutionary timescales because closely related species share a common library of these
 1655 sequences, with quantitative changes brought on by differential amplification. Investigations
 1656 suggested that the satDNA libraries can disappear or be formed de novo following cladogenetic
 1657 events (Camacho *et al.*, 2022). According to this theory, the acquisition of a biological function
 1658 that will ultimately be preserved by natural selection is necessary for conservation over a lengthy
 1659 evolutionary time. Although both species analyzed retained about half of their satDNA families,

1660 evidencing a common library between them, the observed differences in the abundance of these
1661 shared families are also remarkable, a fact predicted by the library hypothesis (Fry and Salser,
1662 1977). Among the 38 shared satDNAs, six of them were selected for FISH experiments (**Table**
1663 **S4**) and revealed the same accumulation pattern in both species.

1664 The heterochromatic regions differ substantially between *Pyrrhulina* species, with large
1665 accumulations in centromeric and telomeric regions, as well as pericentromeric and interstitial
1666 regions (Moraes *et al.*, 2017; Moraes *et al.*, 2019; Moraes *et al.*, 2021). The karyotype of *P.*
1667 *semifasciata* has considerable accumulations of heterochromatin in centromeres and telomeres
1668 (Moraes *et al.*, 2019), whereas *P. marilynae* has these accumulations mainly in the centromeric
1669 region of most chromosomes (Moraes *et al.*, 2021). In the same way, the *in situ* mapping revealed
1670 a predominance of PseSatDNAs in the centromeric regions of *P. semifasciata* (**Figure 2**). This
1671 type of association can be suggestive of a probable relationship with centromere development,
1672 as well as an essential role in genome integrity by preserving the higher-level nucleus structure
1673 (Podgornaya, 2022). Although satellite DNA sequences are often abundant in heterochromatic
1674 regions (Thakur *et al.*, 2021; Šatović-Vukšić and Plohl, 2023), as indicated in *P. semifasciata*,
1675 their occurrence in euchromatic regions has been emphasized in many species, including
1676 bivalves (Tunjić-Cvitanić *et al.*, 2021), insects (Cabral-de-Mello *et al.*, 2021; Pereira *et al.*, 2021;
1677 Flynn *et al.*, 2023), mammals (Valeri *et al.*, 2021), and fishes (Silva *et al.*, 2017; dos Santos *et*
1678 *al.*, 2021; Crepaldi *et al.*, 2021), as well as *P. marilynae* (**Figure 1**). PmaSat01 constitutes
1679 approximately 4% of the *P. marilynae* genome (**Table S1**), while the most abundant satellite of
1680 *P. semifasciata* (PseSat01) only represents about 0.5% of its genome (**Table S2**). However, the
1681 satellitomes of both species are very similar in the number of clusters recovered by TAREAN
1682 (i.e., 70 PmaSatDNAs and 71 PseSatDNAs). Among fishes, other Characiformes species, such
1683 as representatives of *Astyanax*, *Characidium*, and *Psalidodon*, also carry similar numbers of
1684 satDNA families (Serrano-Freiras *et al.*, 2020; Goes *et al.*, 2023). However, species with more
1685 satDNAs have previously been identified, such as in *Megaleporinus*, demonstrating a great
1686 dynamic of such sequences in fish genomes. Owing to the various processes involved in their
1687 dynamics throughout cladogenetic genomic development, the variety of satellitomes among
1688 different species of animals and plants is rather significant, both in terms of the number of
1689 satDNA families and the proportion of the genome they occupy (Garrido-Ramos, 2017; Šatović-
1690 Vukšić and Plohl, 2023).

1691

1692 4.2. *Satellite DNA Contribution in the Significant 2n Reduction Observed in P.*

1693 *marilynae*

1694 *P. marilynae* stands out for presenting the most rearranged karyotype among all *Pyrrhulina*
1695 species, with $2n = 32$ and formed by large and unusual metacentric pairs (Moraes *et al.*, 2021).
1696 Many studies have found that satellite DNAs can induce chromosomal rearrangements and thus
1697 have a direct impact on karyotype evolution due to their dynamic and fast-evolving nature (Paço
1698 *et al.*, 2013; Vieira-da-Silva *et al.*, 2015; Gatto *et al.*, 2018; Escudeiro *et al.*, 2019; de Lima and
1699 Ruiz-Ruano, 2022). Thus, the occurrence of centric fusions and fissions is frequently associated
1700 with the fast dynamics of satDNAs, which are located mostly in the centromeric and
1701 pericentromeric regions of chromosomes (Slamovits *et al.*, 2001; Ugarković and Plohl, 2014;
1702 Kopecna *et al.*, 2014; Vozdova *et al.*, 2019). Interestingly, our experiments demonstrate that
1703 PmaSatDNAs hybridized at telomeres or centromeres of *P. marilynae* chromosomes, including
1704 bitelomeric signals from PmaSat04 and PmaSat10, and pericentromeric signals on both arms
1705 with PseSat01 (**Figure 1**). These results imply that chromosomal reduction in *P. marilynae* is
1706 directly linked to centric fusion processes that result in the large metacentric chromosomes found
1707 in this species' karyotype. Notably, the satellite DNA sequences did not experience any
1708 accumulation or loss after the fusion process.

1709 PmaSatDNAs 04, 07, 09, and 10 accumulate in telomeres and (peri)centromeres,
1710 especially in the large metacentric pairs. These large chromosomes probably originate from
1711 chromosome fusions, restricting recombination to the distal ends (Franchini *et al.*, 2017;
1712 Franchini *et al.*, 2020; Vara *et al.*, 2021). Repetitive sequences, such as satellites and rDNAs,
1713 often make up the subtelomere region, also known as the buffer zone between the internal
1714 chromosome and telomere. Given that the latter is made up of telomeric motifs interspersed with
1715 other repeated sequences (Naish *et al.*, 2021), such subtelomere sequences can also be found in
1716 interstitial telomeric sites (ITSs). As sub and telomeric arrays help to stabilize new ends (Yang
1717 *et al.*, 2005), it is likely that the FISH signals observed directly represent the fusion process that
1718 *P. marilynae* went through throughout its karyotypic reduction (**Figure 1**). The expansion and
1719 contraction of those telomere-associated satellite motifs that remained even after the inactivation
1720 of the telomeric region near the newly formed centromere may be fostered by repair mechanisms
1721 (Kipling *et al.*, 1991). This scenario is not exclusive to *P. marilynae*. Other fish species also
1722 carry a series of repetitive DNA in their chromosome fusion points, as observed in *Rineloricaria*
1723 (Glugoski *et al.*, 2022; Glugoski *et al.*, 2023), for example.

1724 SatDNAs are a significant and prominent component of the so-called “dark matter of
1725 genomes” (Sedlazeck *et al.*, 2018). In fact, multiple pieces of evidence show that satellite DNAs

1726 are sequences that can participate in centromere and telomere formation besides presenting
1727 fundamental roles and specific functions in the genome (Garrido-Ramos, 2017; Louzada *et al.*,
1728 2020; dos Santos *et al.*, 2021; Montiel *et al.*, 2022). Although no functional experiments have
1729 been performed here, the majority of the PmaSatDNAs are found in centromeric and telomeric
1730 regions and may be directly linked to their formation, in addition to possibly playing a role in *P.*
1731 *marilynae*'s reduction and karyotypic evolution.

1732

1733 4.2. *SatDNAs and the Evolution of Multiple Sex Chromosomes*

1734 Repetitive sequences are great tools for the study of sex chromosomes, where species with
1735 heteromorphic sex chromosomes show a difference in the accumulation of some sequences
1736 between males and females, emphasizing the existence of several W/Y-specific satDNAs
1737 (Ferretti *et al.*, 2020; Sember *et al.*, 2021; Cabral-de-Mello *et al.*, 2023; Flynn *et al.*, 2023).
1738 Despite the presence of a well-differentiated X1X2Y sex chromosome system, minor differences
1739 in haplotype accumulation between males and females were observed (**Figure 6**). Although four
1740 PseSatDNAs were mapped in this study to either X1, X2, or neo-Y chromosomes, no neo-Y-
1741 specific satDNA was identified (**Figure 5**), contrasting with *Eneoptera surinamensis* (Palacios-
1742 Gimenez *et al.*, 2017) and *Ronderosia bergii* (Ferretti *et al.*, 2020), which show a large
1743 accumulation of satDNAs in neo-sex chromosomes. These species, however, lack synapses
1744 between sex chromosomes, demonstrating significant differentiation between them. Multiple-
1745 sex chromosome systems, in contrast to simple ones, are known to have a more recent origin and
1746 still exhibit considerable recombination rates, resulting in few or no sex-specific sequences
1747 (Sember *et al.*, 2021). A similar scenario has already been reported in other animal species, such
1748 as the frog *Proceratophrys boiei*. Despite having a simple and heteromorphic ZZ/ZW sex
1749 chromosome system, it is distinguished by the absence of sex-specific satDNAs and low sex
1750 divergence, indicating their early stage of sex chromosome differentiation (da Silva *et al.*, 2023).

1751 There are no dated phylogenetic reconstructions for *Pyrrhulina* species. As a result,
1752 determining when the multiple-sex chromosome system emerged is not feasible, regardless of
1753 other cytogenetic traits that suggest its recent origin. The X1, X2, and Y sex chromosomes lack
1754 strong differences in size and accumulation of heterochromatic regions (Moraes *et al.*, 2019), as
1755 in the satellite distribution. Accordingly, the MST generated for PseSat55 also did not point to
1756 any difference in the abundance of the haplotypes obtained from reads of females and males
1757 (**Figure 6**). Such low heterochromatin is also observed in other species with recent
1758 diversification of multiple sex chromosomes, such as *Hoplias malabaricus* and *Erythrinus*
1759 *erythrinus* (Bertollo *et al.*, 1997; Bertollo *et al.*, 2004). Considering the formation of a trivalent

1760 during the meiosis process, multiple-sex chromosome systems (such as the X1X2Y of *P.*
1761 *semifasciata*) could not accumulate large heterochromatic blocks; otherwise, they could impair
1762 its correct segregation (Cioffi *et al.*, 2012). In this sense, the presence of PseSatDNAs in the
1763 homologous regions of the multiple sex chromosomes of *P. semifasciata* can be indicative of
1764 their role in the modulation of gene expression. Under stress circumstances, euchromatic copies
1765 of pericentromeric satDNAs in *Tribolium castaneum* are functionally relevant in modifying
1766 chromatin and the expression of adjacent genes (Feliciello *et al.*, 2015). In *Drosophila*
1767 *melanogaster*, more than a thousand euchromatic copies of satDNAs are mainly found near genes
1768 and are thought to have a function in the modulation of gene expression (Kuhn *et al.*, 2012).
1769 Similarly, those euchromatin-dominant satellite DNAs share characteristics regarding their
1770 structure, organization, and evolution (reviewed in Šatović-Vukšić and Plohl (2023) and Plohl
1771 *et al.* (2008).

1772 Despite the absence of neo-Y-specific satDNA sequences in *P. semifasciata*, we
1773 demonstrate that several motifs are shared between this species' sex chromosome and the proto-
1774 sex pairs in other *Pyrrhulina* representatives (**Figure 5**). Considering the absence of specific
1775 sequences such as PseSat38 in *P. obermulleri*, it is also noteworthy to emphasize the high
1776 dynamism of these sequences in the cladogenetic history. Both a seemingly complete absence
1777 of these sequences and their low-copy numbers can be explained by the absence of detectable
1778 FISH signals. Unequal crossing over between sister chromatids or intra and interchromosomal
1779 recombination may significantly decrease the copy number of satellite DNAs (Pralhongcheep *et*
1780 *al.*, 2017). On the other hand, sequences such as PseSat01, PseSat04, and PseSat55 suffered
1781 expansions and retractions in the number of loci, including changes between both proto-sex
1782 pairs. In some instances, site-directed recombination between homologous motifs in satellite
1783 repeats and in the target genomic sequence, most likely mediated by extrachromosomal circular
1784 DNA, can explain the dispersion of satellites (Feliciello *et al.*, 2020). Alternatively, such
1785 translocation can be due to transposable elements (TEs) that are known to participate in the
1786 origin and the dispersal of satDNA repeats (Zattera and Bruschi, 2022). Through amplifying
1787 tandem repeats within them, TEs may also capture satDNA motifs and generate new satDNAs,
1788 which can then be disseminated over other regions of the genome and preserved through
1789 nonreciprocal transfer mechanisms such as unequal crossover (Scalvenzi and Pollet, 2014).
1790 Indeed, TEs such as Rex3 were already mapped in *Pyrrhulina* chromosomes, showing a high
1791 dispersal tendency (Moraes *et al.*, 2017). However, the extremely similar size and shape of those
1792 chromosomes, as well as the frequent translocations between them, might also be the result of
1793 putative pseudo-homologous regions (PHRs), which are thought to be due to recombination

1794 between non-homologous sequences (Guarracino *et al.*, 2023) or due to the presence of
1795 pseudoautosomal regions (PARs) with high recombination rates (Yazdi *et al.*, 2023) in these
1796 proto-sex chromosomes.

1797 It is noteworthy that some conserved PseSatDNAs across distinct *Pyrrhulina* species
1798 (**Figure 4**) are present in the pericentromeric region of the sex chromosomes in *P. semifasciata*
1799 and the proto-sex pairs of *P. brevis*, *P. obermulleri*, and *P. marilynae*. From the canonical model
1800 of sex chromosome evolution, when the recombination between the sex-related chromosomes is
1801 ceased, the sex-specific chromosome is invaded by several repetitive sequences, including
1802 satDNAs (reviewed in Kratochvíl *et al.* (2023)). However, the presence of such satDNAs in the
1803 proto-sex chromosomes leads us to two main questions: i) Can the accumulation of the same
1804 PseSatDNAs (i.e., PseSat01, PseSat04, PseSat38, and PseSat55) in proto-sex and multiple-sex
1805 chromosomes indicate the presence of a plesiomorphic and homomorphic XX/XY in *P. brevis*,
1806 *P. obermulleri*, and *P. marilynae*? Or ii) Were those sequences simply conserved in these
1807 acrocentric pairs, given their putative role in the centromeric structure and genome integrity? To
1808 fully solve these questions, however, a high-quality reference genome is mandatory, and the next
1809 steps involve generating a high-quality genome assembly with PacBio having access to an end-
1810 to-end solution.

1811

1812 **References**

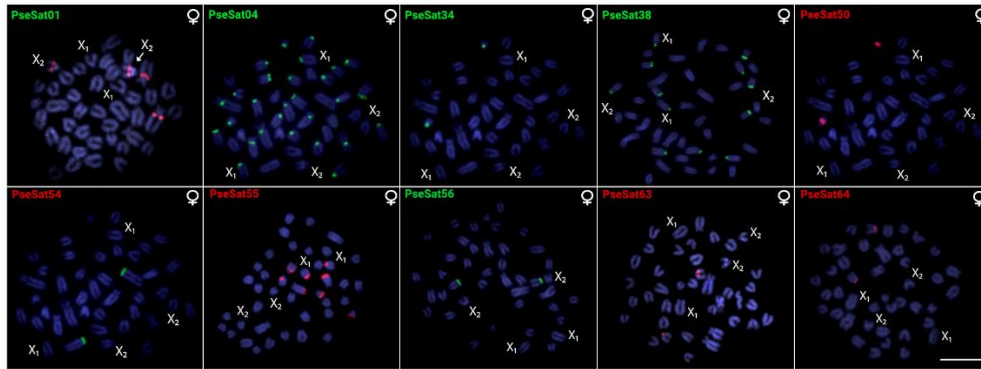
1813 All references are compiled in the end of this thesis.

1814

1815 **Supplementary Materials**

1816 The following supporting information can be downloaded at <https://www.mdpi.com/1422-0067/24/17/13654/s1>.

1818 **Figure S1:** Females metaphase plates of *Pyrrhulina semifasciata* highlighting the chromosomal
1819 location of 10 satDNA. The satDNA family names are indicated on the left top, in red (ATTO550
1820 labeled) or green (ATTO488 labeled). The sex chromosomes (X₁X₂Y) are shown. Scale bar =
1821 10 μm.



1822

1823

1824 **Supplementary Table 1.** Main characteristics of 71 satDNAs found in *Pyrrhulina marilynae*.

1825 The sequences highlighted in blue correspond to those selected for the FISH experiments.

1826

Familia de satDNAs	RUL	Abundância	Divergência	A+T (%)
PmaSat01-1627	1627	0.0395879278883	1.33	58.6
PmaSat02-68	68	0.0126290012853	2.63	66.2
PmaSat03-45	45	0.0083896090511	2.92	44.4
PmaSat04-50	50	0.00772308401902	3.93	60
PmaSat05-226	226	0.00728803566553	9.69	64.2
PmaSat06-198	198	0.00647761332963	9.25	67.2
PmaSat07-45	45	0.00639111613516	5.97	62.2
PmaSat08-33	33	0.00268802096213	2.10	57.6
PmaSat09-335	335	0.00220671410467	9.24	70.1
PmaSat10-4663	4663	0.00209498220866	5.93	43.6
PmaSat11-2486	2486	0.00207120592574	10.40	62.4
PmaSat12-842	842	0.00204339498168	9.60	63.5
PmaSat13-4322	4322	0.00196875721573	13.26	63.7
PmaSat14-54	54	0.00185443026527	3.79	57.4
PmaSat15-1437	1437	0.0015994228488	8.96	58.1
PmaSat16-670	670	0.000982230583972	7.52	59.4
PmaSat17-192	192	0.000746618253954	10.82	63
PmaSat18-42	42	0.000666838894057	4.21	64.3
PmaSat19-84	84	0.000628643771793	13.99	53.6
PmaSat20-142	142	0.000590982313911	3.14	66.2
PmaSat21-712	712	0.000582114970286	1.67	62.2
PmaSat22-32	32	0.000555307988527	3.71	53.1
PmaSat23-23	23	0.000553234717251	7.65	52.2
PmaSat24-1283	1283	0.000550808970056	13.84	56.5
PmaSat25-36	36	0.000541725784436	5.34	44.4
PmaSat26-21	21	0.000528704967553	17.33	47.6
PmaSat27-39	39	0.000519611880924	8.11	64.1
PmaSat28-165	165	0.000493380147786	7.48	66.7
PmaSat29-51	51	0.000480608836328	7.36	39.2
PmaSat30-1062	1062	0.00047705239391	8.96	64.8
PmaSat31-47	47	0.000450014718642	5.81	59.6
PmaSat32-33	33	0.000425481998641	3.84	60.6
PmaSat33-176	176	0.00040900473953	4.45	64.8
PmaSat34-1411	1411	0.000394930455293	0.99	58
PmaSat35-845	845	0.000394410652323	3.59	62.7
PmaSat36-445	445	0.00032788478302	4.71	57.1
PmaSat37-28	28	0.000311260988976	9.21	60.7
PmaSat38-162	162	0.000284214402801	4.71	66
PmaSat39-88	88	0.000276674784478	8.15	68.2

PmaSat40-211	211	0.000276362902695	6.43	59.2
PmaSat41-915	915	0.000237961839444	1.67	67.4
PmaSat42-314	314	0.000236262826307	5.27	58.3
PmaSat43-165	165	0.00023088459824	4.09	64.8
PmaSat44-43	43	0.000227744988298	11.66	48.8
PmaSat45-568	568	0.000214584567189	5.78	59
PmaSat46-470	470	0.000206393462476	5.08	61.3
PmaSat47-672	672	0.000203039000641	3.93	58.5
PmaSat48-31	31	0.000193220170055	5.51	67.7
PmaSat49-80	80	0.00017571122581	17.60	67.5
PmaSat50-428	428	0.000172995379053	7.23	57.2
PmaSat51-414	414	0.000172949834411	7.17	61.6
PmaSat52-387	387	0.000167174575885	4.40	58.1
PmaSat53-36	36	0.000162056744354	7.38	61.1
PmaSat54-44	44	0.000156811189807	4.92	61.4
PmaSat55-231	231	0.000144396314672	6.74	55
PmaSat56-544	544	0.000139795315808	4.75	58.8
PmaSat57-98	98	0.00013769828211	7.53	61.2
PmaSat58-165	165	0.000130510149605	6.24	63.6
PmaSat59-167	167	0.000125421031	6.72	70.7
PmaSat60-31	31	0.000124081424488	7.00	51.6
PmaSat61-142	142	0.000117378441422	8.02	71.8
PmaSat62-47	47	0.000115912101995	4.91	59.6
PmaSat63-33	33	0.000114132890685	2.66	60.6
PmaSat64-39	39	0.0001140388311	5.89	66.7
PmaSat65-64	64	0.000106678421039	2.74	54.7
PmaSat66-188	188	0.000101115044104	8.31	66.5
PmaSat67-39	39	0.0000989358	4.82	53.8
PmaSat68-173	173	0.0000899655	8.21	62.4
PmaSat69-53	53	0.000078606	4.77	56.6
PmaSat70-33	33	0.0000701149	4.78	51.5

1827

1828 **Supplementary Table S2.** Main characteristics of 70 satDNAs found in *Pyrrhulina*
1829 *semifasciata*, highlighting, in blue, those chosen for FISH mapping. The asterisk (*) indicates
1830 the satDNAs mapped in the sex chromosomes.

1831

Família de satDNA	RUL	Abundância (M)	Abundância (F)	Abundância (M/F)	Divergência (M)	Divergência (F)	A+T (%)
PseSat01- 304*	304	0,005606905	0,006386826	0,877885927	9,78	9,65	68
PseSat02- 45	45	0,005289071	0,00496321	1,065655359	4,97	4,98	62,2
PseSat03- 68	68	0,005288433	0,005331731	0,991879186	2,52	2,54	66,1
PseSat04-226*	226	0,004975278	0,005546355	0,897035567	9,76	9,62	64,6
PseSat05 - 45	45	0,004215905	0,004087883	1,03131743	4,4	4,43	44,4
PseSat06- 198	198	0,002799141	0,003195114	0,876069106	8,88	8,81	66,6
PseSat07- 174	174	0,002764281	0,002730314	1,012440816	4,55	4,66	62,6
PseSat08- 2005	2005	0,002341543	0,00191567	1,222310384	10,37	10,38	62,3
PseSat09- 50	50	0,002080652	0,001881225	1,10600892	8,37	9,01	60
PseSat10- 610	610	0,001957573	0,001948731	1,004537311	16,83	16,92	66
PseSat11-2510	2510	0,001864105	0,001601655	1,163861305	12,58	11,71	62
PseSat12- 2219	2219	0,001725149	0,001426195	1,209616448	3,71	3,84	63,8
PseSat13- 35	35	0,001527915	0,001394119	1,095972222	1,86	1,8	57,1
PseSat14- 1235	1235	0,001207345	0,001038919	1,162116533	11,49	11,91	57,4
PseSat15- 38	38	0,001082321	0,001210707	0,893957307	13,9	14,32	63,1
PseSat16- 42	42	0,00096017	0,000568407	1,689228734	7,36	7,61	59,5
PseSat17- 381	381	0,000850538	0,000685979	1,23988987	8,74	8,25	61,4
PseSat18- 615	615	0,000729584	0,000612211	1,191720497	6,62	6,4	58,2

PseSat19- 461	461	0,000715265	0,000645695	1,10774328	11,51	9,8	63,5
PseSat20- 1284	1284	0,000705413	0,00074095	0,952039049	20,91	20,17	56,3
PseSat21- 42	42	0,000696777	0,000711353	0,979510398	4,22	4,15	64,2
PseSat22- 54	54	0,000664187	0,000593948	1,118258389	6,05	6,44	57,4
PseSat23- 155	155	0,000658736	0,000516891	1,274418737	6,28	6,5	63,8
PseSat24- 84	84	0,000643957	0,000633686	1,016208869	14,6	14,94	0,535714
PseSat25- 52	52	0,000643279	0,000613842	1,047954794	13,95	14,18	0,557692
PseSat26- 828	828	0,000613564	0,000594593	1,03190528	7,57	7,25	0,509662
PseSat27- 422	422	0,000581057	0,000722512	0,804218246	6,35	6,6	0,575829
PseSat28- 14	14	0,000557749	0,000571732	0,975542154	6,92	6,86	0,785714
PseSat29- 6	6	0,000552197	0,000573221	0,963321905	26,22	26,24	0,5
PseSat30- 192	192	0,000529303	0,0005363	0,986953819	15,32	15,9	0,640625
PseSat31- 51	51	0,000441051	0,000393715	1,120227305	9,09	9,1	0,392157
PseSat32- 186	186	0,000390964	0,000658971	0,593294997	8,44	8,02	0,709677
PseSat33- 880	880	0,000336683	0,000305781	1,101059365	3	3,46	0,669318
PseSat34-165	165	0,000282004	0,000328703	0,857928629	6,61	6,58	0,642424
PseSat35- 23	23	0,000282019	0,000250551	1,125598016	11,53	12,52	0,521739
PseSat36- 195	195	0,000237211	0,000183166	1,295058399	3,36	3,42	0,707692
PseSat37- 1041	1041	0,000231577	0,000229568	1,008752672	10,1	9,49	0,623439
PseSat38- 300*	300	0,000230661	0,000059944	3,847935851	4,96	6,47	0,576667
PseSat39- 80	80	0,000225943	0,000317697	0,711188427	15,55	15,44	0,6625
PseSat40- 39	39	0,000215363	0,000275735	0,781050911	10,74	9,56	0,641026
PseSat41- 21	21	0,000203179	0,000205974	0,986431944	17,77	16,97	0,47619
PseSat42- 1093	1093	0,000198728	0,000179851	1,104957057	1,5	1,56	0,600183
PseSat43- 124	124	0,000194009	0,000155268	1,249512671	7,66	8,11	0,564516
PseSat44- 28	28	0,00019343	0,000196448	0,984637156	9,47	9,48	0,571429
PseSat45- 445	445	0,00018569	0,000175259	1,059515613	3,95	4,07	0,573034
PseSat46- 837	837	0,000176346	0,000178717	0,986731375	7,57	7,21	0,624851
PseSat47- 21	21	0,000174861	0,000236993	0,737829475	11,25	11,75	0,666667
PseSat48- 32	32	0,000171967	0,000124967	1,376098287	5,94	7,75	0,53125
PseSat49- 33	33	0,000170543	0,000131041	1,301441784	6,45	7,5	0,606061
PseSat50- 1125	1125	0,000160486	0,000123408	1,300450538	9,97	12,7	0,656
PseSat51- 713	713	0,000146761	0,00014616	1,004109652	5,34	5,72	0,622721
PseSat52- 673	673	0,000141336	0,000132213	1,069004987	7,81	7,72	0,576523
PseSat53- 23	23	0,000138389	0,000075714	1,827790545	8,88	10,24	0,565217
PseSat54- 159	159	0,00013754	0,000194867	0,705815943	5,1	4,7	0,672956
PseSat55- 43*	43	0,000133589	0,000159353	0,838325057	8,62	7,99	0,488372
PseSat56- 87	87	0,000126526	0,000159655	0,792494666	6,25	5,81	0,678161
PseSat57- 162	162	0,000124983	8,86007E-05	1,410636489	4,99	5,06	0,67284
PseSat58- 372	372	0,000122859	0,00012864	0,955063226	2,88	2,95	0,567204
PseSat59- 46	46	0,000116657	0,000119628	0,975167464	12,34	12,69	0,608696
PseSat60- 944	944	0,000116336	0,000101468	1,146528955	7,8	7,73	0,610169
PseSat61- 213	213	0,000109063	0,000137659	0,792264963	5,14	5,29	0,615023
PseSat62- 469	469	0,000103981	0,000108045	0,962379989	4,37	3,96	0,614072
PseSat63- 463	463	0,000100169	0,000113188	0,884981918	3,94	3,69	0,591793
PseSat64- 182	182	0,000098656	5,97373E-05	1,651496552	10,95	13,61	0,681319
PseSat65- 187	187	9,83113E-05	8,62127E-05	1,14033514	5,38	5,61	0,620321
PseSat66- 44	44	8,66047E-05	0,000077618	1,115780704	4,41	4,93	0,613636
PseSat67- 198	198	8,07013E-05	0,000103397	0,780502273	4,81	4,26	0,60101
PseSat68- 179	179	7,91173E-05	7,52593E-05	1,051262745	6,5	6,33	0,614525
PseSat69- 592	592	7,38767E-05	7,23727E-05	1,020781326	4,78	4,41	0,586149
PseSat70- 759	759	7,23553E-05	6,96727E-05	1,038503861	4,52	4,48	0,586298
PseSat71- 182	182	6,96327E-05	6,92727E-05	1,005196855	6,83	7,08	0,538462

1832

1833

1834 **Supplementary Table S3.** PCR conditions (primer, temperature, and concentration of template
1835 DNA) for the optimal amplification of satellite DNAs from *P. marilynae* and *P. semifasciata*.

Satellite	Primer F	Primer R	Anneraling temperature range	[DNA] ng/μl
PmaSat01-1627	5'CACACCTTTGGCATTCTAGC	5'TCTGTAAAGCATGGTGGAGG	56°C – 57,4°C	100
PmaSat04-50	5'GGGTGTGGTTATCTCTGTAC	5'CCCCTCTAAACAGAGTATAAAC	50°C – 51,7°C	100; 10; 1; 0,1
PmaSat05-226	5'GCAAGCTGAATACATTCATG	5'GACTGTCTGAGAGCACAAAC	53°C - 54,5°C	100; 10; 1; 0,1
PmaSat06-198	5'AAGACAGCTTCTGCA TCCATG	5'TTGCAGATTTGCCCAAA AAC	55°C - 55,6°C	100; 10; 1; 0,1
PmaSat07-45	5'CCTCTGTAACACATTAAACTGT	5'TAGGAGAGTGTAGTGTTAGTCT	51,7°C – 58°C	100; 10
PmaSat09-335	5'CTGCAACCACTTCCAGTGAT	5'ACACTTAGTTGTGTCTGAAA	53°C - 53,5°C	100; 10; 1; 0,1
PmaSat10-4663	5'AGAACGGAGGTCTCTTGCGT	5'CTCCATTCATTTCCATCACGC	56°C – 62,5°C	100
PseSat01-304	5'CTGCAACCACTTCCAGTGAT	5'ACACTTAGTTGTGTCTGAAA	53°C - 53,5°C	100; 10; 1; 0,1
PseSat04-226	5'GCAAGCTGAATACATTCATG	5'GACTGTCTGAGAGCACAAAC	53°C - 54,5°C	100; 10; 1; 0,1
PseSat06-198	5'AAGACAGCTTCTGCA TCCATG	5'TTGCAGATTTGCCCAAA AAC	55°C - 55,6°C	100; 10; 1; 0,1
PseSat32-186	5'TGAGAGAAGAC TTTACAAGC	5'TGACACATTTAAGGCAT TTC	50°C - 54,9°C	100
PseSat34-165	5'CATGGCTGATAGGGTAAAAG	5'ATGTGACCACACTGTATCCC	56,5°C - 63°C	1; 0,1
PseSat38-300	5'ATAGACGGATGGATTAACGG	5'AAAGACTGACAGACCA TTAT	53°C - 61°C	100; 10; 1; 0,1
PseSat39-80	5'CTTACTGTCTCATATCTGTG	5'AGTTAAGACCAGTATCTCTA	50,5°C - 57,4°C	100
PseSat50-1125	5'CTGTACAGTGGA TTATGGAG	5'TTCGTGTTACTCAGAATGTC	53 - 53,5	100; 10
PseSat54-159	5'AATCTCTGCATATAAAAATGGC	5'AGATGGACCAAAAAGGTGTAT	50°C - 58°C	100; 10; 1; 0,1
PseSat55-43	5'CTGTGGTGCACCTAACCGA	5'CCCTATCATTTACAGTACA	50°C - 58°C	100; 10; 1; 0,1
PseSat56-87	5'CACCCAGCCACTTTTTTA	5'TGGAGGTAGTTAGTTAGATG	50°C - 51,5°C	100
PseSat57-162	5'AGGGTCAGTACTCTCACT	5'CACTTCATAACAGTCATTTTAA	52°C - 60°C	100; 10; 1; 0,1
PseSat61-213	5'ATCCAGGCAATAATCTGCC	5'CAGGCGAGAATTCTACCACT	53°C - 57,9°C	100; 10; 0,1
PseSat63-463	5'ATTGGTCAGATATTGTGAAG	5'ATTGCGCCGTTTCATATCAC	52°C - 60°C	100; 10
PseSat64-182	5'TTTACTGCTGTAAAGATTTTTC	5'CCTTTGGTAGGACATGTAGC	50°C - 50,7°C	100; 10; 1; 0,1
PseSat67-198	5'CTAACTTCATTCGGC	5'CCACCATGGCACACCT	55°C - 55,6°C	10; 1; 0,1

1836

1837 **Supplementary Table S4.** Shared SatDNA between *P. marilynae* and *P. semifasciata*. The
 1838 sequences highlighted in blue correspond to those selected for the FISH experiments

1839

<i>Pyrrhulina marilynae</i>	<i>Pyrrhulina semifasciata</i>	Classificação
PmaSat02-68	PseSat03-68	SV
PmaSat03-45	PseSat05-45	SV
PmaSat04-50	PseSat09-50	SV
PmaSat05-226	PseSat04-226	SV
PmaSat07-45	PseSat02-45	SV
PmaSat08-33	PseSat13-35	V
PmaSat11-2486	PseSat11-2510	V
PmaSat14-54	PseSat22-54	SV
PmaSat17-192	PseSat30-192	SV
PmaSat18-42	PseSat21-42	SV
PmaSat19-84	PseSat24-84	SV
PmaSat21-712	PseSat51-713	SV
PmaSat22-32	PseSat48-32	SV
PmaSat23-23	PseSat35-23	SV
PmaSat24-1283	PseSat28-1284	V
PmaSat26-21	PseSat47-21	SV
PmaSat27-39	PseSat40-39	SV
PmaSat28-165	PseSat54-159	V
PmaSat29-51	PseSat31-51	SV
PmaSat32-33	PseSat49-33	SV
PmaSat35-845	PseSat46-837	V
PmaSat36-445	PseSat45-445	V
PmaSat37-28	PseSat44-28	SV
PmaSat38-162	PseSat57-162	SV
PmaSat39-88	PseSat56-87	SV
PmaSat40-211	PseSat61-213	V
PmaSat41-915	PseSat33-880	V
PmaSat44-43	PseSat55-43	SV
PmaSat45-568	PseSat69-592	V
PmaSat46-470	PseSat62-469	V
PmaSat47-672	PseSat52-673	V
PmaSat49-80	PseSat39-80	SV
PmaSat52-387	PseSat58-372	V
PmaSat54-44	PseSat66-44	SV
PmaSat12-842	PseSat15-38	SF
PmaSat15-1437	PseSat14-1235	SF
PmaSat66-188	PseSat06-198	SF
PmaSat55-231	PseSat71-182	SF

1840

1841

1842

1843 **Author Contributions**

1844 Formal analysis, J.A.D.V., R.U. and M.d.B.C.; Funding acquisition, T.L. and M.d.B.C.;
1845 Investigation, T.L., R.L.R.d.M., F.d.M.C.S., R.Z.d.S., J.H.F.S., F.P.-F. and M.d.B.C.;
1846 Methodology, R.L.R.d.M., F.d.M.C.S., J.A.D.V., C.A.G.G., R.Z.d.S., J.H.F.S., F.P.-F., R.U. and
1847 M.d.B.C.; Project administration, M.d.B.C.; Software, R.L.R.d.M., J.A.D.V., C.A.G.G., J.H.F.S.
1848 and R.U.; Supervision, M.d.B.C.; Validation, R.L.R.d.M., F.d.M.C.S., J.A.D.V., C.A.G.G.,
1849 R.Z.d.S., F.P.-F., R.U. and M.d.B.C.; Visualization, T.L. and F.d.M.C.S.; Writing—original
1850 draft, R.L.R.d.M., F.d.M.C.S., J.A.D.V. and C.A.G.G.; Writing—review and editing, T.L.,
1851 J.A.D.V., C.A.G.G., R.Z.d.S., J.H.F.S., F.P.-F., R.U. and M.d.B.C. All authors have read and
1852 agreed to the published version of the manuscript.

1853

1854 **Funding**

1855 This work was supported by São Paulo Research Foundation (FAPESP) grants 2022/04964-3
1856 and 2019/25045-3 (RLRDM), 2020/11772-8 (MBC). We also acknowledge support for TL by
1857 the German Research Foundation Projekt-Nr. 512648189 and the Open Access Publication Fund
1858 of the Thueringer Universitaets- und Landesbibliothek Jena. All authors certify that they have
1859 no affiliations with or involvement in any organization or entity with any financial interest or
1860 non-financial interest in the subject matter or materials discussed in this manuscript.

1861

1862 **Institutional Review Board Statement**

1863 Sample was approved by the Brazilian Environmental Agency ICMBIO/SISBIO (License
1864 48628-14) and SISGEN (A96FF09). All experiments followed the guidelines and were approved
1865 by the Ethics Committee on Animal Experimentation of the Universidade Federal de São Carlos
1866 (Process number CEUA 7994170423).

1867

1868 **Informed Consent Statement**

1869 Not applicable.

1870

1871 **Data Availability Statement**

1872 The datasets generated during and/or analyzed during the current study are available from the
1873 corresponding author upon reasonable request. The datasets generated and analyzed during the

1874 current study are available in the GenBank repository under the accession numbers OR094701-
1875 OR094771 and OR094772-OR094841.

1876

1877 **Acknowledgments**

1878 We appreciate the contributions of Elixir CZ, CESNET, and CERIT-SC in the maintenance of
1879 the public Galaxy server where RepeatExplorer2 analysis was performed. The authors are
1880 grateful to Claudio Oliveira for the space on the server and to Francisco J. Ruiz-Ruano for
1881 providing Python scripts to analyze satellite sequences.

1882

1883 **Conflicts of Interest**

1884 The authors declare no conflict of interest.

1885

1886 **References**

1887 All references are compiled in the end of this thesis.

1888

1889

1890

1891

1892

1893

1894

1895

1896

1897

1898

1899

1900

1901

1902

1903

1904

1905

The evolution of Lebiasinidae (Teleostei: Characiformes): Insights from cytogenetics

Renata Luiza Rosa de Moraes, Francisco de Menezes Cavalcante Sassi, Fernando Henrique Santos de Souza, Geize Aparecida Deon, Manoela Maria Ferreira Marinho and Marcelo de Bello Cioffi

Artigo em Submissão

1907

1908

1909

1910

Abstract

1911 Cytogenetics and molecular data play critical roles in understanding the evolution of non-
1912 model species. When coupled, they offer an integrated approach that enables a more robust
1913 understanding of genetic diversity, population structure, and phylogenetic relationships within
1914 groups. Cytogenetic and molecular studies on Lebiasinidae fishes are challenging, mainly be-
1915 cause of their small sizes. However, with advancements in cytogenetic and molecular methods,
1916 the number of studies on the family has increased significantly. In this work, we first filled an
1917 important gap by describing, for the first time, the karyotype of a *Copella* species (*C. callole-*
1918 *pis*), showing a $2n = 36$ with a predominance of acrocentric chromosomes and multiple 5S and
1919 18S rDNA sites. Furthermore, by coupling previous phylogenetic studies, a nuclear marker-
1920 based phylogenetic tree, and a NeighborNet network, we were able to achieve a comprehensive
1921 understanding of the genetic relationships among species. In light of these new data and previ-
1922 ous morphology-based phylogenetic analyses, we evaluated the chromosomal evolution pat-
1923 terns of Lebiasinidae and put forth their most plausible evolutionary pathways. There was a
1924 significant karyotypic remodeling pattern in Lebiasinidae fishes, involving different sets of
1925 chromosomal rearrangements. This research is the continuation of a series of previous investi-
1926 gations into the Lebiasinidae family and settles one more step in the elucidation of its evolu-
1927 tionary history.

1928

1929 1. Introduction

1930 Research on non-model species generally presents several challenges when compared
1931 to model ones. Genomic resources, such as scaffold whole genome data or well-annotated ref-
1932 erence genomes, are usually scarce, or even unavailable (Ekblom and Galindo, 2011; Russel *et*
1933 *al.*, 2017). Cytogenetic techniques are a very powerful tool in the study of non-model organ-
1934 isms since they characterize the chromosomal morphologies, ploidy, and position of specific
1935 genomic markers without the need for prior information. As a result, it can aid in clarifying
1936 taxonomic issues and improving comprehension of the relationships between species or popu-
1937 lations. For example, cytogenetics has also contributed to finding cryptic diversity and even
1938 possible species complexes in fishes (Castro *et al.*, 2015; Rocha-Reis *et al.*, 2018). Other ap-
1939 proaches, such as the use of mitochondrial markers like 16S rRNA, cytochrome oxidase I
1940 (COI), and the Control Region (CR) are widely applied to comprehend how different groups
1941 of organisms evolved and study population genetics (Imoto *et al.*, 2013; Bronstein, Kroh and
1942 Haring, 2018). However, mitochondrial DNA analysis can generate distortions in the results
1943 when reticulate events are present since it represents a maternally inherited marker (Toews and
1944 Brelsford, 2012). Sampling nuclear markers is required to overcome such inheritance biases
1945 and provide a more reliable perspective on the evolutionary history of the species under study
1946 (Tollesfrud, 2009). Furthermore, incomplete lineage sorting and other frequent phylogenetic
1947 issues can be resolved with the use of several genetic markers (Mirarab *et al.*, 2016; Simmons
1948 and Gatesy, 2021). Therefore, using complexity reduction techniques that take advantage of
1949 the high throughput of NGS techniques is one of the primary methods used to access the diver-
1950 sity and genetic structure of these species at the nuclear level. This approach allows for the
1951 cost-effective acquisition of a large number of independent genetic markers across the genome
1952 (Davey *et al.*, 2011). Among complexity reduction methods available, DArTseq sequencing
1953 (Diversity Arrays Technology, Canberra, Australia) allows for the enrichment of hypomethyl-
1954 ated regions (Jaccoud *et al.*, 2001; Kilian *et al.*, 2012). Since molecular cytogenetics ap-
1955 proaches primarily focus on repetitive and hypermethylated regions, DArTseq is a useful com-
1956 plementary strategy for cytogenetics investigations (Cioffi *et al.*, 2019; de Oliveira *et al.*, 2019;
1957 Panthum *et al.*, 2021; Schimek *et al.*, 2022; Toma *et al.*, 2023).

1958 The Lebiasinidae family includes seven genera (*Lebiasina*, *Piabucina*, *Derhamia*, *Nan-*
1959 *nostomus*, *Pyrrhulina*, *Copella*, and *Copeina*) and 74 valid species that are native to the Neo-
1960 tropical region and widely spread in South and Central America (Costa Rica and Panama),

1961 except for Chile (Fricke *et al.*, 2024). Two subfamilies are recognized based on morphological
1962 characters: Lebiasininae, which includes *Derhamia*, *Lebiasina*, and *Piabucina*, and Pyrrhulini-
1963 nae, the most varied clade, encompassing the genera *Nannostomus*, *Copeina*, *Copella*, and *Pyr-*
1964 *rhulina* (Géry and Zarske, 2002; Weitzman and Cobb, 1975). Unpublished phylogenetic anal-
1965 ysis, however, recovers *Derhamia* as a basal taxa within the Pyrrhulininae (Marinho, 2014;
1966 Netto-Ferreira, 2010). In general, Lebiasinidae is composed of small-sized fishes that range in
1967 length from 1.5 to 7.0 cm and exhibit a wide diversity of body forms and colors, making them
1968 very appealing to aquarium hobbyists (Weitzman and Weitzman, 2003; Weitzman and Vari,
1969 1988). Due to this richness and to old species description, taxonomic identification of species
1970 is sometimes difficult, demanding the use of additional techniques such as cytogenetics or bar-
1971 coding (Xu *et al.*, 2024). In the same way, issues with phylogenetic placement also occurred.
1972 For a long time, the phylogenetic relationships of Lebiasinidae were uncertain, being related to
1973 different groups of Neotropical fishes. Phylogenetic analysis based on morphological charac-
1974 ters recovered Lebiasinidae as closely related to Erythrinidae, Ctenoluciidae, and Hepsetidae
1975 (Buckup, 1998) and Tarumanidae (de Pinna *et al.*, 2018) whereas those based on molecular
1976 data recovered Lebiasinidae as close to Serrasalminidae, Erythrinidae, and Hepsetidae (Ortí and
1977 Meyer, 1997) or Ctenoluciidae. Combined data have hypothesized Lebiasinidae as a sister to
1978 Ctenoluciidae (Calcagnotto *et al.*, 2005; Oliveira *et al.*, 2011; Arcila *et al.*, 2017; Betancur-R
1979 *et al.*, 2019; Mirande, 2019; Cassemiro *et al.*, 2023; Near and Thacker, 2024;).

1980 Because of their small size, representatives of the Lebiasinidae were little explored cy-
1981 togenetically. One big problem with studying the cytogenetics of such small fish was getting
1982 accurate information on the number and quantity of chromosome spreads. As a result, the stud-
1983 ies were limited to describing haploid and/or diploid chromosome numbers in some species
1984 (Oliveira *et al.*, 1991; Scheel, 1973; Arai, 2011). Thanks to improvements in methods, solid
1985 studies using both classical and molecular cytogenetics have made a considerable difference in
1986 our understanding of how the karyotypes of this group of fish have changed over time (Moraes
1987 *et al.*, 2017; Moraes *et al.*, 2019; Sassi *et al.*, 2019; Toma *et al.*, 2019; Sassi *et al.*, 2020; Sember
1988 *et al.*, 2020; Moraes *et al.*, 2021; Ferreira *et al.*, 2022; Leite *et al.*, 2022; Moraes *et al.*, 2023a).
1989 Such investigations included the first cytogenetic data for *Lebiasina*, *Copeina*, *Nannostomus*,
1990 and *Pyrrhulina*. In general, two evolutionary trends have been proposed for the karyotypic
1991 evolution of Lebiasinidae: 1) the conservation of a plesiomorphic karyotype in the subfamily
1992 Lebiasininae with $2n = 36$ biarmed chromosomes, and 2) the Pyrrhulininae subfamily exhibits
1993 significant variances in diploid numbers and karyotypes, with acrocentric chromosomes pre-
1994 dominating in most species (Sassi *et al.*, 2020). In this scenario, the majority of Pyrrhulininae's

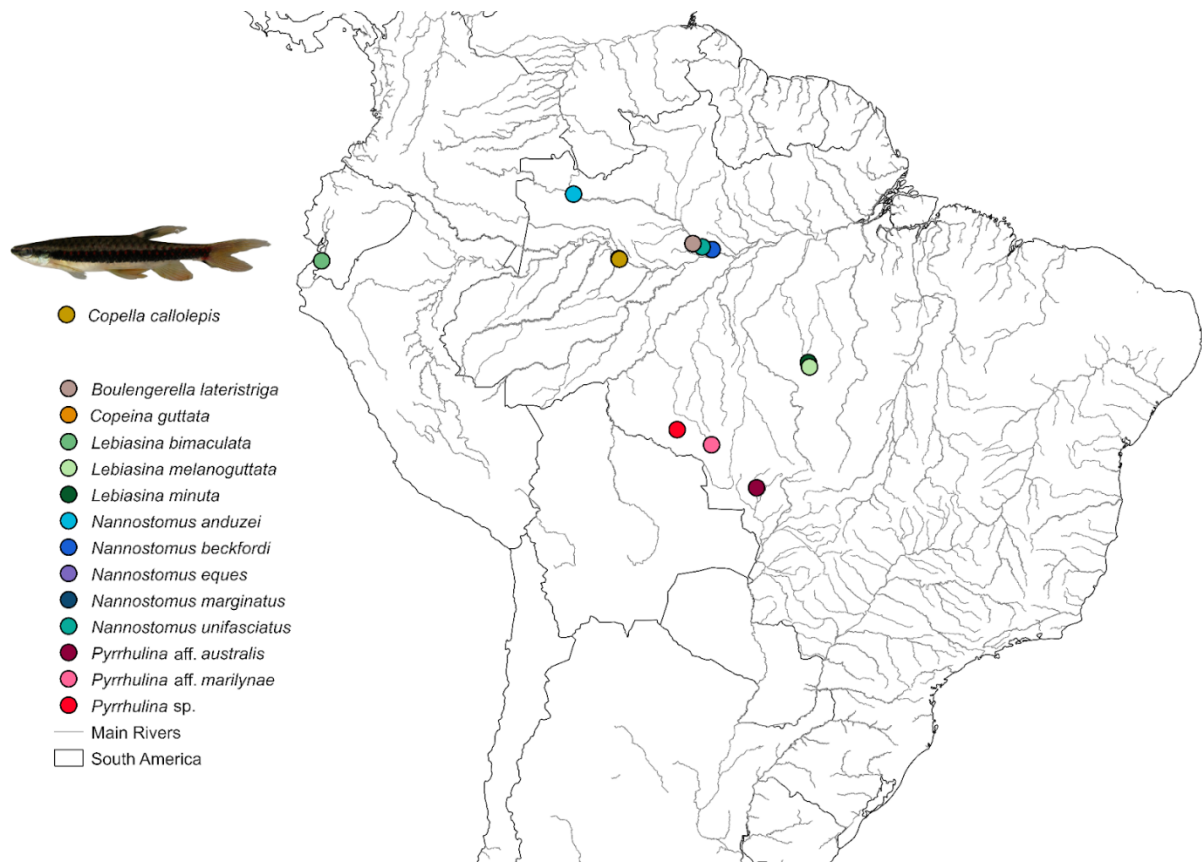
1995 acrocentric chromosomes are the result of rearrangements such as centric fissions (Sassi *et al.*,
1996 2020). However, some exceptions within the subfamily have revealed secondary fusion events,
1997 resulting in metacentric chromosomes in some species and a decrease in $2n$, as seen in *Pyr-*
1998 *rhulina marilynae* ($2n=34$), *Nannostomus anduzei* ($2n= 22$), and *Nannostomus unifasciatus*
1999 ($2n=22$), the last two representing one of the lowest diploid chromosome numbers found among
2000 teleost fishes (Sember *et al.*, 2020; Moraes *et al.*, 2021; Moraes *et al.*, 2023a).

2001 Here, to gain insights into the evolution of Lebiasinidae fishes, we describe, for the first
2002 time, the karyotype of a *Copella* species (named *C. callolepis*), filling an important gap in the
2003 cytogenetics knowledge of the family. Next, we reconstruct the evolutionary relationships
2004 within the family using genome-wide markers. With the assistance of this new data, we as-
2005 sessed the chromosomal evolution patterns of Lebiasinidae and proposed their likely evolu-
2006 tionary pathway.

2007 2. Material and Methods

2008 2.1. Sampling

2009 Thirteen individuals of *Copella callolepis* were collected in Tefé - AM ($3^{\circ}25'50.7''S$,
2010 $54^{\circ}44'54.8''W$). To collect tissues of the liver, kidney, spleen, and gills, a stereomicroscope
2011 was used. Chromosome isolation from collected tissues followed the conventional air-drying
2012 technique (Bertollo, 1978). Following the dissection, the complete fish bodies were preserved
2013 at 100% ethanol and deposited in the tissue bank of the Laboratório de Citogenética de Peixes
2014 of Universidade Federal de São Carlos (São Carlos, São Paulo, Brazil). All individuals were
2015 collected under the appropriate authorization of the Brazilian environmental agency IC-
2016 MBIO/SISBIO (License number 48628-14) and SISGEN (A96FF09). The experiments fol-
2017 lowed ethical standards, and anesthesia followed the Ethics Committee on Animal Experimen-
2018 tation of the Universidade Federal de São Carlos (Process number CEUA 7994170423). A list
2019 of all individuals used in Cytogenetics and sequencing analysis is presented in **Table 1**. Sam-
2020 pling sites for all species are presented in **Figure 1**.



2021
 2022 **Figure 1.** Map of South America with sampling sites indicated as dots. Each color represents a distinct
 2023 species, with colors defined on the legend in the left corner. A *Copella callolepis* individual is presented
 2024 above the legend (photo by José Luis Oliván Birindelli). The map was produced using the software
 2025 QGIS 3.4.4 (<https://qgis.org>), Inkscape 0.92 (<https://inkscape.org>), and Adobe Photoshop CC 2020 (San
 2026 Jose, CA, USA).
 2027

2028 **2.2. Conventional and molecular cytogenetics**

2029 Constitutive heterochromatin was revealed by the application of a standard C-banding proce-
 2030 dure (Sumner, 1972). The 5S and 18S rDNA probes of ribosomal 5S and 18S rDNA were
 2031 isolated from the *Hoplias malabaricus* genome (Cioffi *et al.*, 2009; Pendás *et al.*, 1994). The
 2032 5S rDNA probe included 120 base pairs (bp) of the 5S rDNA gene coding region and 200 bp
 2033 of non-transcribed spacer (NTS) (Pendás *et al.*, 1994). The 18S rDNA probe was composed of
 2034 a 1400-bp-long segment of the 18S rDNA coding region (Cioffi *et al.*, 2009). Both probes were
 2035 directly labeled with the Nick Translation Mix Kit (Jena Bioscience, Jena, Germany) according
 2036 to the manufacturer's instructions, the 18S rDNA probe with Atto488-dUTP and the 5S rDNA
 2037 with Atto550-dUTP. Both rDNA sequences were mapped by fluorescence in situ hybridization
 2038 (FISH) with high stringency conditions (Sassi *et al.*, 2022). Briefly, metaphase chromosomes
 2039 were treated with RNase A (40 g/mL) for 1.5 h at 37°C and the metaphase chromosomes were
 2040 denatured in 70% formamide/2xSSC at 72°C for 3 min. A total of 20 µL of the hybridization
 2041 mixture (2.5 ng/L probes, 50% deionized formamide, and 10% dextran sulfate) was then

2042 applied, and the hybridization process was performed overnight at 37°C in a moist chamber.
 2043 The first post-hybridization wash was performed with 1xSSC for 5 min at 65°C in a shaker,
 2044 followed by 4xSSC/Tween for 5 min at room temperature. Chromosomes were counterstained
 2045 with DAPI in Vectashield (Vector Laboratories, Burlingame, CA, USA).

2046 2.3. Sequencing and obtention of SNPs

2047 We sequenced a total of 41 individuals from 14 different Lebiasinidae species (**Table 1**).
 2048 From each individual, we extracted a small fragment of liver or muscle and stored it in 100%
 2049 ethanol. We performed the DNA extraction according to the protocol described in Sambrook
 2050 and Russell (Sambrook and Russell, 2001). We assessed the DNA quality with NanoDrop (Ther-
 2051 moFisher Scientific, Branchburg, NJ, EUA) and then sent the samples to Diversity Arrays Tech-
 2052 nology Pty Ltd. (Canberra, Australia), for the DArTseq procedure.

2053 DArTseq is based on the use of two distinct restriction enzymes: a frequent cutter and a nucle-
 2054 ase with affinity for hypomethylated regions, generally PstI and SphI (Kilian *et al.*, 2012). The
 2055 sequencing was performed on the Illumina HiSeq 2500 platform, using 3 individuals from each
 2056 species. After sequencing, all generated adapters were trimmed, and sequences went through a
 2057 quality filtering process. The quality of the reads was checked and the resulting reads were pro-
 2058 cessed with proprietary DArT software, resulting in high-quality sequences. We extracted and
 2059 concatenated the sequences of up to 69 bp with the gl2fasta function of the package DArTR
 2060 v.2.9.7 (Gruber *et al.*, 2018) in a dataset for phylogenetic analysis. A final dataset comprising a
 2061 set of Single Nucleotide Polymorphisms (SNP) was generated, with SNPs coded as 1 for heter-
 2062 ozygotes, 0 for reference homozygotes, and 2 for alternate homozygotes.

2063

2064 **Table 1:** Samples used in this study.

Species	2n	Sampling Site	Geographical coordinates	References
<i>Boulengerella lateristriga</i>	36	Novo Airão - AM, Brazil	2°37'28.5"S, 60°58'16.8"W	Souza e Sousa <i>et al.</i> 2017
<i>Copeina guttata</i>	42	Tefé River - AM, Brazil	03°39'49.5"S, 64°59'40"W	Toma <i>et al.</i> 2019
<i>Copella callolepis</i>	36	Tefé River - AM, Brazil	3°25'50.7"S, 54°44'54.8"W	Present study
<i>Lebiasina bimaculata</i>	36	Arenillas River - El Oro, Ecuador	03°30'57.2"S, 80°3'44.2"W	Sassi <i>et al.</i> 2019
<i>Lebiasina melanoguttata</i>	36	Cachoeira da Serra - PA, Brazil	08°46' 59.4"S, 54°58'26.9"W	Sassi <i>et al.</i> 2019
<i>Lebiasina minuta</i>	36	Cachoeira da Serra - PA, Brazil	8°44'39.0"S 55°02'03.0"W	Leite <i>et al.</i> 2022
<i>Nannostomus anduzei</i>	22	Zamula Stream, Barcelos - AM, Brazil	0°04'57.5"S 67°06'23.8"W	Moraes <i>et al.</i> 2023a
<i>Nannostomus beckfordi</i>	44	Agenor Stream - AM, Brazil	2°55'53.9"S 59°58'30.7"W	Sember <i>et al.</i> 2020
<i>Nannostomus eques</i>	36	Cuieiras River - AM, Brazil	2°47'58.1"S 60°29'19.8"W	Sember <i>et al.</i> 2020
<i>Nannostomus marginatus</i>	42	Adolpho Ducke Reserve - AM, Brazil	2°55'53.9"S 59°58'30.7"W	Sember <i>et al.</i> 2020
<i>Nannostomus unifasciatus</i>	22	Cuieiras River - AM, Brazil	2°47'58.1"S 60°29'19.8"W	Sember <i>et al.</i> 2020
<i>Pyrrhulina aff. australis</i>	40	Branco River - MT, Brazil	15°11'28.0"S 57°41'30.7"W	Moraes <i>et al.</i> 2017

<i>Pyrrhulina</i> aff. <i>marilynae</i>	40	12 de Outubro Stream - MT, Brazil	12°58'41.0"S 60°00'34.0"W	Moraes <i>et al.</i> 2021
<i>Pyrrhulina</i> sp.	40	Alto Alegre do Parecis - RO, Brazil	12°11'58.0"S 61°46'47.4"W	Moraes <i>et al.</i> 2021

2065

2066 2.4. *Principal Component Analysis*

2067 To access an overview of the distribution of genetic diversity among samples, we carried
 2068 out a Pearson Principal Component Analysis (PCA). We performed the analysis with two distinct
 2069 datasets, the first comprising data from all species, and the second only with *Nannostomus* data.
 2070 We imported the SNP matrix in RSTUDIO v.4.3.2 as a genlight object, and the PCA was per-
 2071 formed using the Package DArTR v.2.9.7 (Gruber *et al.*, 2018).

2072

2073 2.5. *Species tree*

2074 To better understand the genetic relationships between species, we estimated a maxi-
 2075 mum likelihood species tree using RAxML (Stamatakis, 2014). Before the analysis, we first
 2076 concatenated all sequences from each sample in a PHYLIP format file using the DArTR pack-
 2077 age. Initially, we conducted a model test to define which substitution model better adjusted to
 2078 our data. We estimated the substitution model with the maximum likelihood approach using
 2079 ModelTest-NG (Darriba *et al.*, 2020) with a template parameter adjusted to RAxML, datatype
 2080 set as DNA, and seed number defined as 12345. We set all remaining parameters at default.
 2081 We considered the model with the smallest Bayesian Information Criterion (BIC) as the best
 2082 model. We performed the phylogenetic analysis using the GTR+Gamma+I model with four
 2083 rate categories, setting parameters to generate 100 distinct starting trees, and performed a rapid
 2084 bootstrap analysis. We used a random seed number of 12345 for both the parsimony starting
 2085 trees and the bootstraps. We estimated a consensus tree in GENEIOUS Prime v2023.2. with
 2086 the Majority Rule consensus method, with a support threshold of 70%. The consensus tree is
 2087 based on the 100 trees generated, we exported it and plotted it using FigTree v 1.4.4.

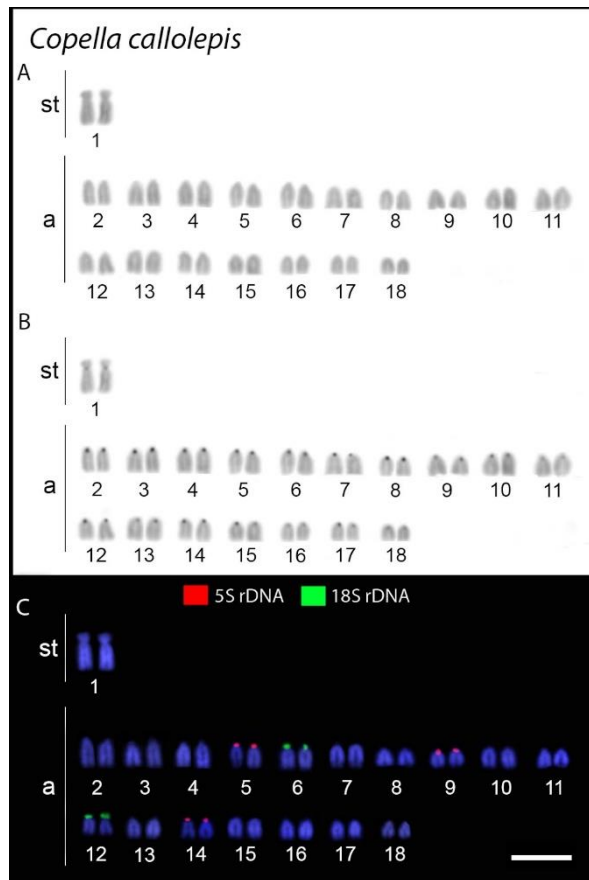
2088 To test for any reticulate structure that deviates from the bifurcating tree-like evolution,
 2089 we implemented a NeighborNet network analysis (Bryant and Moulton, 2004) in SplitsTree
 2090 software.

2091 3. Results

2092 3.1. *Conventional and molecular cytogenetics*

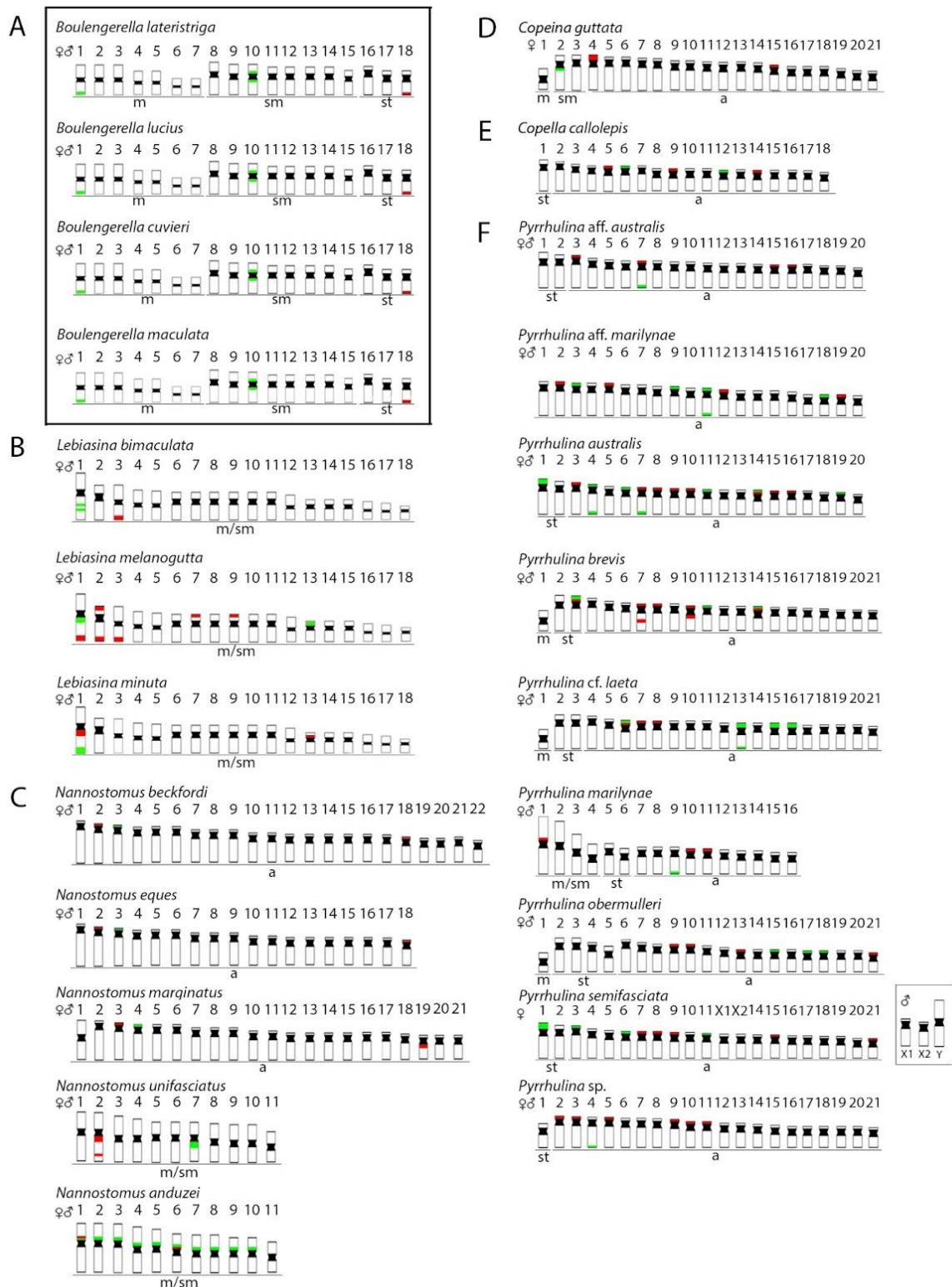
2093 The diploid chromosome number in all analyzed *Copella callolepis* specimens was $2n =$
 2094 36 (**Figure 2**). The karyotype consisted predominantly of acrocentric chromosomes except for
 2095 two subtelocentric chromosomes (**Figure 2A**), with C-positive heterochromatin blocks found in
 2096 the centromeric region of almost all chromosomes (**Figure 2B**). Multiple 5S rDNA and 18S

2097 rDNA sites were found in the centromeric regions of pairs 5, 9, and 14 (5S rDNA) and 6 and 12
2098 (18S rDNA) (**Figure 2C**).



2099
2100
2101
2102
2103

Figure 2. Karyotypes of *Copella callolepis* arranged after different cytogenetic protocols. Giemsa staining (A), C-banding (B), and dual-color FISH with 18S (green) and 5S (red) rDNA probes (C). Chromosomes are counterstained with DAPI (blue). Scale bar = 10 μ m

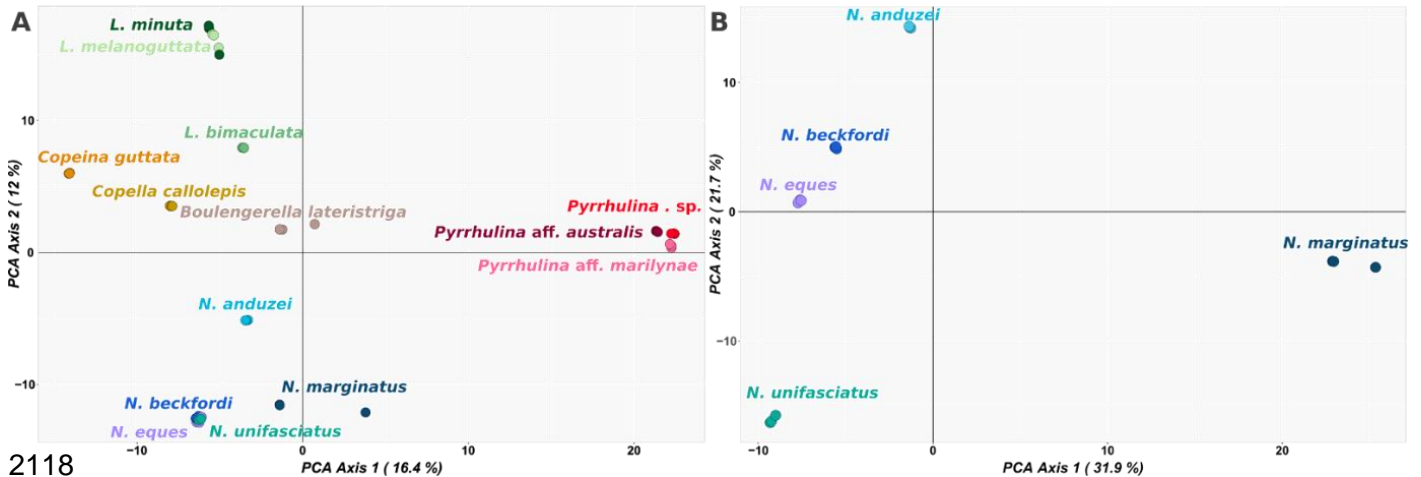


2104
2105
2106
2107
2108
2109
2110
2111

Figure 3. Schematic representation of chromosomes of Lebiasinidae and Ctenoluciidae species, highlighting the position of 18S rDNA (green) and 5S rDNA (red). The small box highlights a sex chromosome system in *Pyrrhulina semifasciata*, while the bigger box highlights the Ctenoluciidae members. FISH data were taken from Souza e Sousa *et al.* 2017; Moraes *et al.*, 2017; Sassi *et al.* 2019; Toma *et al.* 2019; Sember *et al.* 2020; Leite *et al.* 2022; Moraes *et al.*, 2019; Moraes *et al.*, 2021; Moraes *et al.* 2023a. Letters correspond to the genera: (A) *Boulengerella*, (B) *Lebiasina*, (C) *Nannostomus*, (D) *Copeina*, (E) *Copella*, and (F) *Pyrrhulina*.

2112 3.2. *Principal component analysis*

2113 The principal component analysis shows a clear clustering of samples mainly at the genera level, evidencing the genetic differentiation between the species examined (**Figure 4A**), the
2114 era level, evidencing the genetic differentiation between the species examined (**Figure 4A**), the
2115 PCA comprising only *Nannostomus* samples (**Figure 4B**) helps to unravel the differentiation
2116 between *Nannostomus beckfordi*, *Nannostomus eques*, and *Nannostomus unifasciatus* which ap-
2117 peared clustered on the main PCA.



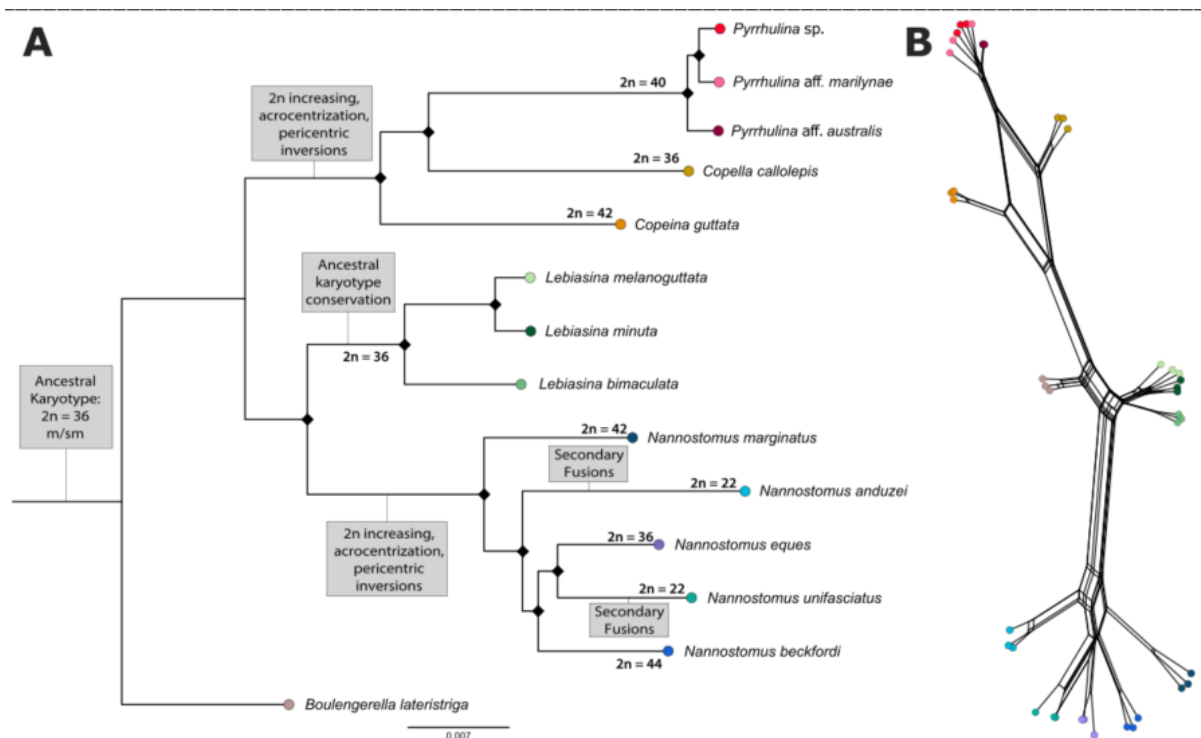
2118 **Figure 4.** Principal component analysis results, each circle represents an individual, species are colored
2119 differently according to the names, percentage values indicate the explanatory capability of each axis,
2120 (A) displays the results for the PCA analysis with the full dataset; (B) displays the results for the dataset
2121 comprising only *Nannostomus* samples.
2122
2123

2124 3.3. *Species tree and Neighbor-net*

2125 The estimated species tree is presented in **Figure 5A**. Individuals of the same species are
2126 collapsed together to simplify visualization, and the full tree is presented in the supplementary
2127 material (**Figure S1**). Overall, the topology is well supported, with all nodes having 100 boot-
2128 strap support. The tree depicts the relationships among sampled Lebiasinidae species, placing
2129 *Copella callolepis* in a broader phylogenetic context with nuclear molecular data for the first
2130 time.

2131 The NeighborNet network (**Figure 5B**) presents a structure congruent to the species tree,
2132 the main difference being a minor clustering of a *Pyrrhulina aff. marilynae* individual with *Pyrr-*
2133 *rhulina* sp. samples.

2134



2135
 2136 **Figure 5.** Maximum likelihood species tree (A), diamond symbols indicate nodes with bootstrap values
 2137 of 100, gray boxes indicate relevant the main cyto-genetic features of each clade. NeighborNet network
 2138 circles are colored in the same scheme as the phylogenetic tree, each circle represents a sample that was
 2139 collapsed into one in the phylogeny (B).
 2140

2141 4. Discussion

2142 This study presents a comprehensive analysis of the cytogenetics of Lebiasinidae, includ-
 2143 ing the karyotype of a *Copella* species (*C. callolepis*), which has now been defined for the first
 2144 time. In addition, by using molecular phylogenetic research and a NeighborNet network, we
 2145 successfully reconstructed a species tree, providing a thorough comprehension of the genetic
 2146 links between Lebiasinidae species. Based on this new information, we analyzed the chromoso-
 2147 mal evolution patterns of Lebiasinidae and proposed their most likely evolutionary pathways.
 2148

2149 4.1. Chromosomal features of *Copella callolepis*

2150 Based on our findings, *C. callolepis* preserved the proposed ancestral 2n for the family
 2151 (2n = 36), but not its karyotype structure. In contrast to the ancestral karyotype, which was
 2152 mostly made up of metacentric chromosomes, *C. callolepis* karyotype exhibited a large number
 2153 of acrocentrics, which reinforces the important role of pericentric inversions in the karyotype
 2154 evolution of the group. Similar scenarios are observed in other fishes, such as the giant trahiras
 2155 *Hoplias* (Sassi *et al.*, 2021), *Nothobranchius* killifishes (Krysanov *et al.*, 2023), *Rineloricaria*
 2156 armored catfishes (Marajó *et al.*, 2023), and *Ictalurus* catfishes (Waldbieser *et al.*, 2023). Be-
 2157 sides pericentric inversions, centromere repositioning (Schubert, 2018) might also explain the

2158 high divergence of acrocentrics between karyotypes of related species. Indeed, a molecular
2159 study in the medaka fish *Oryzias javanicus* suggests the repositioning of centromere-associated
2160 repeats as the main mechanism for the increase of acrocentrics in karyotype, rather than peri-
2161 centric inversions (Ansai *et al.*, 2023). In addition to acrocentrics, the karyotype of *C. callolepis*
2162 has a single pair of large subtelocentric chromosomes, which is very similar in shape and size
2163 to pair 5 of *P. marylinae*, pair 1 of *Pyrrhulina* sp., and pair 2 of *P. obermulleri* and *Pyrrhulina*
2164 cf. *laeta* (Moraes *et al.*, 2021), suggesting that it may have originated before the split of *Pyrrhulina*
2165 and *Copella* (**Figure 5**). The presence of metacentric and submetacentric chromosomes
2166 suggests that the karyotype of *Copeina guttata* retained other features of the basal karyotype
2167 of the family (Toma *et al.*, 2019). However, given their similar sizes, it's also possible that the
2168 subtelocentric pair observed in *Pyrrhulina* and *Copella* is also present in the karyotype of *Co-*
2169 *peina guttata*, either as pair 2, 3, or 4. To shed light on this scenario, additional investigations
2170 employing whole-chromosome painting seem necessary.

2171 While the 2n of other *Copella* species ranges from 24 to 44 chromosomes (Arai, 2011;
2172 Scheel, 1973), these studies were merely descriptive and omitted important details like the
2173 karyotype formula or the number of individuals karyotyped, which impairs their reproducibil-
2174 ity. However, such 2n variation indicates that a series of rearrangements have taken place dur-
2175 ing the chromosomal evolution of the genus, which might have included chromosome fissions,
2176 fusions, translocations, and inversions, as also observed in other lebiasinids (Sember *et al.*,
2177 2020; Moraes *et al.*, 2021; Moraes *et al.*, 2023). Moreover, this series of rearrangements is also
2178 highlighted by the presence of multiple sites for both 5S and 18S rDNA (**Figures 2 and 3**), an
2179 unusual characteristic for fishes (Gornung, 2013; Sochorová *et al.*, 2018). Ribosomal DNAs
2180 are known to spread through the genome either by their association with transposable elements
2181 (TEs) (Garcia *et al.*, 2024) or by the presence of pseudo-homologous regions across heterolo-
2182 gous acrocentric chromosomes, allowing them to recombine and exchange ribosomal repeats
2183 (Guarracino *et al.*, 2023). Given the presence of C-positive heterochromatin in the centromeres
2184 of *C. callolepis* (**Figure 2B**) associated with ribosomal repeats, and hence decreased or re-
2185 pressed recombination (Ellermeier *et al.*, 2010; Roberts, 1965), the association with TEs is
2186 more likely to be the mechanism behind the occurrence of multiple rDNA sites in its karyotype.
2187 Albeit the association of rDNAs and sex chromosomes in several fish species (Cioffi and Ber-
2188 tolo, 2012), the multiple X_1X_2Y that arose by a Robertsonian translocation in *P. semifasciata*
2189 (Moraes *et al.*, 2019) do not accumulate such sequences. Nevertheless, repeated DNA differ-
2190 ences between the sexes supported the likely ZZ/ZW sex system of *L. bimaculata* (Sassi *et al.*,
2191 2019). Regretfully, although *C. callolepis* exhibits parental care and sexual dimorphism

2192 (Marinho and Menezes, 2017), our study was unable to access the female karyotype to detect
2193 any sex-related variations using cytogenetic analysis.

2194

2195 4.2. Trends in karyotype evolution of Lebiasinidae in light of new genomic data

2196 According to TimeTree 5 (Kumar *et al.*, 2022), the split between *Lebiasina* (Lebi-
2197 asinidae) and *Boulengerella* (Ctenoluciidae) occurred around 70 million years ago (mya), while
2198 the one between *Lebiasina* and *Nannostomus* occurred 65 mya. By that time, with the uplifting
2199 of the Andes Mountain range, several river capture events occurred, raising diversification rates
2200 and creating an extraordinary richness in South American fishes, mostly through allopatric
2201 speciation events (Boschman *et al.*, 2023; Casemiro *et al.*, 2023). In contrast, the split between
2202 *Pyrrhulina* and *Copella* took place more recently, around 55 mya, during the Paleogene. This
2203 is associated with the Paleocene–Eocene thermal maximum, which raised temperatures and
2204 significantly increased carbon input into the ocean and atmosphere. Given the unique commu-
2205 nity structures identified in fossilized ray-finned fish, this split indicates the age of modern
2206 fishes (Haynes and Hönisch, 2020). As most Lebiasinidae populations are small and allopatric,
2207 both hypotheses support the large cytogenetic diversity observed within the family. The con-
2208 servation of the ancestral karyotype in Lebiasininae (which, according to morphological data,
2209 includes *Derhamia*, *Lebiasina*, and *Piabucina*) and extensive rearrangements leading to the
2210 formation of acrocentrics in the karyotypes of Pyrrhulininae (including *Copeina*, *Copella*, *Nan-*
2211 *nostomus*, and *Pyrrhulina*) were the two main evolutionary pathways that occurred in Lebi-
2212 asinidae, as proposed by Sassi *et al.* (2020). In the light of molecular data, however, a distinct
2213 scenario is proposed. In light of recent molecular studies that included Lebiasinidae represent-
2214 atives, the position of *Nannostomus* in Pyrrhulininae is contested (Casemiro *et al.*, 2023) and
2215 herein reinforced. Our molecular phylogeny based on DArTseq SNPs suggests that *Nannosto-*
2216 *mus* is more likely to be a sister genus to *Lebiasina* and these two genera to be sisters of the
2217 clade composed of *Copeina*, *Copella*, and *Pyrrhulina* (**Figure 5**). By that, it is possible to infer
2218 that Lebiasininae is likely to be composed of *Lebiasina* and *Nannostomus*, while Pyrrhulininae
2219 comprises *Copeina*, *Copella*, and *Pyrrhulina* (**Figure 5**). Although nearly all phylogenetic re-
2220 search on Lebiasinidae is not congruent in terms of species samples, up to date, no species tree
2221 includes all recognized species. On the other hand, these investigations provide us with predic-
2222 tions of relationships between genera and occasionally between species. Even though most of
2223 their samples consisted of species not included in our analysis, our results line up with those of
2224 Casemiro *et al.* (2023), who identified *Pyrrhulina* as a sister genus to *Copella* and *Lebiasina*
2225 as a sister genus to *Nannostomus*. Four different *Nannostomus* species—*N. marginatus*, *N.*

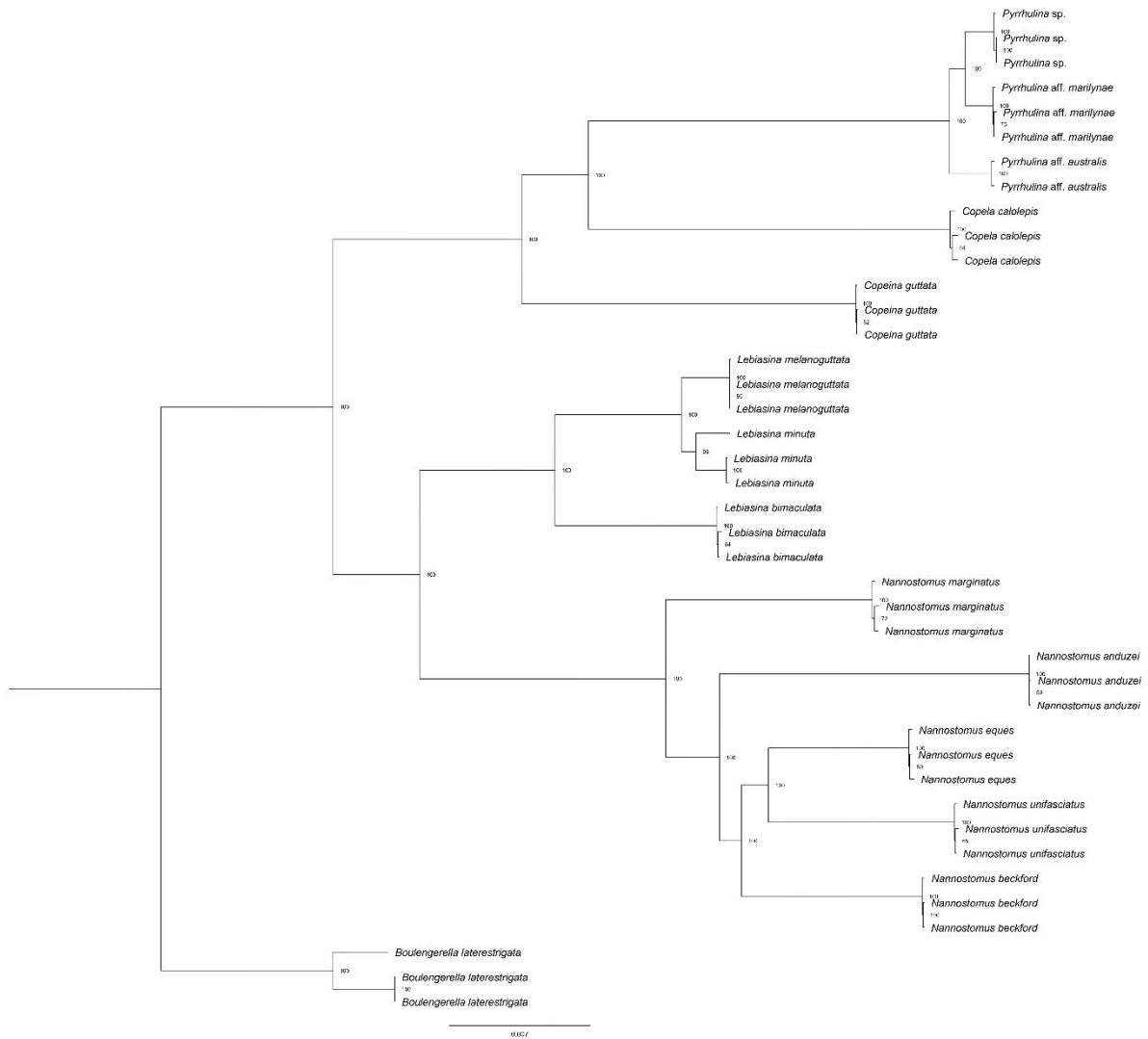
2226 *beckfordi*, and *N. unifasciatus*—had their mitogenomes constructed in a recent work (Xu *et al.*,
2227 2024). The estimated phylogeny tree retrieved *N. beckfordi* and *N. unifasciatus* as closely re-
2228 lated, with *N. marginatus* positioned more distant from both. This result is consistent with both
2229 the PCA and our phylogenetic analysis (**Figures 4 and 5**).

2230 We can see from these phylogenetic studies that the ancestral 2n of the family (36),
2231 which is the same in both Lebiasinidae subfamilies, is shared by both *C. callolepis* and *Lebia-*
2232 *sina* species. This indicates that Lebiasinidae represents another Neotropical Characiform fam-
2233 ily with extensive interspecific karyotype diversity, along with Erythrinidae (Bertollo, 2007;
2234 Cioffi *et al.*, 2012) and Characidae (Arefjev, 1990; Pazza and Kavalco, 2007; Soto *et al.*, 2018).
2235 Although the majority of *Nannostomus* and *Pyrrhulina* have higher 2n and a karyotype domi-
2236 nated by acrocentric chromosomes, some species exhibit metacentric chromosomes that result
2237 from secondary fusions (Sember *et al.*, 2020; Moraes *et al.*, 2023). This feature and the molec-
2238 ular phylogeny indicate that the two evolutionary pathways proposed by Sassi *et al.* (2020)
2239 may only partially reflect the evolutionary history of Lebiasinidae. With that in mind, we can
2240 now focus on a primary pattern of high karyotypic reorganization that results in acrocentrics
2241 dominating Pyrrhulininae karyotypes. As for Lebiasininae, while the ancestral karyotype is
2242 fully conserved in *Lebiasina* (Sassi *et al.*, 2019; Leite *et al.*, 2022), it has experienced substan-
2243 tial modification in *Nannostomus*, leading to karyotypes made up of acrocentrics, which in
2244 certain species may undergo full secondary fusion into metacentrics. As was already indicated,
2245 a small number of studies on *Copella* species have previously reported the 2n with reliable
2246 results (**Table 1**) nonetheless, these studies, when combined with our findings, suggest that this
2247 genus also experiences processes similar to the evolution of *Nannostomus* karyotypes.

2248 Recent molecular research suggests that *Nannostomus* is classified under the Lebi-
2249 asininae subfamily (Cassemiro *et al.*, 2023). However, the cytogenetic and taxonomy data
2250 available so far align with the patterns proposed by Sassi *et al.* (2020). Future investigations
2251 on *Derhamia* and other unstudied species might enhance our comprehension of the evolution-
2252 ary connections within this family. Moreover, the integration of additional morphological, mo-
2253 lecular, and cytogenetic studies with a larger sample size might establish a conclusive Lebi-
2254 asinidae phylogeny, enhancing comprehension of their evolutionary pathways.

2255 **Supplementary Materials**

2256 **Figure S1:** Maximum likelihood species tree with all sampled individuals in this study. Values
2257 close to each node indicate bootstrap values.



2258

2259 **References**

2260 All references are compiled in the end of this thesis.

2261 5. Considerações Finais

2262 A família Lebiasinidae é um grupo desafiante por conta das dificuldades de coleta,
2263 identificação, obtenção cromossômica e manuseio de animais tão pequenos. Entretanto, ao
2264 longo dos anos com os avanços metodológicos foi possível analisar citogenética e
2265 molecularmente uma diversidade de espécies da família que contribuíram significativamente
2266 para os avanços sobre o grupo. Sendo assim, nesse trabalho foram caracterizadas
2267 citogeneticamente cinco espécies de *Pyrrhulina* que resumidamente apresentaram i) um 2n
2268 conservado variando entre 40-42 cromossomos; ii) acúmulo de heterocromatina C-positiva
2269 principalmente nas regiões pericentroméricas/centroméricas e teloméricas; iii) múltiplos sítios
2270 de DNAr 18S e 5S; iiiii) cariótipos marcados majoritariamente por cromossomos acrocêntricos.
2271 Adicionalmente foi observada a presença de um cariótipo diferenciado entre as espécies
2272 estudadas, das quais *P. marilynae* apresentou uma redução cariotípica ($2n=32$) com a presença
2273 de quatro cromossomos metacêntricos grandes e incomuns oriundos de possíveis fusões
2274 secundárias.

2275 Os experimentos de hibridização genômica comparativa, pintura total cromossômica e
2276 análises de DNA satélite auxiliaram na compreensão das relações entre as espécies de
2277 *Pyrrhulina*, a redução cariotípica ocorrida em *P. marilynae* e a origem do único sistema
2278 heteromórfico X_1X_2Y observado na família. Assim, a presença do sistema sexual múltiplo
2279 observado em *P. semifasciata* foi confirmada por experimentos de WCP, os quais evidenciaram
2280 três cromossomos ($1m+2a$) não pareados e totalmente marcado nos machos da espécie e dois
2281 pares de cromossomos totalmente marcados tanto nas fêmeas da espécie como em outras
2282 espécies do gênero sugerindo que formação do cromossomo neo-Y desse sistema fosse a fusão
2283 de dois cromossomos acrocêntricos não homólogos. Ainda nesse cenário, sequências de DNA
2284 satélite foram utilizadas para auxiliar na corroboração da hipótese da origem desse sistema
2285 (X_1X_2Y), assim, a presença de poucos sinais sexo específicos e a ausência de sequências
2286 exclusivas dos cromossomos sexuais, levaram a crer que o sistema sexual presente em *P.*
2287 *semifasciata* seria evolutivamente recente. Além disso, todos os satDNAs presentes em
2288 cromossomos sexuais de *P. semifasciata* hibridizaram em suas espécies próximas,
2289 corroborando assim com a possível formação do sistema por fusão cêntrica. Sendo assim, a
2290 presença marcante dos cromossomos sexuais heteromórficos em *P. semifasciata* podem ter
2291 contribuído significativamente para o aumento da diferenciação genética na espécie.

2292 Com relação a redução cariotípica de *P. marilynae* não foi possível concluir efetivamente
2293 as causas desse processo, entretanto as hibridizações genômicas comparativas mostraram que

2294 tal espécie apresenta uma gama de regiões espécie-específicas indicando uma diferente
2295 tendência evolutiva quando comparada com outras espécies do gênero. Além disso, foi
2296 observado também um acúmulo de satDNAs na região centromérica dos cromossomos da
2297 espécie sugerindo que tais sequências podem estar relacionadas as possíveis fusões que
2298 geraram a redução do cariótipo de *P. marilynae*. Em um contexto geral foi possível observar
2299 que embora as nove espécies de *Pyrrhulina* compartilhem uma gama de características
2300 cariotípicas e genômicas, foram evidenciadas uma série de particularidades em cada uma das
2301 espécies, identificando diferentes processos evolutivos entre elas.

2302 Por fim foi caracterizado pela primeira vez o cariótipo de *Copella* que preservou o $2n$
2303 ancestral proposto para família ($2n=36$), mas não sua estrutura cariotípica. Em contraste com
2304 o cariótipo ancestral que era composto principalmente de cromossomos metacêntricos, *C.*
2305 *callolepis* exibiu um grande número de acrocêntricos, reforçando o importante papel das
2306 inversões pericêntricas na evolução do cariótipo do grupo. Sabe-se que duas tendências
2307 evolutivas foram sugeridas, para as subfamílias de Lebiasinidae: i) um cariótipo conservado
2308 com $2n=36$ composto exclusivamente por cromossomos meta/submetacêntricos representando
2309 a condição basal do grupo, como visto em *Lebiasina*; e ii) um cariótipo com $2n$ mais elevado,
2310 rearranjos cromossômicos estruturais e um cariótipo majoritariamente acrocêntrico. Sendo
2311 assim, teríamos a subfamília Lebiasininae composta por *Lebiasina* e *Dehamia*, e Pyrrhulilinae
2312 composta por *Copeina*, *Copella*, *Nannostomus* e *Pyrrhulina*. Embora essas tendências tenham
2313 sido reafirmadas mais de uma vez em diferentes estudos, e os dados citogenéticos e
2314 taxonômicos até então relatados corroborem com essas tendências, nossos estudos moleculares
2315 propuseram algumas mudanças nesse cenário, tais como a inclusão de *Nannostomus* dentro de
2316 Lebiasininae. Mesmo com o conjunto de todos esses dados ainda sim fica evidente a
2317 necessidade de maiores estudos envolvendo principalmente as relações internas da família,
2318 bem como a inclusão de estudo citogenéticos envolvendo *Dehamia*, dados esses ausentes até o
2319 presente momento.

2320 6. Referências bibliográficas

- 2321 Ahmad, S.F., Singchat, W., Jehangir, M., *et al.* (2020). Dark Matter of Primate Genomes: Sat-
2322 ellite DNA Repeats and Their Evolutionary Dynamics. *Cells* 9, 2714.
2323 doi:10.3390/cells9122714
- 2324 Albert, J.S., Craig, J.M., Tagliacollo, V.A., *et al.* (2018). Upland and Lowland Fishes: A Test
2325 of the River Capture Hypothesis. *Mt. Clim. Biodivers* 273.
- 2326 Albert, J.S., Tagliacollo, V.A., Dagosta, F. (2020). Diversification of Neotropical Freshwater
2327 Fishes. *Annual Review of Ecology, Evolution, and Systematics* 51(1), 27-53.
- 2328 Albert, J.S., Bernt, M.J., Fronk, A.H., *et al.* (2021). Late Neogene megariver captures and the
2329 Great Amazonian biotic interchange. *Global and Planetary Change* 205, 103554. doi:
2330 10.1016/j.gloplacha.2021.103554
- 2331 Alkimim, E.R., Caixeta, E.T., Sousa, T.V., *et al.* (2018). High-throughput Targeted
2332 Genotyping Using Next-Generation Sequencing Applied in Coffea Canephora Breeding.
2333 *Euphytica* 214(3), 1–18. doi:10.1007/s10681-018-2126-2
- 2334 Allen, W.R., Ternetz, C., Meyers, G.S., and Myers, G.S. (1926). Descriptions of a New Char-
2335 acin Fish and a New Pygidiid Catfish from the Amazon Basin. *Copeia* 156, 150–152.
2336 doi:10.2307/1436719
- 2337 Altschul, S.F., Gish, W., Miller, W., *et al.* (1990). Basic local alignment search tool. *J. Mol.*
2338 *Biol.* 215, 403-410. doi: 10.1016/S0022-2836(05)80360-2
- 2339 Ansai, S., Toyoda, A., Yoshida, K., *et al.* (2023). Repositioning of centromere-associated
2340 repeats during karyotype evolution in *Oryzias* fishes. *Mol. Ecol.* doi: 10.1111/mec.17222
- 2341 Arai, R., 2011. Fish karyotypes: a check list. *Springer Science and Business Media*
- 2342 Arcila, D., Ortí, G., Vari, R., *et al.* (2017). Genome-wide interrogation advances resolution of
2343 recalcitrant groups in the tree of life. *Nat. Ecol. Evol.* 1, 0020. doi: 10.1038/s41559-016-
2344 0020
- 2345 Arefjev, V. (1990). Problems of karyotypic variability in the family Characidae (Pisces,
2346 Characiformes) with the description of somatic karyotypes for six species of tetras.
2347 *Caryologia* 43, 305–319. doi: 10.1080/00087114.1990.10797009
- 2348 Balini, L. C., Fernandes, C. A., Portela-Castro, A. L. D. B., *et al.* (2024). Initial Steps of XY
2349 Sex Chromosome Differentiation in the Armored Catfish *Hypostomus albopunctatus*
2350 (Siluriformes: Loricariidae) Revealed by Heterochromatin
2351 Accumulation. *Zebrafish* 21(3), 265-273. doi: 10.1089/zeb.2023.0100
- 2352 Barby, F.F., Bertollo, L.A.C., de Oliveira, E.A., *et al.* (2019). Emerging patterns of genome
2353 organization in Notopteridae species (Teleostei, Osteoglossiformes) as revealed by Zoo-
2354 FISH and Comparative Genomic Hybridization (CGH). *Sci. Rep.* 9, 1112.
- 2355 Bardella, V.B., Milani, D., Cabral-de-Mello, D.C. (2020). Analysis of *Holhymenia histrio* ge-
2356 nome provides insight into the satDNA evolution in an insect with holocentric chromo-
2357 somes. *Chromosome Res.* 28, 369-380. doi: 10.1007/s10577-020-09642-1
- 2358 Basset, P., Yannic, G., and Hausser, J. (2008). Chromosomal Rearrangements and Genetic
2359 Structure at Different Evolutionary Levels of the *Sorex araneus* Group. *J. Evol. Biol.* 21,
2360 842–852. doi:10.1111/j.1420-9101.2008.01506.x
- 2361 Bateson, W. “Heredity and variation in modern lights”. In Seward A.C (ed.) **Darwin and mod-**
2362 **ern Science**. Cambridge: Cambridge University Press, pp 85-101, 1909.
- 2363 Beaudry, F.E.G., Barrett, S.C.H., Wright, S.I. (2019). Ancestral and Neo-sex Chromosomes
2364 Contribute to Population Divergence in a Dioecious Plant. *Evolution* 74(2), 256–269.
2365 doi:10.1111/evo.13892
- 2366 Benzaquem, D.C., Oliveira, C., da Silva Batista, J., *et al.* (2015). DNA Barcoding in Pencil-
2367 fishes (Lebiasinidae: *Nannostomus*) Reveals Cryptic Diversity across the Brazilian Ama-
2368 zon. *Plos One* 10, e0112217. doi: 10.1371/journal.pone.0112217
- 2369 Bertaco, V.A., Ferrer, J., Carvalho, F.R., *et al.* (2016). Inventory of the Freshwater Fishes from

- 2370 a Densely Collected Area in South America—a Case Study of the Current Knowledge of
 2371 Neotropical Fish Diversity. *Zootaxa* 4138(3), 401–440.
 2372 doi:10.11646/ZOOTAXA.4138.3.1
- 2373 Bertollo, L.A.C., Cioffi, M.B., Moreira-Filho, O. “Direct chromosome preparation from
 2374 freshwater teleost fishes”. In: Ozouf-Costaz, C., Pisano, E., Foresti, F.; Almeida-Toledo,
 2375 L.F. (eds.) **Fish Cytogenetic Techniques (Chondrichthyans and Teleosts)**. Florida:
 2376 CRC Press, pp. 21–26, 2015.
- 2377 Bertollo, L.A.C., Fontes, M.S., Fenocchio, A.S., *et al.* (1997). The X 1 X 2 Y sex chromosome
 2378 system in the fish *Hoplias malabaricus*. I. G-, C- and chromosome replication banding.
 2379 *Chromosome Res.* 5, 493–499. doi: 10.1023/A:1018477232354
- 2380 Bertollo, L.A.C., Born, G.G., Dergam, J.A., *et al.* (2000). A biodiversity approach in the
 2381 neotropical Erythrinidae fish, *Hoplias malabaricus*. Karyotypic survey, geographic
 2382 distribution of cytotypes and cytotaxonomic considerations. *Chromosom. Res.* 8, 603–61.
- 2383 Bertollo, L.A.C., Oliveira, C., Molina, W.F., *et al.* (2004). Chromosome evolution in the
 2384 erythrinid fish, *Erythrinus erythrinus* (Teleostei: Characiformes). *Heredity* 93, 228–233. doi:
 2385 10.1038/sj.hdy.6800511
- 2386 Bertollo, L. (1978). Cytotaxonomic considerations on *Hoplias lacerdae* (Pisces, Erythrinidae).
 2387 *Braz. J. Genet.* 1, 103–120.
- 2388 Bertollo, L.A.C. (2007). Chromosome evolution in the Neotropical Erythrinidae fish family:
 2389 an overview. *Fish Cytogenet.* 195, 211.
- 2390 Betancur-R, R., Arcila, D., Vari, R.P., *et al.* (2019). Phylogenomic incongruence, hypothesis
 2391 testing, and taxonomic sampling: The monophyly of characiform fishes. *Evolution* 73, 329–
 2392 345. doi: 10.1111/evo.13649
- 2393 Biémont, C. and Vieira, C. (2006). Junk DNA as an evolutionary force. *Nature* 443, 521–524.
 2394 doi: 10.1038/443521a
- 2395 Blackburn, E.H. (1994). Telomeres: no end in sight. *Cell* 77(5), 621–623.
- 2396 Blanco, D.R., Vicari, M.R., Artoni, R.F., *et al.* (2012). Chromosomal Characterization of
 2397 Armored Catfish *Harttia longipinna* (Siluriformes, Loricariidae): First Report of B
 2398 Chromosomes in the Genus. *Zoolog. Sci.* 29(9), 604–609. doi:10.2108/zsj.29.604
- 2399 Blough, R.I., Heerema, N.A., Ulbright, T.M., *et al.* (1998). Interphase chromosome painting
 2400 of paraffin-embedded tissue in the differential diagnosis of possible germ cell tumors. *Mo-*
 2401 *dern pathology: an official journal of the United States and Canadian Academy of Patho-*
 2402 *logy, Inc* 11(7), 634–641.
- 2403 Bolger, A.M., Lohse, M., Usadel, B. (2014). Trimmomatic: a flexible trimmer for Illumina
 2404 sequence data. *Bioinformatics* 30, 2114–2120. doi: 10.1093/bioinformatics/btu170
- 2405 Bolzán, A.D. (2017). Interstitial telomeric sequences in vertebrate chromosomes: Origin,
 2406 function, instability and evolution. *Mutation research/Reviews in mutation research* 773,
 2407 51–65. doi: 10.1016/j.mrrev.2017.04.002
- 2408 Boschman, L.M., Carraro, L., Cassemiro, F.A.S., *et al.* (2023). Freshwater fish diversity in the
 2409 western Amazon basin shaped by Andean uplift since the Late Cretaceous. *Nat. Ecol. Evol.*
 2410 7, 2037–2044. doi: 10.1038/s41559-023-02220-8
- 2411 Bouckaert, R., Heled, J., Kühnert, D., *et al.* (2014). BEAST 2: a software platform for Bayesian
 2412 evolutionary analysis. *Plos computational biology* 10(4), e1003537. doi:
 2413 10.1371/journal.pcbi.1003537
- 2414 Brajković, J., Feliciello, I., Bruvo-Mađarić, B., *et al.* (2012). Satellite DNA-like elements
 2415 associated with genes within euchromatin of the beetle *Tribolium castaneum*. *G3: Genes*
 2416 *Genomes Genetics*, 2(8), 931–941. doi: 10.1534/g3.112.003467
- 2417 Bronstein, O., Kroh, A., Haring, E. (2018). Mind the Gap! The Mitochondrial Control Region
 2418 and Its Power as a Phylogenetic Marker in Echinoids. *BMC Evolutionary Biology* 18(1),
 2419 80. doi:10.1186/s12862-018-1198-x.

- 2420 Bryant, D. and Moulton, V. (2004). Neighbor-net: an agglomerative method for the
2421 construction of phylogenetic networks. *Mol. Biol. Evol.* 21, 255–265.
2422 doi:10.1093/molbev/msh018
- 2423 Buckup, P.A., Malabarba, L.R., Reis, R.E., *et al.* (1998). Relationships of the Characidiinae
2424 and phylogeny of characiform fishes (Teleostei: Ostariophysii). *Phylogeny and classifica-*
2425 *tion of neotropical fishes*, 123-144.
- 2426 Cabral-de-Mello, D.C., Zrzavá, M., Kubičková, S., *et al.* (2021). The role of satellite DNAs in
2427 genome architecture and sex chromosome evolution in *Crambidae* moths. *Front in Genet.*
2428 12, 661417. doi: 10.3389/fgene.2020.661417
- 2429 Cabral-de-Melo, D.C., Mora, P., Rico-Porras, J.M., *et al.* (2023). The spread of satellite DNAs
2430 in euchromatin and insights into the multiple sex chromosome evolution in Hemiptera re-
2431 vealed by repeatome analysis of the bug *Oxycarenus hyalinipennis*. *Insect Mol Biol.* 12868.
2432 doi: 10.1111/imb.12868
- 2433 Calcagnotto, D., Schaefer, S.A., DeSalle, R. (2005). Relationships among characiform fishes
2434 inferred from analysis of nuclear and mitochondrial gene sequences. *Mol. Phylogenet.*
2435 *Evol.* 36, 135–153. doi: 10.1016/j.ympev.2005.01.004
- 2436 Camacho, J.P.M., Cabrero, J., López-León, M.D., *et al.* (2022). Satellitome comparison of two
2437 oedipodine grasshoppers highlights the contingent nature of satellite DNA evolution. *BMC*
2438 *Biol.* 20, 1-24. doi: 10.1186/s12915-021-01216-9
- 2439 Carvalho, P.C., de Oliveira, E.A., Bertollo, L.A.C., *et al.* (2017). First chromosomal analysis
2440 in Hepsetidae (Actinopterygii, Characiformes): Insights into relationship between African
2441 and Neotropical fish groups. *Front. Genet.* 8, 203. doi:10.3389/fgene.2017.00203.
- 2442 Casemiro, F.A., Albert, J.S., Antonelli, A., *et al.* (2023). Landscape dynamics and
2443 diversification of the megadiverse South American freshwater fish fauna. *Proc. Natl.*
2444 *Acad. Sci.* 120, e2211974120. doi: 10.1073/pnas.2211974120
- 2445 Castro, R., and Polaz, C.N. (2020). Small-sized fish: the largest and most threatened portion of
2446 the megadiverse neotropical freshwater fish fauna. *Biota Neotropica* 20, e20180683. doi:
2447 10.1590/1676-0611-BN-2018-0683
- 2448 Castro, J.P., Moura, M.O., Moreira-Filho, O., *et al.* (2015). Diversity of the *Astyanax*
2449 *scabripinnis* species complex (Teleostei: Characidae) in the Atlantic Forest, Brazil:
2450 species limits and evolutionary inferences. *Rev. Fish Biol. Fish.* 25, 231–244. doi:
2451 10.1007/s11160-014-9377-3
- 2452 Charlesworth, B. *Evolution in age-structured populations*. Cambridge: Cambridge University
2453 Press, 1994.
- 2454 Cioffi, M.B., Kejnovský, E., Marquioni, V., *et al.* (2012). The key role of repeated DNAs in
2455 sex chromosome evolution in two fish species with ZW sex chromosome system. *Mol.*
2456 *Cytogenet.* 5, 1-7. doi: 10.1186/1755-8166-5-28
- 2457 Cioffi, M.B., Martins, C., Centofante, L., *et al.* (2009). Chromosomal Variability among
2458 Allopatric Populations of Erythrinidae Fish *Hoplias malabaricus*: Mapping of Three
2459 Classes of Repetitive DNAs. *Cytogenet. Genome Res.* 125, 132–141. doi:
2460 10.1159/000227838
- 2461 Cioffi M.B., Martins C., Bertollo L.A.C. (2010). Chromosome spreading of associated
2462 transposable elements and ribosomal DNA in the fish *Erythrinus erythrinus*. Implications
2463 for genome change and karyoevolution in fish. *BMC Evol Biol.* 10, 271. doi:
2464 10.1186/1471-2148-10-271.
- 2465 Cioffi, M.B., Sánchez, A., Marchal, J.A., *et al.* (2011). Whole chromosome painting reveals
2466 independent origin of sex chromosomes in closely related forms of a fish species.
2467 *Genetica*, 139(8), 1065-1072.
- 2468 Cioffi, M.B. and Bertollo, L. (2012). Chromosomal distribution and evolution of repetitive
2469 DNAs in fish. *Repetitive DNA* 7, 197–221.

- 2470 Cioffi, M.B., Moreira-Filho, O., Ráb, P., *et al.* (2018). Conventional cytogenetic approaches—
 2471 Useful and indispensable tools in discovering fish biodiversity. *Curr. Genet. Med. Rep.* 6,
 2472 176–186.
- 2473 Cioffi, M.B., Ráb, P., Ezaz, T., *et al.* (2019). Deciphering the evolutionary history of arowana
 2474 fishes (Teleostei, Osteoglossiformes, Osteoglossidae): Insight from comparative
 2475 cytogenomics. *Int. J. Mol. Sci.* 20. doi: 10.3390/ijms20174296
- 2476 Coyne, J.A. and Orr, H.A. (2004). Speciation: a catalogue and critique of species concepts.
 2477 *Philosophy of biology: an anthology*, 272-92.
- 2478 Crepaldi, C., Martí, E., Gonçalves, E.M., *et al.* (2021). Genomic differences between the sexes
 2479 in a fish species seen through satellite DNAs. *Front. Genet.* 12, 728670. doi:
 2480 10.3389/fgene.2021.728670
- 2481 da Silva, M.J., Gazoni, T., Haddad, C.F.B., *et al.* (2023). Analysis in *Proceratophrys boiei*
 2482 genome illuminates the satellite DNA content in a frog from the Brazilian atlantic forest.
 2483 *Front. Genet.* 14, 1101397. doi: 10.3389/fgene.2023.1101397
- 2484 Dagosta, F.C. and De Pinna, M. (2019). The fishes of the Amazon: distribution and
 2485 biogeographical patterns, with a comprehensive list of species. *Bulletin of the American*
 2486 *Museum of Natural History*, 2019(431), 1-163.
- 2487 Dagosta, F.C.P. and De Pinna, M.C.C. (2021). Two New Catfish Species of Typically
 2488 Amazonian Lineages in the Upper Rio Paraguay (Aspredinidae: Hoplomyzontinae and
 2489 Trichomycteridae: Vandelliinae), with a Biogeographic Discussion. *Pap. Avulsos Zool.*
 2490 61, e20216147. doi:10.11606/1807-0205/2021.61.47.
- 2491 Dai, W., Zou, M., Yang, L. *et al.* (2018). Phylogenomic Perspective on the Relationships and
 2492 Evolutionary History of the Major Otocephalan Lineages. *Sci Rep* 8, 205. doi:
 2493 10.1038/s41598-017-18432-5
- 2494 Darriba, D., Posada, D., Kozlov, A.M., *et al.* (2020). ModelTest-NG: A New and Scalable Tool
 2495 for the Selection of DNA and Protein Evolutionary Models. *Mol. Biol. Evol.* 37, 291–294.
 2496 doi: 10.1093/molbev/msz189
- 2497 Davey, J.W., Hohenlohe, P.A., Etter, P.D., *et al.* (2011). Genome-wide genetic marker
 2498 discovery and genotyping using next-generation sequencing. *Nat. Rev. Genet.* 12, 499–
 2499 510. doi: 10.1038/nrg3012
- 2500 de Lima, L.G. and Ruiz-Ruano, F.J. (2022). In-depth satellitome analyses of *Drosophila* spe-
 2501 cies illuminate repetitive DNA evolution in the *Drosophila* genus. *Genome Biol. Evol.* 14,
 2502 evac064. doi: 10.1093/gbe/evac064
- 2503 de Oliveira, E.A., Bertollo, L.A.C., Rab, P., *et al.* (2019). Cytogenetics, genomics and
 2504 biodiversity of the South American and African Arapaimidae fish family (Teleostei,
 2505 Osteoglossiformes). *Plos One* 14, e0214225. doi: 10.1371/journal.pone.0214225
- 2506 de Pinna, M., Zuanon, J., Rapp Py-Daniel, L., *et al.* (2018). A new family of neotropical
 2507 freshwater fishes from deep fossorial Amazonian habitat, with a reappraisal of
 2508 morphological characiform phylogeny (Teleostei: Ostariophysi). *Zool. J. Linn. Soc.* 182,
 2509 76–106.
- 2510 de Souza e Sousa, J.F., Guimarães, E., Pinheiro-Figliuolo, V., *et al.* (2021). Chromosomal
 2511 Analysis of *Ctenolucius hujeta* Valenciennes, 1850 (Characiformes): A New Piece in the
 2512 Chromosomal Evolution of the Ctenoluciidae. *Cytogenet. Genome Res.*, 1–8.
 2513 doi:10.1159/000515456.
- 2514 de Souza e Sousa, J.F., Viana, P.F., Bertollo, L.A.C., *et al.* (2017). Evolutionary relationships
 2515 among *Boulengerella* species (Ctenoluciidae, Characiformes): genomic organization of
 2516 repetitive DNAs and highly conserved karyotypes. *Cytogenet. Genome Res.* 152, 194–
 2517 203. doi:10.1159/000480141.
- 2518 Ditcharoen, S., Sassi, F.M.C., Bertollo, L.A.C., *et al.* (2020). Comparative chromosomal
 2519 mapping of microsatellite repeats reveals divergent patterns of accumulation in Siluridae

2520 (Teleostei: Siluriformes) species. *Genet. Mol. Biol.* 43. doi:10.1590/1678-4685-GMB-
2521 2020-0091.

2522 Dobzhansky, T. (1933). On the sterility of the interracial hybrids in *Drosophila pseudoobscura*.
2523 *Proc Natl Acad Sci USA* 19, 397-403. doi:10.1073/pnas.19.4.397

2524 Dornburg, A. and Near, T.J. (2021). The emerging phylogenetic perspective on the evolution
2525 of actinopterygian fishes. *Annual Review of Ecology, Evolution, and Systematics*, 52(1),
2526 427-452. doi: 10.1146/annurev-ecolsys-122120-122554

2527 dos Santos, L.L., Benone, N.L., Brasil, L.S., *et al.* (2022). The use of taxonomic families as
2528 biological surrogates of the diversity of the Amazonian stream fish. *Ecol Ind* 141, 109094.
2529 doi: 10.1016/j.ecolind.2022.109094

2530 dos Santos, R.Z., Calegari, R.M., Silva, D.M.Z.D.A., *et al.* (2021). A long-term conserved sa-
2531 tellite DNA that remains unexpanded in several genomes of Characiformes fish is actively
2532 transcribed. *Genome Biol Evol.* 13, evab002. doi: 10.1093/gbe/evab002

2533 Eaton, D.A.R. and Overcast, I. (2017). Ipyrad V. 0.7. Available at: [https://github.](https://github.com/dereneaton/ipyrad)
2534 [com/dereneaton/ipyrad](https://github.com/dereneaton/ipyrad)

2535 Eaton, D.A.R. (2014). PyRAD: Assembly of De Novo RADseq Loci for Phylogenetic
2536 Analyses. *Bioinformatics* 30(13), 1844–1849. doi:10.1093/bioinformatics/btu121

2537 Eigenmann, C.H. and Kennedy, C.H. (1903). On a Collection of Fishes from Paraguay, with a
2538 Synopsis of the American Genera of Cichlids. *Proc. Acad. Nat. Sci. Phila.* 55, 497–537.

2539 Ekblom, R. and Galindo, J. (2011). Applications of next generation sequencing in molecular
2540 ecology of non-model organisms. *Heredity* 107, 1–15. doi: 10.1038/hdy.2010.152

2541 Ellermeier, C., Higuchi, E.C., Phadnis, N., *et al.* (2010). RNAi and heterochromatin repress
2542 centromeric meiotic recombination. *Proc. Natl. Acad. Sci.* 107, 8701–8705. doi:
2543 10.1073/pnas.0914160107

2544 Escudeiro, A., Ferreira, D., Mendes-da-Silva, A., *et al.* (2019). Bovine satellite DNAs—a his-
2545 tory of the evolution of complexity and its impact in the Bovidae family. *The European*
2546 *Zool. Journal* 86, 20-37. doi: 10.1080/24750263.2018.1558294

2547 Faircloth, B.C., Alda, F., Hoekzema, K., *et al.* (2020). A target enrichment bait set for studying
2548 relationships among ostariophysan fishes. *Copeia*, 108(1), 47-60.

2549 Faria, R. and Navarro, A. (2010). Chromosomal speciation revisited: rearranging theory with
2550 pieces of evidence. *Trends in Ecology and Evolution* 25, 660-669. doi:
2551 10.1016/j.tree.2010.07.008

2552 Feliciello, I., Akrap, I., Ugarković, Đ. (2015). Satellite DNA modulates gene expression in the
2553 beetle *Tribolium castaneum* after heat stress. *Plos Genetics* 11, e100566. doi:
2554 10.1371/journal.pgen.1005547

2555 Feliciello, I., Pezer, Ž., Kordiš, D., *et al.* (2020). Evolutionary history of alpha satellite DNA
2556 repeats dispersed within human genome euchromatin. *Genome biology and evolution*,
2557 12(11), 2125-2138. doi: 10.1093/gbe/evaa224

2558 Ferreira, P.H.N., Souza, F.H.S, Moraes, R.L.R.M., *et al.* (2022). The genetic differentiation of
2559 *Pyrrhulina* (Teleostei, Characiformes) species is likely influenced by both geographical
2560 distribution and chromosomal rearrangements. *Front Genet.* 13, 869073.
2561 doi:10.3389/fgene.2022.869073

2562 Ferretti, A.B.S.M., Milani, D., Palacios-Gimenez, O.M., *et al.* (2020). High dynamism for neo-
2563 sex chromosomes: satellite DNAs reveal complex evolution in a grasshopper. *Heredity*
2564 125, 124-137. doi: 10.1038/s41437-020-0327-7

2565 Flynn, J.M., Hu, K.B., Clark, A.G. (2023). Three recent sex chromosome-to-autosome fusions
2566 in a *Drosophila virilis* strain with high satellite DNA content. *Genetics* 224(2), iyad062.
2567 doi: 10.1093/genetics/iyad062

2568 Foll, M. and Gaggiotti, O. (2008). A Genome-Scan Method to Identify Selected Loci Appropriate for Both Dominant and Codominant Markers: a Bayesian Perspective. *Genetics* 180(2), 977–993. doi:10.1534/genetics.108.092221

2570
2571 Foresti, F., Almeida-Toledo, L.F., Toledo-Filho, S.A. (1981). Polymorphic nature of nucleolus
2572 organizer regions in fishes. *Cytogenet. Genome Res.* 31, 137–144. doi:
2573 10.1159/000131639

2574 Franchini, P., Irisarri, I., Fudickar, A., *et al.* (2017). Animal tracking meets migration ge-
2575 nomics: transcriptomic analysis of a partially migratory bird species. *Mol. Ecol.* 26, 3204-
2576 3216. doi: 10.1111/mec.14108

2577 Franchini, P., Kautt, A.F., Nater, A., *et al.* (2020). Reconstructing the evolutionary history of
2578 chromosomal races on islands: a genome-wide analysis of natural house mouse popula-
2579 tions. *Molecular Biology and Evolution* 37, 2825-2837. doi: 10.1093/molbev/msaa118

2580 Freitas, N.L., Al-Rikabi, A.B.H., Bertollo, L.A.C., *et al.* (2018). Early stages of XY sex
2581 chromosomes differentiation in the fish *Hoplias malabaricus* (Characiformes,
2582 Erythrinidae) revealed by DNA repeats accumulation. *Curr. Genomics* 19, 216–226.
2583 doi:10.2174/1389202918666170711160528.

2584 Fricke, R., Eschmeyer, W. N., van der Laan, R. Eschmeyer’s Catalog of Fishes: Genera,
2585 Species, References. 2021 Available online:
2586 <http://researcharchive.calacademy.org/research/ichthyology/catalog/fishcatmain.as>
2587 (accessed on 2 September 2021).

2588 Fricke, R., Eschmeyer, W.N., van der Laan, R. Eschmeyer’s Catalog of Fishes: Genera, Spe-
2589 cies, References. 2023. Available online: [http://researcharchive.calacademy.org/re-](http://researcharchive.calacademy.org/research/ichthyology/catalog/fishcatmain.asp)
2590 [search/ichthyology/catalog/fishcatmain.asp](http://researcharchive.calacademy.org/research/ichthyology/catalog/fishcatmain.asp). (accessed on 12 July 2023).

2591 Fricke, R., Eschmeyer, W.N., van der Laan, R. Eschmeyer’s catalog of fishes: Genera, Species,
2592 References. 2024. Available online:
2593 <http://researcharchive.calacademy.org/research/ichthyology/catalog/fishcatmain.asp>
2594 (accessed on 24 may 2024).

2595 Froese, R. and Pauly, D. FishBase: World Wide Web electronic publication. 2014. Available
2596 online: <http://www.fishbase.org> (accessed on 22 april 2014).

2597 Froese, R. and Pauly, D. FishBase: World Wide Web electronic publication. 2018. Available
2598 online: <http://www.fishbase.org> (accessed on 14 april 2018).

2599 Froese, R. and Pauly, D. Fish Base: World Wide Web electronic publication. 2023. Available
2600 online: <http://www.fishbase.org>. (accessed on 22 July 2023).

2601 Froese, R. and Pauly, D. Fish Base: World Wide Web electronic publication. 2024. Available
2602 online: <http://www.fishbase.org>. (accessed on 26 July 2024).

2603 Fry, K. and Salser, W. (1977). Nucleotide sequences of HS- α satellite DNA from kangaroo rat
2604 *Dipodomys ordii* and characterization of similar sequences in other rodents. *Cell* 12, 1069-
2605 1084. doi: 10.1016/0092-867(77)90170-2

2606 Galetti Jr, P.M., Mestriner, C.A., Venere, P.C., *et al.* (1991). Heterochromatin and karyotype
2607 reorganization in fish of the family Anostomidae (Characiformes). *Cytogenetic and*
2608 *Genome Research* 56(2), 116-121.

2609 Garcia, S., Kovarik, A., Maiwald, S., *et al.* (2024). The dynamic interplay between ribosomal
2610 DNA and transposable elements: a perspective from genomics and cytogenetics. *Mol. Biol.*
2611 *Evol.* 41, msae025. doi: 10.1093/molbev/msae025

2612 Garrido-Ramos, M.A. (2017). Satellite DNA: an evolving topic. *Genes* 8, 230. doi: 10.3390/ge-
2613 nes8090230

2614 Gatto, K.P., Mattos, J.V., Seger, K.R., *et al.* (2018). Sex chromosome differentiation in the frog
2615 genus *Pseudis* involves satellite DNA and chromosome rearrangements. *Front. Genet.* 9,
2616 301. doi: 10.3389/fgene.2018.00301

2617 Géry, J. and Zarske, A. (2002). *Derhamia hoffmannorum* gen. et sp. n.-a new pencil fish

- 2618 (Teleostei, Characiformes, Lebiasinidae), endemic from the Mazaruni River in Guyana.
 2619 *Zool. Abh.-Staatl. Mus. Tierkd. Dresd.* 52, 35–47.
- 2620 Géry, J. (1997). Characoids of the world.
- 2621 Glugoski, L., Deon, G., Schott, S., *et al.* (2020). Comparative cytogenetic analyses in *Ancistrus*
 2622 species (Siluriformes: Loricariidae). *Neotrop. Ichthyol.* 18, 1–16.
- 2623 Glugoski, L., Nogaroto, V., Deon, G.A., *et al.* (2022). Enriched tandem repeats in chromoso-
 2624 mal fusion points of *Rineloricaria latirostris* (Boulenger, 1900) (Siluriformes: Loricari-
 2625 dae). *Genome* 65, 479-489. doi:10.1139/gen-2022-0043
- 2626 Glugoski, L., Deon, G.A., Nogaroto, V., *et al.* (2023). Robertsonian fusion site in *Rineloricaria*
 2627 *pentamaculata* (Siluriformes: Loricariidae): involvement of 5S rDNA and satellite
 2628 sequences. *Cytogenet. Genome Res.* doi: 10.1159/000530636
- 2629 Goes, C.A.G., Santos, R.Z., Aguiar, W.R.C., *et al.* (2023). Revealing the satellite DNA history
 2630 in *Psalidodon* and *Astyanax* characid fish by comparative satellitomics. *Front Genet.* 13,
 2631 884072. doi: 10.3389/fgene.2022.884072
- 2632 Gornung, E. (2013). Twenty years of physical mapping of major ribosomal RNA genes across
 2633 the teleosts: A review of research. *Cytogenet. Genome Res.* 141, 90–102.
 2634 doi:10.1159/000354832
- 2635 Gruber, B., Unmack, P.J., Berry, O.F., *et al.* (2018). dartr: An r package to facilitate analysis
 2636 of SNP data generated from reduced representation genome sequencing. *Mol. Ecol.*
 2637 *Resour.* 18, 691–699. doi:10.1111/1755-0998.12745
- 2638 Gržan, T., Dombi, M., Despot-Slade, E., *et al.* (2023). The Low-Copy-Number Satellite DNAs
 2639 of the Model Beetle *Tribolium castaneum*. *Genes* 14, 999. doi: 10.3390/genes14050999
- 2640 Guarracino, A., Buonaiuto, S., de Lima, L.G., *et al.* (2023). Recombination between heterolo-
 2641 gous human acrocentric chromosomes. *Nature* 617, 335-343. doi: 10.1038/s41586-023-
 2642 05976-y
- 2643 Guerra, M.S. (1988). *Introdução à citogenética geral*. Guanabara Koogan
- 2644 Guzmán-Markevich, K., Roco, A.S., Ruiz-García, A., *et al.* (2022). Cytogenetic analysis in the
 2645 toad species *Bufo spinosus*, *Bufotes viridis* and *Epidalea calamita* (Anura, Bufonidae)
 2646 from the mediterranean area. *Genes* 13, 1475. doi: 10.3390/genes13081475
- 2647 Haerter, C. A. G., Blanco, D. R., Traldi, J. B., *et al.* (2023). Are scattered microsatellites weak
 2648 chromosomal markers? Guided mapping reveals new insights into *Trachelyopterus*
 2649 (Siluriformes: Auchenipteridae) diversity. *Plos one* 18(6), e0285388. doi:
 2650 10.1371/journal.pone.0285388
- 2651 Haldane, J. B. S. (1922). Sex Ratio and Unisexual Sterility in Hybrid Animals. *J. Gen.* 12, 101–
 2652 109. doi:10.1007/bf02983075
- 2653 Haynes, L.L. and Hönisch, B. (2020). The seawater carbon inventory at the Paleocene–Eocene
 2654 Thermal Maximum. *Proc. Natl. Acad. Sci.* 117, 24088–24095.
 2655 doi:10.1073/pnas.2003197117
- 2656 Henikoff, S., Ahmad, K., Malik, H.S. (2001). The centromere paradox: Stable inheritance with
 2657 rapidly evolving DNA. *Science* 293, 1098-1102. doi: 10.1126/science.1062939
- 2658 Howell, W.M.T. and Black, D.A. (1980). Controlled silver-staining of nucleolus organizer
 2659 regions with a protective colloidal developer: a 1-step method. *Experientia* 36.8: 1014-
 2660 1015.
- 2661 Ijdo, J. W., Wells, R. A., Baldini, A., *et al.* (1991). Improved telomere detection using a
 2662 telomere repeat probe (TTAGGG)_n generated by PCR. *Nucleic Acids Res.* 19, 4780
- 2663 Imoto, J.M., Saitoh, K., Sasaki, T., *et al.* (2013). Phylogeny and Biogeography of Highly
 2664 Diverged Freshwater Fish Species (Leuciscinae, Cyprinidae, Teleostei) Inferred from
 2665 Mitochondrial Genome Analysis. *Gene* 514(2), 112–24. doi:10.1016/j.gene.2012.10.019.
- 2666 Jaccoud, D., Peng, K., Feinstein, D., *et al.* (2001). Diversity arrays: a solid state technology for
 2667 sequence information independent genotyping. *Nucleic Acids Res.* 29, e25–e25.

2668 doi:10.1093/nar/29.4.e25

2669 Kejnovský, E., Michalovova, M., Steflova, P., *et al.* (2013). Expansion of microsatellites on
2670 evolutionary young Y chromosome. *Plos One* 8, e45519.
2671 doi:10.1371/journal.pone.0045519.

2672 Khosraviani, N., Ostrowski, L.A., Mekhail, K. (2019). Roles for non-coding RNAs in spatial
2673 genome organization. *Front. Cell Develop. Biol.* 7, 336. doi: 10.3389/fcell.2019.00336

2674 Kilian, A., Wenzl, P., Huttner, E., *et al.* (2012). Diversity arrays technology: a generic genome
2675 profiling technology on open platforms. *Data Prod. Anal. Popul. Genomics Methods*
2676 *Protoc.* 67–89. doi:10.1007/978-1-61779-870-2_5

2677 Kipling, D., Ackford, H.E., Taylor, B.A., *et al.* (1991). Mouse minor satellite DNA genetically
2678 maps to the centromere and is physically linked to the proximal telomere. *Genomics* 11,
2679 235–241. doi:10.1016/0888-7543(91)90128-2

2680 Kitano, J. and Peichel, C.L. (2012). Turnover of Sex Chromosomes and Speciation in Fishes.
2681 *Environ. Biol. Fish.* 94(3), 549–558. doi:10.1007/s10641-011-9853-8

2682 Kitano, J., Ross, J. A., Mori, S., *et al.* (2009). A Role for a Neo-Sex Chromosome in
2683 Stickleback Speciation. *Nature* 461(7267), 1079–1083. doi:10.1038/nature08441

2684 Kopecna, O., Kubickova, S., Cernohorska, H., *et al.* (2014). Tribe-specific satellite DNA in
2685 non-domestic Bovidae. *Chromosome Res.* 22, 277–291. doi: 10.1007/s10577-014-9401-4

2686 Kopelman, N.M., Mayzel, J., Jakobsson, M., *et al.* (2015). Clumpak: a program for identifying
2687 clustering modes and packaging population structure inferences across K. *Molecular ecol-*
2688 *ogy resources*, 15(5), 1179–1191. doi: 10.1111/1755-0998.12387

2689 Kratochvíl, L., Stöck, M., Rovatsos, M., *et al.* (2021). Expanding the classical paradigm: what
2690 we have learnt from vertebrates about sex chromosome Evolution. *Phil. Trans. R. Soc. B.*
2691 376, 20200097. doi:10.1098/rstb.2020.0097

2692 Krysanov, E., Yu., Nagy, B., Watters, B.R., *et al.* (2023). Karyotype differentiation in the
2693 *Nothobranchius ugandensis* species group (Teleostei, Cyprinodontiformes), seasonal
2694 fishes from the east African inland plateau, in the context of phylogeny and biogeography.
2695 *Comp. Cytogenet.* 17, 13–29. doi:10.3897/compcytogen.v7.i1.97165

2696 Kubat, Z., Hobza, R., Vyskot, B., *et al.* (2008). Microsatellite accumulation in the Y
2697 chromosome of *Silene latifolia*. *Genome* 51, 350–356. doi:10.1139/G08-024.

2698 Kuhn, G.C., Küttler, H., Moreira-Filho, O., *et al.* (2012). The repetitive DNA of *Drosophila*:
2699 concerted evolution at different genomic scales and association with genes. *Mol. Biol.*
2700 *Evol.* 29, 7–11. doi:10.1093/molbev/msr173

2701 Kumar, S., Suleski, M., Craig, J.M., *et al.* (2022). TimeTree 5: An Expanded Resource for
2702 Species Divergence Times. *Mol. Biol. Evol.* 39, msac174. doi: 10.1093/molbev/msac174

2703 Lafontaine, D.L.J. and Tollervey, D. (2001). The function and synthesis of ribosomes. *Nature*
2704 *Reviews Molecular Cell Biology* 2(7), 514.

2705 Leite, P.P.D.M., Sassi, F.M.C., Marinho, M.M.F., *et al.* (2022). Tracking the evolutionary
2706 pathways among Brazilian *Lebiasina* species (Teleostei: Lebiasinidae): a chromosomal
2707 and genomic comparative investigation. *Neotropical Ichthyol.* 20, e210153.
2708 doi:10.1590/1982-0224-2021-0153

2709 Levan, A. (1964). Nomenclature for centromeric position on chromosomes. *Hereditas.* 52,
2710 201–220. doi:10.1111/j.1601-5223.1964.tb01953.x

2711 Lindholm, A. and Breden, F. (2002). Sex Chromosomes and Sexual Selection in Poeciliid
2712 Fishes. *Am. Nat.* 160(S6), S214–S224. doi:10.1086/342898

2713 Lisachov, A., Rumyantsev, A., Prokopov, D., *et al.* (2023). Conservation of major satellite
2714 DNAs in snake heterochromatin. *Animals* 13, 334. doi: 10.3390/ani13030334

2715 Liu, H., Sun, C., Zhu, Y., *et al.* (2020). Mitochondrial genomes of four American characins
2716 and phylogenetic relationships within the family Characidae (Teleostei: Characiformes).
2717 *Gene* 762, 145041. doi: 10.1016/j.gene.2020.145041

- 2718 López-Flores, I., Garrido-Ramos, M.A. “The repetitive DNA content of eukaryotic genomes”.
- 2719 In Garrido-Ramos, M.A (ed.) **Repetitive DNA**. Switzerland: Karger Publishers, pp. 1–28,
- 2720 2012.
- 2721 Louzada, S., Lopes, M., Ferreira, D., *et al.* (2020). Decoding the role of satellite DNA in genome
- 2722 architecture and plasticity—An evolutionary and clinical affair. *Genes* 11, 72.
- 2723 doi:10.3390/genes11010072
- 2724 Lui, R.L., Blanco, D.R., Moreira-Filho, O., *et al.* (2012). Propidium iodide for making
- 2725 heterochromatin more evident in the C-banding technique. *Biotech. Histochem.* 87, 433–
- 2726 43.
- 2727 Machado, C.A., Haselkorn, T.S., Noor, M.A.F. (2007). Evaluation of the Genomic Extent of
- 2728 Effects of Fixed Inversion Differences on Intraspecific Variation and Interspecific Gene
- 2729 Flow in *Drosophila pseudoobscura* and *D. persimilis*. *Genetics* 175 (3), 1289–1306.
- 2730 doi:10.1534/genetics.106.064758
- 2731 Malabarba, L.R. and Malabarba, M.C. “Phylogeny and classification of Neotropical fish”. In:
- 2732 Baldisseroto, B., Urbinati, E.C., Cyrino, J.E.P. (eds.) **Biology and physiology of**
- 2733 **freshwater neotropical fish**. Amsterdam: Elsevier, 2020.
- 2734 Marajó, L., Viana, P.F., Ferreira, A.M.V., *et al.* (2023). Chromosomal rearrangements and the
- 2735 first indication of an ♀X1X1X2X2/♂X1X2Y sex chromosome system in *Rineloricaria*
- 2736 fishes (Teleostei: Siluriformes). *J. Fish Biol.* 102, 443–454. doi:10.1111/jfb.15275.
- 2737 Margarido, V.P., Galetti Junior, P.M. (2000). Amplification of a GC-rich heterochromatin in
- 2738 the freshwater fish *Leporinus desmotes* (Characiformes, Anostomidae). *Genetics and Mo-*
- 2739 *lecular Biology* 23(3), 569-573.
- 2740 Margarido, V.P. and Galetti Junior, P.M. (1999). Heterochromatin patterns and karyotype
- 2741 relationships within and between the genera *Brycon* and *Salminus* (Pisces, Characidae).
- 2742 *Genetics and Molecular Biology* 22(3), 357-361.
- 2743 Marinho, M.M.F. (2014). Relações filogenéticas e revisão taxonômica das espécies do gênero
- 2744 *Copella* Myers, 1956 (Characiformes: Lebiasinidae). Universidade Estadual Paulista
- 2745 (UNESP).
- 2746 Marinho, M.M.F. and Menezes, N.A. (2017). Taxonomic review of *Copella* (Characiformes:
- 2747 Lebiasinidae) with an identification key for the species. *PloS One* 12.
- 2748 doi:10.1371/journal.pone.0183069
- 2749 Martins, C. (2007). Chromosomes and repetitive DNAs: a contribution to the knowledge of
- 2750 fish genome. *Fish cytogenetics* 421, 452.
- 2751 Mayr, E. (1963). *Animal Species and Evolution*. Cambridge: Harvard University Press.
- 2752 Mayr, E. (1999). *Systematics and the Origin of Species, from the Viewpoint of a Zoologist*.
- 2753 Cambridge: Harvard University Press.
- 2754 McGaugh, S.E. and Noor, M.A.F. (2012). Genomic Impacts of Chromosomal Inversions in
- 2755 parapatric *Drosophila* species. *Phil. Trans. R. Soc. B* 367(1587), 422–429.
- 2756 doi:10.1098/rstb.2011.025010.1186/1471-2164-14-570
- 2757 McKee, B.D., Wilhelm, K., Merrill, C., *et al.* (1998). Male Sterility and Meiotic Drive
- 2758 Associated with Sex Chromosome Rearrangements in *Drosophila*: Role of X-Y Pairing.
- 2759 *Genetics* 149(1), 143–155. doi:10.1093/genetics/149.1.143
- 2760 McTaggart, S.J., Dudycha, J.L., Omilian, A., *et al.* (2007). Rates of recombination in the
- 2761 ribosomal DNA of apomictically propagated *Daphnia obtusa* lines. *Genetics* 175, 311–
- 2762 320.
- 2763 Melo, B.F., Sidlauskas, B.L., Near, T.J., *et al.* (2021). Accelerated Diversification Explains the
- 2764 Exceptional Species Richness of Tropical Characoid Fishes. *Syst. Biol.*
- 2765 doi:10.1093/sysbio/syab040.
- 2766 Melo, B.F., Sidlauskas, B.L., Near, T.J., *et al.* (2022). Accelerated diversification explains the
- 2767 exceptional species richness of tropical characoid fishes. *Systematic Biology*, 71(1), 78–

2768 92. doi: 10.1093/sysbio/syab040

2769 Melville, J., Haines, M.L., Boysen, K., *et al.* (2017). Identifying Hybridization and Admixture
2770 Using SNPs: Application of the DArTseq Platform in Phylogeographic Research on
2771 Vertebrates. *R. Soc. Open Sci.* 4, 161061. doi:10.1098/rsos.161061

2772 Merlo A., Cross I., Palazón JL., *et al.* (2007). Chromosomal mapping of the major and minor
2773 ribosomal genes, (GATA) n and (TTAGGG) n by one-color and doublecolor FISH in the
2774 toadfish *Halobatrachus didactylus* (Teleostei: Batrachoididae). *Genetica* 131, 195–200.

2775 Mirande, J.M. (2019). Morphology, molecules and the phylogeny of Characidae (Teleostei,
2776 Characiformes). *Cladistics* 35, 282–300. doi:10.1111/cla.12345

2777 Mirarab, S., Bayzid, M.S., Warnow, T. (2016). Evaluating Summary Methods for Multilocus
2778 Species Tree Estimation in the Presence of Incomplete Lineage Sorting. *Systematic
2779 Biology* 65(3), 366–80. doi:10.1093/sysbio/syu063.

2780 Montiel, E.E., Panzera, F., Palomeque, T., *et al.* (2021). Satellitome analysis of *Rhodnius pro-*
2781 *lixus*, one of the main Chagas disease vector species. *Int J Mol Sci.* 22(11), 6052.

2782 Montiel, E.E., Mora, P., Rico-Porrás, J.M. *et al.* (2022). Satellitome of the red palm weevil,
2783 *Rhynchophorus ferrugineus* (Coleoptera: Curculionidae), the most diverse among insects.
2784 *Front. Ecol. Evol.* 10, 826808. doi: 10.3389/fevo.2022.826808

2785 Moraes, J.N., Viana, P.F., Favarato, R.M., *et al.* (2022). Karyotype variability in six
2786 Amazonian species of the family Curimatidae (Characiformes) revealed by repetitive
2787 sequence mapping. *Genetics and molecular biology*, 45, e20210125. doi: 10.1590/1982-
2788 0224-2021-0153

2789 Moraes, R.L.R., Bertollo, L.A.C., Marinho, M.M.F., *et al.* (2017). Evolutionary relationships
2790 and cytotaxonomy considerations in the genus *Pyrrhulina* (Characiformes, Lebiasinidae).
2791 *Zebrafish* 14, 536-546. doi: 10.1089/zeb.2017.1465

2792 Moraes, R.L.R., Sember, A., Bertollo, L.A.C., *et al.* (2019). Comparative cytogenetics and neo-
2793 Y formation in small-sized fish species of the genus *Pyrrhulina* (Characiformes, Lebi-
2794 asinidae). *Front Genet.* 10, 678. doi: 10.3389/fgene.2019.00678

2795 Moraes, R.L.R., Sassi, F.M.C., Bertollo, L.A.C., *et al.* (2021). Tracking the evolutionary trends
2796 among small-size fishes of the genus *Pyrrhulina* (Characiforme, Lebiasinidae): New in-
2797 sights from a molecular cytogenetic perspective. *Front Genet.* 12, 769984. doi:
2798 10.3389/fgene.2021.769984

2799 Moraes, R.L.R., Sassi, F.M.C., Marinho, M.M.F., *et al.* (2023). Small Body, Large
2800 Chromosomes: Centric Fusions Shaped the Karyotype of the Amazonian Miniature Fish
2801 *Nannostomus anduzei* (Characiformes, Lebiasinidae). *Genes* 14, 192.
2802 doi:10.3390/genes14010192

2803 Moreira-filho, O. and Bertollo, L.A.C. (1991). *Astyanax scabripinnis* (Pisces, Characidae): A
2804 species complex. *Revista Brasileira de Genética* 14, 331–357.

2805 Muller, H.J. Isolation mechanisms, evolution and temperature. *Biol Symp.* 1942, 6, 71.
2806 Available at:
2807 <https://www.google.de/url?sa=terct=jeq=eescr=sesource=webecd=eved=2ahUKEwiI1OuM3MyAAxXHhv0HHeVXDCAQFnoECBAQAQeurl=https%3A%2F%2Fwww.ucl.ac.uk%2Ftaxome%2Fflit%2Fmuller%25201942%2520new%2520enh.pdf&usg=AOvVaw0Xf86o-hX4H9vA0QhXx295eopi=89978449>

2811 Naish, M., Alonge, M., Wlodzimierz, P., *et al.* (2021). The genetic and epigenetic landscape
2812 of the *Arabidopsis* centromeres. *Science*, 374, eabi7489. doi: 10.1126/science.abi7489

2813 Nascimento, M., Sousa, A., Ramirez, M., *et al.* (2017). PHYLOViZ 2.0: providing scalable
2814 data integration and visualization for multiple phylogenetic inference methods. *Bioinform-
2815 atics* 33, 128-129. doi: 10.1093/bioinformatics/btw582

2816 Navarro, A. and Barton, N.H. (2003). Accumulating postzygotic isolation genes in parapatry:
2817 A new twist on chromosomal speciation. *Evolution*, 57, 447–459.

- 2818 Near, T.J. and Thacker, C.E. (2024). Phylogenetic Classification of Living and Fossil Ray-
2819 Finned Fishes (Actinopterygii). *Bull. Peabody Mus. Nat. Hist.* 65, 3–302. doi:
2820 10.3374/014.065.0101
- 2821 Nelson, J. S., Grande, T.C., and Wilson, M.V.H. (2016). Fishes of the World. *John Wiley e*
2822 *Sons* doi:10.2307/2412830.
- 2823 Netto-Ferreira, A.L. and Marinho, M.M.F. (2013). New species of *Pyrrhulina* (Ostariophysi:
2824 Characiformes: Lebiasinidae) from the Brazilian shield, with comments on a putative mon-
2825 ophyletic group of species in the genus. *Zootaxa* 3664, 369-76. doi:
2826 10.11646/zootaxa.3664.3.7
- 2827 Netto-Ferreira, A.L. (2010). Revisão taxonômica e relações interespecíficas de Lebiasinidae
2828 (Ostariophysi: Characiformes: Lebiasinidae). Universidade de São Paulo (USP).
- 2829 Novák, P., Neumann, P., Macas, J. (2020). Global analysis of repetitive DNA from unassem-
2830 bled sequence reads using RepeatExplorer2. *Nat Protoc.* 15, 3745-3776. doi:
2831 10.1038/s41596-020-0400-y
- 2832 O'Neill, R.J., Eldridge, M.D.B., Metcalfe, C.J. (2004). Centromere dynamics and chromosome
2833 evolution in marsupials. *J. Hered.* 95, 375-381. doi: 10.1093/jhered/esh063
- 2834 Ocalewicz, K. (2013). Telomeres in fishes. *Cytogenetic and genome research*, 141(2-3), 114-
2835 125. doi: 10.1159/000354278
- 2836 Oliveira, E.A., Sember, A., Bertollo, L.A.C., *et al.* (2017). Tracking the evolutionary pathway
2837 of sex chromosomes among fishes: characterizing the unique XX/XY₁Y₂ system in
2838 *Hoplias malabaricus* (Teleostei, Characiformes). *Chromosoma*, 127, 115–128.
- 2839 Oliveira, C., Andreato, A.A., Almeida-Toledo, L.F., *et al.* (1991). Karyotype and nucleolus
2840 organizer regions of *Pyrrhulina* cf. *australis* (Pisces, Characiformes, Lebiasinidae). *Rev.*
2841 *Bras. Genet.* 14, 685–690.
- 2842 Oliveira C., Almeida-Toledo L.F., Foresti F. “Karyotypic evolution in Neotropical fishes”. In:
2843 Pisano E, Ozouf-Costaz C, Foresti F, Kapoor B.G. (eds.) **Fish Cytogenetics**. USA:
2844 Enfield, NH, pp.111-164, 2007.
- 2845 Ortí, G. and Meyer, A. (1997). The radiation of characiform fishes and the limits of resolution
2846 of mitochondrial ribosomal DNA sequences. *Systematic Biology* 46, 75-100.
- 2847 Oliveira, R.R., Feldberg, E., dos Anjos, M.B., *et al.* (2009). Occurrence of multiple sexual
2848 chromosomes (XX/XY₁Y₂ and Z₁Z₁Z₂Z₂/Z₁Z₂W₁W₂) in catfishes of the genus *Ancistrus*
2849 (Siluriformes: Loricariidae) from the Amazon basin. *Genetica* 134, 243-249.
2850 doi:10.1007/s10709-007-9231-9
- 2851 Oliveira, C., Avelino, G.S., Abe, K.T., *et al.* (2011). Phylogenetic relationships within the
2852 speciose family Characidae (Teleostei: Ostariophysi: Characiformes) based on multilocus
2853 analysis and extensive ingroup sampling. *BMC Evol. Biol.* 11, 1–25. doi: 10.1186/1471-
2854 2148-11-275
- 2855 Oliveira, E.A., Perez, M.F., Bertollo, L.A.C., *et al.* (2020). Historical Demography and Climate
2856 Driven Distributional Changes in a Widespread Neotropical Freshwater Species with High
2857 Economic Importance. *Ecography* 43(9), 1291–1304. doi:10.1111/ecog.04874
- 2858 Ortí, G. and Meyer, A. (1997). The radiation of characiform fishes and the limits of resolution
2859 of mitochondrial ribosomal DNA sequences. *Syst. Biol.* 46, 75–100. doi:
2860 10.1093/sysbio/46.1.75
- 2861 Ostberg, C. O., Hauser, L., Pritchard, V. L., *et al.* (2013). Chromosome Rearrangements,
2862 Recombination Suppression, and Limited Segregation Distortion in Hybrids between
2863 Yellowstone Cutthroat Trout (*Oncorhynchus Clarkii* Bouvieri) and Rainbow Trout (*O.*
2864 *mykiss*). *BMC genomics* 14(1), 570–616. doi:10.1186/1471-2164-14-570
- 2865 Oyakawa, O.T. Relações filogenéticas das famílias Pyrrhulinidae, Lebiasinidae e Erythrinidae
2866 (Osteichthyes: Characiformes). Ph.D. Thesis, Universidade de São Paulo, 1998.

- 2867 Paço, A., Chaves, R., Vieira-da-Silva, A., *et al.* (2013). The involvement of repetitive sequen-
 2868 ces in the remodelling of karyotypes: The *Phodopus* genomes (*Rodentia*, *Cricetidae*). *Mi-*
 2869 *cron* 46, 27-34. doi: 10.1016/j.micron.2012.11.010
- 2870 Palacios-Gimenez, O.M., Dias, G.B., De Lima, L.G., *et al.* (2017). High-throughput analysis
 2871 of the satellitome revealed enormous diversity of satellite DNAs in the neo-Y chromosome
 2872 of the cricket *Eneoptera surinamensis*. *Sci. Rep.* 7, 6422. doi: 10.1038/s41598-017-06822-
 2873 8
- 2874 Panthum, T., Singchat, W., Laopichienpong, N., *et al.* (2021). Genome-wide SNP Analysis of
 2875 Male and Female rice Field Frogs, *Hoplobatrachus rugulosus*, Supports a Non-genetic Sex
 2876 Determination System. *Diversity* 13, 501. doi: 10.3390/d13100501
- 2877 Parey, E., Louis, A., Montfort, J., *et al.* (2023). Genome structures resolve the early
 2878 diversification of teleost fishes. *Science* 379(6632), 572-575. doi:
 2879 10.1126/science.abq4257
- 2880 Pavlek, M., Gelfand, Y., Plohl, M., *et al.* (2015). Genome-wide analysis of tandem repeats in
 2881 *Tribolium castaneum* genome reveals abundant and highly dynamic tandem repeat
 2882 families with satellite DNA features in euchromatic chromosomal arms. *Dna*
 2883 *research* 22(6), 387-401. doi: 10.1093/dnares/dsv021
- 2884 Pazza, R. and Kavalco, K.F. (2007). Chromosomal evolution in the neotropical characin
 2885 *Astyanax* (Teleostei, Characidae). *Nucleus-Calcutta*, 50(3), 523.
- 2886 Pendás, A.M., Mórán, P., Freije, J.P., *et al.* (1994). Chromosomal location and nucleotide
 2887 sequence of two tandem repeats of the Atlantic salmon 5S rDNA. *Cytogenet Cell Genet.*
 2888 67. doi: 10.1159/000133792
- 2889 Peona, V., Kutschera, V.E., Blom, M.P., *et al.* (2023). Satellite DNA evolution in Corvoidea
 2890 inferred from short and long reads. *Mol Ecol.* 32, 1288-1305. doi: 10.1111/mec.16484
- 2891 Pereira, J.A., Milani, D., Ferretti, A.B.S., *et al.* (2021). The extensive amplification of hetero-
 2892 chromatin in *Melipona* bees revealed by high throughput genomic and chromosomal anal-
 2893 ysis. *Chromosoma* 130, 251-262. doi: 10.1007/s00412-021-00764-x
- 2894 Pinkel, D., Straume, T., Gray, J.W. (1986). Cytogenetic analysis using quantitative, high-sen-
 2895 sitivity, fluorescence hybridization. *Proc. Natl. Acad. Sci. USA* 83, 2934–2938. doi:
 2896 10.1073/pnas.83.9.2934
- 2897 Plohl, M., Luchetti, A., Meštrović, N., *et al.* (2008). Satellite DNAs between selfishness and
 2898 functionality: structure, genomics and evolution of tandem repeats in centromeric (hetero)
 2899 chromatin. *Gene* 409, 72-78. doi:10.1016/j.gene.2007.11.013
- 2900 Plohl, M., Meštrović, N., Mravinac, B. (2012). Satellite DNA evolution. *Repetitive DNA* 7,
 2901 126-152. doi: 10.1159/000337122
- 2902 Podgornaya, O.I. (2022). Nuclear organization by satellite DNA, SAF-A/hnRNPU and matrix
 2903 attachment regions. *Sem. Cell. Dev. Biol.* 128, 61-68. doi: 10.1016/j.semcdb.2022.04.018
- 2904 Poltronieri, J., Marquioni, V., Bertollo, L.A.C., *et al.* (2014). Comparative chromosomal
 2905 mapping of microsatellites in *Leporinus* species (Characiformes, Anostomidae): unequal
 2906 accumulation on the W chromosomes. *Cytogenet. Genome Res.* 142, 40–45.
 2907 doi:10.1159/000355908.
- 2908 Potter, S., Bragg, J.G., Turakulov, R., *et al.* (2022). Limited Introgression between Rock-
 2909 Wallabies with Extensive Chromosomal Rearrangements. *Mol. Biol. Evol.* 39(1), 333.
 2910 doi:10.1093/molbev/msab333
- 2911 Prakhongcheep, O., Thapana, W., Suntronpong, A., Singchat, W., Pattanatanang, K., Phatcha-
 2912 rakullawarawat, R., Muangmai, N., Peyachoknagul K., Matsubara, K., Ezaz, T., *et al.* Lack
 2913 of satellite DNA species-specific homogenization and relationship to chromosomal rear-
 2914 rangements in monitor lizards (Varanidae, Squamata). *BMC Evol. Biol.* 2017, 17, 1-14.
 2915 doi: 10.1186/s12862-017-1044-6
- 2916 Presgraves, D. C. (2018). Evaluating Genomic Signatures of "the Large X-Effect" during

2917 Complex Speciation. *Mol. Ecol.* 27(19), 3822–3830. doi:10.1111/mec.14777

2918 Raj, A., Stephens, M., Pritchard, J. K. (2014). Faststructure: Variational Inference of

2919 Population Structure in Large SNP Data Sets. *Genetics* 197(2), 573–589.

2920 doi:10.1534/genetics.114.164350

2921 Rambaut, A., Drummond, A. J., Xie, D., *et al.* (2018). Posterior Summarization in Bayesian

2922 Phylogenetics Using Tracer 1.7. *Syst. Biol.* 67(5), 901–904. doi:10.1093/sysbio/syy032

2923 Ravi, V. and Venkatesh, B. (2018). The divergent genomes of teleosts. *Annual review of*

2924 *animal biosciences*, 6(1), 47–68. doi: 10.1146/annurev-animal-030117-014821

2925 Reinhold, K. (1998). Sex Linkage Among Genes Controlling Sexually Selected Traits. *Behav.*

2926 *Ecol. Sociobiol.* 44(1), 1–7. doi:10.1007/s002650050508

2927 Richard, G. F., Kerrest, A., Dujon, B. (2008). Comparative genomics and molecular dynamics

2928 of DNA repeats in eukaryotes. *Microbiology and molecular biology reviews*, 72(4), 686–

2929 727. doi:10.1128/mmbr.00011-08

2930 Rieseberg, L. H. (2001). Chromosomal Rearrangements and Speciation. *Trends Ecol. Evol.* 16

2931 (7), 351–358. doi:10.1016/s0169-5347(01)02187-5

2932 Roberts, P.A. (1965). Difference in the Behaviour of Eu- and Heterochromatin: Crossing-over.

2933 *Nature* 205, 725–726. doi: 10.1038/205725b0

2934 Rocha-Reis, D.A., de Oliveira Brandão, K., de Almeida-Toledo, L.F. (2018). The persevering

2935 cytotaxonomy: discovery of a unique XX/XY sex chromosome system in catfishes

2936 suggests the existence of a new, endemic and rare species. *Cytogenet. Genome Res.* 156,

2937 45–55. doi: 10.1159/000492959

2938 Roy, V., Monti-Dedieu, L., Chaminade, N., *et al.* (2005). Evolution of the chromosomal loca-

2939 tion of rDNA genes in two *Drosophila* species subgroups: *ananassae* and *melanogaster*.

2940 *Heredity* 94, 388–395.

2941 Rozas, J., Ferrer-Mata, A., Sanchez-DelBarrio, J. C., *et al.* (2019). DnaSP Version 6 for 32-bit

2942 and 64-bit Environments.

2943 Ruiz-Ruano, F.J., López-León, M.D., Cabrero, J., *et al.* (2016). High-throughput analysis of

2944 the satellitome illuminates satellite DNA evolution. *Sci Rep.* 6, 28333. doi:

2945 10.1038/srep28333

2946 Sambrook, J. and Russell, D.W. *Molecular Cloning, A Laboratory Manual*. New York: Cold

2947 Spring, Harbor Laboratory Press, 2001

2948 Sumner, A.T. (1972). A simple technique for demonstrating centromeric heterochromatin. *Exp.*

2949 *Cell Res.* 75, 304–306. doi:10.1016/0014-4827(72)90558-7

2950 Sánchez-Sevilla, J.F., Horvath, A., Botella, M.A., *et al.* (2015). Diversity Arrays Technology

2951 (DArT) Marker Platforms for Diversity Analysis and Linkage Mapping in a Complex

2952 Crop, the Octoploid Cultivated Strawberry (*Fragaria* × *Ananassa*). *PLoS One* 10(12),

2953 e0144960. doi:10.1371/journal.pone.0144960

2954 Sassi, F.M.C., Hatanaka, T., Moraes, R.L.R., *et al.* (2020). An Insight into the Chromosomal

2955 Evolution of Lebiasinidae (Teleostei, Characiformes). *Genes* 11, 365. doi:

2956 10.3390/genes11040365

2957 Sassi, F.M.C., Toma, G.A., Cioffi, M.B. “FISH-in fish chromosomes”. In Liehr, T (ed.) **Cyto-**

2958 **genetics and Molecular Cytogenetics**. USA: CRC Press, Boca Raton, pp. 281–297, 2022.

2959 doi: 10.1201/9781003223658

2960 Sassi, F.M.C., Oliveira, E., Bertollo, L.A.C., *et al.* (2019). Chromosomal evolution and evolu-

2961 tionary relationships of *Lebiasina* species (Characiformes, Lebiasinidae). *Int. J. Mol. Sci.*

2962 20, 2944. doi: 10.3390/ijms20122944

2963 Sassi, F.M.C., Perez, M.F., Oliveira, V.C.S., *et al.* (2021). High Genetic Diversity despite

2964 Conserved Karyotype Organization in the Giant Trahiras from Genus *Hoplias*

2965 (Characiformes, Erythrinidae). *Genes* 12, 252. doi: 10.3390/genes12020252

- 2966 Šatović-Vukšić, E. and Plohl, M. (2023). Satellite DNAs—From localized to highly dispersed
2967 genome components. *Genes* 14, 742. doi: 10.3390/genes14030742
- 2968 Scalvenzi, T. and Pollet, N. (2014). Insights on genome size evolution from a miniature in-
2969 verted repeat transposon driving a satellite DNA. *Mol. Phylogenet. Evol.* 81, 1-9.
2970 doi:10.1016/j.ympev.2014.08.014
- 2971 Scheel, J. (1973). Fish chromosomes and their evolution. *Intern. Rep. Dan. Akvarvum* 22.
- 2972 Schemberger, M.O., Nascimento, V.D., Coan, R., *et al.* (2019). DNA transposon invasion and
2973 microsatellite accumulation guide W chromosome differentiation in a Neotropical fish
2974 genome *Chromosoma*, 128, 547–560.
- 2975 Schimek, C., Shams, F., Miura, I., *et al.* (2022). Sex-linked markers in an Australian frog
2976 *Platyplectrum ornatum* (Limnodynastidae) with a small genome and homomorphic sex
2977 chromosomes. *Sci. Rep.* 12, 20934. doi: 10.1038/s41598-022-25105-5
- 2978 Schmieder, R. and Edwards, R. (2011). Fast identification and removal of sequence contami-
2979 nation from genomic and metagenomic datasets. *PLoS One* 6, e17288. doi:10.1371/jour-
2980 nal.pone.0017288
- 2981 Schubert, I. (2018). What is behind “centromere repositioning”? *Chromosoma* 127, 229–234.
2982 doi: 10.1007/s00412-018-0672-y
- 2983 Sedlazeck, F.J., Lee, H., Darby, C.A., *et al.* (2018). Piercing the dark matter: bioinformatics of
2984 long-range sequencing and mapping. *Nat. Rev. Genet.* 19, 329-346. doi: 10.1038/s41576-
2985 018-0003-4
- 2986 Sember, A., Bertollo, L.A.C., Ráb, P. *et al.* (2018). Sex Chromosome Evolution and Genomic
2987 Divergence in the Fish *Hoplias malabaricus* (Characiformes, Erythrinidae). *Frontiers in*
2988 *Genetics* 5(9).
- 2989 Sember, A., de Oliveira, E.A., Ráb, P., *et al.* (2020). Centric fusions behind the karyotype
2990 evolution of neotropical *Nannostomus pencilfishes* (Characiforme, Lebiasinidae): First
2991 insights from a molecular cytogenetic perspective. *Genes* 11, 91. doi:
2992 10.3390/genes11010091
- 2993 Sember, A., Nguyen, P., Perez, M.F., *et al.* (2021). Multiple sex chromosomes in teleost fishes
2994 from a cytogenetic perspective: State of the art and future challenges. *Phil. Trans. R. Soc.*
2995 *B.* 376, 20200098. doi: 10.1098/rstb.2020.0098
- 2996 Serrano-Freitas, E.A., Silva, A.M.Z.A., Ruiz-Ruano, F.J., *et al.* (2020). Satellite DNA content
2997 of B chromosomes in the characid fish *Characidium gomesi* supports their origin from sex
2998 chromosomes. *Mol. Genet. Genomics* 295, 195-207. doi: 10.1007/s00438-019-01615-2
- 2999 Shao, F., Han, M., Peng, Z. (2019). Evolution and diversity of transposable elements in fish
3000 genomes. *Sci. Rep.* 9, 15399. doi: 10.1038/s41598-019-51888-1
- 3001 Shatskikh, A.S., Kotov, A.A., Adashev, V.E., *et al.* (2020). Functional significance of satellite
3002 DNAs: insights from *Drosophila*. *Front. Cell, Dev. Biol.* 8, 312.
3003 doi:10.3389/fcell.2020.00312
- 3004 Šichová, J., Voleníková, A., Dincă, V., *et al.* (2015). Dynamic karyotype evolution and unique
3005 sex determination systems in *Leptidea* wood white butterflies. *BMC Evol Biol.* 15, 1-16.
3006 doi: 10.1186/s12862-015-0375-4
- 3007 Silva, D.M.D.A., Utsunomia, R., Ruiz-Ruano, F.J., *et al.* (2017). High-throughput analysis un-
3008 veils a highly shared satellite DNA library among three species of fish genus *Astyanax*. *Sci*
3009 *Rep.* 7, 12726. doi: 10.1038/s41598-017-12939-7
- 3010 Simmons, M.P. and Gatesy, J. (2021). Collapsing Dubiously Resolved Gene-Tree Branches in
3011 Phylogenomic Coalescent Analyses. *Molecular Phylogenetics and Evolution* 107092. doi:
3012 10.1016/j.ympev.2021.107092.
- 3013 Slamovits, C.H., Cook, J.A., Lessa, E.P., *et al.* (2001). Recurrent amplifications and deletions
3014 of satellite DNA accompanied chromosomal diversification in South American *tuco-tucos*

3015 (genus *Ctenomys*, Rodentia: Octodontidae): a phylogenetic approach. *Mol. Biol. Evol.* 18,
3016 1708-1709. doi: 10.1093/oxfordjournals.molbev.a003959

3017 Smith, C.J., Castanon, O., Said, K., *et al.* (2020). Enabling large-scale genome editing at
3018 repetitive elements by reducing DNA nicking. *Nucleic Acids Res.* 48, 5183-5195. doi:
3019 10.1093/nar/gkaa239

3020 Sochorová, J., Garcia, S., Gálvez, F., *et al.* (2018). Evolutionary trends in animal ribosomal
3021 DNA loci: introduction to a new online database. *Chromosoma* 127, 141–150. doi:
3022 10.1007/s00412-017-0651-8

3023 Sola, L., Rossi, A.R., Annesi, F., *et al.* (2003). Cytogenetic studies in *Sparus auratus* (Pisces,
3024 Perciformes): molecular organization of 5S rDNA and chromosomal mapping of 5S and
3025 45S ribosomal genes and of telomeric repeats. *Hereditas* 139, 232-236.

3026 Soto, M.Á., Castro, J.P., Walker, L.I., *et al.* (2018). Evolution of trans-Andean endemic fishes
3027 of the genus *Cheirodon* (Teleostei: Characidae) are associated with chromosomal
3028 rearrangements. *Rev. Chil. Hist. Nat.* 91, 8. doi: 10.1186/s40693-018-0078-5

3029 Souza e Sousa, J.F., Viana, P.F., Bertollo, L.A.C., *et al.* (2017). Evolutionary Relationships
3030 among *Boulengerella* Species (Ctenoluciidae, Characiformes): Genomic Organization of
3031 Repetitive DNAs and Highly Conserved Karyotypes. *Cytogenet. Genome Res.* 152. doi:
3032 10.1159/000480141

3033 Souza, J.S. Instituto Nacional de Pesquisas da Amazônia – INPA, Manaus, Brazil. Personal
3034 communication, 2019.

3035 Souza, C.S., Melo, B.F., Mattox, G.M., *et al.* (2022). Phylogenomic analysis of the Neotropical
3036 fish subfamily Characinae using ultraconserved elements (Teleostei:
3037 Characidae). *Molecular Phylogenetics and Evolution*, 171, 107462. doi:
3038 10.1016/j.ympev.2022.107462

3039 Souza, T.B.D., Ferreira, D.C., Silva, H.P.D., *et al.* (2023). DNA Barcoding of *Pyrrhulina*
3040 *australis* (Characiformes: Lebiasinidae) reveals unexpected cryptic diversity in the
3041 group. *Neotropical Ichthyology*, 21(4), e230037. doi: 10.1590/1982-0224-2023-0037

3042 Souza, F.H.S., Sassi, F.M.C., Ferreira, P.H.N., *et al.* (2022). Integrating Cytogenetics and
3043 Population Genomics: Allopatry and Neo-Sex Chromosomes May Have Shaped the
3044 Genetic Divergence in the *Erythrinus erythrinus* Species Complex (Teleostei,
3045 Characiformes). *Biology* 11, 315. doi: 10.3390/biology11020315

3046 Stamatakis, A. (2014). RAxML version 8: a tool for phylogenetic analysis and post-analysis of
3047 large phylogenies. *Bioinformatics* 30, 1312–1313. doi: 10.1093/bioinformatics/btu033

3048 Steane, D.A., Nicolle, D., Sansaloni, C.P., *et al.* (2011). Population Genetic Analysis and
3049 Phylogeny Reconstruction in Eucalyptus (Myrtaceae) Using High-Throughput, Genome-
3050 wide Genotyping. *Mol. phylogenetics Evol.* 59(1), 206–224. doi:
3051 10.1016/j.ympev.2011.02.003

3052 Steindachner, F. Beiträge zuer Kenntniss der Characinen des Amazonenstromes. Wien:
3053 Sitzungsber. Kaiserl. Akad. Wiss., 72, 6, 1876

3054 Symonová, R., Majtánová, Z., Sember, A., *et al.* (2013). Genome differentiation in a species
3055 pair of coregonine fishes: an extremely rapid speciation driven by stress-activated
3056 retrotransposons mediating extensive ribosomal DNA multiplications. *BMC Evol. Biol.*
3057 13, 1–11. doi:10.1186/1471-2148-13-42.

3058 Tagliacollo, V.A., Dagosta F.C.P., de Pinna M., *et al.* (2021). Assessing extinction risk from
3059 geographic distribution data in Neotropical freshwater fishes. *Neotrop Ichthyol.* 19(3),
3060 e210079. doi:10.1590/1982-0224-2021-0079

3061 Tautz, D. “Notes on the defunction and nomenclature of tandemly repetitive DNA sequences”.
3062 In: Pena, S.D.J., Chakraborty, R., Epplen, J.T., Jeffreys, A.J. (eds.) **DNA Fingerprinting:
3063 State of the Science**. Switzerland: Birkhauser, pp 21-28, 1993.

3064 Terencio, M.L., Schneider, C.H., Gross, M.C., *et al.* (2012). Repetitive sequences associated

3065 with differentiation of W chromosome in *Semaprochilodus taeniurus*. *Genetica* 140, 505–
3066 512. doi:10.1007/s10709-013-9699-4.

3067 Thakur, J., Packiaraj, J., Henikoff, S. (2021). Sequence, chromatin and evolution of satellite
3068 DNA. *Int. J. Mol. Sci.* 22, 4309. doi: 10.3390/ijms22094309

3069 Tickner, D., Opperman, J.J., Abell, R., *et al.* (2020). Bending the curve of global freshwater
3070 biodiversity loss: an emergency recovery plan. *BioScience* 70(4), 330-342.
3071 doi:10.1093/biosci/biaa002

3072 Toews, D. P. and Brelsford, A. (2012). The biogeography of mitochondrial and nuclear
3073 discordance in animals. *Molecular ecology* 21(16), 3907-3930. doi: 10.1111/j.1365-
3074 294X.2012.05664.x

3075 Tollesfrud, M.M., Sønstebø, J.H., Brochmann, C., *et al.* (2009). Combined Analysis of Nuclear
3076 and Mitochondrial Markers Provide New Insight into the Genetic Structure of North Eu-
3077 ropean *Picea Abies*. *Heredity* 102 (6), 549–62. doi: 10.1038/hdy.2009.16.

3078 Toma, G.A., Moraes, R.L.R., Sassi, F.M.C., *et al.* (2019). Cytogenetics of the small-sized fish,
3079 *Copeina Guttata* (*Characiformes, Lebiasinidae*): Novel insights into the karyotype differ-
3080 entiation of the family. *Plos One* 14, e0226746. doi: 10.1371/journal.pone.0226746

3081 Toma, G.A., dos Santos, N., dos Santos, R., *et al.* (2023). Cytogenetics Meets Genomics:
3082 Cytotaxonomy and Genomic Relationships among Color Variants of the Asian Arowana
3083 *Scleropages formosus*. *Int. J. Mol. Sci.* 24, 9005. doi: 10.3390/ijms24109005

3084 Tonella, L.H., Ruaro, R., Daga, V.S., *et al.* (2023). Neotropical freshwater fishes: A dataset of
3085 occurrence and abundance of freshwater fishes in the Neotropics. doi: 10.1002/ecy.3713

3086 Tunjić-Cvitanić, M., Pasantes, J.J., García-Souto, D., *et al.* (2021). Satellitome analysis of the
3087 pacific oyster *Crassostrea gigas* reveals new pattern of satellite DNA organization, highly
3088 scattered across the genome. *Int. J. Mol. Sci.* 22, 6798. doi: 10.3390/ijms22136798

3089 Ugarković, Đ. and Plohl, M. (2002). Variation in satellite DNA profiles—causes and effects.
3090 *The EMBO Jornal* 18, 1708-1719. doi: 10.1093/emboj/cdf612

3091 Utsunomia, R., Silva, D.M.Z.D.A., Ruiz-Ruano, F.J., *et al.* (2019). Satellitome landscape
3092 analysis of *Megaleporinus macrocephalus* (*Teleostei, Anostomidae*) reveals intense
3093 accumulation of satellite sequences on the heteromorphic sex chromosome. *Sci Rep.* 9,
3094 5856. doi: 10.1038/s41598-019-42383-8

3095 Valeri, M.P., Dias, G.B., do Espírito Santo, A.A., *et al.* (2021). First description of a satellite
3096 DNA in manatees' centromeric regions. *Front Genet.* 12, 694866. doi:
3097 10.3389/fgene.2021.694866

3098 van der Sleen, P. and Albert, J.S. (eds.) *Field guide to the fishes of the Amazon, Orinoco, and*
3099 *Guianas*. USA: Princeton University Press, 15, 2017.

3100 Van Der Sleen P. and Albert J.S. "Patterns of freshwater wetland fish species diversity". In:
3101 Tockner K, Mehner T, Wittmann F, Junk WJ (eds.) **Encyclopedia of Inland Waters**.
3102 Elsevier, pp 243–255, 2021.

3103 Vara, C., Paytuví-Gallart, A., Cuartero, Y., *et al.* (2021). The impact of chromosomal fusions
3104 on 3D genome folding and recombination in the germ line. *Nat. Commun.* 12, 2981. doi:
3105 10.1038/s41467-021-23270-1

3106 Venere P.C. and Garutti V. *Peixes do Cerrado: Parque Estadual da Serra Azul, rio Araguaia,*
3107 *MT. RiMa* (ed.), São Carlos: Fapemat, 2011.

3108 Vieira, C.P., Coelho, P.A. and Vieira, J. (2003). Inferences on the evolutionary history of the
3109 *Drosophila americana* polymorphic X/4 fusion from patterns of polymorphism at the X-
3110 linked paralytic and elav genes. *Genetics* 164, 1459-1469. doi: 10.1093/genet-
3111 ics/164.4.1459

3112 Vieira-da-Silva, A., Louzada, S., Adegá, F., *et al.* (2015). A high-resolution comparative chro-
3113 mosome map of *Cricetus cricetus* and *Peromyscus eremicus* reveals the involvement of

- 3114 constitutive heterochromatin in breakpoint regions. *Cytogenetic Genome Res.* 145, 59-67.
 3115 doi: 10.1159/000381840
- 3116 Vozdova, M., Kubickova, S., Cernohorska, H., *et al.* (2019). Comparative study of the bush
 3117 dog (*Speothos venaticus*) karyotype and analysis of satellite DNA sequences and their
 3118 chromosome distribution in six species of Canidae. *Cytogenet. Genome Res.* 159, 88-96.
 3119 doi: 10.1159/000503082
- 3120 Vozdova, M., Kubickova, S., Martínková, N. (2021). Satellite DNA in neotropical deer species.
 3121 *Genes* 12, 123. doi: 10.3390/genes12010123
- 3122 Waldbieser, G.C., Liu, S., Yuan, Z., *et al.* (2023). Reference genomes of channel catfish and
 3123 blue catfish reveal multiple pericentric chromosome inversions. *BMC Biol.* 21, 67. doi:
 3124 10.1186/s12915-023-01556-8
- 3125 Wang, Y., Ghosh, G., Hendrickson, E.A. (2009). Ku86 represses lethal telomere deletion
 3126 events in human somatic cells. *Proceedings of the National Academy of Sciences* 106(30),
 3127 12430-12435. doi: 10.1073/pnas.0903362106
- 3128 Wang, M. and Lemos, B. (2017). Ribosomal DNA copy number amplification and loss in hu-
 3129 man cancers is linked to tumor genetic context, nucleolus activity, and proliferation. *PLoS*
 3130 *genetics*, 13(9), e1006994. doi: 10.1371/journal.pgen.1006994
- 3131 Weissensteiner, M.H. and Suh, A. “Repetitive DNA: The dark matter of avian genomics”. In
 3132 Kraus, R (ed.) **Avian genomics in ecology and evolution: From the lab into the wild.**
 3133 Switzerland: Springer, pp 93-150, 2019. doi: 10.1007/978-3-030-16477-5_5
- 3134 Weitzman, M. and Weitzman, S. Family Lebiasinidae. Check List Freshwater Fishes South
 3135 Cent. Am. Porto Alegre: Edipucrs pp 241–250, 2003
- 3136 Weitzman, S.H. and Cobb, J.S. (1975). A revision of the South American fishes of the genus
 3137 *Nannostomus* Günther (Family Lebiasinidae).
- 3138 Weitzman, S.H. and Vari, R.P. (1988). Miniaturization in South American freshwater fishes,
 3139 an overview and discussion.
- 3140 Xu, W., Tai, J., He, K. (2024). Complete Mitochondrial Genomes of *Nannostomus* Pencilfish:
 3141 Genome Characterization and Phylogenetic Analysis. *Animals* 14, 1598. doi:
 3142 10.3390/ani14111598
- 3143 Yang, F., Graphodatsky, A.S. “Animal Probes and ZOO-FISH”. In: Liehr, T. (ed.)
 3144 **Fluorescence In Situ Hybridization (FISH) - Application Guide.** Berlin: Springer
 3145 Protocols Handbooks, p. 323-346, 2009.
- 3146 Yang, F., Trifonove, V., Kosyakova, N., *et al.* “Generation of paint probes by flow-sorted and
 3147 microdissected chromosomes”. In: Liehr, T. (ed.) **Fluorescence In Situ Hybridization**
 3148 **(FISH) - Application Guide.** Berlin: Springer Protocols Handbooks, p. 35-52, 2009.
- 3149 Yang, T.J., Yu, Y., Chang, S.B., *et al.* (2005). Toward closing rice telomere gaps: mapping and
 3150 sequence characterization of rice subtelomere regions. *Theor. Appl. Genet.* 111, 467-
 3151 478. doi:10.1007/s00122-005-2034-4
- 3152 Yang, W., Kang, X., Yang, Q., *et al.* (2013). Review on the Development of Genotyping
 3153 Methods for Assessing Farm Animal Diversity. *J. Anim. Sci. Biotechnol.* 4 (1), 1–6.
 3154 doi:10.1186/2049-1891-4-2
- 3155 Yannic, G., Basset, P., and Hausser, J. (2009). Chromosomal Rearrangements and Gene Flow
 3156 over Time in an Inter-specific Hybrid Zone of the *Sorex araneus* Group. *Heredity* 102
 3157 (6), 616–625. doi:10.1038/hdy.2009.19
- 3158 Yano, C.F., Bertollo, L.A.C., and de Cioffi, M.B.(2017). “Fish-FISH: molecular cytogenetics
 3159 in fish species,” in *Fluorescence in situ hybridization (FISH)* (Springer), 429–443.
 3160 doi:10.1007/978-3-662-52959-1_44.
- 3161 Yano, C.F., Bertollo, L.A.C., Molina, W.F., *et al.*(2014). Genomic organization of repetitive
 3162 DNAs and its implications for male karyotype and the neo-Y chromosome differentiation
 3163 in *Erythrinus erythrinus* (Characiformes, Erythrinidae). *Comp. Cytogenet.* 8, 139.

3164 doi:10.3897/compcytogen.v8i2.7597.
3165 Yano, C.F., Sember, A., Kretschmer, R. *et al.* (2021). Against the mainstream: exceptional
3166 evolutionary stability of ZW sex chromosomes across the fish families Triportheidae and
3167 Gasteropelecidae (Teleostei: Characiformes). *Chromosome Res* 29, 391–416. doi:
3168 10.1007/s10577-021-09674-1
3169 Yazdi, H.P., Olito, C., Kawakami, T., *et al.* (2023). The evolutionary maintenance of ancient
3170 recombining sex chromosomes in the ostrich. *PLoS Genetics* 19, e1010801. doi:
3171 10.1371/journal.pgen.1010801
3172 Zattera, M.L. and Bruschi, D.P. (2022). Transposable elements as a source of novel repetitive
3173 DNA in the eukaryote genome. *Cells* 11, 3373. doi:10.3390/cells11213373
3174 Zwick, M.S., Hanson, R.E., Islam-Faridi, M.N., *et al.* (1997). A rapid procedure for the isolation
3175 of C 0 t-1 DNA from plants. *Genome* 40, 138–142. doi:10.1139/g97-020.